SIMULATION TESTS FOR THE OPERATION OF A WATER MAIN WITH BREAK PRESSURE TANKS

Ismaeel Haroon Tar Ally

BSc(Eng) (Chemical)

Submitted in fulfilment of the academic requirements for the degree of

Master of Science in Engineering

in the

Faculty of Engineering,

University of KwaZulu-Natal, Durban

Supervisor: Professor Michael Mulholland

March 2016

DECLARATION

I, Ismaeel Haroon Tar Ally, declare that

1. The research reported in this thesis, except where otherwise indicated, is my original research.

2. This thesis has not been submitted for any degree or examination at any other university.

3. This thesis does not contain other persons' data, pictures, graphs or other information, unless specifically acknowledged as being sourced from other persons.

4. This thesis does not contain other persons' writing, unless specifically acknowledged as being sourced from other researchers. Where other written sources have been quoted, then:

a. Their words have been re-written but the general information attributed to them has been referenced

b. Where their exact words have been used, then their writing has been placed in italics and inside quotation marks, and referenced.

5. This thesis does not contain text, graphics or tables copied and pasted from the Internet, unless specifically acknowledged, and the source being detailed in the thesis and in the References sections.

Signed

……

Ismaeel Haroon Tar Ally

03/03/2016

As the candidate's Supervisor I agree/do not agree to the submission of this thesis

_____

Michael Mulholland

March 2016

ACKNOWLEDGMENTS

- My family, specifically my parents
- Professor Mulholland – Supervisor
- Professor Buckley – Co-supervisor
- Neil McLeod – Co-supervisor
- Amal Doorgapershad (Knight Piesold), Darren van Rooyen (RHDHV)
- EWS

ABSTRACT

The Ashley Drive break pressure tank (BPT-20 $M\ell$) has been installed on Durban's Western Aqueduct. Its purpose is to release the 20 bar gravity head of the 1.4m trunk main supply from Umgeni Water at Umlaas Road. The expected peak conditions (400 $M\ell/day$) will only allow 14 minutes for valves to close, yet they must be moved slowly in order to avoid dynamic shock. The high pressure upstream supply is admitted to the BPT through a set of thee parallel sleeve valves, which are in a control loop to maintain level in the BPT against the downstream draw. These cavitation-resistant valves cannot be operated without electrical power, so an added complication of the design is a set of 3 hydraulically-operated globe valves which switch in at extreme tank levels.

Though the commissioning of the Ashley Drive BPT is already in progress, it is important to simulate the overall operation of the system for projected future flows, in order to detect possible operational problems, and to build in solutions if necessary. Optimisations include such issues as the valve closing sequence and speeds, settling level variations, and smoothness of the draw from Umgeni Water.

The simulation study involved the modelling of the trunk main, the Ashley Drive BPT, the downstream Wyebank BPT and the reservoirs drawing from the trunk main before and after these two BPTs. Data handling techniques were developed in order to formulate the daily demand profiles for each of the reservoirs. Design information was used to calculate the hydraulic parameters that featured in the simulation, and to determine the residual pressures at the inlet valve sets of the BPTs. Implicit calculations with the Newton-Raphson iterative method were employed in order to obtain a pressure distribution across the BPT valves. Simple mechanisms were built into the MATLAB® program in order to accommodate the complexities of the system, e.g. the possibility of power loss, valve or BPT chamber maintenance, or the deliberately slowed movement of the valves to avoid pressure surges within the pipeline.

The analysis of the results of the simulation study involved examining the efficacy of the control set-points and valve sequencing, and determining whether these settings satisfy the design specifications. Random and anticipated scenario testing was carried out within the study in order to accommodate for situations such as electricity outages or unusual consumer demands. The BPT control system was analysed to assess its adequacy and the risks associated with the proposed *staggered* sleeve valve control scheme.

The results of this investigation are presented as multiple time-sequence graphs depicting the results of the different scenario tests. Support for the design concept, additional recommendations and indications of adverse scenarios, have emerged from this study. The original design is found to be capable of duty within the ranges of expected normal operation in 2036, and the system was observed to be capable of conveying a throughput greater than that of the design. The normal operating level was also found to be higher than intended, and valve oscillations were deemed a significant concern. It was established that operation with just two sleeve valves active within each BPT would achieve better correspondence to the design specifications. The revised control system (Control 2.0) was found to be better suited to the application, but was also diagnosed to be too slow to react under certain circumstances.

TABLE OF CONTENTS

LIST OF FIGURES

LIST OF TABLES

LIST OF ABBREVIATIONS

Abbreviation	Definition
AD	Ashley Drive
BPT	Break pressure tank
NOL	Normal operating level
SOP	Standard operating procedure
WA	Western Aqueduct
WDS	Water distribution system
WR	Wyebank Road

1 INTRODUCTION

The right of access to water, for every citizen, is enshrined in Act 108 of 1996, Chapter 2 of the Bill of Rights of the South African Constitution. Section 27.1 States that "Everyone has the right to have access to... sufficient food and water and ...". According to Section 27.2 of this Act, it is within the duties of the state to enact "reasonable legislative and other measures, within its available resources to achieve the progressive realization of these rights."(Muller, 2011). Pursuant to this legislation, The Water Services Act of 1997 and The National Water Act of 1998, provide the general structure for the framework within which water supply services and water resource management and usage. In addition to this, the National Water Act aims to promote equitable access to water. The role of municipalities and water service providers are governed by the Water Services Act of 1997, whose objectives include, but are not limited to, setting of national standards for tariffs, the Establishment of water services institutions and water boards and monitoring service provision. The Municipal Structures Act of 1998 together with the Municipal Structures Amendment Act of 2000, determine the separation of responsibilities and functions between municipalities, including sewage disposal, bulk treatment and bulk water supply. Category C (District) municipalities are allocated the responsibilities of "potable water systems" and "domestic sewage and wastewater" (Department of Water Affairs and Forestry., 2009).

The eThekwini Water and Sanitation Unit (EWS) is an award-winning, pioneering unit of the eThekwini (Metropolitan) municipality whose responsibilities include the provision of potable water and sanitation to residents within the municipal locality. The municipality includes

Durban and surrounding towns, and as the third largest municipality in South Africa, caters to 3 442 398 people (2011 census) (eThekwini Municipality., 2013). In support of the pioneering aims of EWS, a co-operative research agreement with UKZN is currently in place (eThekwini Municipality., 2012).

EWS has an extensive infrastructure network that facilitates the efficient distribution of potable water that ensures the availability of a distribution point within 200 m of each resident. Figure 1 is a GIS mapping of the existing water distribution infrastructure. Bulk water is either purchased from Umgeni Water, a state-owned parastatal, or sourced through one of the four EWS-operated water treatment plants (eThekwini Municipality., 2011b).

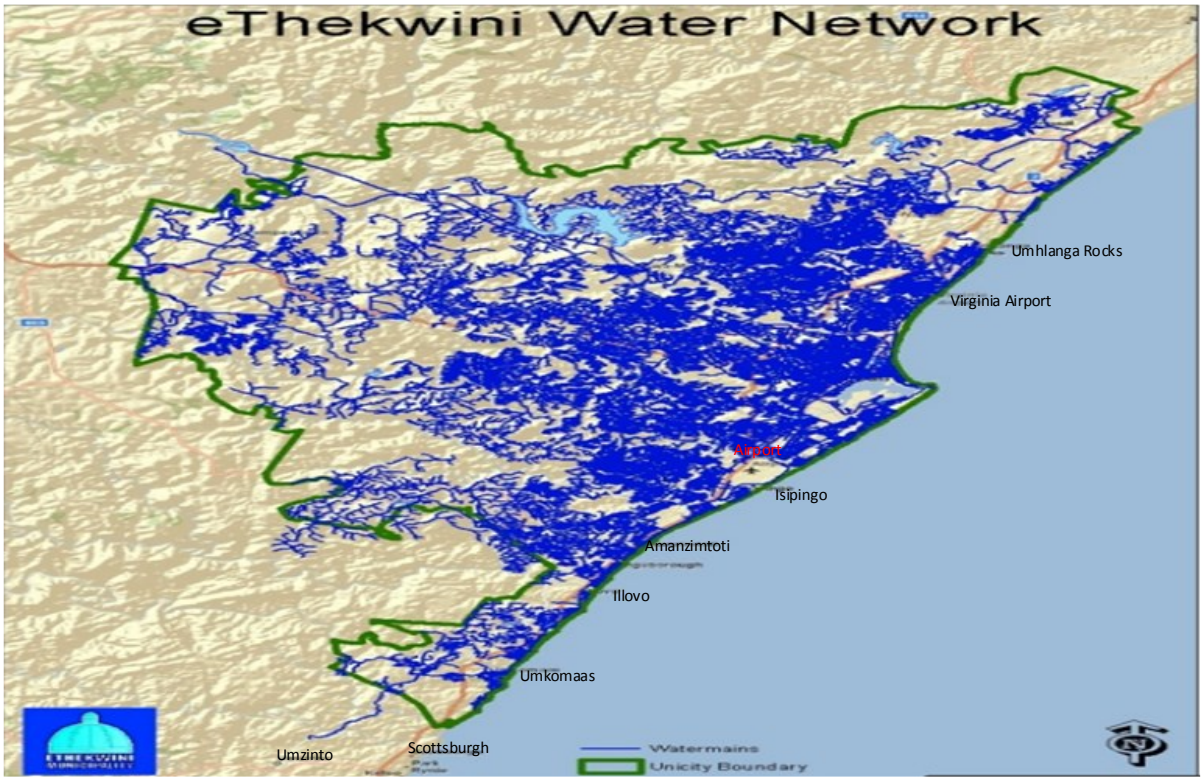

Figure 1 - GIS mapping of the eThekwini water distribution network (eThekwini Municipality., 2011b)

1.1 Aqueduct Projects

A spate in urbanization has vastly increased the population within the jurisdictional locality of EWS. In the period spanning 2000-2014 alone, 1.3 million extra people had been granted access to piped water facilities. In 2010 alone, 30 000 families were connected to the piped water network, and by 2030, a 20% increase in the eThekwini metropolitan population is

forecasted. This has led to a surge in the demand for bulk water and has stressed existing, often dated, infrastructure (SAinfo reporter., 2014). In response to the challenges posed by the ever increasing demand for water, and a forecasted impending catastrophic water supply shortage, EWS has commissioned two major aqueduct projects – The Western Aqueduct Project and The Northern Aqueduct Augmentation Project. These projects are intended to bolster supply capacity in the long term (30 years – 2036).

The Northern Aqueduct Augmentation Project consists of three phases, each prioritised according to its distinct purpose. The project was conceived due to the near-capacity operation of the existing northern aqueduct bulk supply lines, particularly in the Ntuzuma, Mzinyathi and Senzokuhle areas, and a resulting low residual pressure issue in the Umhlanga region. This project also establishes the supply network to the Cornubia Housing development (Phase One), and connects the Western and Northern Aqueducts (Phase Two). Phase Three includes the construction of pipelines, reservoirs, a pump booster station and a pumping main (Macleod, 2013).

The Western Aqueduct Project was conceived in order to relieve the excess loading and resultant capacity issues that plagued the Outer West areas. Internal pipe damage and erosion on existing infrastructure have already been observed as a result of excess supply velocities which result from demand flows that exceed the design limits. In addition to this, supplemental supply (shed demand) had become necessary to meet increased demands in the high-density residential areas (Ntuzuma and surrounding areas), as the pumping stations that supply the areas north of the Durban Heights Waterworks had reached capacity.

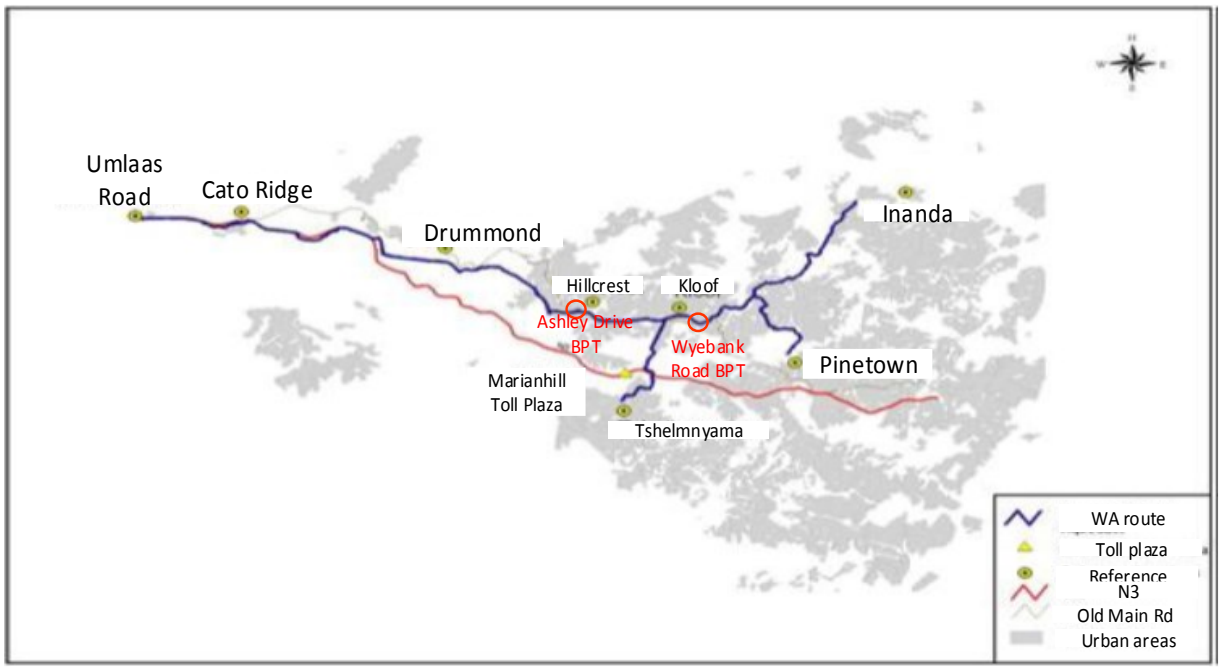

Figure 2 - Western Aqueduct route from Umlaas Road to Ntuzuma (eThekwini Municipality., 2011b).

The eventual design route for the Western Aqueduct bulk supply route thus begins at Umlaas Road (west- near Cato Ridge), goes through the Inner West and Outer west areas, and ends to the North at Ntuzuma. The pipeline tends to follow the N3 highway from Umlaas Road to Inchanga, where the two diverge, with the pipeline cutting through the Hillcrest area. The pipeline then tracks the path of the M13 freeway, through Wyebank and Mount Moriah until it ends at Ntuzuma (Facts About Durban., 2009). Figure 2 is the proposed route for the Western Aqueduct bulk supply pipeline. The total estimated cost of the project is R1.2 Billion Rand (eThekwini Municipality., 2011b). The total pipeline length is 75 km and the design incorporates two break pressure tanks (BPT). The Ashley Drive (Kloof) break pressure tank has a total capacity of 20 $M\ell$ and the Wyebank break pressure tank has a capacity of 10 $M\ell$. The Western Aqueduct is envisaged to fortify existing water supply by boosting supply capacity by 400 $M\ell/day$. The total consumption for Durban in 2011 was 950 $M\ell/day$ (eThekwini Municipality., 2011a). The project is expected to reach completion and be fully operational by mid-2017 (Tancott, 2014). The initial portion of the Western Aqueduct pipeline (Inchanga to Ashley Drive) began commissioning during February 2015, and the revised estimated completion date for the Ashley Drive BPT, at the time, was the third quarter of 2015. The contract for the construction of the Wyebank BPT was awarded during the third quarter of

2015. The construction of the trunk mains from the Ashley Drive BPT to NR5 (Ntuzuma Reservoir 5) is in progress. The pipelines to Haygarth Road and Tshelnyama were scheduled to start in April 2015 (Daily News Reporter., 2015). The BPTs were initially intended to serve as hydroelectric generators, in order to supply "green energy" to the communities surrounding the tanks (eThekwini Municipality., 2011a).

The route was selected primarily based upon the following criteria:

- To incorporate as much of the existing infrastructure within the current registered infrastructural network.
- To minimize the use of pumping stations in order to avoid extraneous energy usage and to circumvent potential supply disruptions due to pump failures/maintenance.
- To avoid impacting and destroying cultural and heritage sites, and environmentally sensitive areas.

Measures were also devised to avoid public disruption. These measure included rapid reinstatement of the working corridor, the sealing of the corridor to prevent animal access and restriction of the latest working time to 18:00 in residential areas. Where roads were affected, they were also repaired immediately (Facts About Durban., 2009).

Despite the claimed meticulous adherence to protocols in the tender awarding process, the project implementation was delayed by an entire year. Three rejected bidders objected against the decision of the eThekwini Municipality to award the tender to the EsorFranki and Cycad Pipelines joint venture. A court application was also lodged against the municipality. Factors purported to have been considered in the evaluation of tenders include the BEE status of the bidder, the compliance with tender conditions, the quotation price and the quality. The current status of the construction of the Western Aqueduct, at the time of writing is listed in Table 1.

Table 1 - The current progress of the Western Aqueduct project construction.

Contract #	Description	Status
1	Inchanga to Alverstone Nek	Complete
2	Alverstone Nek to Ashley Drive	Complete

3	Ashley Drive to Ntuzuma	in progress (estimated completion 2017)
4	Branch line from Maytime to Tshelimnyama	in progress (estimated completion 2017)
5	Branch line from Wyebank to Mount Moriah	On hold
6	Ashley Drive BPT	Complete
7	Wyebank BPT	estimated to start Jan 2016

The need for a working model of existing, and especially new infrastructure is well-established amongst the engineering and allied fraternities. The presence of a model allows for increased levels of service delivery and heightened awareness of the system's behaviour. It also allows for improved emergency preparedness and for informed decisions to be made, particularly regarding master planning. Such meticulous planning is essential for EWS to establish confidence in their ability to uphold high standards of service delivery, to maintain the pristine reputation of EWS, as a reliable, award-winning municipal division, and to prevent a deterioration in the relationship with the public. The eThekwini Municipalities EWS division, through their strategic research relationship with the University of KwaZulu-Natal initiated this project. The foundational directive issued, pertained to the focussed analysis of the Ashley Drive BPT's response to failure-states. The outcomes and objectives of this research study were thus determined through ensuing sessions in which the expectations and requirements of the relevant personnel were discussed and analysed. The scope of this study was thus expanded to include the span of the Western Aqueduct, which includes the Wyebank Road BPT. Situational analyses were also augmented to the project to include various other possible failure scenarios within a series of systematic simulation executions. These results could then be analysed to deepen the understanding of the control and operation of the system, and provide valuable insight to possible problem situations.

1.2 Aims

- Develop a working, realistic, robust model of the Western Aqueduct
- Assess the performance of the Western Aqueduct under stress conditions

1.3 Objectives

- Build a mathematical representation of the Western Aqueduct to evaluate the daily behaviour of the system
- Identify and execute stress-tests that can be used as an assurance to the adequacy of the design of the Western Aqueduct and to improve the emergency response preparedness of the operators
- Deconstruct the model to allow for users to understand its components
- Critically assess the accuracy of the simulation in order to identify possible improvements
- Evaluate the results of the simulation

1.4 Thesis structure

Figure 3 presents a visual summary of the content of the thesis, and the interaction between the chapters. The intent of each chapter is described briefly below.

Chapter 1: Is an introduction to the Durban Aqueduct projects and the Western Aqueduct. The basis of this project, its aims and objectives are also detailed within this chapter.

Chapter 2: Presents a literature review of the underlying theory and subject matter that relates to the project and the physical system. Similar and related projects have been outlined within this chapter.

Chapter 3: Describes the Western Aqueduct from a macroscopic and a microscopic perspective. The macroscopic description pertains to the overall route and topography, while the microscopic description incorporates the BPTs and their internal components (control system, valve arrangements etc.)

Chapter 4: Describes in detail, the modelling approach that was undertaken to formulate the mathematical model of the WA. This chapter essentially is a development/user manual for the model. The description will enable the user to seamlessly edit the program to adjust parameters according to the latest developments.

Chapter 5: Presents the results of the scenario tests on the model of the WA. The results are analysed to assess the performance of the WA under varying conditions.

Chapter 6: Presents the conclusions of this study, and the recommendations that have arisen from it.

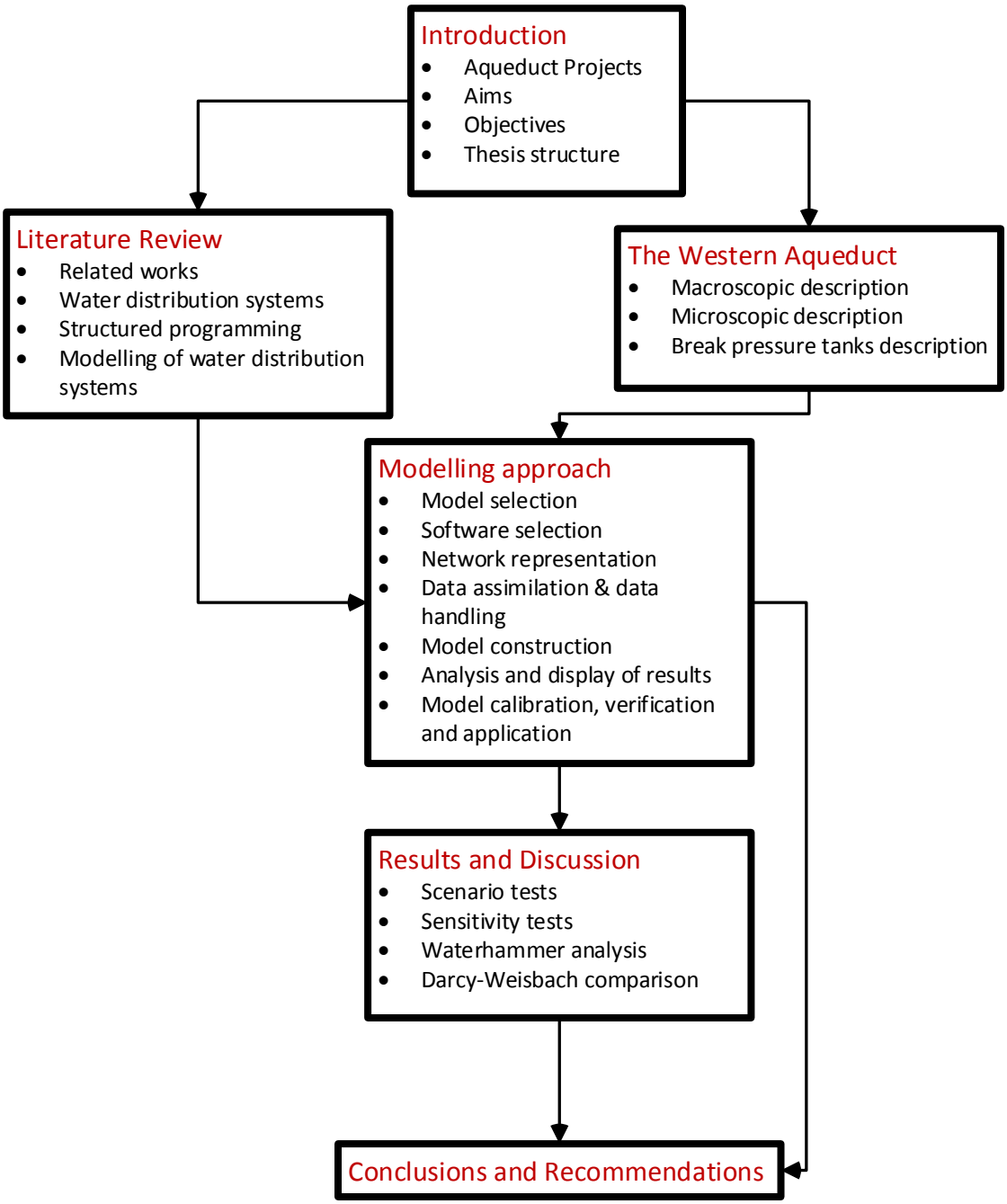

Figure 3 - Visual summary of the content of the thesis.

2 LITERATURE REVIEW

2.1 Related Works

Soldi et al. (2015) presented a framework to assess the resilience and vulnerability of a water distribution system (WDS). A hydraulic model together with simulations was employed to compute the stress of the materials of construction for varying service levels. EPANET was used to model the system in order to produce a decision support tool that would aid in identifying system vulnerabilities and in isolating pipes with high stress exposure. The framework was tested on active water distribution systems.

Dasic and Djordjevic (2004) developed a method to simultaneously analyse the mechanical and hydraulic reliability of a water distribution system (WDS). The presented model, NETREL, which is capable of accepting input for systems of varied configurations and sizes, uses a genetic algorithm to assess the optimum distribution for maximum reliability. The framework was tested on an imaginary network to illustrate its effectiveness in identifying system vulnerabilities.

Hopkins (2012) used a modified version of the gravity model for transportation in order to evaluate the systems exposure to threats, without using hydraulic evaluations for each conceivable failure state. The modelling of the hypothetical system was conducted in MATLAB and WaterCAD. The objective of the program was to identify nodes, junctions or pipes that would disable the system if affected or affect the activity of critical service providers. Model simplicity was prioritized in order to ensure that non-professionals may utilise and understand the model. Model outputs were documented using Microsoft Excel.

Zessler et al. (1989) presented a method to institute the optimal operation of WDS using a progressive optimality solution algorithm. The model requires the approaching forecasted daily water demand, reservoir initial and final conditions, the energy cost schedule and the hydraulic parameters for the system. The optimum pump schedule is thus found by iteratively combing through the network fragments over a series of time steps until convergence is attained. The algorithm was applied to a WDS that consisted of seven booster stations and eight storage tanks.

Biscos et al. (2002) undertook a study for the eThekwini Metro, which used MINLP to formulate a method to achieve the real-time optimum operation of a water distribution system. Both discrete (valves, pumps etc.) and dynamic (level, concentration) elements were considered in the constrained optimization. The primary optimization concerns were the maximisation of off-peak electricity usage, and the minimisation of chlorine decay. A model predictive control algorithm was thus formulated to execute an optimization process, at each time interval, to generate a series of optimum control moves for a predefined time frame. The first control move is then immediately implemented, and the optimization process is re-initiated. The researchers used MATLAB to generate inputs to GAMS, which was used to solve the optimization problem. The Southern Aqueduct was modelled in order to demonstrate the ability of the proposed method to optimize the distribution of water within the confines of the eThekwini Metro jurisdiction.

Elker and Kara (2003) undertook to model the Gaziantep City water supply using a nonlinear model. Simulation studies were subsequently carried out in order to validate the model results and to understand the system behaviour. The stability of the flow, the pressure heads in the reservoirs and frictional pressure drops were recorded for sections of the plant. Various flow disturbance scenarios were simulated in order to test the system response.

Kwierniewski (2003) outlined a method to model water distribution systems (WDS) in order to assess their reliability. The model was constructed around the WDS operational data. Parameters to rate the system reliability were defined in order to calculate the probability of unsatisfactory system performance, the frequency of part-fault system states and the intensity and duration of such faults. The reliability parameters were defined through the consideration of the delivery quantity, quality and pressure.

Shuang, Zhang & Yuan (2014) undertook a model-oriented approach to the testing of water distribution system (WDS) reliability under various operating conditions. Cascading failure

conditions in the system were studied in order to identify and subsequently isolate and eliminate the pipe sections that are vulnerable to this type of failure. Reliability coefficients for the system were defined as the ratio of the sum of available flows to that of required flows. EPANET was used as the simulation engine, while MATLAB was used to implement stage-wise modelling in time steps of one hour. The Hazen-Williams formula was used in EPANET for the head loss calculations.

Wright et al. (2015) presented an optimization procedure for the optimum control of pressure reducing valves within water distribution systems, using dynamic topology. A study was conducted on an active WDS, to demonstrate the superiority of the proposed method over previous approaches. The hydraulic model used within the case study incorporated 2 374 nodes and 2 434 pipes.

2.2 Water Distribution Systems

History is testament to the fact that the widespread availability of clean water has been prioritized since early recorded human civilizations. The first documented transport system dates back 3 500 years, to the Crete Island in Greece. Piped water distribution systems existed in Anatolia, Turkey, approximately 3 000 years ago. The Roman Aqueducts of the first century AD, as perhaps the most famous historical piped distribution systems, spanned a length of 420 km and conveyed approximately 1 000 $M\ell/day$ over 90 km to a distribution subnetwork. Despite large volumes of water losses, the system enabled each resident of Ancient Greece (app. 1.2 million) access to approximately 500 litres per day of clean, piped water (Trifunovic, 2006). The importance of water distribution systems as assets should not be discounted. Water distribution systems are both capital intensive and serve the general public, and thus require a distinct form of asset management. The Netherlands as an example, invests approximately $500 million per year in order to expand, reconstruct, rehabilitate, manage and maintain their water distribution and treatment infrastructure. A cost study conducted on water systems in the Netherlands (Figure 4) revealed that the transport and distribution of potable water is the major contributor (>50%) to the capital expenditure, while treatment and extraction accounts for a smaller proportion. A large proportion of the transport and distribution capital allocation is consumed by pipes and pipe fittings e.g. joints, valves and service connections (Trifunovic, 2006). The typical constituents of a water distribution system are shown in Figure 5.

Water transport and distribution systems typically serve the purposes of providing potable water for consumption, and for fire protection (Mays and American Water Works Association., 2010). Water distribution systems however, are also critical in the maintenance of public safety, human rights and uninterrupted daily operations (Shuang et al., 2014). This system is a part of a broader process that typically consists of the following functions (Trifunovic, 2006):

1- Raw water extraction and transport – EWS/Umgeni Water
2- Water treatment and storage – EWS/Umgeni Water
3- Clean water transport and distribution – EWS
4- Used water disposal and treatment – EWS/Umgeni Water

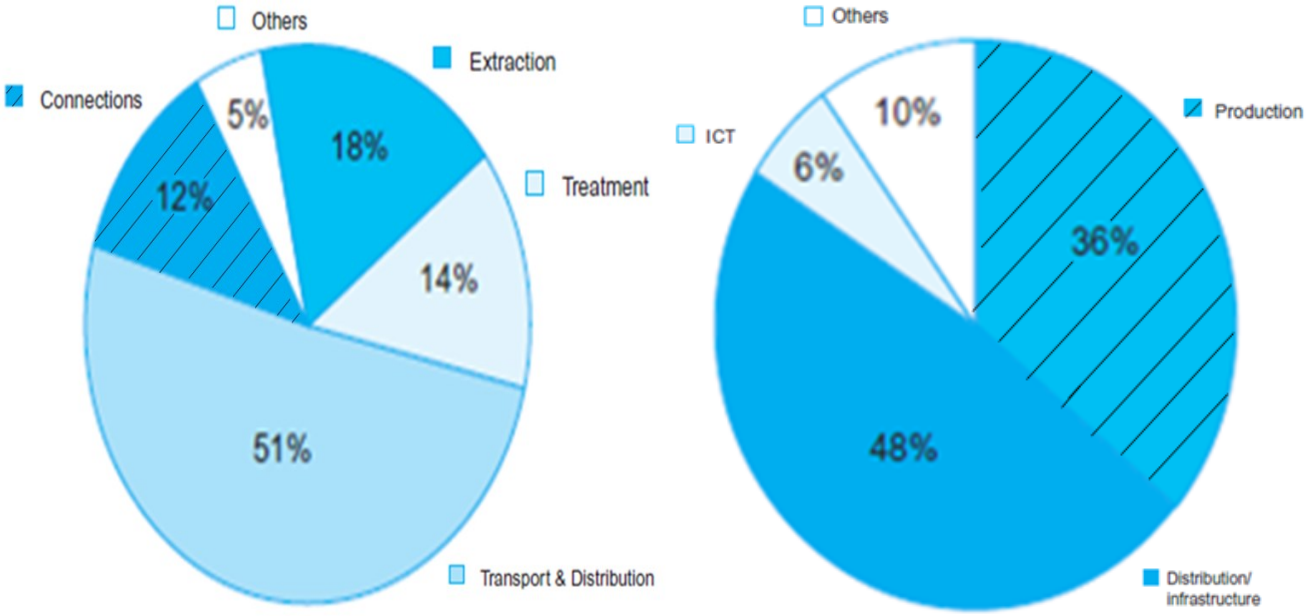

Figure 4- Results of a study into the apportioning of funds dedicated to water provision, amongst the various contributing expenses in the Netherlands (Trifunovic, 2006).

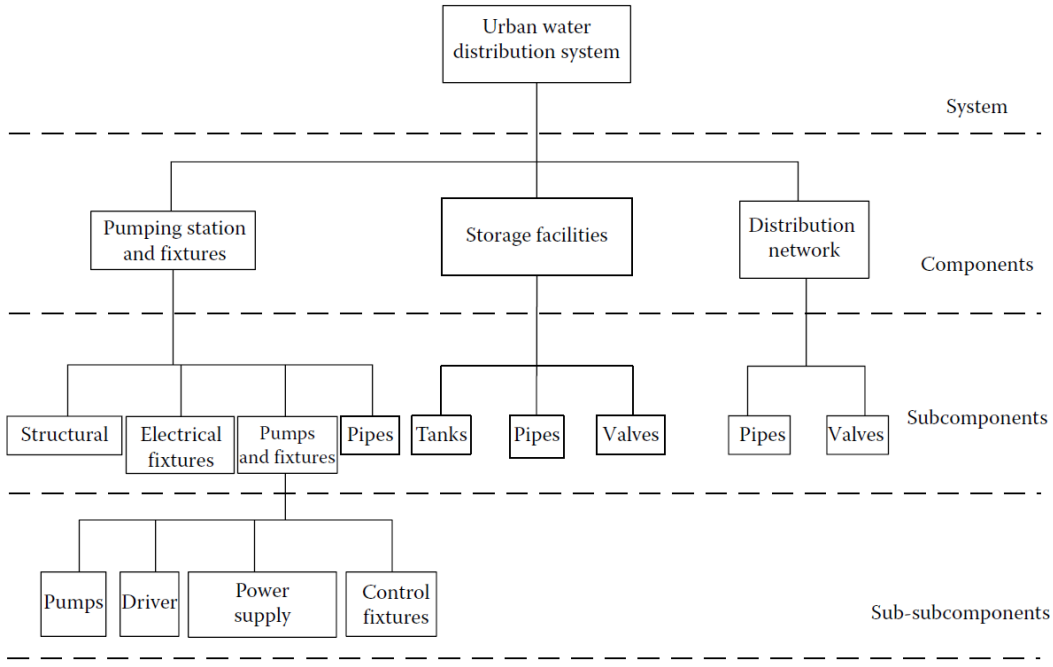

Figure 5 - The typical constituents of a water distribution system (Karamouz et al., 2010).

The system components that comprise a water distribution system, like the Western Aqueduct, are:

- **Trunk main/ Transmission Lines** – The function of these pipelines is to convey potable water in bulk from treatment plant to distribution infrastructure (service reservoirs, pumping stations etc.) or untreated water from the source to the treatment works (Ratnayaka et al., 2009). Their size is dependent on the consumer demand in regions served by the mains. Trunk main diameters typical range from 100 mm to several metres (Trifunovic, 2006). They are generally straight-run systems, but branching is sometimes possible. Even the largest of consumers are rarely connected directly to the transmission mains (Mays and American Water Works Association., 2010).
- **Secondary mains are smaller pipelines –** These pipelines (typically between 150 mm-400 mm) link the main apparatus of the distribution systems (e.g. pumping stations). They allow for demand-commensurate distribution of water and operation under irregular situations (fire, major pipe burst, maintenance etc.). These lines may be tapped to directly connect large consumers.
- **Distribution mains –** These pipelines function to distribute the flow from within the secondary mains to the community. They are usually laid adjacent to roads, have

multiple service connections and are frequently tapped to accommodate individual users. Valves are carefully placed within the distribution mains in order to maintain adequate supply conditions (Mays and American Water Works Association., 2010).

- **Service lines –** These are small-diameter pipes that serve as connections for each consumer to the distribution mains (Trifunovic, 2006). Private connections link individual consumers to the distribution mains, while public outlets are intended to serve a sub-section of a community (Mays and American Water Works Association., 2010).

2.2.1 Storage in Water Distribution Systems

Storage systems within distribution systems, like the Western Aqueduct, generally take the form of reservoirs (ground-level or buried) or elevation tanks. They are usually situated at elevated locations within the distribution system. Their inclusion within the system is primarily aimed at serving the following purposes (Mays and American Water Works Association., 2010) & (Trifunovic, 2006):

- Accepting variable supply. The modulation of the demand from the source is also of concern.
- Meeting variable demand on the consumer end
- Maintaining sufficient supply for emergency conditions (fire flows, power outages, pump failures etc.)
- Providing stable, adequate pressure to users
- Decreasing pumping costs and flattening pumping variations
- Providing surge relief (see Section 2.2.1.1)
- Blending of water from different sources

The primary purpose of the water storage features is to equalize the supply and demand conditions, thus allowing for the use of smaller pipes. This is due to the buffering function offered by the tanks. The average consumer demand can thus be considered as the design flow, instead of overdesigning to meet the maximum possible demand. Storage systems are thus a justified cost, as other large costs are offset due to it (Trifunovic, 2006). Reservoirs are typically designed to store 20-50% of total maximum daily consumption, in order to maintain a high turnover ratio, which in turn aids in circumventing chlorine degradation and water quality issues. Maintaining a high turnover ratio and good mixing characteristics also mitigates

problems of 'deadzones' within the reservoirs, where water stagnates and thus deteriorates within the reservoir (Mays and American Water Works Association., 2010).

2.2.1.1 Break Pressure Tanks (BPTs)

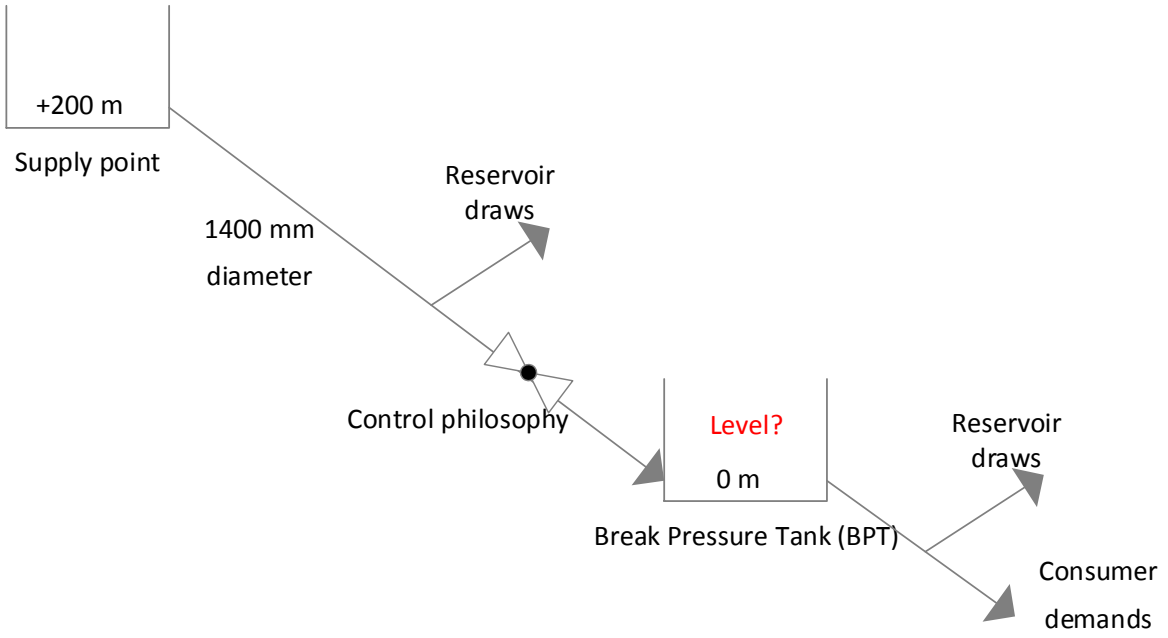

Figure 6 - Simple schematic describing the purpose of a break pressure tank in a gravity-fed water distribution system.

Break pressure tanks, as found within the Western Aqueduct, are primarily used as pressure regulating devices that are ideally paired with balancing tanks. The purpose of a break pressure tank is to return the process fluid to atmospheric pressure, in order to maintain working pressures in the system within economic ranges. In Figure 6, the break pressure tank is tasked with releasing 200 m of head by re-establishing atmospheric pressure, The inlet control system is governed by a control philosophy that must maintain the tank level based upon the variable upstream head, while giving cognisance to downstream demand. It is important to design compartments within the break pressure tank in order to permit easy access for maintenance (Stephenson, 2012). Bypasses around the break pressure tanks should be avoided at all costs, in order to negate the possibility of the high pressure being transmitted to the pipelines downstream of the break pressure tank. The design and location of break pressure tanks should aim to bisect the sum total maximum static head on either side of the break pressure tank (Ratnayaka et al., 2009), or to divide the system into a series of manageable pressure zones

(Groundfos., 2012). BPTs are an invaluable tool in the establishment of pressure zones, which provide advantages by reducing excessive pressure in lower-lying areas (Trifunovic, 2006).

Break pressure tanks also find use as buffering tanks, to ensure that adequate supply is maintained even during peak demands or equipment failures. BPTs also serve to minimize the effect of water hammer surges and to prevent instances of water contamination by eliminating the possibility of backflow (Groundfos., 2012).

The inclusion of break pressure tanks into gravity fed water distributions is integrated within the considerations for the materials of construction and maximum working pressure (Niskanen, 2003). This is due to the radical reduction in working pressure that stands to be realized with the use of BPTs, and the subsequent reduction in the requisite strength of materials, and expected wear on system components. As a heuristic, working pressures should be kept below 20 bar (Stephenson, 2012).

Although BPTs are advantageous in many regards, they do increase the initial capital cost of the system, pose a health risk due to increased microbial growth within the tanks (if the design and turnover ratio is inadequate), and occupy large expanses of land. Some of the advantages associated with the use of BPTs include (Groundfos., 2012):

- Increased robustness due to the storage of large volumes of water
- Increased control of pressure within the pipelines
- Decreased sensitivity to electrical outages
- Decreased capital costs due to the adequacy of lower grade pipeline and fittings materials

2.2.2 Valves

Flow control valves are selected based on their characteristics, which corresponds to the relationship between the flow, pressure drop and % of the trim open. It should be noted that intrinsic characteristics, caused by varying designs of the valve trim, seat, body shape and port dimensions, often differ from the actual operating characteristics of the valve due to the interaction of valve with the characteristics of other system components (Ratnayaka et al., 2009). Typical intrinsic characteristics of different valve designs are shown in Figure 7. The

head loss through a valve can typically be described by Equation [1], which incorporates the intrinsic valve characteristic ($f(x)$), and the valve capacity coefficient (C_v):

$$Q = C_v f(x)\sqrt{\Delta p} \qquad [1]$$

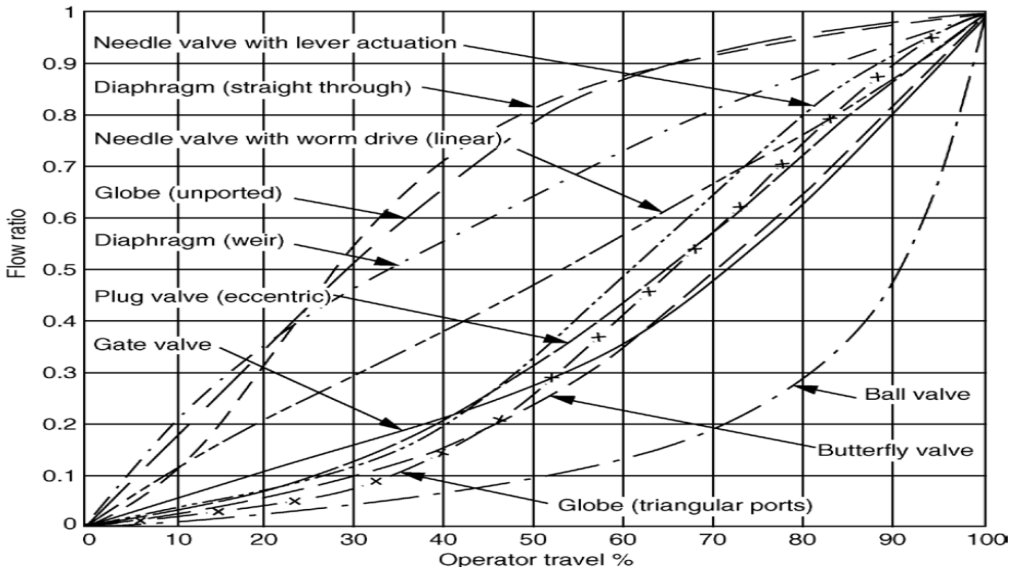

Figure 7 -Representative intrinsic valve characteristics for numerous valve types (American Water Works Association., 2001).

Some operational difficulties with control valves occur as a result of the throttling function of the valve. The valve accelerates the passing fluid at a rapid rate, and the resultant high velocities cause steep transverse velocity gradients to form, due to frictional effects (*no slip*) at the exposed surfaces. The result is large-scale energy dissipation by the conversion of mechanical energy to thermal energy (heat). The desired pressure drop through the valve is thus achieved in conjunction with varying amounts of other less desirable effects such as noise, cavitation and valve chamber wear (Mays, 2000).

The parallel arrangement of valves is advantageous in areas of high pressure variations, and when a single valve (equally sized valve) is unable to accommodate large requisite flows. Apollo Valves. (2014) thus recommends that several smaller pressure reducing valves be installed in parallel when designs are intended to serve future demands. Valve performance is also enhanced when the flow demand range is high (more accurate control due to the divided flow), and maintenance can be easily conducted on individual valves without a total system shutdown (Watts Canada., 2015).

2.2.2.1 Globe Valves

Globe valves, as included within the Western Aqueduct inlet-control design, are linear valves that are also commonly called *y-pattern* valves (American Water Works Association., 2001). Their design, as shown in Figure 8a, closely resembles that of an angle valve, apart from the 90° angular distance between the inlet and outlet chambers in the latter (Mays, 2000). The throttling function of the globe valves, that serves to regulate flow, is achieved through the lowering of a plug/disc into the valve seat. The valve seat is formed from an internal baffle that laterally compartmentalises the valve body. The design of the plug determines the characteristic of the valve. The most common categories of globe valves are linear, equal percentage and fast opening. The design of the globe valve provides for a convoluted flow path. Globe valves primarily find use within pressure-control scenarios, tank level control and surge control (American Water Works Association., 2001). The advantages of globe valves include a good sealing capacity (preventing of leakage and thus contamination) and a heightened resistance to wear. Globe valves however offer a high resistance to flow, even in their open positions, and are vulnerable to the deposits of sediment and other particles within their chambers. Figure 8a is a diagram of the operation of a typical globe valve (American Water Works Association., 2001).

Self-actuated valves, also known as hydraulically operated valves, utilize the process fluid pressure in order to adjust their position. This renders them free of any dependence on electricity, and an attractive option in the case of power outages. Self-actuated control valves can either be backpressure control, where an upstream pressure is used to adjust the valve position, or pressure control, where a downstream pressure is used to throttle the control valve, and is thus controlled. The latter makes use of a tapping that connects the bonnet diaphragm to a downstream location, giving the bonnet access to the pressure at such a location. An increase in the downstream pressure beyond a setpoint thus forces fluid into the bonnet, which applies an increased force onto the diaphragm, thus closing the valve. The valve closure causes the downstream pressure to retreat to the setpoint. If the downstream pressure falls to below the setpoint level, the process fluid is drawn back into the downstream pipe from the bonnet, thus decreasing the force applied to the valve diaphragm, which opens the valve. Fluid flow is thus increased due to a reduction in the system resistance, and the downstream pressure is thus increased. The back-pressure control valve uses an analogous operational philosophy, except

that an increase in pressure on the diaphragm forces open the valve. The structure of a self-actuated globe valve is shown in Figure 8b (Enggcylcopedia., 2012).

a

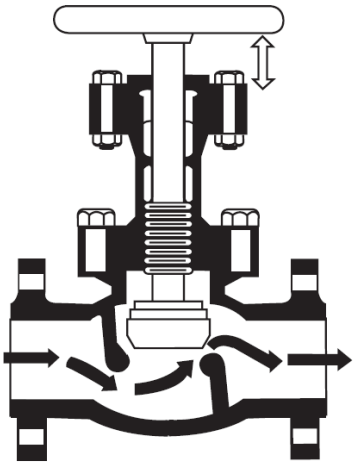

b

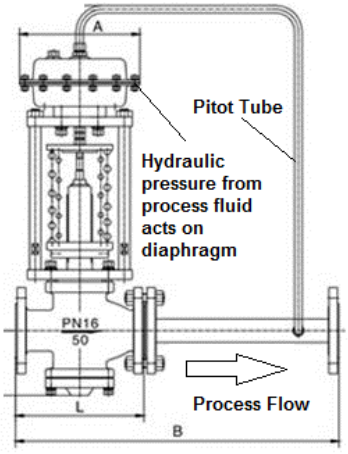

Figure 8 – (a) Schematic of a globe valve operation (left) and (b) the operation of a hydraulically operated pressure-regulating globe valve (right) (American Water Works Association., 2001) & (Enggcylcopedia., 2012).

2.2.2.2 Sleeve Valve (Fixed Cone Valves)

The design of sleeve valves render them particularly well-suited to high-pressure, high-volume, energy intensive applications. The valve operation is able to achieve massive energy dissipation and is vibration-free and resistant to cavitation (Ithuba Valves.). The valve consists of an external tubular sleeve which moves across the inner sleeve's discharge port, thereby altering the valve resistance to flow (Figure 9a). An alternate, more common design (Figure 9b) consists of an external sleeve which is made to move relative to the porous inner sleeve. This movement regulates the volumetric liquid flowrate through the valve, by varying the exposure of the inner sleeve to the incoming liquid, and thereby adjusting the resistance of the valve (American Water Works Association., 2001).

The inner sleeve has meticulously designed nozzles (ports), that may be tapered, that ultimately determine the incremental change of volumetric flow through the valve per incremental change in the valve position. This, together with the number of nozzles determines the valve characteristics, which is designed according to the pressure and flow conditions that the valve

is intended to regulate. Valve maintenance is prevented by design, as the nozzles balance flow and direct the liquid jets to collide, thereby protecting the valve inner surfaces and minimizing operational costs (Henry Pratt Company., 2008).

Sleeve valves are most commonly used at the outlets to dams, in water distribution networks and in turbine systems. They are generally installed to discharge to atmosphere, but are capable of discharging to a immersed outlet in order to prevent erosion of equipment due to jetting (Henry Pratt Company., 2008). The valve may be manufactured from cast iron, graphite, steel or stainless steel. In-line maintenance and replacement of valve seals can be easily undertaken with the use of upstream isolation valves (Ithuba Valves.).

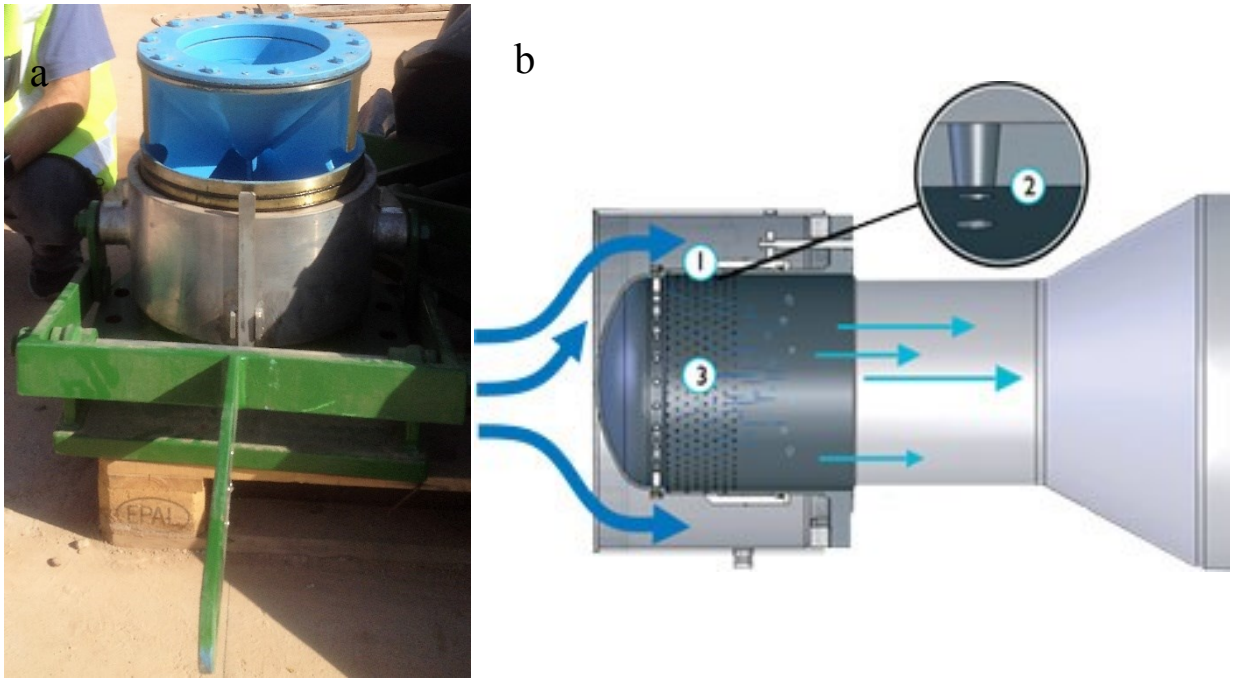

Figure 9 – (a) Sleeve valve at the Ashley Drive break pressure tank site - prior to installation - (left). (b) Cross section of a sleeve valve (alternative design) demonstrating its operation (right) (Bailey Valves., 2013).

2.2.2.3 Gate Valves

Gate valves, as included within the sleeve valve isolation chambers in the Western Aqueduct design, consist of a circular/rectangular gate that is lowered into the valve bore in order to control the rate of flow through the valve. Gate valves are advantageous when low frictional drops are preferred, and it renders gate valves ideal to on/off toggle applications and isolation responsibilities (Cameron., 2015). Gate valves cannot be used for flow control or regulation,

as their characteristics are unsuitable, and vibrational problems plague their stems. Gate valves have developed significantly over the past century to mitigate operational problems that plagued them. Gate valves must be frequently operated in order to prevent the build-up of dirt and grit within the machined grooves, and to keep the threads in the nuts and stem clear (Ratnayaka et al., 2009). The schematic of a gate valve is presented in Figure 10.

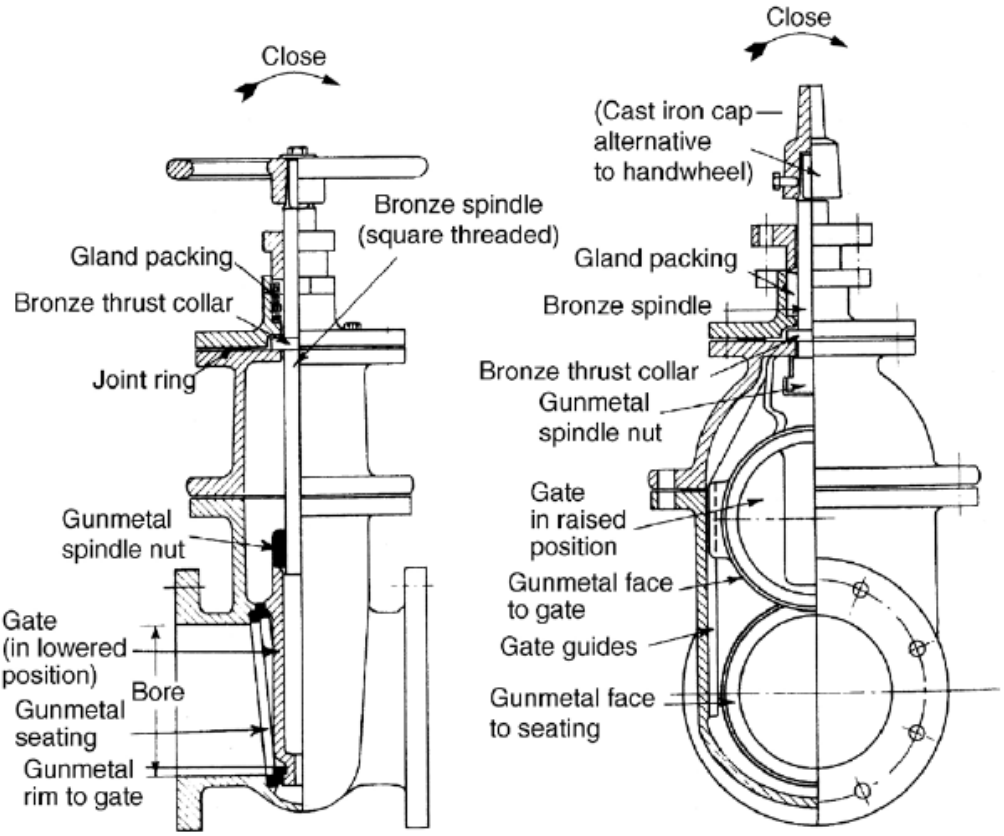

Figure 10 - Gate valve internals - DN300 bore (Ratnayaka et al., 2009).

2.2.2.4 Butterfly valves

Butterfly valves are relatively simple valves, both in terms of their minimalistic design, and construction. They are commonly used within water distribution systems, including the Western Aqueduct, as isolation valves. They consist of a centrally pivoted disc that is able to rotate against oncoming flow, thus enabling operation even in unbalanced pressures. Butterfly valves are ideally suited to isolation applications but find limited use within flow control and regulation due to potential damage to the seals. Butterfly valves can be fabricated to large diameters (>10 m), and have operated successfully under conditions of high oncoming velocity and upstream heads (Mays, 2000).

2.3 Structured Programming

Structured programming, also commonly termed *modular programming*, is a programming technique that is commonly used to construct mathematical models of water distribution systems. This programming formulation is a subsection of procedural programming that allows for the development of a faster, less complex and a more efficient program that is easier to understand and adapt. It strictly discourages the use of the "*goto*" statement and encourages the use of a top-down analysis format. The programme structure is mapped into a series of distinct operations/functions that contribute to the overall programme operation through function calls within the main script. This modular format allows for the re-use of the modular subroutines and a more discernible and memory efficient code (Rouse, 2014). Modules are themselves organized in a structured code, and are rigorously tested prior to integration within the main structure. Structured programs are easily graphically represented through the use of flow diagrams (California Polytechnic State University, 2008).

The use of loops ("for", "while" etc.), conditional statements and logic blocks are encouraged, resulting in greater productivity through the following (California Polytechnic State University, 2008):

1- Less time-intensive coding, debugging and testing
2- More reliability due to fewer logical and organizational errors
3- Easier maintenance and editing of the program for further use

Object oriented programming (OOP) is an advanced, altered form of structured programming that makes extensive use of self-contained, interacting sub-programs within the main program. It is characterized by classes that represent distinct functions of the overall program. Structured programming is better suited to small-medium sized programs, while OOP is only encouraged for mega-scale programming initiatives, due to the time-intensive nature of developing of function classes (Neely and Obbayi, 2010).

2.4 Modelling of Water Distribution Systems (WDS)

The use of computer aided modelling of water distribution systems in contemporary times, has found use primarily in the design of these systems, and is being used increasingly to assess the effects of the design on the water quality. Hydraulic models are also often used as an inexpensive alternative to the building and testing of a prototype prior to accepting a design. For these applications, numerical models are advantageous in terms of modern technology's

ability to rapidly generate results, the ease with which the model may be amended and adjusted, and the fact that the usage of the model poses no financial or physical risks that a physical prototype does (Mays, 2000).

With the progress of technology, the classical trial-and-error method has given way to more complex methods of design that exploit the ability of modern computers to process large amounts of information in short periods of time. Models find use in the testing, operation and optimization of water distribution networks, and aid in the strategic management, long-range planning and decision-making processes of these system (Brebbia and Kungolos, 2007). Water quality management and contaminant testing has also emerged as a major use of network modelling. Models can also be used for transient analyses or network troubleshooting and for the purposes of rehabilitation (Walski and Haestad Methods, 2003). Hydraulic models are highly beneficial for utility controllers, but require periodic updates in order to remain relevant to the ever-evolving conditions of distribution systems. The following are some of the more notable applications of computer aided modelling of WDS. (Mays, 2000):

- For network improvements and network expansions in the planning and design stages.
- Planning of forecasted maintenance operations that may remove system components from their functions e.g. valve or reservoir maintenance.
- In determining the optimum placement of specific components, either through manual iterative or optimisation strategies.
- To develop operator skills, formulate SOPs (standard operating procedures), to arrange pump schedules for energy optimisation and to analyse water quality.
- In the analysis of the system's adequacy in accommodating fire flows with regards to the available flow and pressure. Insurance companies generally make extensive use of these in order to assess the risk status of their clients.
- For reliability and vulnerability analyses, to test the exposure of the system to risk scenarios under extenuating circumstances that cannot always be reasonably considered in the purview of the designers during the design phases. Such circumstances include pathogenic/toxic contamination of the water, at source or within the network, power outages, burst-pipes, water shortages etc. Furthermore, network security has recently come under increasing scrutiny to ensure that failures (natural and deliberate attacks) are eliminated or in the very least anticipated and mitigated correctly. Numerous studies have focussed on the analyses of systems with cognisance on this aspect. (Albert et al.,

2000), for example, have reported that scale-free networks are robust in dealing with random variations, but are fragile under deliberate attack. This implies that under circumstances of natural or deliberate disasters, the system may experience cascading failures that propagate from the affected node through the system.

Perhaps the most important benefit of a model, lies in its assistance in forecasting of the results of predetermined actions and conditions that may be physically impossible to implement, thereby increasing the understanding of the system and its behaviour in response to possible changes in its operation. Other important advantages of numerically modelling within a computer program are (Mays, 2000):

- Having a structured format that allows for flexibility in terms of input parameters
- The model results can be displayed in an unambiguous manner through the use of colour-coded plots, tables, histograms etc.
- Spreadsheets can be used to store data in a neat manner.
- Model adaptations allow for other analyses to be carried out e.g. water quality analysis, pump schedule (energy efficiency) etc.

Model complexity is primarily based on the layout of the network, the level of detail required, the acceptable error that can be tolerated for the ultimate application of the model and the availability of required information. The trade-off between available information and technological sophistication vs modelling and execution time is thus a limiting factor in the plausible depth of the model (Trifunovic, 2006).

2.4.1.1 Types of Hydraulic Models

Hydraulic model simulations are of two types (American Water Works Association., 2005) and (Walski and Haestad Methods, 2003):

1. **Steady State Simulations** – These represent the system's equilibrium state at an instant of time, for the given inputs. These generally find use in design and sizing problems, and are typically run for 'worst-case' scenarios e.g. power outages, fire flow usage etc.
2. **Extended Period Simulations (EPS)** – involve the assessment of the system response over a longer period of time. It is commonly a string of steady state simulations that are evaluated for a given period of time at specified intervals. EPSs thus enable the study of the effects of the varying user demands and reservoir levels on the system, as well as a more realistic study of the system response to a change in input conditions, thus

providing valuable information that can be used in order to adjust parameters that define control systems. In order to formulate an EPS, the accumulation within each storage tank must be accounted for, by solving the differential equation that describes the state of the tank i.e.

$$\frac{dV_{res}}{dt} = Q_{in} - Q_{out} \qquad [2]$$

The most basic solution method, the explicit Euler Method, is a first order finite-difference method whose global error is proportional to the size of the forward step (Mays, 2000). The discretized form of Equation NNN, which results from the application of the Euler Method, is presented as

$$V_{res}(t+\Delta t) = V_{res}(t) + \Delta t(Q_{in}(t) - Q_{out}(\mathrm{t})) \qquad [3]$$

Mays (2000) suggests that the Euler method typically produces acceptable results, even with hour-long timesteps, provided rapid flow changes are not experienced. Mays (2000) also endorses EPS using this solution method as sufficiently accurate for practical usage for the aforementioned implementations.

In addition to these, the model can be classified according to the underlying mathematical formulae that are used to construct the numerical representation of the system. The following are the main types of mathematical models (Mays 2000)

1. Mass Balance Model: This simple model focusses on the conservation of mass in a system. For a single tank, the model would simplify to equating the difference of the flow into and out of the tank to the time rate of change of volume through the tank. Pressure requirements are neglected, and thus cannot be analysed through this model. The model uses a sweeping assumption that the liquid head will suffice, or adequate pumping facilities are available, as long as flows are within an acceptable range. Multidimensional mass balance models can also be executed by employing weighted equations for system parameters.

   These models are well-suited to applications that require large amounts of simulation results, or for major transmission pipelines only. The model's usefulness however, severely impacted for use in pumping-cost and pressure analyses.

2. Regression Models: This type of model allows for the accurate incorporation of the system's non-linear hydraulics by employing non-linear regression relations. The

regression can be executed by a regression scheme to a set of results from repeated simulations of a well-calibrated model under different loading and flow conditions, or from measurements of a physical system at several locations. The use of this class of models becomes limited in the event of system infrastructural changes, because of the highly-specific nature of the models. The outcome is that in this case, or in the case of system loads outside of the simulated range, highly erroneous results are produced. Errors may also be compounded by generating regression curves that are an inaccurate representation of the system.

3. Simplified Hydraulic Models: These models represent a transition from the simple regression models to a full-scale nonlinear network model. In this model, network hydraulic behaviour is typically represented by a network-wide model or by a system of linearized hydraulic equations. The model is generally skeletonized in scrupulous manner to drastically reduce the model complexity.
4. Complete Hydraulic Model (non-linear): These models allow for the hydraulic behaviour of a network to be calculated by rigorously solving the highly non-linear, coupled hydraulic equations that describe the system. This model is highly adaptive to infrastructure and demand allocation changes, and is able to model looped and branched configurations satisfactorily. These models require large amounts of data in order to compile, and are difficult to accurately calibrate. Furthermore, these models are time-consuming to build and are computationally resource-intensive to solve.

2.4.1.2 Model Implementation

Although many model implementation procedures have been formulated, the complete development of a hydraulic model can be grouped into three broad, interconnected categories, each of which has multiple phases;

- Model Development
- Model Calibration
- Simulation, Analysis and Optimization

2.4.1.3 Model development

Model development is initiated by the mandate to undertake the stated task. As such, the purpose of the model must be clearly specified in order to define the scope and boundaries of

the hydraulic model. This will allow for the prevention of unnecessary resource and time expenditure.

2.4.1.3.a Data Assimilation and Data Handling

The information necessary to compile the model can then be identified, and can be obtained from a variety of sources. System maps, contoured topographical maps and/or GIS/SCADA systems outputs can be used to collect information on the topography of the system, location of pertinent equipment, lengths of pipes and other background information. Sizes of equipment can generally be obtained from the designer in the form of technical drawings, or from asset management software. As-built drawings should be used in the case of any alterations made during the construction phase of the equipment. Physical inspections/measurements may be necessary if critical information cannot be obtained or estimated with reasonable accuracy (Walski and Haestad Methods, 2003). Data for consumer demands (diurnal patterns), growth factors and peak factors can be obtained from the billing division of the water authority. Other requisite information includes the initial conditions of all system components e.g. pumps, control valves, reservoirs etc. In addition, schedules for pump and valve controls, or the control settings that govern the operation of these elements should be obtained from the relevant personnel.

It remains important to evaluate and record the quality and applicability of the data to the system in order to identify any errors and to assist in future enhancements of the model. This also aids in the assessment of the level of confidence in the model, and its use in planning and troubleshooting, and determines the appropriate amount of resources to be expended in securing the information. Information should also be ranked according to the estimated impact on the model results, so that commensurate attention can be afforded to the verification of the accuracy of such critical information.

Water Demand Forecasting

The total water demand and its spatial distribution have a major impact on the system performance (Mays, 2000). Accurate forecasting of water demands is thus of critical importance in the evaluation of the hydraulic performance and reliability of the system. This information is also critical in the design of reservoir, pumping stations and distribution networks. Water usage profiles are typically presented as diurnal demand profiles (hydrographs) that indicate the rate of withdrawal from a reservoir over the period of one day

(Trifunovic, 2006). The information necessary to estimate system regional demands can be sourced from four possible data sources. These are (in order of decreasing accuracy); billing information from each meter, meter routes, dwellings classification and amounts and land-use classification (Mays, 2000). Although numerous intertwined factors affect the estimation of usage profiles of supply areas from dwellings and land-use classifications, the following factors are sufficient in in defining/developing accurate diurnal usage profiles (Trifunovic, 2006) and (Mays, 2000).

i. Area classification – The dominant classification of the supply region with regards to purpose of the water supplied. These classifications generally include urban (domestic), industrial, rural, tourism etc. The classification is often complicated by the lack of demarcation of areas, although a dominant pattern is typically apparent.

ii. User demographics - Similar areas may exhibit different usage patterns due to demographical differences that exist amongst consumers. Major demographical and similar influences include culture, education, technological incorporation and climate.

iii. Water value – Conditions of supply and cost impact on the water usage patterns. Expensive water, unreliable supply, inadequate supply and no access to municipal water all significantly affect usage profiles.

Furthermore, seasonal variations exist, which must be accounted for. In the vast majority of developing countries, including South Africa and neighbouring SADC countries, non-domestic (agricultural and industrial) use far surpasses domestic usage. Additionally, factors such as high leakage levels may influence the diurnal patterns. Apart from seasonal variations, usage profiles are also observed to vary between weekdays, weekends and public holidays (Trifunovic, 2006).

Stephenson (2012) undertook a study to develop diurnal demand curves for residential (high and low income – middle income was found to be almost identical to low income) and industrial areas in South Africa.

Skeletonization

It is often inconceivable to include every pipe of a physical water distribution system into the model. Furthermore, data handling for such an exhaustive model is a tedious task and model outputs are complex, since the complexity of the model and its outputs are proportional to the size of the modelled system. It thus becomes necessary to use sound engineering judgement in

order to only select pipelines that are critical to the network portion being modelled, without significantly impacting on the accuracy of the model (Trifunovic, 2006). This process, which is usually initiated by selecting a threshold pipeline diameter for the model, is termed *skeletonization* or *schematisation*. All pipe runs that exceed the threshold value, as well as critical pipelines that are judged to substantially affect the flow within the above-threshold pipes (e.g. large user connections, high velocity flows, parallel connections etc.) are then included into the model. For design purposes, models exceeding 1000 pipes are rarely relevant in its entirety. Similar deductions can be made for models that incorporate pipes of diameters below 100mm. In addition to the selection of pipes exceeding the threshold diameter, the following rules to the skeletonization process (Trifunovic, 2006):

- Proximate demand nodes can be lumped into a single demand.
- Branched pipes can be represented by their straight-run equivalents, and dead ends can be neglected.
- Equivalent diameters are used.
- All demands, even for excluded portions of the network, must be accounted for.
- The impact of all storage tanks, valves and pumps must be accounted for.
- The fundamental structure of the system should remain unaltered, and no major loops should be dismantled.

The major benefits of skeletonization include the lightening of the computational burden necessary to solve the model and attainment model simplicity. The result is a model that is easier to understand, debug, verify and calibrate. The two extreme levels of skeletonization modelling result in the transmission-mains model and the all-mains model. The former only includes main pipelines through the system, large users, pumps, reservoirs and storage tanks, and control valves. The latter aims to include practically all system connections barring those to individual users. Although many computer programs may be capable of executing all-mains models, the marginal increase in accuracy provided by it is seldom deemed beneficial when contrasted to a well-skeletonized system. The large demand for network information that is present in all-mains models usually calls for extrapolative action to satisfy, and could thus render the large model less accurate than a skeletonised representation of it. The skeletonization process is illustrated in Figure 11 (Trifunovic, 2006).

This information can then be used together with the relevant hydraulic equations and a software package to build the program into a working mathematical model that can correctly represent the mandated physical system. Pertinent hydraulic theory is presented in Section 2.4.2.

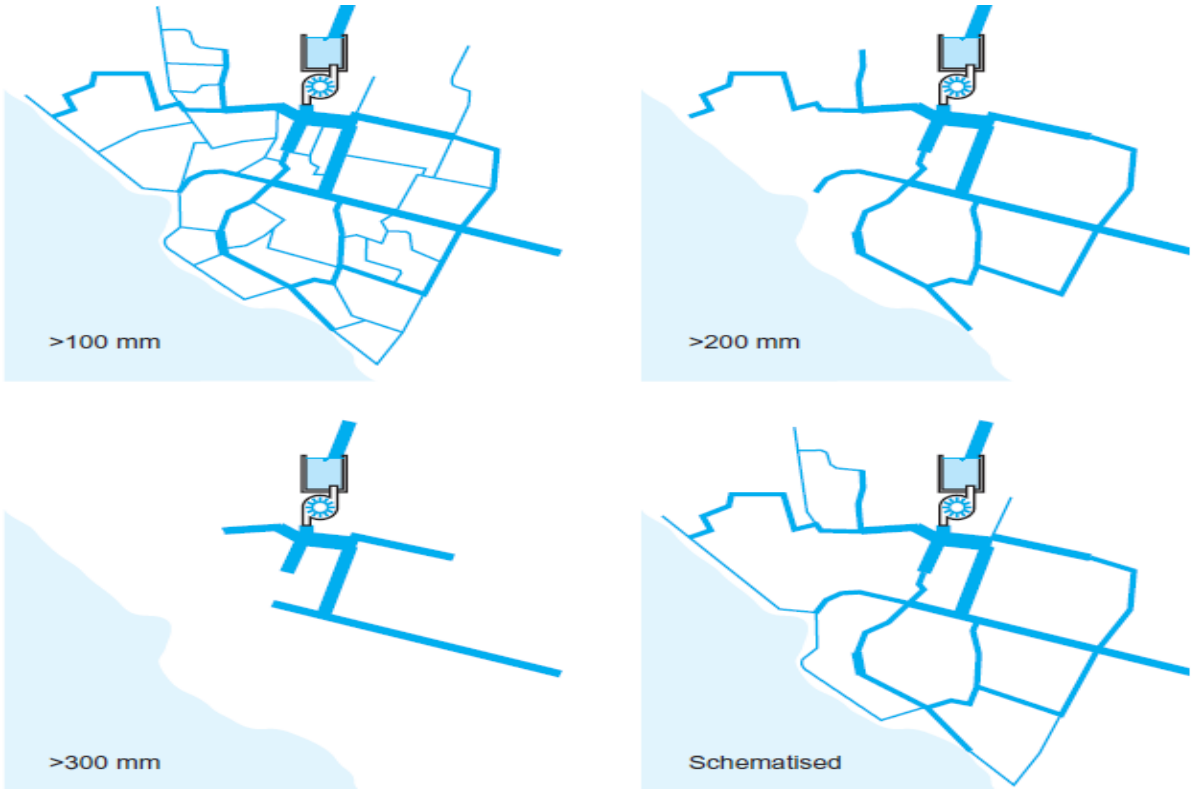

Figure 11 - Illustration of the skeletonization process for a hydraulic model of a system in Hodeidah. The graphics illustrate the skeletonization process outcomes for the removal of pipes below 100 mm, 200 mm, 300 mm in diameter, and the final representation (Trifunovic, 2006).

Software Selection

Numerous software packages exist for the purpose of hydraulic modelling and simulation. EPANET is one such widely-used software package that is capable of performing extended period simulations. It was first released in 1993 by the United States Environmental Protection Agency as a public domain software that can be freely distributed and copied. Its capabilities include the modelling of highly complex networks, tanks of any shape, control valves, and pipe fittings. It can also complete hydraulic calculations using numerous calculation methods; calculate energy expenditures and accommodate time-varying demand patters. EPANET also is able to track multiple variables, including; nodal pressures, level, flowrate, network-wide

chemical composition and water age. Energy optimization, fire flow evaluations and water age minimization are amongst the numerous uses of the program. EPANET can be interfaced in a variety of programming languages including C++, Pascal and Delphi (US Environmental Protection Agency., 2015). EPANET can be used in conjunction with MATLAB through the EPANET toolkit within the MATLAB package (EPANET .DE., 2011). WaterGEMS, HAMMER, KYPipe (Pipe2014) and Bentley AutoPIPE are other commercial software suites that have similar, and perhaps more advanced capabilities than EPANET (Cook, 2012).

Model calibration

The model must be calibrated in order to verify the accuracy of the predicted (theoretical) representation to the empirical results of the actual operation of the system. A calibrated model can provide invaluable inputs into the engineering and strategic decision making processes, and can safeguard from potentially disastrous errors that may arise from improper model results.

Model calibration involves the *tweaking* of model parameters (pipe roughness, usage profiles etc.) in order to ensure that results from the model, for a specified input, agree with those of the physical system under the same conditions, within an acceptable error range. This correspondence should be achieved in each of the following; reservoir levels, individual pipe flowrates and nodal pressures. The effect of scaling and tuberculation (a constant decrease in pipe diameter), can also be incorporated into the friction factor estimate through calibration. The field data collection is achieved through the extensive collation of field data preferably at the extremities of the system. Flow results are generally more sensitive to input adjustments, and should thus be preferentially reconciled (Mays, 2000). The calibration process may uncover errors or inaccuracies within the model, but may also indicate the neglect of system parameters, controls or constraints. System parameters, assumptions and extrapolations in the model, may need to be adjusted, although caution should be exercised, as measured data itself could be inaccurate and even wrong. Data adjustments should therefore be made only after careful analysis and only with sufficient justification. Repetition of this process may become necessary upon updating of the model or alterations to the physical system (American Water Works Association., 2005).

The degree of calibration is ultimately governed by the intended purpose of the model. The calibration process should thus aim to only reconcile the required results of the model to

measured data, in order to streamline the model development process (Walski and Haestad Methods, 2003).

Simulation, analysis and optimization phases

The Simulation, Analysis and Optimization phase is marked by the evaluation of the system's state either at an instant in time (steady state), or for a specified duration (EPS – typically 24 hours). The distribution system is generally tested at limiting scenarios in order to assess the performance of the system under stress. The results are then processed into tabular or graphic formats for further decision-making. A visual summary of the model development and implementation process is presented in Section 4. The results of the simulations have innumerable uses, some of which are listed below (The New Zealand Water & Wastes Association Wairos Actearoa., 2009) and (American Water Works Association., 2005):

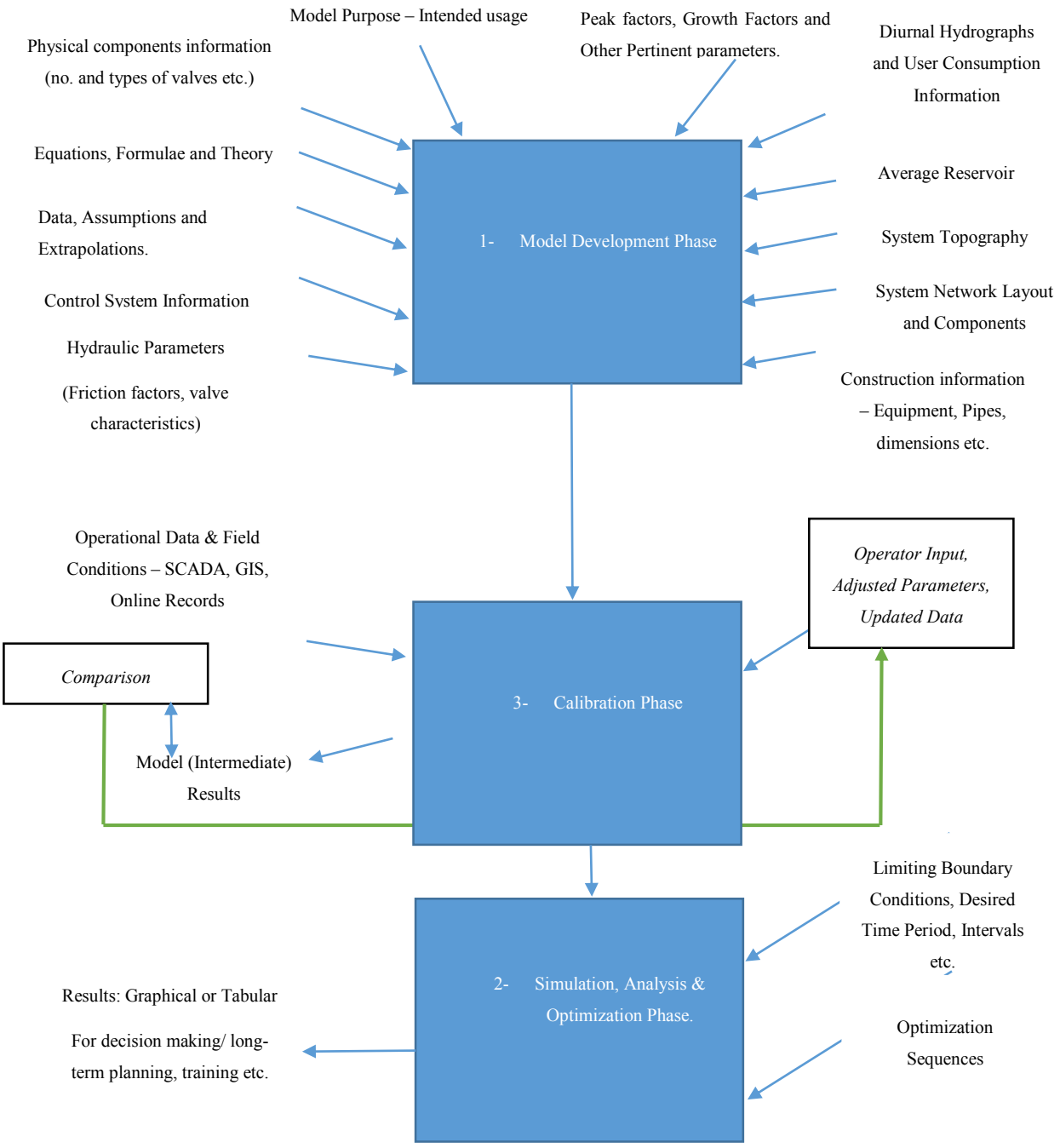

Figure 12 - Representation of the model development and implementation process.

2.4.2 System Hydraulic Representation

The hydraulic laws and equations that govern the flow of water form the basis of water distribution system design and operation. It is thus imperative that these very hydraulics be used to characterize the system model, so as to minimize the absolute error between the model and the physical system. Pressurized flow, which is governed by its own set of hydraulics, occurs in pipelines in which a pressure considerably higher than atmospheric pressure is maintained (Mays, 2000).

The system hydraulics govern two primary aspects of a systems characteristics; its hydraulic capacity – capability to convey design flows, and the manner in which the instituting of design flows and rectification of deviations are controlled. It should however be noted that the successful implementation of a pipeline system is contingent upon the collaboration of parties responsible for the hydraulic design, structural aspects, construction, mechanical and geotechnical surveyors. Additionally, social acceptance, environmental impact and legal aspects must be navigated in order to successfully implement a water distribution system design (Trifunovic, 2006).

Equation [4] is simply a restatement of the law of mass conservation, in volumetric terms. The application of this relation requires the definition of a 'control volume'- a fixed region that is within an area referred to as the 'control space'. The continuity equation simply expresses the relation between the accumulation of fluid in the control volume ($\frac{dV}{dt}$) to the volumetric flows into (Q_{in}) and out of (Q_{out}) it. For an incompressible fluid in an isothermal system, the continuity equation is expressed as (Mays, 2000):

$$\frac{dV}{dt} = Q_{in} - Q_{out} \qquad [4]$$

The concept of steady flow simply implies that there is no accumulation within the defined control volume (Equation [5]), and thus the rate of flow into the control volume is equal to that out of the system. This equation is analogous to Kirchoff's Law for electrical current, when a node has no capacity to accumulate fluid (zero volume - i.e. pipe junction) (Mays, 2000).

$$Q_{in} = Q_{out} \qquad [5]$$

Newton's second law (Equation [6]) allows for the calculation of the forces exerted on the system components ($\sum F_{ext}$) through the time rate of change of velocity ($\frac{dv}{dt}$) and the mass of the fluid (m). The principal forces that are exerted in a pressurized piping system are the fluid weight, friction and hydrostatic pressure (Mays, 2000).

$$\sum F_{ext} = m\frac{dv}{dt} = ma \qquad [6]$$

The flow of a fluid through a conduit causes the distribution of the total energy within the fluid, between the various forms of mechanical energy, to change. The Bernoulli equation (Equation [7]) accounts for the changes that occur during the movement of a fluid under pressure, to a different elevation at a varying velocity. The Bernoulli equation however neglects frictional energy dissipation, which is accompanied by an energy loss, usually through incremental temperature changes within the fluid. Bernoulli's equation is expressed as

$$\frac{p_1}{g\rho} + \frac{u_1^{\,2}}{2g} + z_1 = \frac{p_2}{g\rho} + \frac{u_2^{\,2}}{2g} + z_2 \qquad [7]$$

The first term ($\frac{p_1}{g\rho}$) is the pressure head that corresponds to the flow work, and is related to the pressures at the start (p_1) and end points (p_2) and the fluid density (ρ). The potential energy due to gravity (z) and the kinetic energy ($\frac{u_1^{\,2}}{2g}$) are also considered at the start and end points to complete the energy balance. Either side of the equality represents the total head at the specified point, while the sum of the potential energy and kinetic energy terms represent the piezometric head which forms the hydraulic grade line (HGL). The Bernoulli equation however, must be amended to include the head loss term (h_f) to account for frictional energy dissipation (Trifunovic, 2006).

$$\frac{p_1}{\gamma} + \frac{u_1^{\,2}}{2g} + z_1 = \frac{p_2}{\gamma} + \frac{u_2^{\,2}}{2g} + z_2 + h_f \qquad [8]$$

The head loss, in laminar flow ($Re < 2\,000$ for cylindrical piped flow), is postulated to be caused by events that are elucidated with the use of the boundary layer theory. This theory underscores the 'no-slip' condition, which states that when a fluid passes over a surface, the

fluid layer that is in direct contact with the surface attains the velocity of the surface. Successive layers (further from the surface) then assume a greater velocity in the direction of the bulk movement of the fluid. The impeding force (shear stress) on a fluid layer is due to the viscosity of the fluid that allows for the slower-moving neighbouring layer, that is closer to the surface, to decelerate the subsequent layer. The result is that for cylindrical piped flows, the greatest velocity is attained at the centreline, where the shear stress is zero. Velocity and shear stress gradients are thus observed in opposing directions within the pipeline. The head loss for turbulent flow however, cannot be elucidated using this theory, as turbulence causes unsystematic, irregular flow patterns that are not definable in simplistic terms. Turbulent flow (Re>4 000 for cylindrical piped flow) is characterized by the formation of eddy currents due to the fluid contact with the rough (conduit) surface (Trifunovic, 2006). The formation of eddy currents is commensurate with the bulk mean velocity of the fluid. The eddy currents promote a phenomenon termed 'turbulent mixing', where adjacent fluid pockets dissipate matter and energy to each other due to the eddy currents. The Reynolds number is the primary measure of the turbulence of the fluid, and is defined for cylindrical piped flow in terms of the pipe diameter (d), the fluid bulk velocity (u) and the fluid density and viscosity (μ) as Equation [9] (Mays, 2000).

$$\mathrm{Re} = \frac{du\rho}{\mu} \qquad [9]$$

The zone between laminar and turbulent flow is named transitional flow, wherein the effect of the Reynolds number on the head loss is restricted.

The majority of engineering applications usually operate within the turbulent flow regime despite the inability to categorically analyse the complex interactions and ostensibly unstructured flow patterns within the fluid. Empirical formulations are thus accepted as sufficiently accurate, in order to avoid resource-intensive solutions to a multiplicity of intertwined complex equations that result from detailed studies of the velocity variations within turbulent regimes.

There are two widely accepted relations that are able to relate the discharge rate (Q) to the head loss (h_f) that is encountered due to frictional forces along the pipe wall. Both equations are accommodated for within the EPANET software package ((US Environmental Protection Agency., 2015)).

The Darcy-Weisbach (1845) Equation (Mays, 2000): This empirical equation is useful in determining the frictional head loss that is associated with a specified flowrate in a pipe. It entails the use of a dimensional friction factor (λ) that accounts for the roughness of the pipe inner surface. The Darcy-Weisbach equation prescribes a relationship of direct proportionality of the frictional pressure drop (Δp) to the pipeline length (l) is described as

$$\Delta p = \frac{\lambda l}{d_h} \times \frac{\rho u^2}{2} \qquad [10]$$

The hydraulic diameter for a duct, which reduces to the actual diameter for a circular duct, is defined in terms of the cross-sectional area (A_x) and wetted perimeter of the conduit (p_{wetted}), as

$$d_h = \frac{4A_x}{p_{wetted}} \qquad [11]$$

The Darcy-Weisbach equation demonstrates that the pressure loss is directly proportional to the length of the conduit, friction factor, density and the square of the velocity, yet inversely proportional to the diameter of the conduit. An increase in length or roughness of the inner surface of the pipe ensures that the fluid experiences more surface friction, while for an increase in pipe diameter, the shear force from the walls is somewhat diminished. The equation also has a highly nonlinear relation with the discharge rate and conduit diameter, resulting in large head losses for exceedingly small pipes (Trifunovic, 2006).

The Colebrook-White (1937) equation (Equation [12]) can be used to determine the friction factor for flows within the turbulent regime, provided the roughness (ε) of the conduit inner surface is known. The relative roughness can be obtained from pipe manufacturers, who determine the parameter through rigorous experimentation. This equation is highly nonlinear and implicit, and is therefore useful for modelling and design purposes only when computational exertion is not a limiting factor. The Moody (1944) Diagram (Figure , Appendix A) is a graphical alternative to the Colebrook-White equation that allows for the friction factor to be determined by following the appropriate roughness curve to its intersection with the applicable Reynold's Number. Usage of the Moody diagram however becomes tedious when iterative calculations are conducted. Alternative, explicit methods

based upon the Colebrook-White equation, such as the equation presented by Swamee and Jain (1976), are thus used in the design and modelling of these systems in programmes such as EPANET (Trifunovic, 2006).

$$\frac{1}{\sqrt{f}} = -2\log\left(\frac{e/D}{3.7} + \frac{2.51}{\mathrm{Re}\sqrt{f}}\right) \qquad [12]$$

- The Hazen-Williams equation (Equation [13]) is an alternate equation that relinquishes the dependency of the head loss (Δp) on the friction factor and Reynold's Number. It utilizes the Hazen-Williams roughness coefficient (C) and takes the form of:

$$\Delta p = 10.654\left(\frac{Q}{C}\right)^{\frac{1}{0.54}} \frac{l}{d^{4.87}} \qquad [13]$$

The superiority of the Darcy-Weisbach equation over the Hazen-Williams equation has been repeatedly demonstrated, and lies in the fact that the former is theoretically based, while the latter is purely empirical (Trifunovic, 2006).

2.4.3 Fluid Transient Phenomena: Water Hammer

Water Hammer is a potentially dangerous transient flow phenomenon that involves the propagation of acoustic waves within pipelines. It is caused by rapid changes in the velocity of the fluid that flows through the pipeline, and is commonly accompanied by an unpleasant characteristic banging/hammering sound. These rapid changes may be a result of sudden, large valve movements, pump toggles or disturbances within the pipeline (obstructions, collapses, vibrations or deformation) (Mays, 2010). The most severe disturbance occurs in the event of power failures, where pumps are unable to maintain supply flows (Stephenson, 1972). The resultant acoustic waves constitute an additional pressure force, in addition to the mechanical forces due to loading, fluid pressure and other steady-state forces that must be withstood by the pipe material. In the case of a valve suddenly closing, a pressure wave is generated at the upstream side of the valve. The wave is then propagated upstream at a velocity close to speed of sound in the fluid medium (u_c). At the instant of the wave generation and subsequent propagation, the fluid between the wave front and the valve is stagnant, while the fluid upstream is at the original velocity (u). The pressure at the valve is that of the initial pressure (p_o) added to the overpressure generated by the rapid closing of the valve (p_{gen}). The propagated wave, upon reaching the upstream end of the pipe results in the reverse flow of the

fluid at the initial velocity (u). The wave is then propagated back to the valve. This back-and-forth wave motion subsequently continues, but is dampened by frictional forces in the pipeline (Mays, 2010). Water column separation, vapourization and cavitation may result due to pressure drops caused by the generated overpressures and that may be exacerbated by the topography of the pipeline (Stephenson, 1972).

The Joukowsky equation (Equation [14]) is used to obtain estimates of the waterhammer overpressures generated during transient flows. The derivation of the Joukowsky equation neglects the frictional effects and boundary effects at the pipe extremities (Mays, 2000).

$$p_{gen} = \rho_{fluid} \times u \times u_c \quad [14]$$

$$\Delta h_{wh} = \pm \frac{a}{g} \Delta u \quad [15]$$

The Joukowsky relation (Equation [15]), can be used to estimate the peak head change (Δh) for a given change in velocity of the fluid. a is the propagation velocity of the wave that is usually equivalent to the speed of sound in the fluid, and g is the gravitational acceleration. Typical values of $\frac{a}{g}$ tend to be larger than 100 s (Mays, 1999). The wave propagation velocity can be calculated through Equation [16], which utilizes the modulus of elasticity of the fluid (E_F), that of the pipe wall (E_R), the pipe wall thickness (s) and the Poisson Number (μ_p) (KSB Aktlengesellschaft., 2006):

$$a = \sqrt{\frac{1}{\frac{\rho}{E_F} + \frac{\rho \times d_i \times (1 - \mu_p{}^2)}{E_R \times s}}} \quad [16]$$

The Joukowsky relation accounts for the compressibility of the fluid and the elasticity of the pipe wall, but its application is severely limited due to its underlying assumption of an instant valve closure. Moreover, the equation fails to account for any column separation that may occur and cause additional overpressures. The relation cannot be applied to systems whose pressure could drop to below the fluid vapour pressure. The Joukowsky relation is applicable to systems that abide by following (Netrium., 2014a):

- An unbranched, linear system – branches allow for the reflection of pressure waves and thus for constructive interference to occur within the pipeline.

- The system frictional pressure dissipation patterns should resemble that of a water distribution system.
- The valve closure time should be less that the pressure wave communication time (Equation [17]). The communication time is the length of time that passes from the instant a wave is emitted, to the moment it reaches a source. Its importance within transient analysis is that any event whose duration is shorter than the communication time, is classified as instantaneous. The communication time can be calculated from the pipeline length (l) and the wave propagation velocity (a), through the use of the following equation (Netrium., 2014b):

$$\Delta t_{ct} = \frac{2l}{a} \qquad [17]$$

In light of the abovementioned limitations of the Joukowsky relation, another simple relation exists that aids in benchmarking the results of the Joukowsky relation. The 's*teel pipe analogy*', (Equation [18]) is a simple analogy that circumvents the use of complex partial differential equations in order to examine the system transients. The PDEs that describe fluid transients are derived through a combinatorial application of the wavespeed relation, Newton's Second Law and the conservation of mass and energy equations. The PDEs are highly complex and are thus solved in dedicated programs such as Pipenet, HAMMER, Hytran, Hypress, Impulse etc. (Ghidaoui et al., 2005).

The '*steel pipe analogy*' involves the visualisation of the fluid in the pipe through its inertial properties. This analogy ignores the finite compressibility of the water, the elasticity of the water and that of the conduit wall, and is therefore limited in its application. The '*steel pipe analogy*', whcih is derived from Newton's Second Law, thus predicts the overpressure through the rate of change of the velocity of the fluid ($\frac{\Delta u}{\Delta t}$). The '*steel pipe analogy*' can be stated as (KSB Aktlengesellschaft., 2006):

$$\Delta p_{wh} = \frac{l\rho}{\Delta t}\Delta u \qquad [18]$$

Protective measures against the effects of water hammer include (Stephenson, 1972):

- Regulated (slowed) control of control valves, and pumps.
- Installation of air vessels to mitigate pump failures by resuming the interrupted supply.

- Installation of a reflux non-return valve around the pump to limit the pressure difference between the pump discharge and suction.
- Using the pump inertia to prevent an interruption to the supply, thereby relieving the severity of water hammer overpressures.
- Installation of surge tanks (open-to-atmosphere) to reduce the effect of water surges by ‘absorbing’ sudden changes of fluid flow. Break pressure tanks often serve the purpose of alleviating the severity of this phenomenon.

3 THE WESTERN AQUEDUCT

The Western Aqueduct project forms part of a larger scheme to address the ever-increasing water demand that is in part due to a spate in urbanization within the region. The population growth rate in the eThekwini municipal jurisdiction is thus above the national average, while the municipal operational area has drastically increased within the last decade. The resulting overburden on the existing supply networks resulted in forecasts of impending water supply shortages (Anderson, 2013).

The aqueduct augmentation projects, which include both the Western and Northern Aqueducts, was thus conceived to bolster the supply capability of EWS and to circumvent service delivery issues. The two aqueducts, upon completion, will be intimately related, with the Western Aqueduct supplementing the Northern Aqueduct. The NA will transport water to the Northern extents of the eThekwini municipal area including Umhlanga, Waterloo and Phoenix.

The design and monitoring of the WA and its construction and subsequent commissioning was awarded to a joint venture between Knight Piesold, Naidu Consulting and Royal Haskoning DHV (Tancott, 2014). The joint venture is known as the Western Aqueduct Consultants' Joint Venture (WAC JV). Knight Piesold is the lead member of the joint venture, Royal Haskoning DHV is the lead design member, and Naidu Consulting is a participant consultant. The initial investigations and designs for the Western Aqueduct (Project No. 4 918) were launched in the year 2000. In 2006, the first preliminary design for the first phase of the WA was submitted by the Knight Piesold and Naidu Consulting to the EWS. The WAC JV was subsequently

appointed in 2008 to execute the detailed design and construction monitoring of Phase 2 of the WA. Phase 2 includes the BPTs and their associated equipment (Fischer, 2014).

3.1 Western Aqueduct Macroscopic Description

3.1.1 Route

The Western Aqueduct route, as shown in the plan view (Figure 13), falls within the jurisdictional areas of two, neighbouring municipalities. The project is thus divided between Umgeni Water and EWS. Phase 1 consists of the initial stretch of the pipeline, which links the Midmar Dam water works potable supply (Camperdown) to the Inchange Railway Station. This 17 km pipeline, which terminates at the eThekwini Metropolitan boundary known as "Point M", is called the "57 Pipeline and is managed by Umgeni Water. Phase 2 is composed of 56 km of pipeline that terminates in Inanda and Pinetown, and falls under the management of EWS (Anderson, 2013).

The WA route design prioritized the incorporation of the WA into the existing water pipeline infrastructure. This allows for maximum infrastructural overlap in order to drive down costs associated with incorporating the new system into the associated, existing infrastructure. The pipeline route design also included considerations to eliminate the need for any pump stations. This inherently decreases the chances of service failures due to power outages and pump faults or maintenance. Long-term operational costs are thus also decreased through the elimination of electricity dependence. The current potable water supply infrastructure, particularly in the higher-lying service areas, make extensive use of pumping stations (Anderson, 2013).

Additionally, in order to obtain permission for the construction to commence, the pipeline route had to satisfy the requirements of the KwaZulu-Natal Department of Agriculture and Environmental Affairs and the KwaZulu-Natal Heritage Act. This included the preservation of sites of heritage importance and environmentally sensitive areas. Cognisance was also given to the inconvenience to the general public during construction periods, which would require a working access strip of up to 30 m in width (Anderson, 2013).

The pipeline route, as presented in Figure 2, commences at Umlaas Road, after which it largely maintains adjacency to the N3 highway. The pipeline remains parallel to the N3 throughout its passage through Camperdown and Cato Ridge toward the Inchanga Railway Station. The route subsequently begins to diverge from the N3 as it traverses the Outer West supply area, moving

towards Drummond, Assegai, Waterkloof and Hillcrest. The main pipeline then restarts a new adjacency, to the M13 freeway, as it leads through Gillits, Everton and Kloof toward Wyebank Road. The pipeline then follows the M13 toward its termination at Ntuzuma near Inanda. Along this main route, there are two branches, which serve to supply water to strategic locations that lie away from the main route. The first branch extends from the main pipeline in Haygarth Road in Kloof, and cuts across the N3 toward Tshelmnyama near Pinetown. The second branch extends out of the pipeline that stretches toward Ntuzuma, to serve the other portion of the Inner West supply area through the Mount Moriah reservoir.

Figure 13 - Plan view of the WA route up to the AD BPT, showin/g the location of offtakes and reservoirs (Fischer and van Rooyen, 2013)

The WA route allows for the provision of potable water to eight critical supply reservoirs that will service areas within the Outer West and Inner West supply areas. A list of reservoirs that are directly connected to the Western Aqueduct mains, together with their estimated draws and their yearly growth rates is provided in Table 2 (Anderson, 2013). The augmentation feature of the WA to the NA is also a significant function, as new developments at the King Shaka International Airport, the Dube Trade Port and the Cornubia residential development are

forecasted to place additional strain onto the northern supply service infrastructure (Macleod, 2013).

3.1.2 Topography

The large descents in altitude along the path of the WA allow for the WA to be a gravity-fed system, thus eliminating the reliance of the system on booster/pumping stations. The large descents however necessitate the inclusions of BPTs within the system in order to reduce the maximum working pressures to manageable, reasonable pressures and to divide the system into separate pressure zones. The maximum working pressure is limited due to its influence on the diameters of pipes, the pipe materials, and the working life of the system components (including pipes, fittings, valves etc.). The BPTs are situated at Ashley Drive (Hillcrest) and at Wyebank Road (New Germany). The maximum static pressure (elevation difference) between the Umlaas Road reservoir and the Ashley Drive BPT is 194 m, while the elevation difference between the two BPTs is 183.5 m. This corresponds to the recommendations by Ratnayaka et al. (2009) to equalize the maximum static head on either side of the BPT. Additionally, it is advantageous in terms of economies of scale, as it allows for the pipe material on either side of the BPTs to be of similar grades. Furthermore, the maximum static head is kept to below 20 bar, as per the heuristic suggested by Stephenson (2012).

The longitudinal section diagram (Figure 14) shows the heights of the BPTs and reservoir offtakes along the pipeline route. The WA route can be seen to be extremely hilly, with the multiple localized peaks and troughs throughout the longitudinal section, presenting a jagged appearance. The entire route can be observed to lie below the hydraulic grade line of the system (see Section 2.4.2), and the fluid is thus adequately pressurized. In general, the reservoir offtakes are at successively lower levels, thus avoiding the use of pumps. The positioning of air valves, scour valves and isolating valves along the pipeline route are also shown in Figure 14.

3.1.3 Reservoirs

The WA conveys potable water to its service areas though multiple reservoirs, that are either connected directly to the trunk mains, or are connected through other reservoirs. A complete list of reservoirs connected directly to the trunk mains is provided in Table 2. The list is in sequential order of the connections along the pipeline route. The average estimated consumer demand on each reservoir, the forecasted year-on-year (y/y) growth rate and the peak-to-mean

factor for each reservoir is provided alongside the reservoir name. It can be seen that the Ntuzuma - NR5 (80.9 $M\ell/day$), Alverstone Nek (28.3 $M\ell/day$), Mount Moriah (27.7 $M\ell/day$) and Tshelmnyama (18.8 $M\ell/day$) reservoirs have the largest consumer demands. These demands are especially significant considering the sizes of the BPTs (20 $M\ell$ & 10 $M\ell$). The draw schedules of these reservoirs thus have a major effect on the operation of the BPTs.

Table 2 - List of reservoirs connected directly to the WA. The y/y growth factors, yearly demands and peak to mean factors are also listed for each.

Reservoir #	Reservoir	Growth Factor (y/y)	2006 Demand (Mℓ/day)	2015 Demand (Mℓ/day)	2036 Demand (Mℓ/day)	Peak/Mean Factor	Basis of demands
0	Georgedale	2,0%	7,3	8,7	13,2	1,2	UW sales meters
1	Cato Ridge	2,5%	5,0	6,2	10,5	1,2	UW sales meters
2	Sterkspruit Res	0,5%	0,0	2,1	2,3	1,2	Estimate
3	Hammarsdale HL Res	2,0%	7,7	9,2	13,9	1,2	Logging by EWS
4	Alverstone Nek Res	1,0%	21,0	23,0	28,3	1,2	Logging by EWS
5	Summerveld Elev Tank	1,0%	0,5	0,5	0,7	1,2	Logging by EWS
6	West Riding Res	2,0%	5,8	6,9	10,5	1,2	Logging by EWS
7	Knelsby Res	1,0%	2,0	2,2	2,7	1,2	Estimate
8	Emoyeni Res	1,0%	3,5	3,8	4,7	1,2	Logging by EWS
9	Emberton Res	1,0%	5,3	5,8	7,1	1,2	Logging by EWS
10	Haygarth Rd Res	1,5%	10,0	11,4	15,6	1,2	Umgeni Water report
11	Tshelimnyama M1B Res	1,5%	12,0	13,7	18,8	1,2	Umgeni Water report
12	Abelia Rd Res	1,0%	6,2	6,8	8,4	1,2	Logging by EWS
13	Jerome Drv Res	1,0%	6,0	6,6	8,1	1,2	Umgeni Water report
14	Wyebank Res	0,5%	3,8	4,0	4,5	1,2	Logging by EWS
15	Mount Moriah Res	0,5%	23,9	25,0	27,7	1,2	UW sales meter
16	KwaDabeka 1 Res	1,0%	11,0	12,1	14,9	1,2	UW sales meter
17	Ntuzuma 5 Res	1,0%	60,0	65,6	80,9	1,2	Restor Africa logging
18	Duffs Rd				100,0		
	Total demand		**191,0**	**213,6**	372,7		

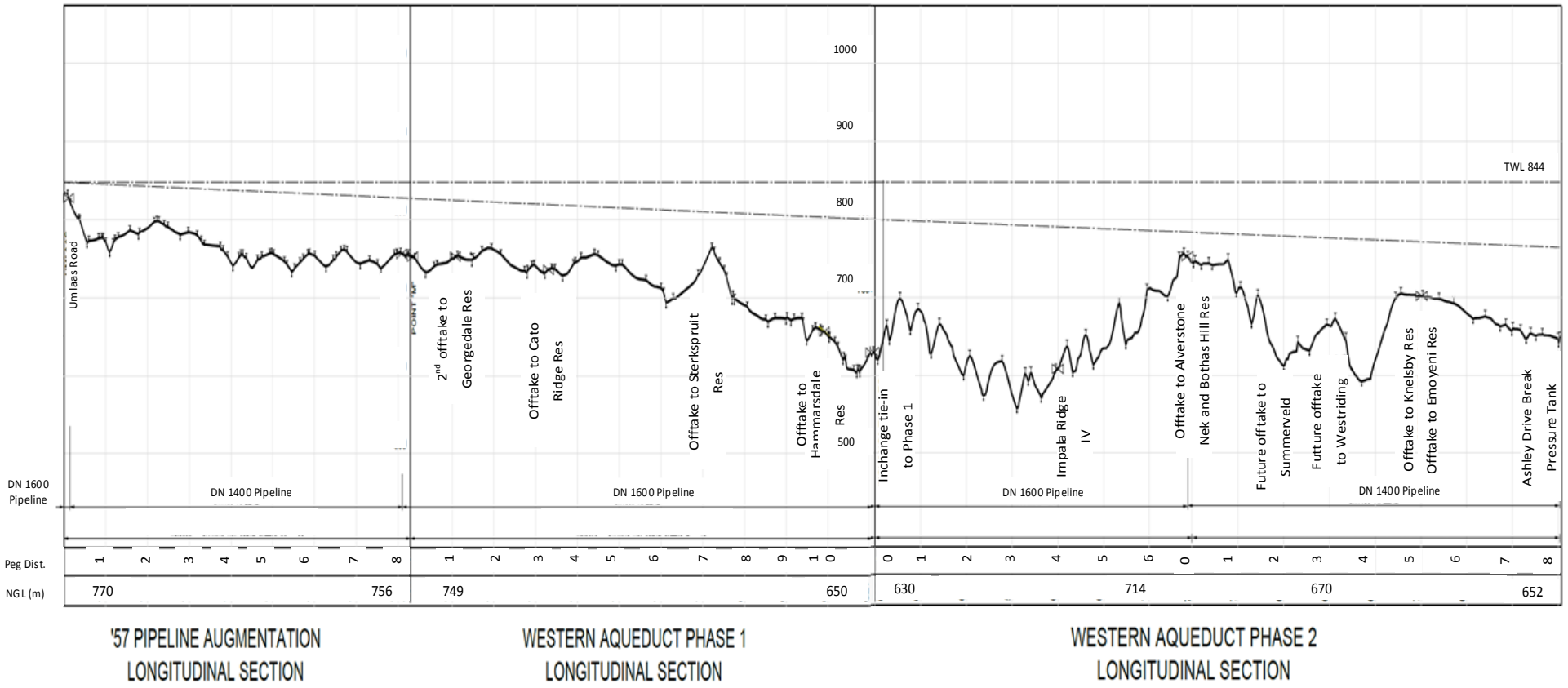

Figure 14 - Longitudinal Section of the WA route including the "57 pipeline up to the AD BPT (Fischer, 2014) .

3.1.4 Pipes

The WA trunk mains are constructed solely of pipes of nominal diameters of 1 400 mm or 1 600 mm. The section between the Umlaas Road reservoir and "point M" is constructed of 1 400 mm diameter pipe. The subsequent trunk mains, up to the Alverstone Nek reservoir offtake, are constructed of 1 600 mm diameter pipes whereafter all ensuing pipes on the trunk mains are 1 400 mm in diameter. The diameter of the pipes were selected in order to limit the fluid flow velocity to 3 m/s, at 400 $M\ell/day$ supply. Another concern was the required gently modulating velocity within the pipelines in order to avoid highly fluctuant draws from the Umgeni Water supply node (Fischer and van Rooyen, 2013).

Figure 15 - Photograph of a 1.4m, 400 $M\ell/day$ pipe at the AD BPT site.

The constructions of the WA pipelines were awarded as separate contracts through a highly publicised and somewhat disputed tender process. The first of the six contracts that comprise the WA, which includes the 7 km of pipeline leading to the Alverstone Nek offtake was awarded to Cycad Pipelines. The second contract, which involves the pipeline from the Alverstone Nek reservoir to the AD BPT was awarded to WK SA Construction. Esor Construction won the last contract, which involves the largest pipeline stretch, from the AD BPT to the Ntuzuma 5 (NR5) reservoir in Ntuzuma (Creamer Media., 2015). The other three contracts include one for each BPT, and one for the remaining pipeline branch that leads to Tshelmnyama which was also awarded to Esor Construction (Tancott, 2014). The statuses of the contracts are presented in Table 1.

The trunk main pipeline lengths and diameters are presented in Table 3. The grade of the materials of construction (mild steel) of these pipelines are shown in Table B1, Appendix B. All pipelines have been fortified with corrosion protection. The total pipeline length from the Umlaas Road reservoir to the NR5 reservoir is 60.08 km. Of this, the pipeline length from

Umlaas Road to the AD BPT is 40.01 km, while the pipeline length between the two BPTs is 9.34 km. The total average demand forecasts for each of these three subsections are; 86.8 $M\ell/day$, 58.0 $M\ell/day$ and 227.9 $M\ell/day$ respectively. It should be noted however, that the pipes are in series, and thus the conveyance within the first subsection is the sum total of all three demands (Fischer, 2014).

Table 3 - Trunk main pipeline information (length and diameters) for the WA (Doorgapershad 2015).

Trunk Main Pipeline Information		Length	Diameter
From:	**To:**	km	mm
Umlaas Rd	Point M	8,138	1400
Point M	Georgedale offake	1,194	1600
Georgedale offake	Cato Ridge offtake	2,225	1600
Cato Ridge offtake	Sterkspruit	7,639	1600
Sterkspruit	Hammarsdale HL	4,212	1600
Hammarsdale HL	1000 Hills/Bothas Hill	8,100	1600
1000 Hills/Bothas Hill	Alverstone Nek	0,030	1600
Alverstone Nek	Summerveld Elevation Tank	1,800	1400
Summerveld Elevation Tank	West Riding	1,400	1400
West Riding	Knelsby	1,050	1400
Knelsby	Emoyeni	0,500	1400
Emoyeni	Emberton	4,300	1400
Emberton	Haygarth/M1B	3,300	1400
Haygarth/M1B	Abelia Rd	1,063	1400
Abelia Rd	Jerome Drive	1,140	1400
Jerome Drive	Wyebank	3,500	1400
Wyebank	Mount Moriah offtake	0,429	1400
Mount Moriah offtake	KD1 offtake	2,062	1400
KD1 offtake	NR5	8,000	1400
Mount Moriah offtake	Mount Moriah Res	6,300	1000

3.2 Microscopic Description (BPTs)

3.2.1 BPT design requirements

The BPTs were designed to comply with the following basic requirements that were set by the EWS (Fischer, 2014):

1. The tanks should consist of two compartments in order to facilitate the maintenance, cleaning and scouring of the compartments individually.
2. It should be possible for the gravity feed to discharge into either or both compartments.
3. The inlet flow volumes to the BPT should correspond to the demands on the downstream supply units in order to retain the setpoint water level of the BPT to 50% of its maximum level.
4. A PLC (programmable logic controller) should be used to control the gravity feed into the BPT.

5. The BPT gravity outlet stream should not have a remote override. Manual intervention should thus be necessary for isolation purposes in case of burst pipes or maintenance downstream.

Apart from these conditions, the maximum working pressure, the maximum velocity and the mitigation of surge overpressures also were considered in the design of the BPTs.

* Cogeneration was not accommodated for, since progress was lacking. In order to operate the Western Aqueduct, the current design was thus necessary. The cogeneration at the BPTs is currently the subject of a feasibility study by EWS (Fischer, 2014).

3.2.2 Valves

3.2.2.1 Valve selection & design process

As per the project outcomes, in order to ensure that the design is completely interrogated by the simulation tests, it is important to fully understand the reasons and criteria that governed the valve selection and the structure of the inlet control mechanisms.

3.2.2.1.a Valve usage

The primary consideration for the selection of the valves was the BPT operation during electrical outages, and the possibility of overflows during such outages. As an alternative to control valves, the telemetric opening of downstream reservoirs in order to accept additional flows was considered. This was rejected on the basis of its lack of sustainability (Fischer, 2014).

3.2.2.1.b Valve type

Sleeve valves could not be independently used, as hydraulic actuators (control using pipeline pressure – for power failures) could not be procured as a proprietary design. It would thus be necessary to purpose-design the hydraulic actuators for the WA, which would result in exorbitant costs and lack of reliability testing that accompanies proprietary equipment from reputable suppliers. The use of a petrol or diesel generator could be argued for, as the sleeve valve actuators require a relatively small amount of electricity, and a small generator would thus suffice. This option however could not possibly be instituted due to maintenance and burglary complications. The use of an uninterrupted power supply system was also ruled out on this basis. The use of counterweights to automatically shut the (isolation) butterfly valves upstream of the sleeve valves upon loss of electrical power was rejected. This was due to the

added complications that could arise from the requirement of manual intervention in order to restore water supply

The final design thus advocated for the use of hydraulically-operated globe valves upstream to, and in series with, the sleeve valves. This design allows for the sleeve valves to assume the bulk of the flow regulation responsibilities during normal operation, and the globe valves to maintain service during electrical power outages. Added arguments in favour of the employment of globe valves included their verified reliability and their familiarity to EWS staff, particularly with regards to maintenance and operation.

In order to mitigate cavitation damage and to allow for a high flow rate range, a parallel arrangement of globe valves was deemed necessary. A total of three DN600 valves, in a parallel arrangement of three identical valves, was preferred at each BPT, as an impractically and uneconomically large number of valves would be required for any smaller sized valves. The sleeve valves were sized in order to provide an operational working range between 20% and 80% of their stroke, in order to minimise excessive noise and vibrations. It was decided that a parallel arrangement of three DN300 sleeve valves, downstream and in series with the parallel arrangement of globe valves, would thus be sufficient (Fischer, 2014).

Final-design valve purposes and operation

The sleeve valves were selected as the flow regulating mechanism of choice. This is due to the highly fluctuant upstream pressures and the high range of flows that are expected. In order to mitigate the loss of control that accompanies power outages, hydraulically operated globe valves were placed in series to the sleeve valves. The primary purpose of the globe valves is to shut off inlet flows at high BPT levels to avoid overflows. The issue of disturbed motion along the stroke of the globe valves, which could arise due to their infrequent use, was envisaged to be mitigated through the periodic movement of the globe valves by the central PLC, as the globe valve is not to be used to regulate flow (Fischer, 2014).

3.3 BPT Description

3.3.1.1 AD BPT location and topography

The AD BPT is located at the border of the Emberton Estate Development, at the junction of Ashley Drive and Old Main Road in Hillcrest. The BPT is situated adjacent to a golf course.

The elevation difference between the AD BPT site and the Umlaas Road reservoir supply node is 194 m. The top water level of the BPT is set to 655.2 msl, and the normal operating level (NOL) is 651.2 $m\ msl$ (50 % level of BPT) (Fischer and van Rooyen, 2013).

3.3.1.2 BPT internals

The AD and WR BPTs both consist of two compartments. The dimensions of the AD BPT are 64 m x42 m x8 m and those of the WR BPT are 26 m x52 m x8m. The AD BPT is designed to store 20 Ml of liquid, while the WR BPT is designed to store 10Ml (Van Rooyen, 2015). The internal components of both BPTs, as is described hereunder, are identical.

Simple description (Figure 16): Inlet flows to the BPT are through a 1 400 mm diameter pipe. Three parallel offtakes, each with a globe valve, connect to the inlet pipe on one end, and lead to another 1 400 mm diameter common manifold. Three parallel offtakes, each with a sleeve valve, are connected to the common manifold. These offtakes lead to a common inlet launder that allows flow into the two BPT chambers by overflow over a weir. Butterfly valves are placed around each valve to facilitate isolation, and gate valves allow for drainage of the sleeve valve chambers for maintenance purposes.

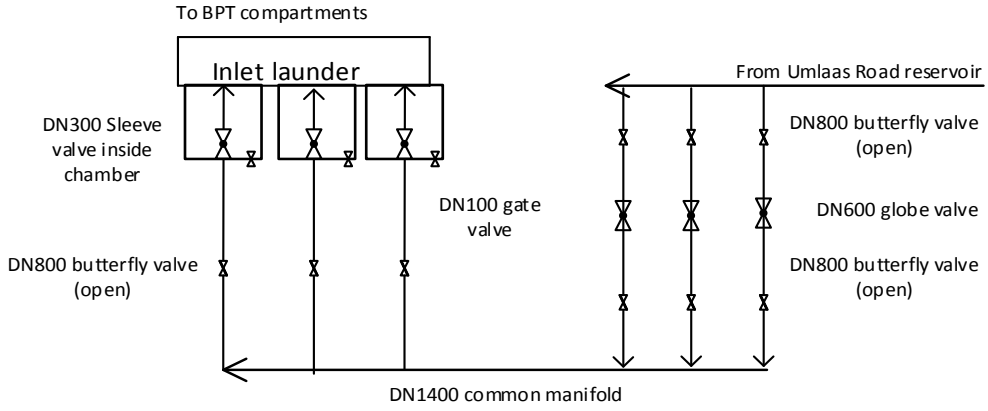

Figure 16 - Simplified schematic of the AD BPT inlet subsystem showing the valves and the major pipework.

Engineering description (Figure 17): The inlet pipe into the BPT is a DN1400 pipe, with a DN1400 bullnose end that is 3 300 mm in length. The pipe has three identical offtakes connected successively to it in a parallel arrangement. These offtakes lead to a common manifold through a single DN600 globe valve on each line. The offtakes that lead toward the globe valves are DN800 PE pipes with flanged ends. A DN800 butterfly valve is situated on

each line before the globe valves to facilitate the isolation of the valves for maintenance or emergency situations. The DN800 butterfly valve is bypassed with two DN100, 90° smooth radius bends that link to the supply and discharge of a DN100 butterfly valve. A 310 mm DN800xDN600 PE reducer is used to connect the DN600 globe valves to the DN800 line. The pipeline leading to the manifold consists of a reducer, butterfly valve and its bypass, in a reverse arrangement that is identical to that explained above. The common manifold is a DN1400 with DN1400 bullnose ends. Three identical DN800 offtakes, also in a parallel arrangement are connected to the manifold with DN1400 tees. Each identical offtake leads through a 7-segment, DN800, 90° duckfoot bend before leading to a DN800 butterfly valve. The butterfly valve is bypassed identically to the butterfly valves in the branched lines leading to the common manifold. A stainless steel DN800xDN300 reducer is used to connect each branch to the DN300 sleeve valve, each submerged within its own chamber, which also contains an anti-erosion plate. A DN100 wedge gate valve is situated on each sleeve valve chamber. The sleeve valve chambers lead to a common inlet launder that has an overflow weir that will allow the water to flow into the BPT compartments. The electric actuators for the sleeve valves are situated prior to the stainless steel reducers. The outlet pipe from the BPT will also be fitted with a DN200 air valve in order to limit damage to the pipeline should drainage be carried out with the outlet shut (Fischer and van Rooyen, 2013). Figure 16 is a simplified schematic of the BPT subsystem, and Figure 17 is a full technical drawing it.

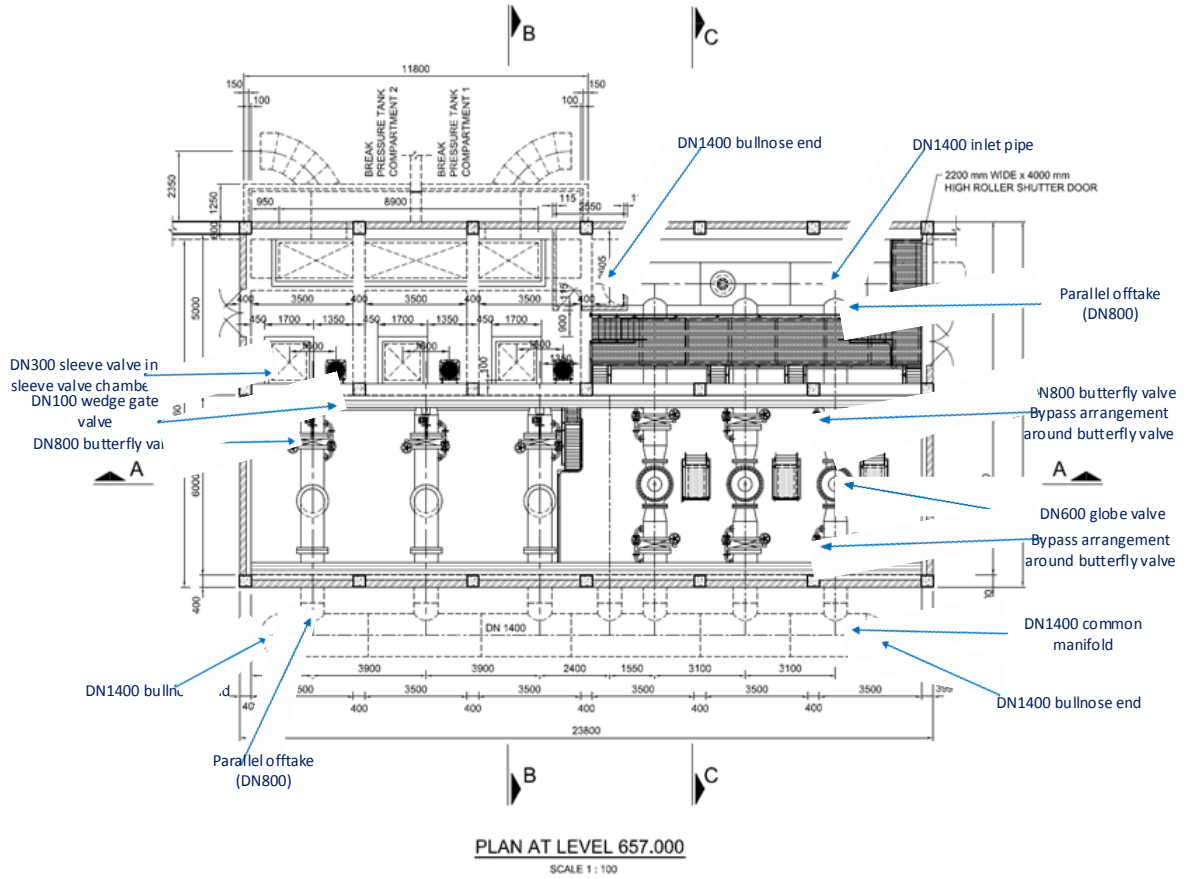

Figure 17 - Full technical drawing of the BPT inlet subsystem, including valves, pipework and dimensions (Fischer and van Rooyen, 2013).

The sleeve valves are placed into a submerged chamber in order to prevent erosion of the floors and walls by water jets. An anti-erosion plate is also provided for this reason. The wedge gate valves allow for the sleeve valve chambers to be drained to allow for maintenance. The sleeve valve chambers lead to a common inlet launder, through a penstock, which contains an overflow weir to pass the water to the BPT compartments. In order to prevent the backflow of water into the sleeve valve chambers, the chambers are configured with an open hole in the wall that can be closed by the installed penstock. This configuration allows for a low pressure loss, and negligible chlorine depletion, but could leak if the penstock is not tightly shut (Fischer, 2014).

The BPT outlet has an overflow chamber, toward which the BPT floor is made to slope, in order to facilitate easy cleaning/scouring. The roof is also sloped toward the overflow chamber in order to pass rainwater runoff to the chamber. The overflow weir from the BPT is designed

for 279 Mℓ/day, which is for 150% of the peak demand (186 Mℓ/day). The overflow weir drains from a hole in the BPT wall into the overflow chamber. In order to mitigate overflow situations, the overflow pipe is designed to convey up to 3 $\frac{k\ell}{s}$, corresponding to the flow through a single DN300 sleeve valve at 80% of its stroke open.

The BPT is designed with various manholes and access ways in order to enable easy cleaning, scouring and maintenance. These also serve to accommodate the fitment of a telemetry system after the construction. The BPT in its entirety, barring the inlet chamber, is situated underground. An underdrain is provided in order to identify leaks, and to account for the possibility of leakage through the BPT floor or floor joints.

The valves have manual overrides, in the form of handwheels, in order to allow operator intervention in emergency situations. Isolating butterfly valves are also provided in order to enable the isolation of the globe valves, sleeve valves or butterfly valves.

Each BPT compartment is equipped with an ultrasound level sensor that relays the liquid level within the compartment to the PLC. The PLC is the controller in the feedback loop, and serves to determine and set the valve positions based upon the level within the BPT compartment. The higher of the two levels is responded to (high select), in order to allow the disabling of a BPT compartment without altering the control system. Each globe valve is equipped with a float valve that will be mounted externally in order to maintain visibility from the control room. The float valves, which provide a contingency for control during power outages, are set to react at different levels in order to limit transient overpressures. The floats are placed within the inlet launder instead of a BPT compartment, so that cleaning/maintenance of the compartments does not affect the valve control. A full technical schematic of the BPT control system is presented in Figure 19.

3.3.2 Control System (Control 1.0)

The Western Aqueduct control philosophy, which is configured through the central PLC, comprises sub-regions that dictate a desired position of the valves. Upon the BPT level entering into the sub-region, the valves are prompted to begin moving toward the pre-configured desired position. The movement of the valves are regulated (slowed rate of movement) in order to mitigate transient overpressure generation. The sleeve valves are intended to traverse their entire workable range (0%-85%) in 5 minutes, and the globe valves (0%-100%) in 7 min and

49 sec. The target normal operating level (NOL) is 50% (Fischer, 2014). A summary of the control system is presented in Figure 18.

During the initial design phases, the peak flow (150 Mℓ/day) provision for the Duffs (Aloes) reservoir was not considered. As such, testing peak factors were reduced, and both sleeve and globe valve movements were slackened (to the aforementioned movement rates) in order to compensate for the inadequate pipe grades and thicknesses. In order to enact adjustments to the globe valve movement rate, orifice plates or needle valves may be used to slow the filling/emptying of liquid into the hydraulically-operated globe valve's bonnet (Fischer and van Rooyen, 2013).

Signal From:		Ultrasonic level / PLC			Float control				Alarms		
Levels	Water	Sleeve Valve No.			Control Valve No.				Description	Local	Remote
% depth	Depth (m)	1	2	3	1	2	3				
103.5%	**8.3**	**0.0**	**0.0**	**0.0**	**C**	**C**	**C**		Overflow	x	x
102.0%	8.2	0%	0%	0%	C	C	C		High-High Water Level	x	x
101.0%	8.1	0%	0%	0%	C	C	C				
100.0%	**8.0**	**0%**	**0%**	**0%**	**C**	**C**	**C**		Break Pressure Tank Full	x	x
99.0%	7.9	25%	0%	0%	C	C	CL		Control Valve 3 starts Closing	x	
94.0%	7.5	25%	0%	0%	C	CL	O		Control Valve 2 starts Closing	x	
87.5%	7.0	25%	0%	0%	CL	O	O		Control Valve 1 starts Closing	x	
81.3%	6.5	25%	25%	0%	O	O	O				
75.0%	6.0	25%	25%	25%	O	O	O				
68.8%	5.5	50%	25%	25%	O	O	O				
62.5%	5.0	50%	50%	25%	O	O	O				
50.0%	**4.0**	**50%**	**50%**	**50%**	**O**	**O**	**O**				
37.5%	3.0	85%	50%	50%	O	O	O				
31.3%	2.5	85%	85%	50%	O	O	O				
25.0%	2.0	85%	85%	85%	O	O	O				
18.8%	1.5	85%	85%	85%	O	O	O				
12.5%	1.0	85%	85%	85%	O	O	O				
6.0%	0.5	85%	85%	85%	O	O	O		Low Water Level	x	
0.0%	**0.0**	**85%**	**85%**	**85%**	**O**	**O**	**O**		Break Pressure Tank Empty	x	x

O - Open
C - Closed
CL - Closing

Figure 18 - BPT control system (Control 1.0) overview (Fischer, 2014).

Consider the scenario wherein the BPT level is relayed to be between 50% (4.0m) and 62.5% (5.0m), and all sleeve valves are at 50% and globe valves at 100% open. In this case, no valve movements will be initiated. When the BPT level exceeds 62.5% (5.0 m), sleeve valve three is prompted to move to 25%. The valve however, is governed to move at a rate of 17% of its stroke per minute. It will thus move successively toward 25%, provided the level does not breach the 62.5% (5.0 m) or 68.8% (5.5 m) barriers (current sub-region boundaries). The globe valves are programmed to move in much the same manner. If the valve positions are

inconsistent with the requirements of the PLC control algorithm, simultaneous valve movements will occur, still at the restricted movement rate, until the BPT levels and valve positions correspond to the control algorithm requirements. This could occur immediately after power is restored, if the BPT levels are within the upper 20% of the BPT.

3.3.3 Control 2.0

Control 2.0 is a revised control system for the WA that was finalized at the end of January 2016. This complete overhaul of the original control system had become necessary due to concerns that were supported with the preliminary results of this study. Table 4 presents the lookup-table that describes the PLC decision process for Control 2.0.

Table 4 - Decision lookup-table for Control 2.0 (Fischer and van Rooyen, 2015).

Valve Position	Water Level >4,5m	Water Level <3,5m
0%	Decrease position ↑	Increase position ↓
25%		
30%		
35%		
40%		
45%		
50%		
55%		
60%		
65%		
70%		
75%		
80%		
85%		

Control 2.0 operates using a *true deadband* philosophy, in combination with sequential, individual (sleeve) valve movements. The control system, as shown in Table 4, is devised around a central deadband between 3.5 m and 4.5 m, that corresponds to the design intent of maintaining the level setpoint at 50%. Every 30 seconds, any breach of the deadband boundaries triggers the movement of a single valve, which is selected in sequence by the PLC according to its current position. The valve movements are regulated to 5% per 30 second interval, although the movement between 0% and 25% (and its reverse) occurs in a single movement (30 seconds). The globe valves, which are regulated to move their entire workable

range (0%-100%) in 7 minutes 49 seconds, begin simultaneously closing upon the liquid level in the BPT exceeding the high-high BPT level (8.3 m). The aims of Control 2.0 are:

- To limit the maximum inlet flowrate through the sleeve valves to 373 $\frac{M\ell}{day}$
- Utilize the hydraulically actuated (globe) valves as a high-level backup during emergency outages
- Allow the sleeve valves to be manually adjusted through the use of handwheels

Consider the scenario in which the BPT level is to exceed 4.5 m. The control valve at the highest position will be prompted to close by 5%. If the valve is at 25%, it will move to the closed (0%) position. After 30 seconds, if the BPT level is still above 4.5 m, the next *most-open* sleeve valve (currently highest position) will be prompted to move towards its closed position, again at 5%. In this manner, a step-like configuration is formed, where valve movements are alternated between on-duty sleeve valves. The globe valves, as per the design intent, will only begin closing if the liquid level in the BPT exceeds 8.3 m. The globe valves will move simultaneously at their regulated movement rate, in order to supplement the flow control duty of the sleeve valves.

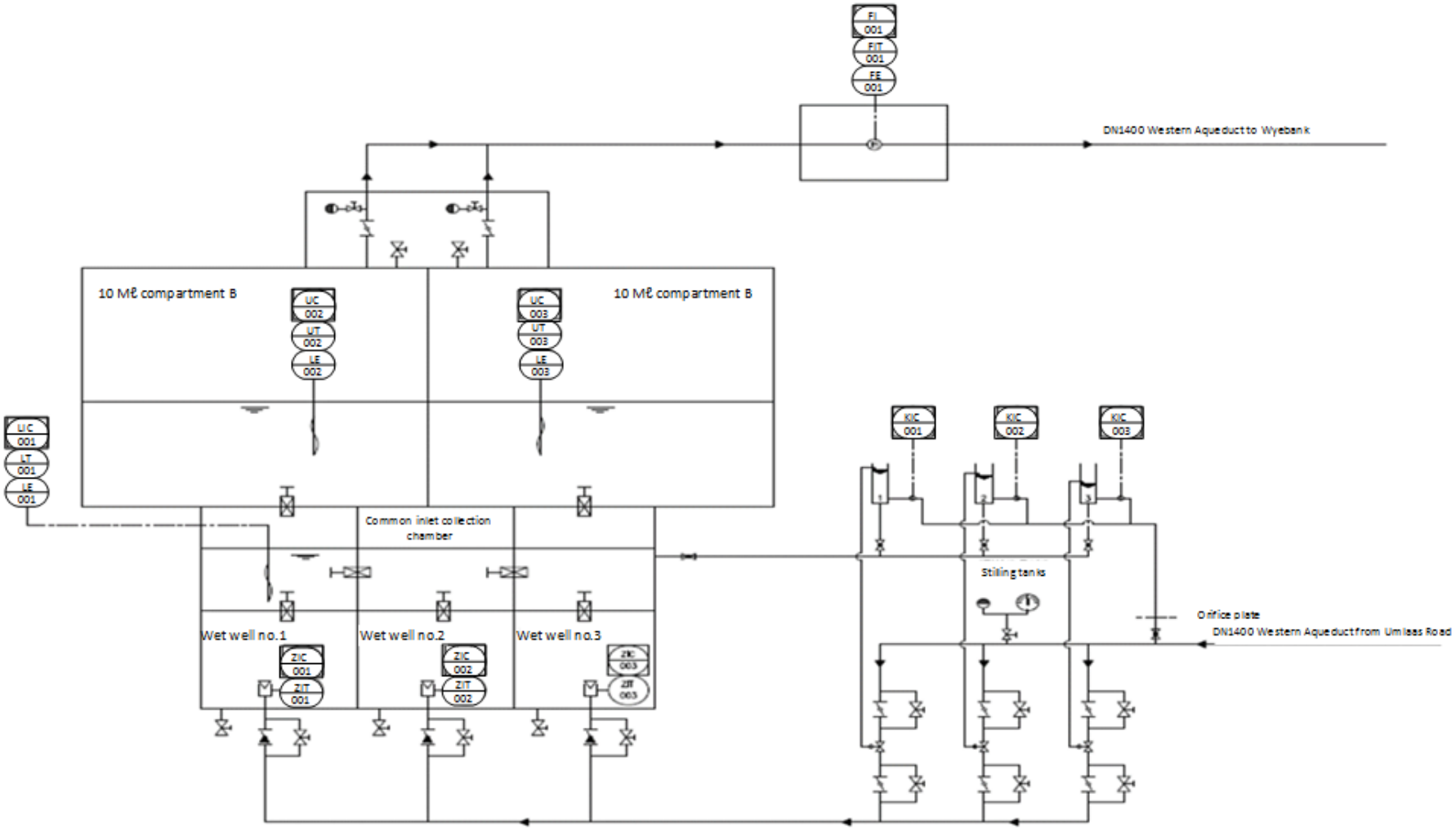

Figure 19 - Technical schematic layout of the Ashley Drive BPT and its inlet controls (Fischer, 2014).

4 MODELLING APPROACH

The model was selected based upon the initial directive issued by the eThekwini Municipality's Water and Sanitation unit (EWS), which formed the basis of the project. The project outcomes were thus defined through this explicit request, and the inference of any other results that would be of benefit to the strategic interests of EWS.

The study outcomes were determined to be a combination of reliability tests, system behaviour analyses and vulnerability assessments. Although the analysis of the system's ability to withstand failure scenarios was deemed to be of primary importance, surface-concepts from all the above were utilised within the processes followed within this study. The modelling method presented by Clark et al. (1988) was loosely followed in the delineation of the project and construction of the model. The adapted method is shown in Figure 20.

4.1 Model Selection

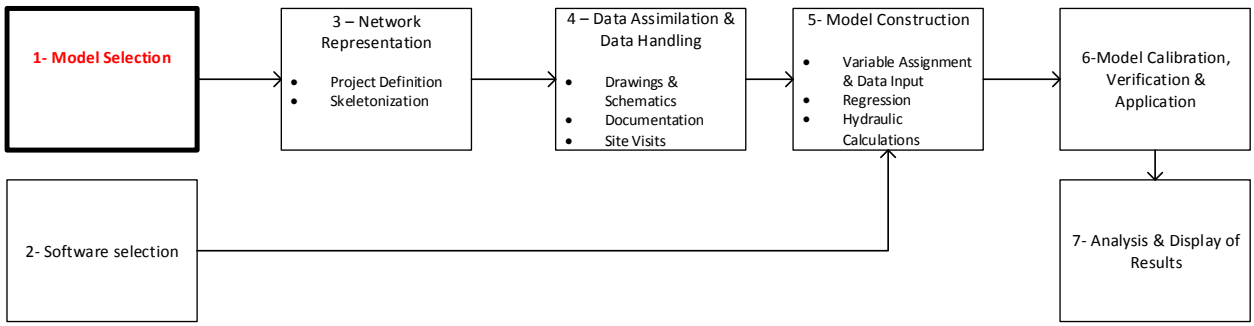

Figure 20 - The modelling process followed. Adapted from Clark et al. (1988).

It was decided that in order to adequately assess the performance of the system and to facilitate master planning and operator training, an extended period simulation (EPS) would be necessary. A simple mass balance evaluative model, however was ruled out due to its drawback of not sufficing for any level of pressure analysis. A cross-mixture of the simplified hydraulic model in conjunction with the regression model (Section 2.4.1.1) was thus selected in order to best suit the intended application and required outcomes. This model was envisaged to be robust enough to accommodate any construction-phase changes, and would be simple to calibrate. This model was preferred over the complete hydraulic model due to time limitations and the increased versatility offered by the former, in terms of the ability to quickly solve the model on possibly-dated computers.

4.2 Software Selection

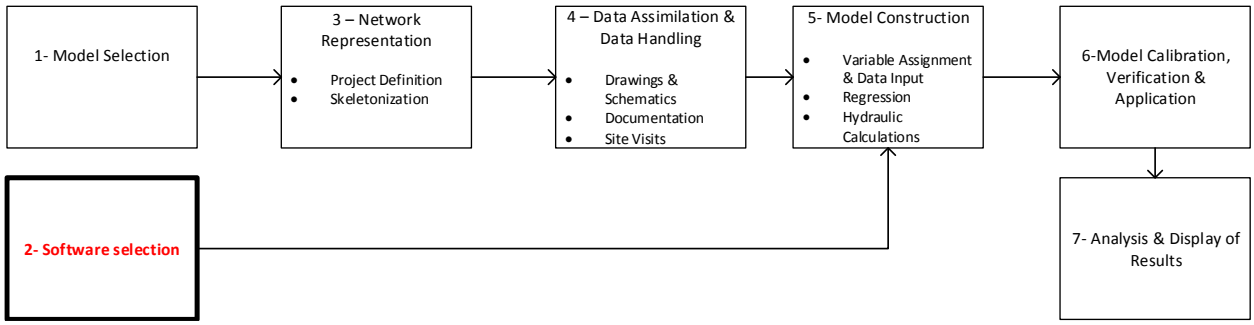

MATLAB was selected as the programming package due to its widespread availability in South Africa, its flexibility and popularity amongst members of the applied mathematics, engineering and allied fields. MATLAB also features a plethora of inbuilt commands, features and toolboxes and is able to represent results in a neat, discernible graphical manner. The intuitive language, extensive help resources, online support forums and the researcher's experience with the program also contributed to its selection over EPANET and GAMS.

Structured programming was used in order to maintain a desirable level of simplicity within the interconnected program code. Furthermore, basic coding language was used, and explanations were included in the form of comments, in order to improve the readability of the code. For the same reasons, an input data panel is included at the top of the code, with the required measurement units included as comments. All required input data can thus be easily entered into the data panel, eliminating the need to sift through the code to locate the necessary inputs. Every effort was made to ensure that the program could emulate possible real-world application conditions e.g. the inclusion of a (past) layered stack for the control valve

movements. Furthermore, function calls were programmed in a generic manner, thus allowing them to be reused multiple times, and avoiding the need to edit the function for a change in the form of inputs (e.g. number of co-ordinate pairs for regression, number. of reservoir volumes to integrate etc.).

The MATLAB program includes the programming for the generation of pertinent graphs in order to display results and relationships in an easy-to-analyse manner. The data storage need was addressed through the use of the "xlswrite" function that allows MATLAB to print specified results into an Excel spreadsheet. The supplied spreadsheet is equipped with headers and labels as well as graphs for the input data. The advantage of the spreadsheet storage system is the increased readability of the results and the malleability of the graphing software through Excels graphical user interface. The presentation graphic in the Excel spreadsheet is shown in Figure C1, Appendix C.

4.3 Network Representation

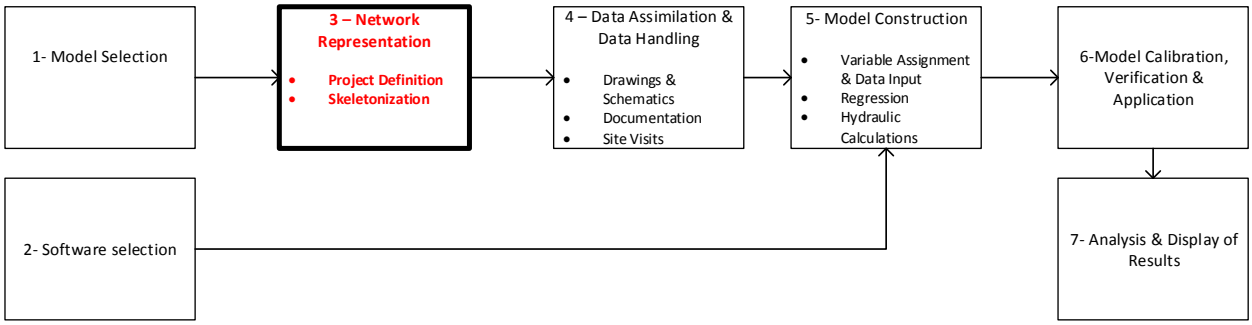

4.3.1 Project Definition

The project definition process was initiated by a data surveying phase. Data surveying was conducted in order to define the boundaries of the scope of the project. During this phase, the necessary and available data, for use within the model, was identified and compared. Data acquisition was subsequently initiated using a top-down approach, thereby decomposing the entire system into more specific subsystems. The macroscopic data, which includes the Western Aqueduct (WA) layout and topography were initially collected in order to completely understand the extents of the WA system, and its effect on the projected trajectory of the study. The acquisition of the microscopic data involved meetings with the EWS consultants that were tasked with the design, implementation and construction of the system, in which the system together with other related background material were discussed. This was seen as necessary in

order to ensure that no misunderstandings would undermine the quality of the study, thus avoiding time-consuming errors. These meetings were also essential to ensure that the expectations of EWS was aligned to the projected outcomes of the study.

4.3.2 -Skeletonization

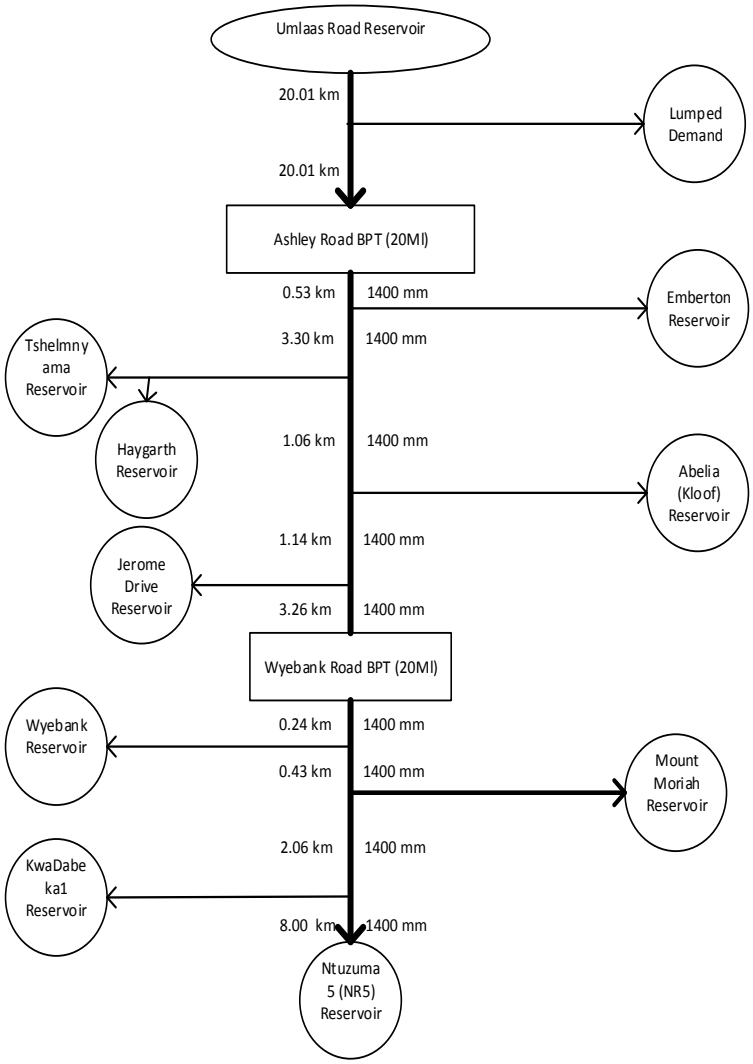

Figure 21 - Skeletonized representation of the WA.

The skeletonization was carried out according to the procedure outlined in Section 2.4.1.3.a. The aim of the skeletonization procedure was to simplify the modelling and calculation procedure without significantly affecting the accuracy of the model results.

With a complete understanding of the requisite outcomes of the project, it was decided that the pressure profile of the trunk main 'central spine' (Figure 21) would be necessary, yet in order to ensure that the accuracy of the pressure profile, the mass balance of the system would have

to be conserved. This was achieved by ‘fixing’ the value and location of offtake draws, allowing for the dynamic losses within the trunk mains to be accurately calculated while accounting for the change in flowrate due to each offtake draw.

The ‘fixing’ of offtake flows was achieved through the assumption that the offtake flows (to reservoirs) can be accurately represented by the ‘characteristic flow’ – the flow that occurs in a reservoir intake line when its valve or pump is activated. The characteristic flow was calculated by the procedure outlined in Section 4.4.3, by examining level-time graphs for each reservoir, allowing for simultaneous outflow to consumers. The reservoir offtakes after the Ashley Road BPT were considered individually, as the impact of their drawing schedules, which is determined by their inlets switching at upper and lower levels, in response to varying consumer demands, were projected to have an appreciable impact on the operation of the BPTs.

In the case of reservoirs supplied from the aqueduct between Umlaas Road and the Ashley Drive BPT, these were lumped into a single, static demand draw at the midpoint (see Figure 21). The value of the static (constant) demand draw was calculated as the sum total of the average consumer draws on each of the included reservoirs, for the specified year. This was deemed as pragmatic, as these early draws are relatively small and the focus of the study leans more heavily towards the performance of the BPTs.

By eliminating the consideration of pressure profiles within the offtake branches and fixing the value of offtake flows as each reservoir draws, the trunk main’s pressure profile is thus decoupled, allowing for its determination directly through the hydraulic calculations and a trunk mains and offtake mass balance, rather than through the solution of a highly-coupled, network-wide pressure balance that is expected to only marginally improve calculation accuracy for the desired pressures.

The system was then inspected to confirm that the fundamental structure of the system remained unaltered, and that no significant portions of the distribution system were unaccounted for. This was followed by the construction of a flowchart of the skeletonized system, in order to understand the outstanding data requirements, and formulate a basic mathematical strategy to represent the system. The skeleton flowchart also served the purpose of providing the foundation to begin the evaluation of solution strategies and the assessment of the impact of the accuracy of information and approximations on the results of the model. The outstanding data requirements were then requested from the relevant parties (data types and sources are presented in Table 6).

Table 5 - Data sources, their estimated impact on the model, their estimated accuracy, and recommendations on their usage.

Data	Source	Impact on model	Estimated accuracy	Recommendation(s)
System (macroscopic) Layout	EWS/Consultants	High	+++++	Adjustment only necessary if changes to infrastructure are planned.
System Topology	EPANET Model Results	High	+++++	-
System (microscopic) Layout	EWS/Consultants & Construction Supervisor (Site Inspection)	High	+++++	Adjustment only necessary in case of maintenance or changes to infrastructure are planned.
BPT Dimensions and Construction Plans	Construction Supervisor (Site Inspection)	High	+++++	Adjustment only necessary in case of maintenance or changes to infrastructure are planned.
Pipe Lengths	EWS/Consultants	High	+++++	-
Pipe Diameters	EWS/Consultants	High	+++++	-
Pipe Materials	EWS/Consultants	Medium	+++++	Factors based on this can be adjusted during model calibration or to accommodate for scaling/corrosion.
Equipment (Valve No., Types etc.)	Construction Supervisor (Site Inspection)	High	+++++	Changes may be necessary if valve types differ from initial plans.
Valve Characteristics (Sleeve)	Manufacturer	High	+++++	-
Valve Characteristics (Globe)	Competitor Manufacturer	Medium	+++	It would be prudent to update this if the information becomes available.
BPT Control System	EWS/Consultants	High	+++++	Can be adjusted for optimization/planning purposes.
Reservoir Control Scheme	Inferences Based on Visit to EWS Pinetown Control Centre	High	++	Must be adjusted according to planned control scheme. Recommend increasing monitoring, automation and telemetry.
Reservoir Characteristic Draws	Calculations Based on Data Accumulated from Visit to EWS Pinetown Control Centre	High	++	Must be accurately measured and updated. The system is not operational and accuracy may thus be compromised.
Reservoir Mean Demands and Peak Factors	EWS/Consultants	High	+++++	Only amend if more accurate information is attained.
Area Classifications for hydrograph development	Based on observed patterns vs those from Stephenson (2012)	Medium	+++	Change if more accurate information is attained.
Reservoir Diurnal Consumption patterns	Calculated based on mean demands and peak factors, together with hydrographs from Stephenson (2012) and area classifications	Medium	+++	Only amend if necessary.

4.4 Data Assimilation & Data Handling

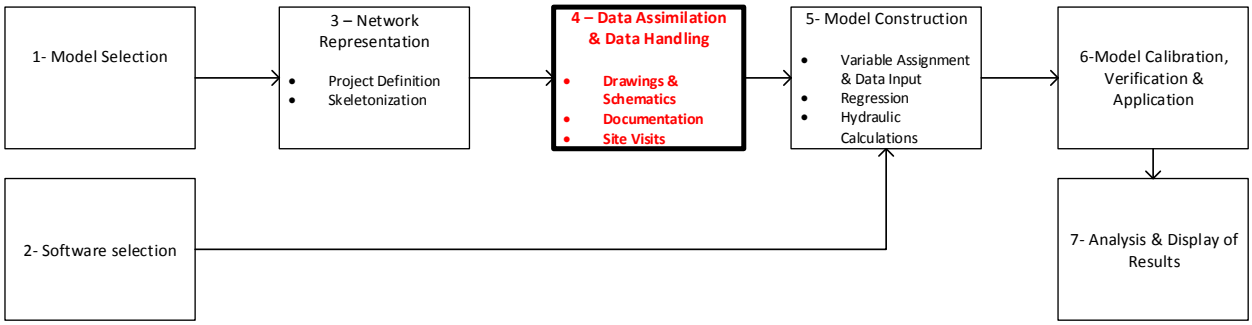

The collected data was then assimilated into individual formats that are easy to understand and interpret. This was done in order to simplify the construction of the model and to maintain a uniform level of simplicity with the model and associated information. It also aids in the verification of the interpretation of given information through cross-checking of the reformatted data with the original source, or with the author of the data. This prudent measure in turn provides for an invaluable level of certainty throughout the model construction and allows for the avoidance of time-consuming errors. Another appealing advantage of this method is that it provides a basis for clear, uncluttered, graphics-based reporting. An example of the benefits of this step is the 'flattening' and linearization of the Western Aqueduct route (Figure 21) and supply points into the simple schematic that is used in the reporting of results (Figure 21).

The data handling phase involved the extraction of relevant data, re-working of data into a meaningful form, extrapolating of data in order to meet requirements and the formation of reasonable assumptions. It is necessary to elucidate this aspect in order to ensure a proper understanding of the model operation through the understanding of its formative foundations.

All physical data was collected from reputable handbooks and databases under the assumption of the prevailing atmospheric temperature of 25°C and a pressure of 1 atm. Water was also assumed to be incompressible. Table 6 presents a summary of the input data necessary to execute the model simulations.

Table 6 - Summary of the requisite input data for the model.

Variable	Description	Input Units	Designation
Break Pressure Tanks			
Total Capacity (fixed volume)	AD and WR BPTs	m^3	V_{AD}, V_{WR}
Surface Area		m^2	A_{AD}, A_{WR}
Control Philosophy	In the form of a lookup table in (valve) positioner functions	-	-
Reservoirs			
Total Capacity (fixed volume)	For all reservoirs considered individually (all between AD and including NR5)	m^3	V_i (i=res #)
Surface Area		m^2	A_i (i=res #)
Control Philosophy	In the form upper and lower deadband limits	-	-
Characteristic draws	For all reservoirs considered individually (all between AD and including NR5)	$\frac{m^3}{s}$	Q_{resi} (i=res #)
Pipes			
Length	For all pipe segments, on the trunk main, from the Umlaas Road reservoir to the WR BPT.	m	l_i (i=pipe segment #)
Diameter	For all pipe segments, on the trunk main, from the Umlaas Road reservoir to the WR BPT.	m	d_i (i=pipe segment #)
Thickness	For all pipe segments, on the trunk main, from the Umlaas Road reservoir to the WR BPT.	m	S_i (i=pipe segment #)
Physical Parameters			
Density of Water		$\frac{kg}{m^3}$	ρ_w
Viscosity of Water		Pa.s	μ_w
Bulk Modulus of Water		Pa	E_w
Bulk Modulus of Pipe Materials		Pa	E_s
Poisson's Ratio of Pipe Materials		dimensionless	μ_s
Globe valve characteristic curve coordinates		coordinates	x_i, y_i
Sleeve valve characteristic curve coordinates		coordinates	x_i, y_i

4.4.1 Drawings and Schematics

As per the skeletonization, the WA macroscopic route was mapped into a simple, flattened schematic, to which the pipe lengths and diameters were added (Figure 21). The pipe diameters were obtained from the Western Aqueduct layout drawing (Figure B1, Appendix B), while the list of pipe lengths were supplied separately (Table 3).

The microscopic system, relating to the internal BPT structure, was also requested in the form of a technical drawing (Figure 17). This form of data presentation is desired as the level of

certainty in the obtained data is increased. The technical drawing was thus simplified into a simple schematic of the pipe and valves arrangements (Figure 16). The internal structure of the BPTs is discussed in Section 3.3.1.2. The BPT volumes and heights, and the volumes and heights of the individual tank sections within the BPT were also computed and noted from these diagrams.

The system topography was presented in the form of a longitudinal section diagram (elevation vs. distance) which also contained information regarding the placement of air valves and scour valves along the trunk-main pipeline route (Figure 14). This diagram was used in conjunction with results from the EPANET simulation, that were presented in the final amendment of the Western Aqueduct design report, to obtain the elevations of the system components (BPTs, supply etc.).

Furthermore, according to the recommendation by Walski and Haestad Methods (2003), a site visit to the Ashley Drive construction site was conducted, in order to verify the obtained information. This confirmed that the number of valves, types of valves, BPT dimensions and the pipe sizes were being implemented according to the design specifications. This visit also served to deepen the understanding of the system and to ensure that the physical scale of the system was fully grasped.

4.4.2 Documentation

The Ashley Drive BPT (Western Aqueduct) design report was utilized in order to obtain a large proportion of the remaining data. This report contained a written description of the BPT systems, descriptions of its interactions and operations within the larger system, and provided reasons for the selection of the components of the system. This report also elucidated the details of the BPT control scheme in terms of its movement schedules and the regulated movement of the valves. The report also contained the details of the globe valves (size, commercial product name and manufacturer) which were used to obtain the valve characteristics.

The sleeve valve characteristics that were provided in a graphical form within the report, in addition to the Bermad globe valve manufacturer-supplied characteristics, required curve fitting in order to render them useful to the model.

Additional documentation that was generously supplied by EWS, included:

i. A complete database of all reservoirs in the eThekwini region. This exhaustive record contained amongst other information, the capacities, top water level, floor level and locations of the reservoirs.

ii. Explicit timings for the regulated movements of the valve positions. The sleeve valves are set to move over their entire range (0% to 85%) in 5 minutes, while the globe valves average 7 minutes and 49 seconds over their entire range.

iii. Pipe descriptions including the thickness and material for each individual pipe grouped by nominal diameter.

iv. A reservoir datasheet that listed for each reservoir the average daily demand, the projected yearly growth rate and the peak factors (peak to mean ratio).

4.4.3 Site Visits

Reservoir information was obtained through a visit to the EWS Operations Centre, which provided direct, intimate access to the telemetry system. The information acquired included the individual reservoir control policies, the diurnal (consumer) demand profiles, and the 'characteristic flows' of each reservoir. The characteristic flow of a reservoir is the mean inlet flow upon the toggling of the valve/pump in order to initiate filling of the reservoir. This is a reasonably good approximation to the actual operation of the reservoirs, although variations in the rate, based on the liquid height within the reservoir and the pressure within the trunk main at the supply node, are expected.

The reservoir control policy could not be determined with certainty, due to the fact that no automatic controllers were in place. Human intervention was used in order to maintain reservoir levels within practical ranges, yet no set policy was followed. The lack of a stringent standard control policy was in part due to a severe drought that required a dynamic 'balancing act' in terms of level control throughout the complex distribution system. The control system was thus inferred to have a deadband control system with upper and lower limits of 80% and 20% of the total reservoir height respectively.

The lack of online measuring devices or access to temporary measuring devices also complicated the estimation of the individual **reservoir characteristic flows**. The telemetry system only provided time-series graphs of the reservoir level over a 24 -48 hour period (Figure B2, Appendix B). These graphs were collected for each reservoir that was to be connected to

the Western Aqueduct, and examined in order to estimate the required inlet flow rate. The following procedure was followed, and is illustrated in Figure B3, Appendix B:

i. For every available pump toggle (ON) or control valve opening (Point A), the average previous negative gradient was extrapolated in the forward direction. This line represents the level decline at the previous draw rate for no inlet flow. (Point A) is detected by the sustained increase in the level of the reservoir.

ii. The average gradient of the refill period, from (Point A) to the point of the pump toggle (OFF) or control valve closure ('Point B) was then estimated.

iii. The level difference (Δh) between the extrapolated negative and estimated positive gradient lines at the abscissa of Point B was measured to be the level difference over the refill period. This was then divided by the time (Δt) of the refill period (abscissa of Point B – abscissa of Point A) in order to obtain the level change per second of inflow. The floor area ($A_{reservoir}$) of the reservoir was then used to calculate the average volumetric inlet rate for that period.

iv. For reservoirs in series, the above procedure was executed on each reservoir, and the results were added.

The results of this procedure for all contributing reservoirs are presented in Table 7. It should be noted that the telemetry system provided records of existing operations (not WA) only. It is for this reason that the obtained values can only be used as a guideline until operational data is for the Western Aqueduct system is available. Furthermore, the estimates obtained from this procedure (Table 7) resulted in a few instances of improbable results, when compared to average reservoir (consumer) demands. These anomalies could be attributed to the numerous instances of missing data or erroneous measurements. The anomalous results were thus ignored and an average of the factor of the plausible characteristic flows to their average demands, was computed in order to maintain uniformity. The estimated characteristic flow for each reservoir in the Western Aqueduct was thus concluded to be twice that of the yearly average flow.

Table 7 - Table showing the results obtained during the process of calculating the characteristic flows of each reservoir

Reservoir	Reading 1 (m/h)	Reading 2 (m/h)	Reading 3 (m/h)	Area 1 (m^2)	Area 2 (m^2)	Area 3 (m^2)	Char Flow (m3/h)	Ave Flow (m3/h)	Average factor
Emberton	0,41	0,09		522,37	396,69		250,29	241,52	1,59
Haygarth Rd	0,02			647,50			13,26	476,41	
Tshelimnyama M1B	0,68	0,75		590,55	590,55		844,18	571,69	
Abelia Rd	0,16	0,16		517,41	1021,11		250,97	282,54	
Jerome Drive	0,74	0,18		626,17	527,28		559,87	273,42	
Wyebank	0,71			623,13			439,74	167,35	
Mount Moriah	0,23			5435,79			1255,24	1039,81	
KwaDabeka 1	0,38	0,14		17,63	15,56		8,99	502,78	
Ntuzuma 5	0,56	0,43	0,24	1036,59	3913,38	3913,38	3194,62	2734,21	

Reservoir diurnal profiles: Due to the lack of measuring devices, a clear operating policy and the availability of telemetry records, diurnal profiles for each reservoir could not be directly attained. Furthermore, limited access to meter route readings, individual user billing information, dwellings classifications and amounts, and land-use classifications prevented the use of any of the preferred methods of profile development. Given the available information, the following procedure was developed in order to obtain an accurate demand profile for each reservoir:

i. Normalized hydrographs for South African regions (urban, rural and industrial) were obtained from Stephenson (2012) (Figure A2, Figure A3 and Figure A4 in Appendix A, respectively). The specificity of the hydrographs to South African demographics and water value provided a greater degree of certainty to the hydrograph development process,

ii. The reservoir level time-series graphs (Figure B2, Appendix B) were inspected to identify pertinent features that could aid in the classification of the areas served by the reservoir. This was preferred to the use of an area classification, as some reservoirs are supplied through other reservoirs. A list of pertinent features that correspond to the features observed in the hydrographs of Stephenson (2012) are presented in Table 8.

The reservoir diurnal profile was then formulated by stretching the hydrographs about the normalized mean to obtain agreement between the supplied peak factor and that of the hydrograph. The mean was then scaled to correspond the reservoir mean. The results of this process are shown in Figure 22.

Table 8 – Observations from the reservoir draw pattern characterization process. These observations arise from the time-series graphs obtained for each reservoir from the control centre.

Reservoir	Feature 1	Feature 2	Feature 3	Characterization
Emberton	Large draw - 5.30	Flat around Midnight	Concave draw profile	**Upper income**
Abelia Road	Sustained afternoon draw	Reservoir fills late at night		**Industrial**
Jerome drive	Early morning and evening draws	Reservoir fills late at night		**Lower Income**
Tshelmnyama M1B	Sustained afternoon draw	Reservoir fills late at night		**Industrial**
Haygarth Rd	Large Early morning draw	Evening draw		**Lower Income**
Wyebank	Major afternoon draws	steady draw through the day		**Industrial**
Mt Moriah	Early morning and evening draws	Reservoir fills late at night		**Lower Income**
KwaDabeka 1	Sustained afternoon draw	Reservoir fills late at night		**Industrial**
Ntuzuma5	Large early morning draw, sustained	Flat around Midnight		**Upper income**

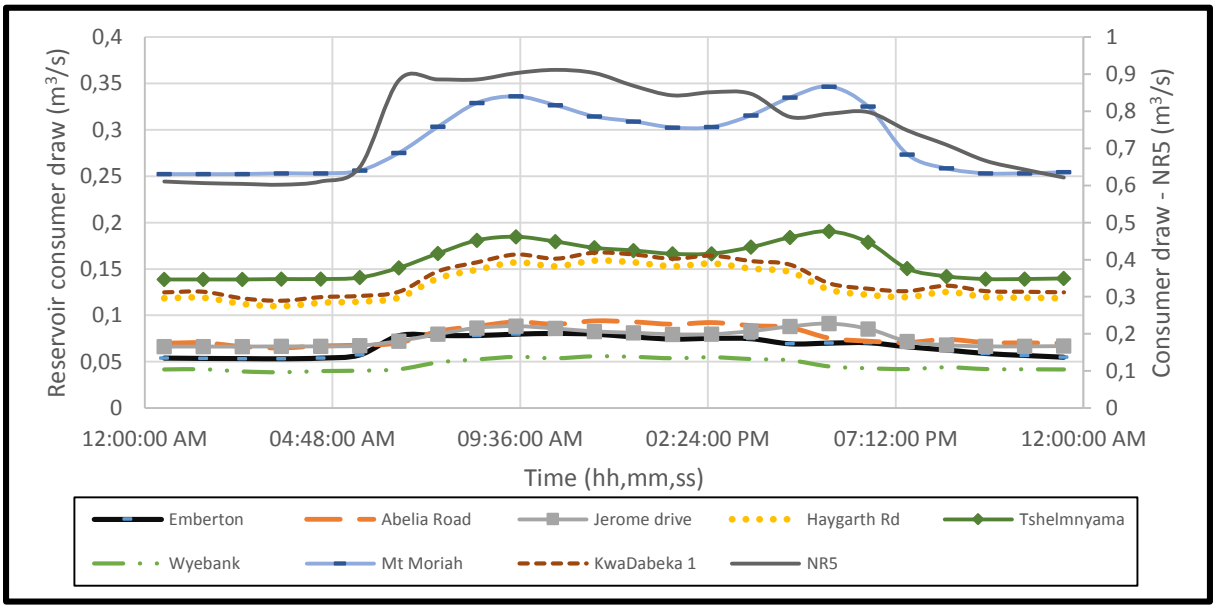

Figure 22 - Results (diurnal pattern) of the reservoir demand profile development process.

4.5 Model Construction

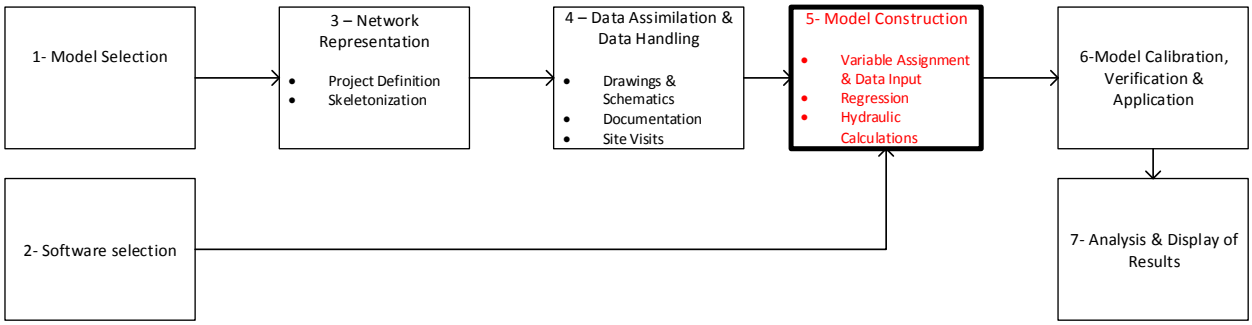

The network representation was built upon the existing skeletonized system. The link-node analysis method outline in Section 4.3 was followed in order to lay the foundations of a working, accurate mathematical representation of the physical system. All pipes that are separated by a node, as well as each node itself, were individually named in order to avoid confusion in coding and in the reporting of the data. The operational flowchart of the model is presented in Figure 23.

4.5.1 Data Preparation

In order to ensure conformity of the program to both the physical system, and user requirements, an input configuration module is provided. The configuration module consists of a time-loop configuration block and a physical parameter block.

4.5.1.1 Time-loop configuration

The code is commenced with the time loop configuration block. This block accepts as inputs; the total required time for the EPS, the simulation start time ($hh, \frac{mm}{60}$) and the length of the time increments (in seconds) and the year for which results are required. The program is configured to calculate the total number of increments required, which is then used in conjunction with the increment length to set the length of the time loop, and subsequently to initialize the vectors.

4.5.1.2 Physical data and parameters and initial conditions

The physical parameters required to execute the hydraulic calculations, is accommodated within the physical parameter block. The initial conditions for the system components, that is required to initiate the simulation sequence, are also input into this block. The requisite input variables are summarized in Table 6.

The a parameter is solely dependent on the physical parameters of the system. It is calculated using Equation [19] and the required physical parameters, for use within the Joukowsky Equation (1898) (Equation [14]).

$$a = \sqrt{\frac{1}{\frac{\rho}{E_F} + \frac{\rho \times d_i \times (1 - \mu_p{}^2)}{E_R \times s}}} \qquad [19]$$

4.5.1.3 Initialization

Vector initializations (creation of arrays of zeros) are aimed at increasing the computational speed of the program. The pre-allocation of the vectors allows for the circumvention of a vector size increase with every (time) step ahead in the approaching loop.

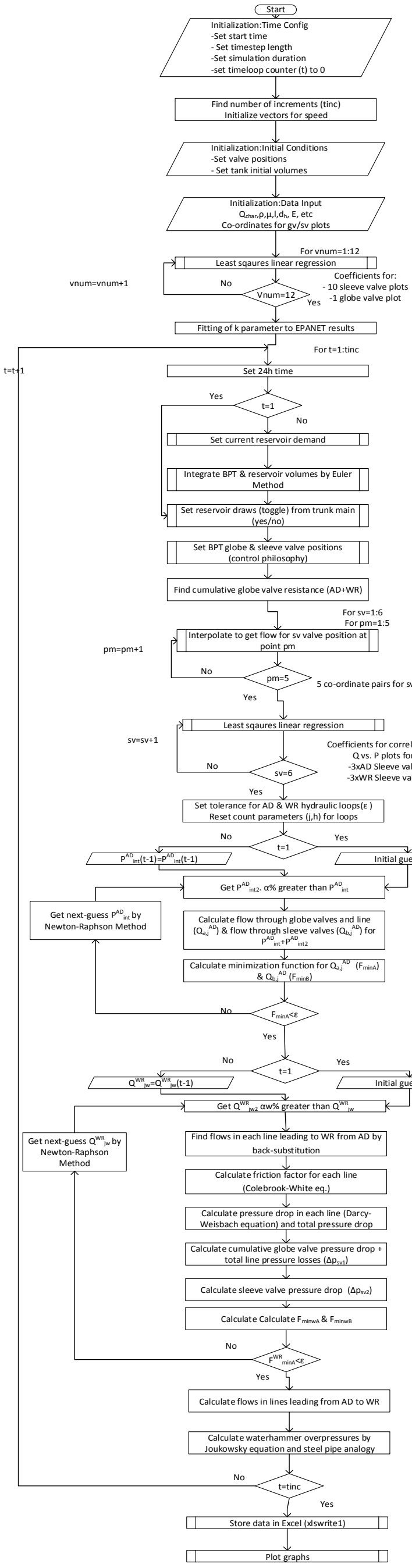

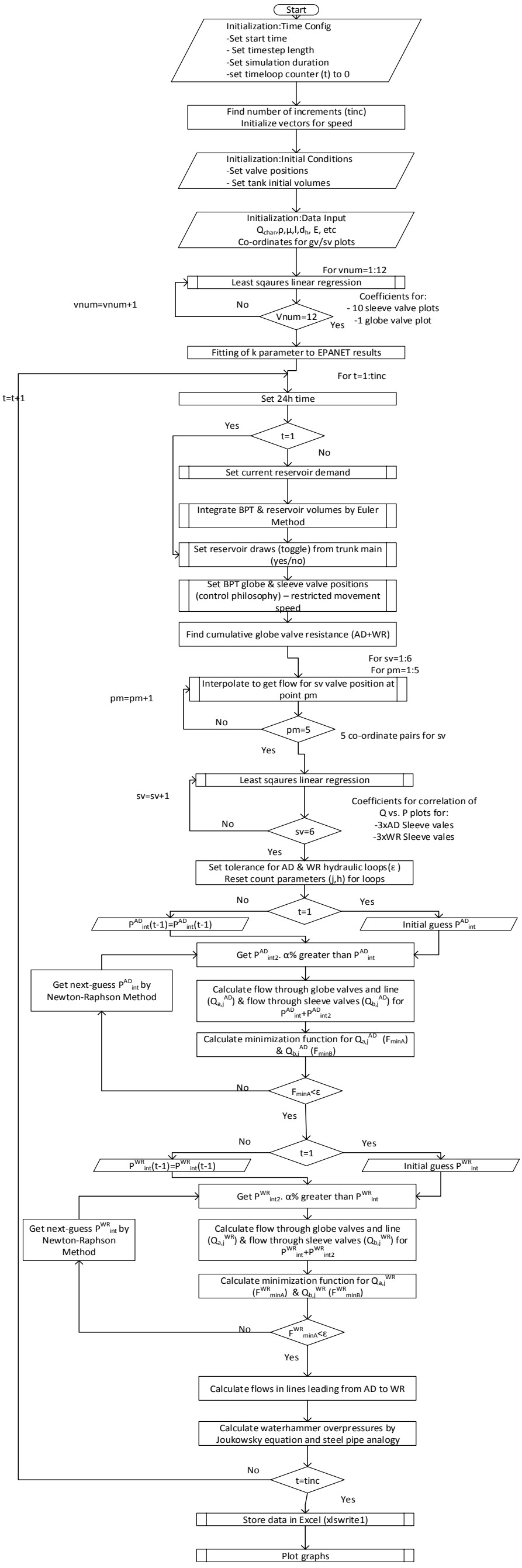

Figure 23 - Flowchart of the program operation, with the Darcy-Weisbach Equation (left) and the regression-type calculation (right).

4.5.2 Regression

4.5.2.1 Valve characteristics

In order to obtain a mathematical representation of the relationship between flow and pressure drop across the valves, for use within the hydraulic calculations, a regression routine is employed. The regression routine, which is accessible from the main code, generates parameters of an equation of the relationship describing the co-ordinates of the valve's flow (F_k) vs. pressure (P_{svk}) plots. The sleeve valve characteristic data was obtainable only in the graphical form presented in Figure 24.

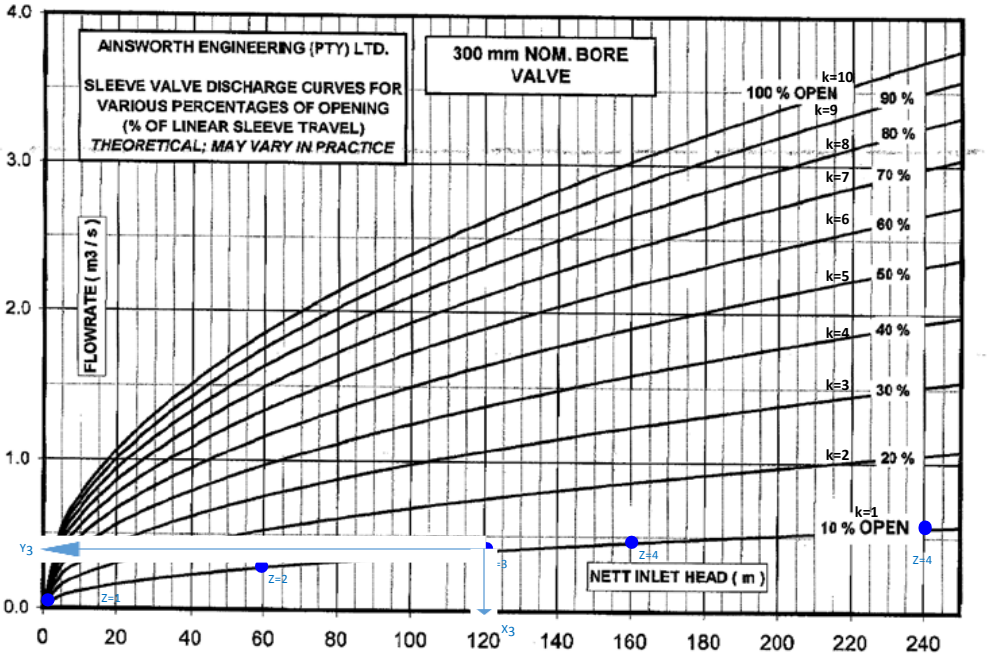

Figure 24 - BPT sleeve valve characteristics - flowrate vs. nett inlet head for deciles of the valve position (Fischer, 2014).

The regression for each of the ten sleeve valve flow characteristic (decile) plots, is achieved through the use of an external function call. This function is a matrix (linear) regression function that uses the least-squared error technique to obtain the best fit to the curves presented in . The function accepts two corresponding ordinate and abscissa vectors, and returns the vector of coefficients (β) for the desired mathematical function, and thus must be called each time a regression is conducted. The least squares, matrix (linear) regression solution, for an equation described by Equation [20], is represented by Equation [21]

$$Y = X\beta \quad [20]$$

$$\beta = (X'.\mathrm{X}^{-1}).X'.Y \quad [21]$$

The format of the abscissa vector (X), the ordinate vector (Y) and the equations coefficients (β) are shown below as Equation [22], Equation [23] & Equation [24] respectively. It should be noted that X and Y may vary in size due to the amount of co-ordinate pairs used (z), yet β will remain constant, as the regression is for a single curve (k). z is the number of co-ordinate pairs used within the regression.

$$X = \begin{pmatrix} \frac{P_{sv1}}{100} & \sqrt{\frac{P_{sv1}}{100}} \\ \vdots & \vdots \\ \frac{P_{svz}}{100} & \sqrt{\frac{P_{svz}}{100}} \end{pmatrix} \quad [22]$$

$$\beta = \begin{pmatrix} a \\ b \end{pmatrix} \quad [23]$$

$$Y = \begin{pmatrix} F_1 \\ \vdots \\ F_z \end{pmatrix} \quad [24]$$

The presented function returns two coefficients (g, h) based on an equation that sequentially includes a linear and a square root term. The equation selected for the characterisation of the k^{th}position of the sleeve valve flow characteristic plot is thus:

$$F_k = gP_{svk} + h\sqrt{P_{svk}} \quad [25]$$

It was decided, after a rigorous analysis of the trade-off between descriptive accuracy, and code and computational complexity, that this equation form describes the valve plots with sufficient accuracy. The marginal increase in accuracy for the inclusion of the quadratic and constant term ($SSE = 0.12$, $R^2 = 9.16$) as opposed to the accuracy for the simpler linear and square root function ($SSE = 0.43$, $R^2 = 9.17$), was deemed to be negligible when the accompanying drastic increase in computational complexity was considered. The inclusion of the quadratic term necessitates the inclusion of an added iterative loop that must be independently solved within the Darcy-Weisbach (1845) solution algorithm, as an explicit

solution is impossible. Furthermore, this added iterative loop was found to be unstable and resulted in a radical increase (~60 sec to ~12 214 sec) in the code execution time. The program that incorporates the quadratic and square root regression is however provided as an accompanying resource. The globe valve characteristics for an equivalent Bermad model, was regressed to a quadratic equation by implementing a simple modification to the above code. This quadratic regression function is also provided as an addendum.

An added regression sequence is also employed after the positioning of the valves in each time-step. The regression function is re-used to obtain a mathematical representation of the sleeve valves at the specified position. The Y-vector for the re-regression step is obtained through linear interpolation between the relevant (initially) regressed curves. This is done by placing the valve position between two predefined curves, and subsequently carrying out a linear interpolation at each required abscissa.

*The usage of a matrix necessitated the division of the pressure by a factor of 10^2 in order to circumvent the formation of a near-singular matrix.

4.5.2.2 k-value regression

Since the Midmar Dam Water Works supply system's behaviour was deemed to be outside of the scope of this study, the skeletonization incorporated a lumped demand term midway along the route to Ashley Drive. Additionally the representation of a non-operational physical system called for the use of a regression model-type nonlinear equation, since calibration to the physical system cannot be achieved. This limit the achievable accuracy when using the simplified and complete hydraulic models. The use of a regression model would furthermore simplify calibration and allow for better correspondence to the EPANET design model. This would also account for all pipe fittings (bends, air valves, scour valves, butterfly valves etc.) since their resistance would already be incorporated into the (design) lumped parameter. As such, the system pressure/flow relationship was regressed according to Equation [26] to the EPANET model, to obtain a value for k.

$$\Delta p_{line} = kQ^2 \qquad [26]$$

In order to mitigate the concerns expressed in Mays (2000) regarding the accuracy of a regression model outside of its simulated (input) range, an average of four k values was obtained, incorporating those for peak factors of 1.2 and 1.5 multiples of the flow. In calculating the k, the change in diameter (between 1 400 mm and 1 600 mm) and flowrate

encountered in the pipeline from Umlaas Road to Ashley Drive had to be accounted for. This was achieved through the relationship between the diameter and pressure drop, obtainable from the Darcy-Weisbach (1845) equation (Equation [10]). The calculation to obtain the *k* is presented below;

Simple mathematical manipulations of Equation [10] are used to incorporate the pipe diameter into the Darcy-Weisbach equation (1845), yielding Equation [27].

$$\Delta p = \frac{8\rho\lambda}{\pi^2} \times l \times \frac{Q^2}{d_h{}^5} \quad [27]$$

It is thus established that Δp has a relationship to the pipe hydraulic diameter ($d_h{}^5$) that is described by $\frac{1}{d_h{}^5} \propto \Delta p$,. Furthermore, the initial factor shown in Equation [27] can be equated to an adapted k_x factor to obtain the following, simplified form of the Darcy-Weisbach equation (1845) – Equation [28].

$$\Delta p = k_x \times l \times \frac{Q^2}{d_h{}^5} \quad [28]$$

The relationship between the k_x factor for the 1 400 mm (k_{1400}) and 1600 mm (k_{1600}) (Equation [29]) allows the exclusive use of the k_{1400}, which therefore also applies to the pipes downstream of the AD BPT.

$$k_{1400} = \frac{k_{1600}}{1.4^5} \times 1.6^5 \quad [29]$$

The final form of the regression equation, that accounts for the lumped halfway (fractional) offtake ($q_{o,year}$) and the change, from and to the 1 400 mm diameter pipe follows from Equation [28] and Equation [29], and is thus presented as Equation [30]

.

$$k = \frac{\Delta p}{Q^2 \times [l_1 + l_2 \times \frac{1.6^5}{1.4^5} + l_3 \times \frac{1.6^5}{1.4^5} \times (1 - q_{o,year})^2 + l_4 \times (1 - q_{o,year})^2]} \quad [30]$$

4.5.3 Time-based hydraulic calculations

4.5.3.1 Time loop

The time loop is commenced with the use of a *for* loop, with a specified termination length, equal to the total number of increments that is calculated from the user inputs into the time loop configuration block. The time is initially set to the user-specified starting time. Each subsequent progression through the loop causes an incremental move ahead in time, equal to the user-specified time increment length

4.5.3.2 Reservoir consumer demands and inlet draws

Using the calculated time, and user-specified year, an external function delivers the consumer demand on each reservoir at the specified time. This function is configured with the format of a time-based lookup table, which was generated according to the procedure outlined in Section 4.4.3. An allowance for the projected yearly demand growth for each reservoir is included within the computation.

The reservoir draws from the trunk mains, at the current time-step ($time = t$), are determined through the use of an external function that accepts as inputs; the current reservoir levels, the lower and upper reservoir (deadband) control limits and the previous state of the reservoir draw ($\kappa_{act}(t-\Delta t)$), all in vector form. The function compares the current level of each reservoir to its upper and lower control limits, and enacts adjustments to the output vector only when these limits are transgressed (deadband' control philosophy). The adjustments to the output vector ($\kappa_{act}(t)$) are in the form of a binary toggle (1=draw, 0=no draw). No control action is taken when the reservoir levels are within the specified deadband limits, and the result is thus the value of the previous entry.

The function is built in a generic format, and was thus used in its identical form for both sets of reservoirs (between Ashley Drive and Wyebank Road BPTs and after Wyebank Road BPT). The reservoirs are divided into distinct sets in order to facilitate their independence within the simulation phase, particularly when their control systems are overridden during stress tests.

4.5.3.3 Volume integration

The initial ($time = 0$) volumes of the BPTs together with those for the reservoirs and the initial conditions of the valves are set within the initial conditions block. For all other time ($time > 0$) the volumes of the BPTs and reservoirs are calculated using the Euler Method

(Equation [3]), which takes on the form of Equation [31] for the reservoirs and Equation [32] for the BPTs. The Euler Method was accepted as sufficiently accurate, without hesitation, due to the assurance provided by Mays (2000), as detailed in Section 2.4.1.1.

All reservoir volumes are thus integrated through an external function call that simultaneously integrates for each reservoir. The BPT and reservoir volumes are subsequently divided by their respective surface areas, as per Equation [34] , in order to calculate the current level of water within the tank. The reservoir integration function provides for a saturation volume to be reached in order to represent reservoir overflow conditions. The same is not provided for the BPTs, as it would affect the analysis of the efficacy of the control system and its ability to manage large flows. κ_{act} is the activator binary variable that toggles the inflow to the reservoir based on the reservoir level.

$$V_{res}(t) = V_{res}(t-\Delta t) + \Delta t(Q_{in}(t-\Delta t) - Q_{out}(\mathrm{t}-\Delta t)) \quad [31]$$

$$V_{BPT}(t) = V_{BPT}(t-\Delta t) + \Delta t(Q_{in}(t-\Delta t) - Q_{out}(\mathrm{t}-\Delta t)) \quad [32]$$

$$V_{res}(t) = V_{res}(t-\Delta t) + \Delta t(Q_{char} \times \kappa_{act}(t-\Delta t) - Q_{demand}(\mathrm{t}-\Delta t)) \quad [33]$$

$$h_{res}(t) = \frac{V_{res}(t)}{A_{res}(t)} \quad [34]$$

4.5.3.3.a Level based decisions

The volume integration calculations enables the control mechanisms to reach a preferred valve/pump setting for the time-step ($time = t$). The positioning functions (globe valves and sleeve valves independently) utilize the BPT levels at $time = t$, and the control system settings (Figure 18) that are located within their respective external functions in the form of a lookup table. The lookup table provides the target valve positions (x_p) for the current level, to which the valve position must move, at its regulated rate. This ramped (regulated) valve movement is built into the external function through a calculation (Equation [35]) that involves the following inputs: the desired movement limit (fraction of stroke - m_{ps}), the length of the interval for which this movement is specified (t_{ps}) and the duration of each time step (Δt).

$$m_{\Delta t} = \frac{m_{ps}}{t_{ps}} \Delta t \quad [35]$$

The calculated movement ($m_{\Delta t}$) is then allowed for, from the previous valve position (at $time = t - 1$). The ramped movement of the valves however, necessitates the following logic in order to account for a previous valve position ($x_{t-\Delta t}$) that would not permit the movement at the allowed rate (i.e. a movement at the calculated rate ($m_{\Delta t}$) would cause the valve movement to exceed its target position (x_p)).

if $x_{t-\Delta t} < x_p$ **&** $x_{t-\Delta t} + m_{\Delta t} \leq x_p$

$$x_t = x_{t-\Delta t} + m_{\Delta t}$$

elseif $x_{t-\Delta t} > x_p$ **&** $x_{t-\Delta t} + m_{\Delta t} \geq x_p$

$$x_t = x_{t-\Delta t} - m_{\Delta t}$$

else $x_t = x_p$

Although the control settings for the Ashley Drive and Wyebank Road BPTs are envisioned to be identical, provision is made for alterations in either control system by utilizing separate external functions. Control system settings may require alteration due to interaction between the two BPTs that may prove to be particularly burdensome on the Ashley Drive BPT, or if new valve settings are determined by optimization.

The program incorporates a data stack for the BPT control valve positions. This is included in order to emulate the workings of a real-world control model, where data cannot be indefinitely stored. The control valve position stack contains two levels of data; the current valve positions ($time = t$) in row 2, and the previous positions ($time = t - 1$) in row 1. The valve positions at $time = t - 1$ are required in order to regulate the movement of the valves as required by the control system.

4.5.3.4 Calculation of hydraulic parameters

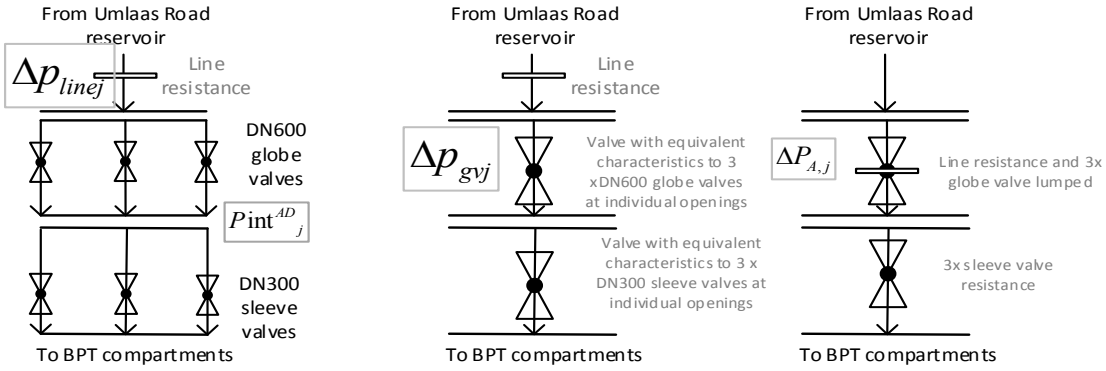

Figure 25 - Demonstration of the transformation of the individual flow factors into lumped terms to solve the hydraulic equations.

The combined effect of the globe valves (for each BPT) is computed through the addition of the product of the Kv and $f(x)$ terms for all three valves, as presented in Equation [36]. The Kv value is constant, but $f(x)$ is dependent on the current valve position, and is thus calculated through the regressed parameters (Section 4.5.2).

$$R_{gv,BPT} = \sum_{l=1}^{3} (Kv \times f(\mathrm{x}))_l \qquad [36]$$

The format of the data supplied for the sleeve valves (Figure 24) however, required an additional processing step prior to this addition step. The additional processing involves the mentioned linear interpolation (Section 4.5.2.1) of the flowrate (ordinate), for the given valve position, from the nearest supplied valve position curve above and below the valve position at $time = t$. The interpolation is carried out through an external function that contains a lookup table of data coordinates for each (k^{th}) sleeve valve flow vs head curves.

The interpolation function utilizes the current valve position (x_t) and a logical statement to place the current valve position between the two closest valve positions that correspond to the supplied characteristic curves (deciles). The coefficients for these two valve positions, that are obtained from the previous regression (Section 4.5.2.1), are used to find the flows ($F_{specP_{sv,k}}|_{upper}$ & $F_{specP_{sv,k}}|_{lower}$) at the specified pressure (P_{sv}). The interpolation is subsequently carried according to Equation [37].

$$F_k = F_{specP_{sv,k}}\,|_{lower} + \frac{F_{specP_{sv,k}}\,|_{upper} - F_{specP_{sv,k}}\,|_{lower}}{x_{upper} - x_{lower}} \times (x_k - x_{lower}) \qquad [37]$$

Re-regression (see Section 4.5.2.1) is then conducted using the results of the linear interpolation, in order to obtain a usable analytical equation that could be summed to obtain the combined effect of the sleeve valves, without compromising the accuracy of the model.

4.5.3.5 Hydraulic Loop- AD BPT

The attainment of the collective characteristics of each group of valves in series at $time = t$ allows for the commencement of the Newton-Raphson Method iteration loop. This method is used to iteratively solve for the flow through the AD BPT system, which is dependent on the interplay between the available head, the pipeline frictional effects and the resistance of the valves. The problem was constructed to manipulate a variable (Q) other than that utilised in its convergence criterion (P). This was done in order to negate the interference of the relaxation parameter (ω) on the convergence criterion.

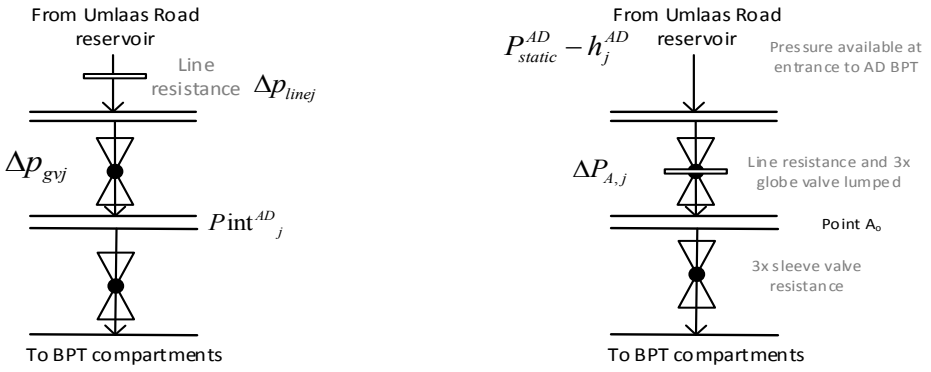

Figure 26 - Visualization of the parameters used in the hydraulic calculations for the AD BPT.

4.5.3.5.a Hydraulic calculations – k-value

Objective: *The objective of the hydraulic solution loop is to determine the flowrate that is permitted through the BPT system at the current valve positions. The flowrate through the system is governed by three, interacting resistances (the line resistance, globe valves resistance and sleeve valve resistance). The attainment of the pressure between the globe valves and sleeve valves ($P\text{int}^{AD}$) will allow for the flowrate upstream and downstream of this point (Point A_o) to be calculated explicitly. The hydraulic solution loop thus utilises the Newton-Raphson method to equate the flows upstream and downstream of Point A_o, by adjusting the*

intermediate pressure ($P\text{int}^{AD}$). Figure 26 is a visualization of the parameters used within the hydraulic loop.

The procedure is initiated by estimating the pressure ($P\text{int}^{AD}{}_{j}|_{j=0}$) loss through sleeve valves at $time = t$. j is the Newton-Raphson iteration number. This in turn enables the calculation of a combined pressure loss ($\Delta P_{A,j}$) for the line (Δp_{linej}) and globe valves (Δp_{gvj}) corresponding to the initial guess (Equation [38]). The unit of measurement for all pressure terms is meters of water.

$$\Delta P_{A,j} = (\Delta p_{linej} + \Delta p_{gvj})_{j=0} \quad [38]$$

This combined pressure loss is then calculated, according to Equation [39] by subtracting the initial guess for the sleeve valve pressure loss, from the available head. The available head is the total static head (P_{static}^{AD}) less the level of liquid in the BPT (h_j^{AD}) (BPT is bottom-fed).

$$\Delta P_{A,j} = P_{static}^{AD} - h_j^{AD} - P\text{int}^{AD}{}_{j} \quad [39]$$

These initial pressure loss guesses are then used to calculate the corresponding flow through the line and globe valves ($Q_{A,j}^{AD}|_{j=0}$), and through the sleeve valves ($Q_{\mathrm{B},j}^{AD}|_{j=0}$). Equation [40] presents the relationship between the combined line and globe valve pressure loss and the flowrate through the system. Equation [41] is its explicit solution for the flowrate through the system.

$$\Delta P_{A,j} = (Q_{A,j}^{AD})^2 \times (k + \frac{1}{R_{gv,AD}}) \quad [40]$$

$$Q_{A,j}^{AD} = \sqrt{\frac{P_{static}^{AD} - h_j^{AD} - P\text{int}^{AD}{}_{j}}{k + \frac{1}{R_{gv}}}} \quad [41]$$

The flow through sleeve valve i ($Q_{\mathrm{Bu},j}^{AD}$) is obtained from Equation [42] which utilises the coefficients from the regression carried out in Section 4.5.2.1 for the current valve positions (x_t).

$$Q_{\mathrm{Bu},j}^{AD} = v_{1u}(\frac{P\text{int}_j}{100}) + v_{2u}\sqrt{\frac{P\text{int}_j}{100}} \quad [42]$$

The flowrate through each sleeve valve i, is then summed (Equation [43]) to obtain the total flowrate through the parallel configuration of the valves ($Q_{\mathrm{B},j}^{AD}$).

$$Q_{\mathrm{B},j}^{AD} = \sum_{u=1}^{3} Q_{\mathrm{Bu},j}^{AD} \qquad [43]$$

4.5.3.5.b Newton Raphson solution

The minimization function for the Newton-Raphson Method ($\mathrm{f}(P\mathrm{int}^{AD})$) is shown in Equation [44]

$$\mathrm{f}(P\mathrm{int}^{AD}) = (Q_A^{AD} - Q_{\mathrm{B}}^{AD})_j \qquad [44]$$

According to the Newton-Raphson method, the corresponding next guess is calculated by Equation [45]. j is the iteration number, which is 0 for the initial guess.

$$P\mathrm{int}^{AD}{}_{j+1} = P\mathrm{int}^{AD}{}_j - \omega \frac{\mathrm{f}(P\mathrm{int}^{AD})}{\frac{\partial \mathrm{f}(P\mathrm{int}^{AD})}{\partial P\mathrm{int}}\Big|_{Pi_j}} \qquad [45]$$

The procedure of re-generating a next-guess pressure is repeated until the minimization function is within a specified tolerance (ε). A tolerance of $1\mathrm{x}10^{-3}$ $\frac{m^3}{s}$ was deemed to be suitable as a convergence criterion for the model. The relaxation parameter was set to $5\mathrm{x}10^{-3}$ in order to avoid observed 'sawtooth' overshooting of the root, thus speeding up convergence. The gradient $\frac{\partial \mathrm{f}(P\mathrm{int}^{AD})}{\partial P}$ was calculated through the simultaneous evaluation of the flows at a pressure α% greater than $P\mathrm{int}^{AD}{}_j$, according to Equation [46]. The evaluation parameter (α) is included as a user-adjustable variable.

$$\frac{\partial \mathrm{f}(P\mathrm{int}^{AD})}{\partial P\mathrm{int}}\Big|_j = \frac{\mathrm{f}(P\mathrm{int}^{AD})_{\mathrm{A}} - \mathrm{f}(P\mathrm{int}^{AD})_{\mathrm{B}}}{P\mathrm{int}_A - P\mathrm{int}_B}\Big|_j \qquad [46]$$

In order to optimize the algorithm for speed, the converged (final) $P\mathrm{int}_j|_{j=j,t=t-1}$ at the previous timestep ($time = t-1$) is used as the initial guess ($P\mathrm{int}_j|_{j=0,t=t}$) at the current timestep ($time = t$) for all $t > 1$, as this is expected to be a close approximation, particularly at small time increments.

4.5.3.6 Hydraulic Loop- WR BPT

The Wyebank Drive BPT solution loop, in the regression model form, follows much the same format as that of the Ashley Drive BPT. The primary difference is the scaling of the per-metre k value, which is achieved by the multiplication of the length of the pipe segment being considered, according to Equation [28]. Figure 27 is a visualization of the parameters used within the hydraulic loop.

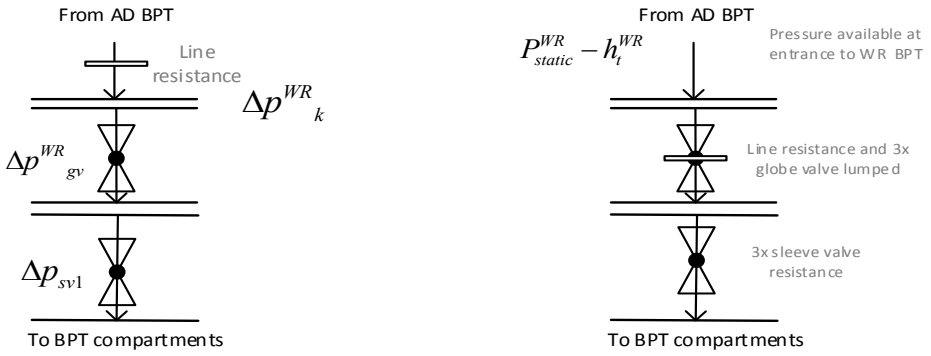

Figure 27 - Visualization of the parameters used in the hydraulic calculations for the AD BPT.

The inclusion of the Darcy-Weisbach (1845) equation however, necessitates a complete overhaul of the structure of the loop. This loop commences with an initial guess ($t = 0$) of the flow through the network ($Q_j^{WR}|_{j=0}$) that is also equated to the previous converged flow value $Q_j^{WR}|_{j=j,t=t-1}$ for every subsequent time-step ($t > 1$). The flowrate through each pipe run, from the Ashley Drive BPT to the Wyebank Road BPT is then computed through a series of backward-substitution type calculations.

4.5.3.6.a Hydraulic calculations (Darcy-Weisbach method)

Objective: *The objective of the hydraulic solution loop is to determine the flowrate that is permitted through the BPT system at the current valve positions. The flowrate through the system is governed by three, interacting resistances (the line resistance, globe valves resistance and sleeve valve resistance). The Darcy-Weisbach equation introduces an added complexity, due to the equation being implicit with the flowrate. The solution procedure is thus amended to adjust the flowrate based upon the Newton-Raphson technique through the calculated*

pressure losses. The line and globe valve pressure losses are all determinable with a flowrate estimate.

The initial guess of flow through the WR BPT ($Q_j^{WR}|_{j=0}$) allows for the flow within each successive upstream line ($k-1$) leading to the WR BPT ($Q_j^{WR}{}_{k-1}$) to be calculated, through the knowledge of the current offtakes ($Q_{char,\text{res}}$ - Section 4.5.3.2) according to Equation [47]

$$Q_j^{WR}{}_{k-1} = Q_j^{WR}{}_k + \sum_{y=1}^{y}[\kappa_{act}(t) \times Q_{char,\text{res}}]_y \quad [47]$$

The dimensionless friction factor (λ) is then calculated through an external function call that solves the Colebrook-White equation (Equation [12]) for the friction factor, through successive substitution, according to Equation [48].

$$f_{k,z} = \frac{1}{-2\log(\frac{e/D_k}{3.7} + \frac{2.51}{\text{Re}_k\sqrt{f_{k,z-1}}})}^2 \quad [48]$$

The friction factor, together with the other requisite physical parameters are then utilised within a Darcy-Weisbach (1845) (Equation [10]) external function, to calculate the pressure drop Δp_k for each pipe segment (k).

$$\Delta p^{WR}{}_k = \sum_{k=0}^{5}\Delta p_k \quad [49]$$

The sum of the pressure drops ($\Delta p^{WR}{}_k$) is then calculated through Equation [49], and subsequently subtracted from the total *available* static head in order to calculate the pressure available upstream of the globe valves. The total pressure drop across the three globe valves ($\Delta p^{WR}{}_{gv}$) is obtained through Equation [50] which requires the regressed valve characteristic coefficients (Section 4.5.2) and the flowrate estimate ($Q_j^{WR}|_{j=0}$).

$$\Delta p^{WR}{}_{gv} = (\frac{Q_j^{WR}}{R_{gv,WR}})^2 \quad [50]$$

This enables the calculation of the estimated pressure drop across the sleeve valves (Δp_{sv1}) through Equation [51].

$$\Delta p_{sv1} = P_{static}^{WR} - h_t^{WR} - \Delta p^{WR}{}_k - \Delta p^{WR}{}_{gv} \quad [51]$$

Using the same flowrate estimate ($Q_j^{WR}|_{j=0}$), the pressure drop Δp_{sv2} through the set of sleeve valves can be calculated from the regressed equations (Section 4.5.2.1) and the quadratic equation. Equation [52] represents the explicit solution for the total flow through the sleeve valves (Q_{SV}^{WR}) by summing the expressions for the individual flowrates through each valve in the parallel arrangement.

$$Q_{SV}^{WR} = (v_{11} + v_{12} + v_{13}) \times \frac{\Delta p_{sv2}}{100} + (v_{21} + v_{22} + v_{23}) \times \sqrt{\frac{\Delta p_{sv2}}{100}} \qquad [52]$$

Simple mathematical manipulations of Equation [52], yields the quadratic expression shown in Equation [53].

$$0 = \frac{v_{11} + v_{12} + v_{13}}{100} \Delta p_{sv2}{}^2 + \frac{(v_{21} + v_{22} + v_{23})}{100} \Delta p_{sv2} - (Q_{SV}^{WR})^2 \qquad [53]$$

The quadratic formula is then used to provide an explicit solution (Equation [54]) for the pressure drop through the sleeve valve arrangement (Δp_{sv2}). The subtraction of the square root term was found to produce the only viable root over the entire plausible range of flows.

$$\Delta p_{sv2} = \frac{-\frac{(v_{21} + v_{22} + v_{23})}{100} \pm \sqrt{\frac{(v_{21} + v_{22} + v_{23})^2}{100} - 4 \times \frac{v_{11} + v_{12} + v_{13}}{100} \times (Q_{SV}^{WR})^2}}{2 \times \frac{v_{11} + v_{12} + v_{13}}{100}} \qquad [54]$$

The usage of the marginally more accurate quadratic-root regression equation for the sleeve valve flow-pressure relationship requires the inclusion of yet another inner loop, which was found to be unstable, particularly at low flowrates. The extra loop is required for root-finding purposes, as the root cannot be found directly. The inclusion of this loop drastically increased the computation time, regardless of the root-finding algorithm or relaxation parameter used. The linear-root equation however, possesses an explicit solution that takes the form of the quadratic equation, whose non-complex solution over the entire pressure/flow range, corresponds to the subtraction of the square root term.

4.5.3.6.b Newton Raphson minimisation

The minimization function for this loop is constructed in terms of pressure in order to circumvent the aforementioned interference of the relaxation parameter in the convergence criteria. The minimization function ($f(Q^{WR})$) is thus constructed as Equation [55].

$$f(Q^{WR}) = |\Delta p_{sv2} - \Delta p_{sv1}|_j \quad [55]$$

According to the Newton-Raphson method, the corresponding next guess is calculated by

$$Q^{WR}_{j\ j+1} = Q^{WR}_{j\ j} - \omega \frac{f(Q^{WR})}{\frac{\partial F_{\min}}{\partial f(Q^{WR})}|_{Qw_j}} \quad [56]$$

where j is the iteration number, which is 0 for the initial guess. The procedure of re-generating a next-guess pressure is repeated until the minimization function is within a specified tolerance (ε). The tolerance and relaxation parameter were maintained at the values specified for the AD BPT solution, and the gradient evaluations were conducted at the same (adjustable) percentage distance.

After each Newton Raphson solution convergence, the pertinent variables are stored into separate vectors, in order to avail them for storage and further calculations. The iteration number parameter j is then reset to zero, and all the variable vectors are re-used for the next time-step.

4.5.3.7 Fluid transient analyses

The next section of the program incorporates the water hammer calculations that are described in Section 2.4.3. The inclusion of both calculations to estimate the water hammer overpressure is discussed in Section 2.4.3. The Joukowsky overpressure estimation simplifies to Equation [57] and the *steel pipe analogy* simplifies to Equation.[58] l_{up} is the length of the pipeline upstream to the valve and Q_j^{BPT} is the converged flow rate from the BPT hydraulic loop, at the indicated time step.

$$\Delta h_{wh} = \frac{\pm a_{jou} \times \rho \times (Q_j^{BPT}(t) - Q_j^{BPT}(t - \Delta t))}{250 \times \pi \times d_h{}^2} \quad [57]$$

$$\Delta h_{wh} = \frac{l_{up} \times \rho \times (Q_j^{BPT}(t) - Q_j^{BPT}(t - \Delta t))}{250 \times \pi \times d_h{}^2 \times \Delta t} \quad [58]$$

4.6 Analysis and Display of Results

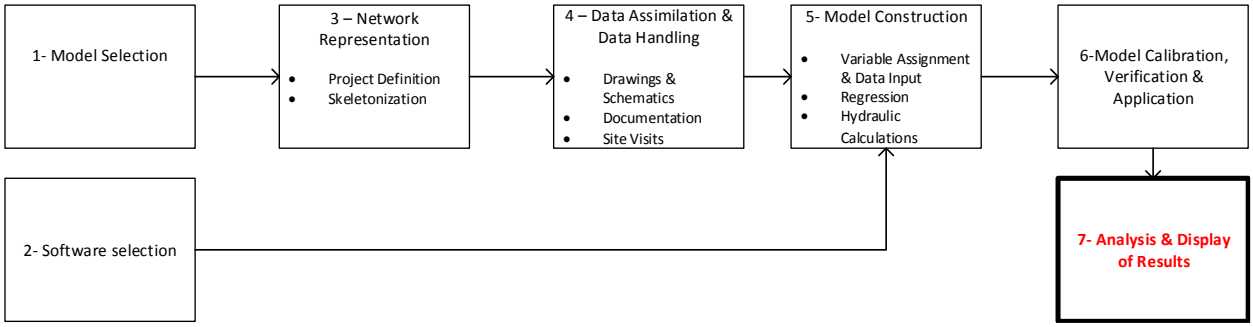

A plotting facility is provided in order to graphically display the calculated parameters against the time, in order to display the large volumes of data in a concise manner. These plots are intended to expedite decision-making processes and allow for the easy identification of system vulnerabilities. The selection of ordinate-abscissa pairs was scrupulously carried out in order to highlight interactions between system components. The final portion of the program uses a modified version of the inbuilt 'xlswrite.m' function in order to drastically decrease the execution-time of the program. The function script was obtained from the Mathworks online forum (Swartz, 2006). The storage utility was deemed to be of utmost importance in the field-use of the program, as each re-run of the program overwrites any past data generated. Microsoft Excel © was selected as the spreadsheet facility of choice, due to its widespread acceptance. A template .xlsx file, which is provided with the code, contains readymade data headers and plots as shown in Figure C1, Appendix C.

4.7 Model Calibration, Verification & Application

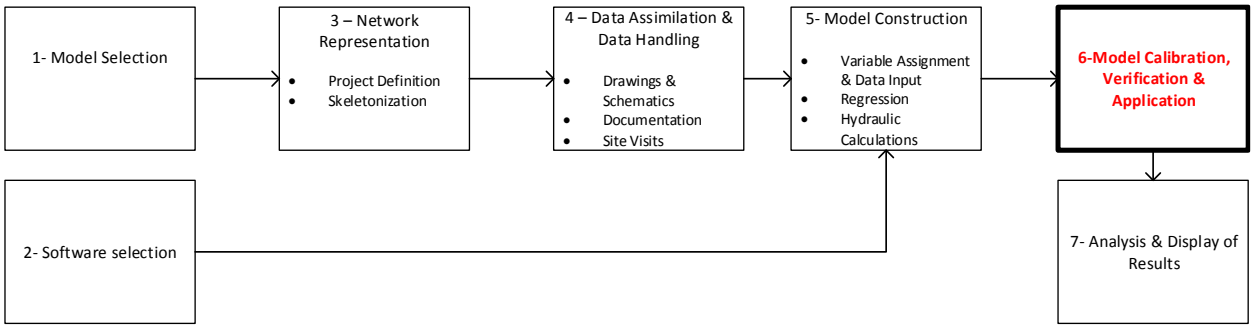

Model calibration could not be achieved as the Western Aqueduct is not currently operational. The regression model-type calculations however, do provide a welcome degree of certainty with regards to the correspondence of the model results to the EPANET simulation.

Model verification was achieved through the use of numerous localized mass balances and an overall mass balance. The balancing of the mass balance itself provides an assurance of the

veracity of the computational elements of the model. Furthermore, simplified, disentangled scenarios were developed in order to assess the correspondence of the behaviour of the system to anticipated behaviour, and to ensure that the model is accurate.

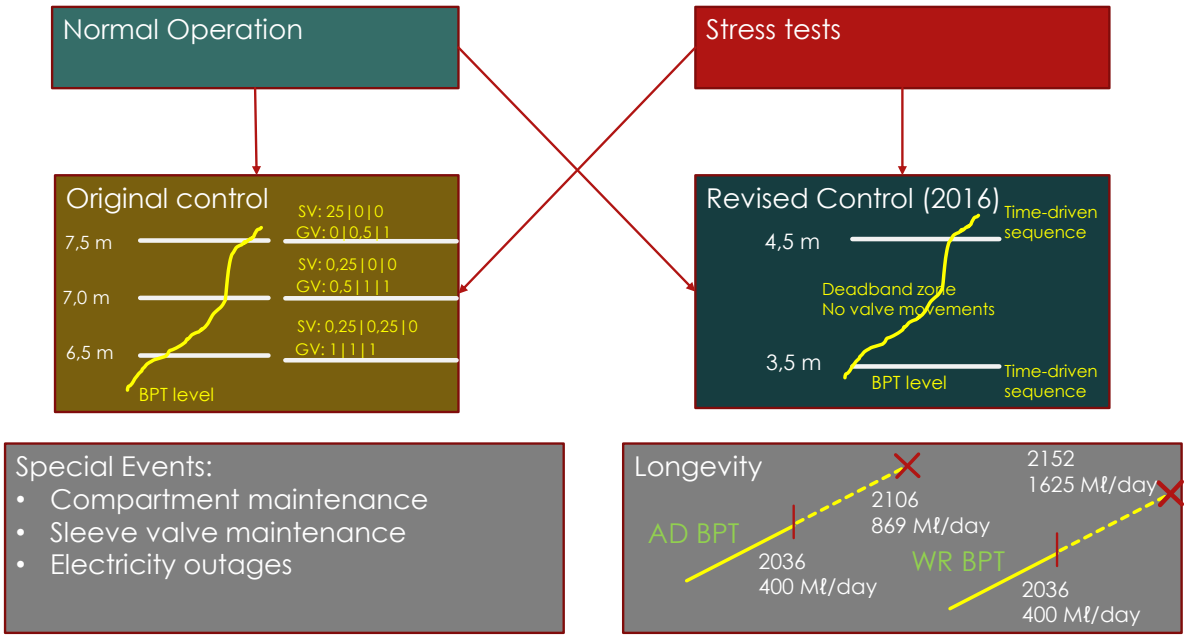

Figure 28 - Visusal presentation of the factors involved within the conception of the simulation test scenarios.

The model application involved the conception and execution of multiple scenarios in order to assess the system performance and behaviours under pre-selected conditions. Both normal operational tests and stress-tests were conducted on the system. Normal operation involves the consumer usage draws at their estimated draw rates and schedules, while the reservoir control philosophy governs the reservoir draws from the trunk mains. Stress-tests however involve the overriding of the reservoir control system to manually set the binary toggle for reservoir draws from the trunk mains, thus ignoring the breaching of the high or low deadband limits within each reservoir. Reservoirs were set to draw either individually or simultaneously, as presented in Table 10. These operating conditions were then permutated in succession with the original control philosophy (Control 1.0) and the revised control strategy (Control 2.0). Special events, which bore much significance within the conceptual stages of the Western Aqueduct design, such as BPT compartment maintenance, sleeve valve maintenance and operation under power outage conditions, were also tested for each control philosophy. Longevity tests included simulations over much longer time-periods. These tests thus negated the effects of the control system, and were used to evaluate the ability of the Western Aqueduct to be able to supply

growing (y/y increase) consumer demands, based upon upstream heads, and the line resistance. Figure 28 graphically represents the permutative setup of the generation of scenario test conditions.

The triple step test is a stress test that uses a maximum/zero/maximum schedule in order to test the adequacy of the BPTs when responding to massive changes in the throughput. The first 120 minutes of this test sees the system being operated at the maximum throughput, which is followed by 120 minutes of no reservoir draws from the trunk mains. At 240 minutes, all reservoirs are again manually overridden to draw at their characteristic flow from the trunk mains.

The last test (8.0) involved the assessment of the time taken for the BPTs to overflow should the valves stick at their fully open positions. An exhaustive list of the functions developed for, and used within, the model are presented in Table 9. A summary of the scenarios, and an assigned number for each is presented in Table 10, and a graphical representation of the permutations are presented in Figure 29.

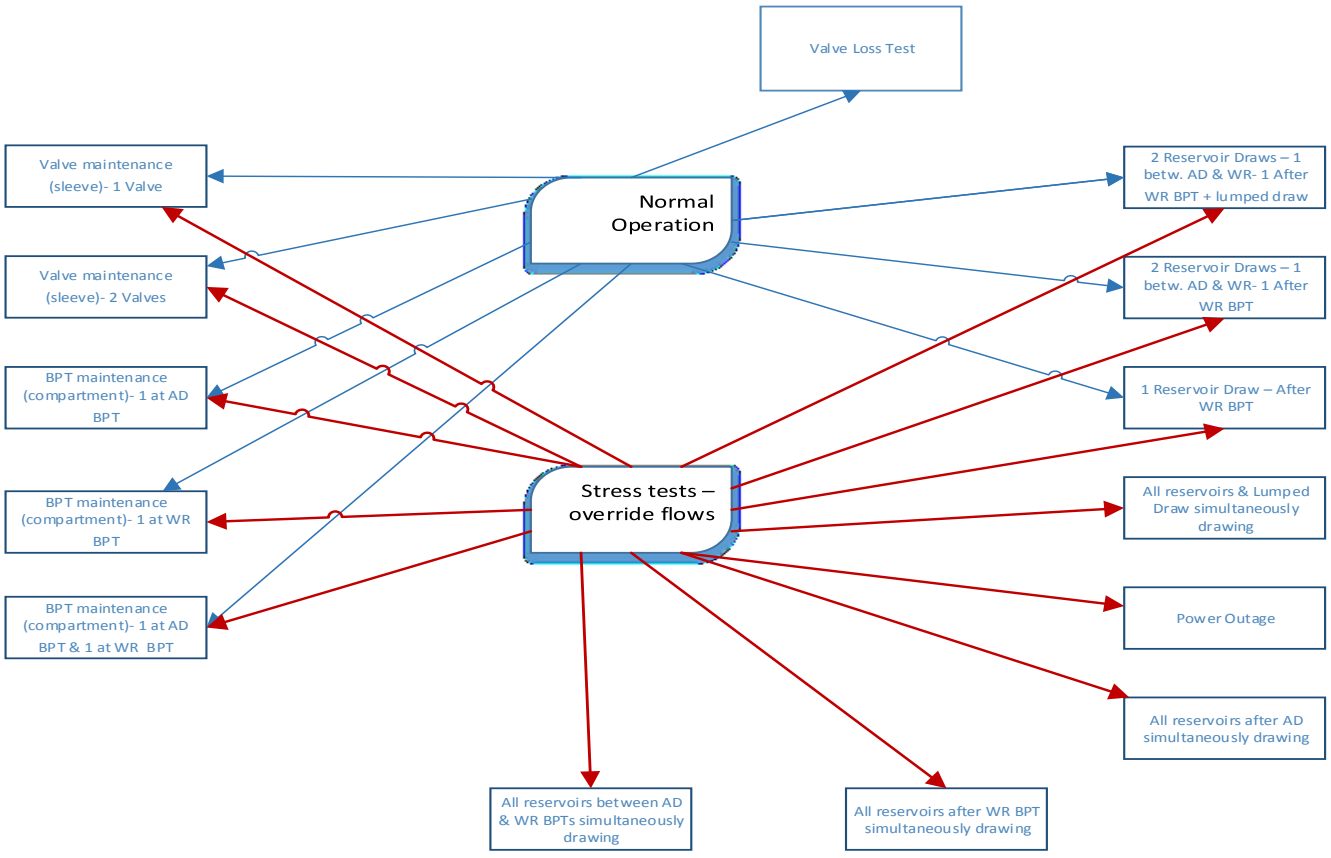

Figure 29 - Summary of scenario test combinations

Table 9 - List of external functions used in the model execution. All functions were developed for use within the model – Bolded inputs indicate vectors

Function Name	Purpose	Inputs
sleeve1.m	Linear regression of sleeve valve characteristics	**X co-ordinates**, **Y co-ordinates**
globe1.m	Linear regression of sleeve valve characteristics	**X co-ordinates**, **Y co-ordinates**
demand.m	Set reservoir consumer demands for current time step (Reservoirs between Ashley Drive and Wyebank Road BPTs).	24 hr time, year
Demand2.m	Set reservoir consumer demands for current time step (Reservoirs after the Wyebank Road BPT).	24 hr time, year
voladd.m	Integrate reservoir volumes. Incorporates a tank saturation feature	**Previous reservoir volumes, reservoir characteristic flows, previous time-step reservoir consumer demands,** length of time increment, **reservoir capacities**
SpositionerA.m	Set valve position for current time-step based on Ashley Drive BPT control strategy. Incorporates a valve-movement time regulating feature.	BPT level at current time-step, sleeve valve position at past time step, length of time increment
GpositionerA.m	Set valve position for current time-step based on Ashley Drive BPT control strategy. Incorporates a valve-movement time regulating feature.	BPT level at current time-step, sleeve valve position at past time step, length of time increment
SpositionerW.m	Set valve position for current time-step based on Wyebank Road BPT control strategy. Incorporates a valve-movement time regulating feature.	BPT level at current time-step, sleeve valve position at past time step, length of time increment
SpositionerW.m	Set valve position for current time-step based on Wyebank Road BPT control strategy. Incorporates a valve-movement time regulating feature.	BPT level at current time-step, sleeve valve position at past time step, length of time increment
valveinterp.m	Linearly interpolate for a single point between the curves immediately above and below it, according to the previously regressed equation.	Current valve position, head across the valve
activator.m	Toggle the binary activation parameter to set the flow into individual reservoirs between Ashley Drive and Wyebank Road BPTs. Parameter is toggled based on the programmed control strategy for each reservoir.	**Reservoir levels, lower deadband limits, upper deadband limits, previous toggle parameter values**
activatorw.m	Toggle the binary activation parameter to set the flow into individual reservoirs after the Wyebank Road BPT. Parameter is toggled based on the programmed control strategy for each reservoir.	**Reservoir levels, lower deadband limits, upper deadband limits, previous toggle parameter values**
lambdafun.m	Calculate the friction factor for each pipe segment based on the Colebrook-White Equation.	Pipe relative roughness, **pipe diameters**, liquid density, **current iteration (j) flowrate through the pipes,** fluid viscosity, initial friction factor guess.
pdrops.m	Calculate the pipeline pressure drops according to the Darcy-Weisbach Equation.	Density, **pipeline friction factors, pipeline lengths, current iteration (j) flowrate through the pipes, pipe diameters**.

Table 10 -Summary of simulated scenarios

Number	Scenario Description (year)	Reservoir Initial Conditions	BPT Initial Conditions	Reservoir Draws
0	Normal operation test (2036)	50% Full	70% Full	Normal operation
1.1	Interaction test	50% Full	10% Full	Only NR5
1.2			50% Full	
1.3			99% Full	
2.1	consistency test (model verification)		10% Full	NR5 & Haygarth
2.2			50% Full	
2.3			99% Full	
3.1	Simple operation test (2036)		10% Full	NR5 & Haygarth & lumped draw before AD BPT
3.2			50% Full	
3.3			99% Full	
4.1	Stress test (2036)	50% Full	50% Full	All reservoirs after WR BPT
4.2				All reservoirs after AD BPT
4.3				All reservoirs between AD & WR BPTs
4.4				All reservoirs & lumped draw before AD BPT
5.1	Triple-step Test – Stress Test (2036)	50% Full	50% Full	Start: No reservoirs draw 90 min: All reservoirs & lumped term draw 180 min: No reservoirs draw
6.0	Power Outage (2036)	50% Full	50% Full	Normal Operation
6.1	Stress test + Power Outage (2036)	50% Full	50% Full	All reservoirs & lumped draw before AD BPT
6.2	Triple-step Test – Stress Test + Power Outage (2036)			Start: No reservoirs draw 90 min: All reservoirs & lumped term draw 180 min: No reservoirs draw
7.1a **7.1b** **7.1c**	Stress Test – Ashley Drive BPT compartment maintenance testing – (b – triple step test, c – triple step + power outage) (2036)	50% Full	70% Full	Normal Operation Start: No reservoirs draw 90 min: All reservoirs & lumped term draw 180 min: No reservoirs draw
7.2a **7.2b** **7.2c**	Stress Test – Wyebank Road BPT compartment maintenance testing – (b – triple step test, c – triple step + power outage) (2036)	50% Full	70% Full	Normal Operation Start: No reservoirs draw 90 min: All reservoirs & lumped term draw 180 min: No reservoirs draw
7.3a **7.3b** **7.3c**	Stress Test – One compartment in each BPT maintenance testing – (b – triple step test, c – triple step + power outage) (2036)	50% Full	70% Full	Normal Operation Start: No reservoirs draw 90 min: All reservoirs & lumped term draw 180 min: No reservoirs draw
7.4a **7.4b** **7.4c** **7.4d**	Sleeve Valve Maintenance (a – one in each BPT, b - two in each BPT, c – 2 in Wyebank Road BPT, d – 2 in Ashley Drive BPT) (2036)	50% Full	70% Full	Start: No reservoirs draw 90 min: All reservoirs & lumped term draw 180 min: No reservoirs draw
7.5a		50% Full	70% Full	Normal Operation

7.5b **7.5c** **7.5d**	Sleeve Valve Maintenance (a – one in each BPT, b - two in each BPT, c – 2 in Wyebank Road BPT, d – 2 in Ashley Drive BPT) (2036)			
8.0	Valve loss test (2036)	50% Full	50% Full	All valves suddenly open after 120 mins

5 DISCUSSION

After attaining a complete, working mathematical model that can compute the system response to a set of input conditions, simulations were carried out in assess the performance of the proposed Western Aqueduct (WA), to gain an understanding of the interactions within the system, and to determine limits of the operability of the WA. Preconceived scenarios were preferred to stochastic simulations and Monte Carlo methods, as an understanding of the systems behavior is required. These methods can still be used with the model for future work, and may find use in the optimization of the control system. These methods could also find use if the model is paired with modifications to the methods presented by Biscos et al. (2002), in order to optimise the scheduling for turbine generators at the BPTs or micro and pico-stations at the reservoirs, as per the development plans of the eThekwini Metropolitan.

Multiple scenarios were formulated and simulated within the model in order to delineate the effects of each of the components of the system, or to stress the system in order to understand the extents of the system operation. The simulated scenarios ranged from minor alterations that could be used to identify the effect of input conditions on the system behaviour, to step demand changes and simulations of power failures and maintenance situations, with various permutations of each. The stress tests, maintenance and power failure scenarios enable an understanding of how the operation of the system and its PLC control system are affected when placed under intense strain. This understanding allows for emergency preparedness and for the formulation of SOPs for such situations. Stress tests were preferred to stochastic simulations or Monte-Carlo type tests, as they can be carefully constructed to match a specific set of circumstances. The stress tests are also useful in determining the extents of the WA's ability to

perform satisfactorily. The simulation results, including those of the base case operation, can also be used as a precursor to the optimisation of the control system should any results not be within their intended ranges.

5.1 Scenario 1.1: Imposed steady draw at Ntuzuma (9) – Control 1.0

- All reservoir control systems overridden: Only Ntuzuma (NR5) draws continuously, at a steady rate.
- The imposed steady draw rate of Ntuzuma is that of its characteristic draw rate.
- NR5 has the largest individual reservoir draw, and is at the extreme end of the aqueduct.
- Draw rate based on projections for 2036 flows.
- Purpose:
    - Simple operational test to verify model performance and understand system interactions.
    - Neglects the impact of reservoir consumer demands and control systems on the performance of the WA system.
    - Provides insight to the effect of biased spatial allocations of demand (fire flows, new settlements etc.)

Scenario	**1.1**
Classification	Normal/override
Start time	00:00
Reservoir draws	override (NR5 only)
Sleeve valves active	AD - 3 WR - 3
Globe valves active	AD – 3 WR - 3
Control system	Control 1.0

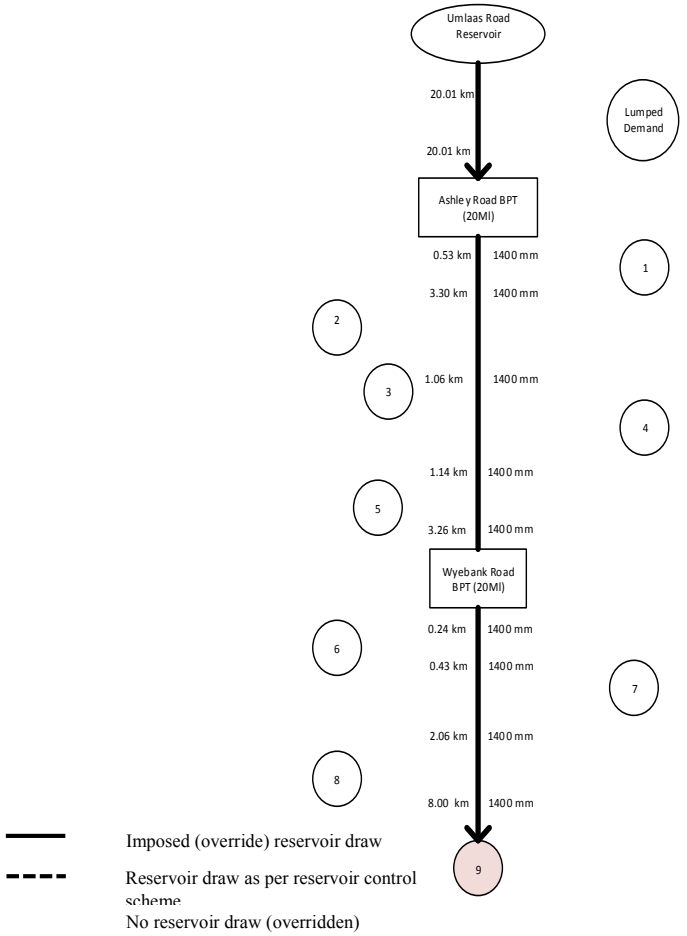

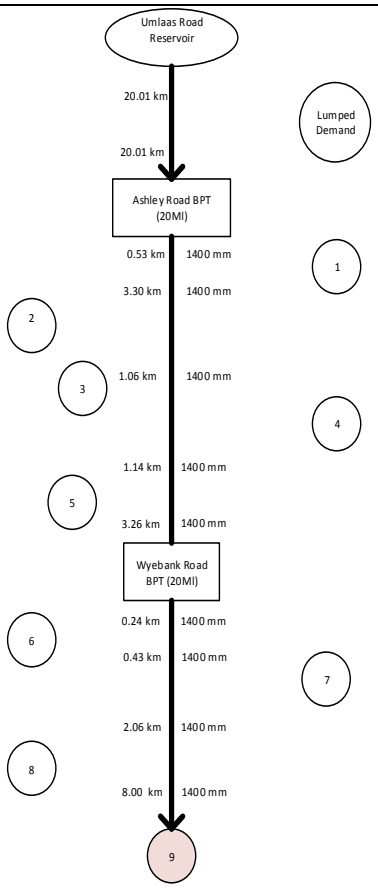

Rates: 2036

1- Simple operational test to verify model performance and understand system interactions.
2- Only NR5 drawing continuously at its steady characteristic flowrate.

Initial Conditions: All valves open, reservoirs 50 %, and BPTs 10% full.

Risk:

1- Valve oscillations - wear risk.
2- Settling level not at NOL (50% level) –overflow risk.
3- Globe valve active during normal operation – deviation from design intent

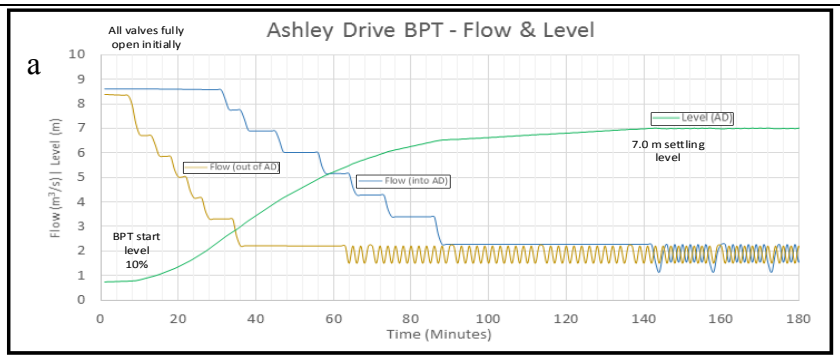

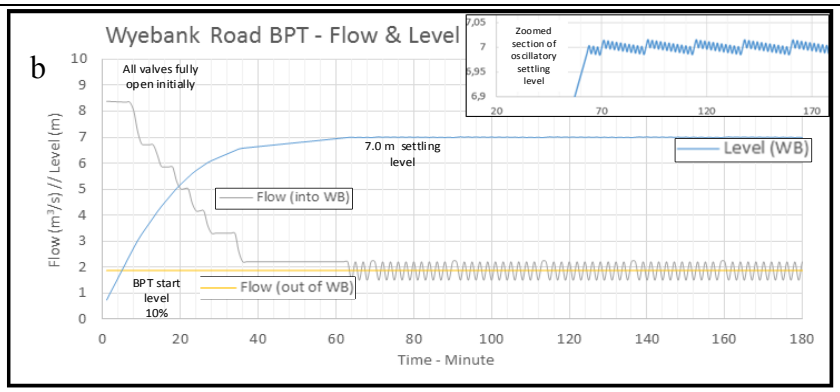

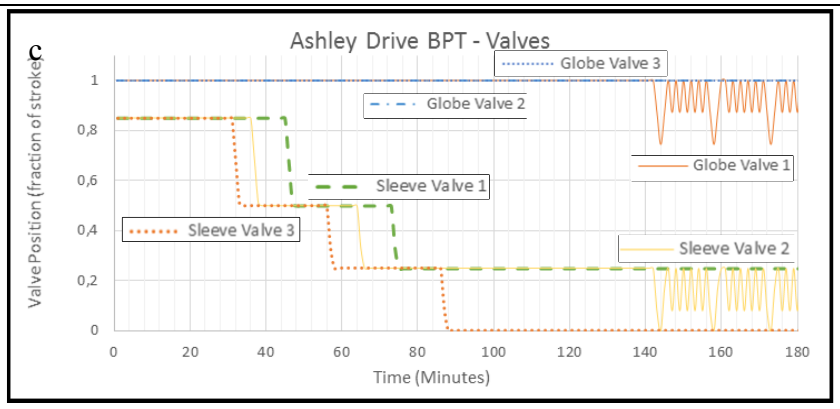

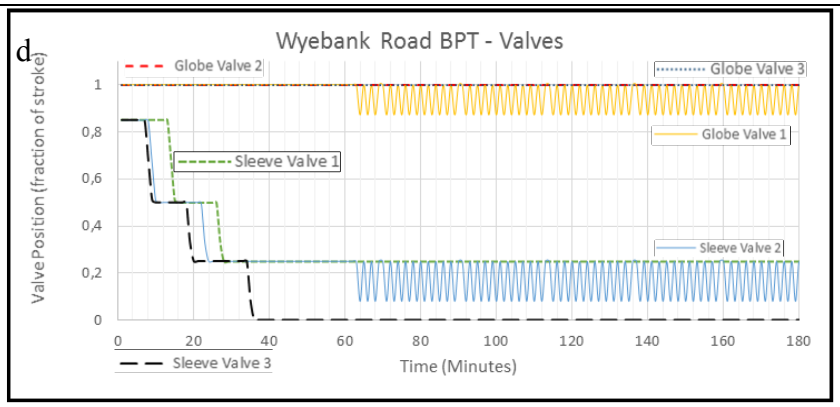

AD Initial: WR Initial

S1=	0.85	G1=	1	L^{AD}_{BPT}= 50% of capacity	S1=0.85	G1=1
S2=	0.85	G2=	1	L^{WR}_{BPT}=50% of capacity	S2=0.85	G2=1
S3=	0.85	G3=	1	L_{res}=50% of capacity	S3=0.85	G3=1

Other Observations:

Both BPTs establish settling levels at 7 m. AD after 140 mins and WR, 60 mins. Globe valve 1 and sleeve valve 2 switch to maintain level in an *oscillatory stable* state.

Figure 30 - Scenario 1.1 results overview – Imposed steady draw at Ntuzuma

- This scenario was envisaged to provide an uncomplicated set of results that could be used to analyse the system behavior in the absence of reservoir draw scheduling effects. It also enables a delineation and decoupling of the system components that interact in a complex manner during regular operation of the system. This test furthermore provides valuable insight into the operation of the system when the consumption demand is shifted toward a specific spatial location. The NR5 reservoir was selected to be overridden to draw constantly, due to it having the greatest consumer demand of the reservoirs downstream to the Wyebank BPT. Its average demand in 2036 represents 43.5% of the total anticipated demand downstream of the AD BPT in that year. It is also suited to the outcomes of this test due to it being at the extreme end of the aqueduct.
- The BPT initial volumes (10%) are representative of a highly unlikely scenario, possibly a rebound from a failure state, or reboot from emergency maintenance. Under normal circumstances, the control system ensures that the volume of liquid within the BPT would remain within the upper 20% of the BPT capacity. The other possible, and an increasingly plausible situation it could accurately represent, is a shortage of potable water supply. According to the control philosophy (Section 3.3.2), the valves would initially adopt a fully-open state in this situation.
- Figure 30a demonstrates the ability of the WR BPT to enact a greater demand draw upon the AD BPT than the AD BPT is able to demand from the supply source. This is understood from the marginal, yet observable difference between the supply and demand flows (AD BPT), despite the absence of direct draws between the AD and WR BPTs, and the presence of a sizable draw downstream of the WR BPT. It is anticipated that this result will be more clearly visible in the presence of direct draw(s) from the AD BPT (to reservoirs that are supplied between the two BPTs e.g. Haygarth Road), and will thus be discussed in more detail in Section 5.2.
- The constant WR BPT draw that is visible between 35 min and ~64 min in both Figure 30a (as the flow out of AD) and Figure 30b (as the flow into WR) corresponds to the lack of valve movements (WR BPT) within this period, as demonstrated in Figure 30d. An equivalent condition for the AD BPT is observed between 90 min and 140 min. This observation is explained by the BPT levels residing within the confines of a control system sub-range (6.5m<h<7.0m), in which no valve changes are stipulated. The prolonged length of these periods is due to the gradual (slowed) closure of the valves in a manner that resembles the action of an integral controller. It is within these periods that the BPT levels

gradually climb to 7 m, where an apparent settling level is consequently established. The control system is then seen to maintain this apparent settling level, thus causing the levels and valve positions to become '*oscillatory stable*'. The lack of visibility of the oscillations in the BPT level curves indicates that valve movement frequency is high enough to attenuate the resultant level oscillation. The presence of the minute oscillations within the level curves is shown in the inset image in Figure 30b and the zoomed section in Figure 31.

- The fitted-operation BPT control system mechanisms can be described through its determination of the systems behavior as presented in Figure 30 (a-d). As described in Section 3.3.2, the system consists of control sub-regions, at whose boundaries the adjustment of one or more control valves are stipulated, giving rise to 'staggered valve movements', as observed in Figure 30c and Figure 30d. This forms a system of *localized bang-bang control* where any flow imbalance will cause the BPT level to gravitate toward a specific sub-region boundary. This boundary is then established as the *settling level* until the downstream demand is altered to a sufficient extent to cause the level to drift to another sub-region boundary. Small flow imbalances will be compensated for through the aforementioned oscillatory movement of the valve around the established settling level. The traversing of a system boundary sets any valve that is programmed to move on a set trajectory toward its required position, governed only by the preset valve movement rate. It is thus likely that the control system will always establish BPT settling levels at these sub-region boundaries. The make-up of Control 1.0 resembles the principle of a proportional controller, where larger outlet flow demands will necessitate further opening of valves, and thus lower BPT levels.

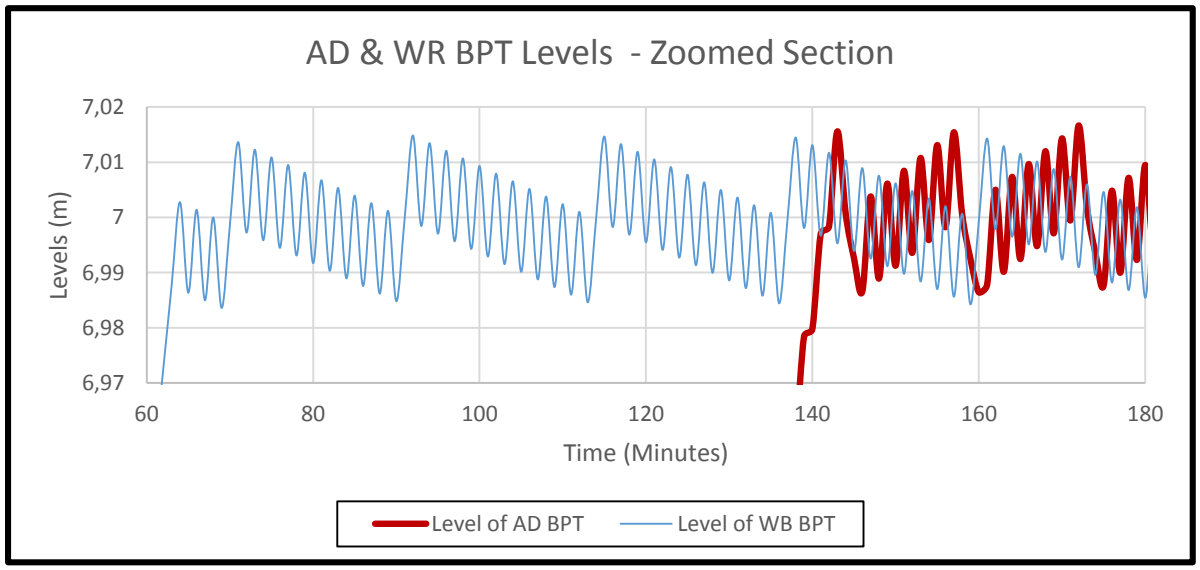

Figure 31 - Zoomed section around the oscillatory settling level of the BPTs.

- The irregular pattern of the oscillations depicted within Figure 31 are due to the difference between the flowrate change for the predetermined, fixed per-interval valve movement, and the outlet (demand) flowrate. The phenomenon will be discussed further in Section 5.2
- The high number of valve movements, required to maintain the '*oscillatory stable*' *settling levels* unintendedly resulting from the stipulated control philosophy (Control 1.0), are undesirable from both an operational, and a maintenance perspective. Such repeated valve movements are unnecessary and can increase the amount of wear on the valves.

5.2 Scenario 0: Normal operation (Base case) test – Control 1.0

- Base case test to represent the behavior of the Western Aqueduct under normal operating conditions
- Reservoir consumer demand draws determined by the consumer diurnal demand profile for the reservoir.
- Reservoir draw schedules (from the trunk mains) determined by the reservoir control system and the reservoir water level.
- Initial BPT volumes and reservoir levels are set to 50%, valves to their fully open states.
- All flows are based upon projections for 2036.
- Purpose:
    - Represents the most-encountered operational scenario. It is thus important to enact an analysis that can assist in the improvement of operations and possibly prompt optimization-based amendments to the system.
    - Determining the adequacy of the system to cope with the daily exertions, and to analyse the system behavior under these conditions
    - Assess the conformity of the system to design expectations

Scenario	**0**
Classification	Normal- Base case
Start time	00:00
Reservoir draws	Diurnal (all)
Sleeve valves active	AD - 3 WR - 3
Globe valves active	AD – 3 WR - 3
Control system	Control 1.0

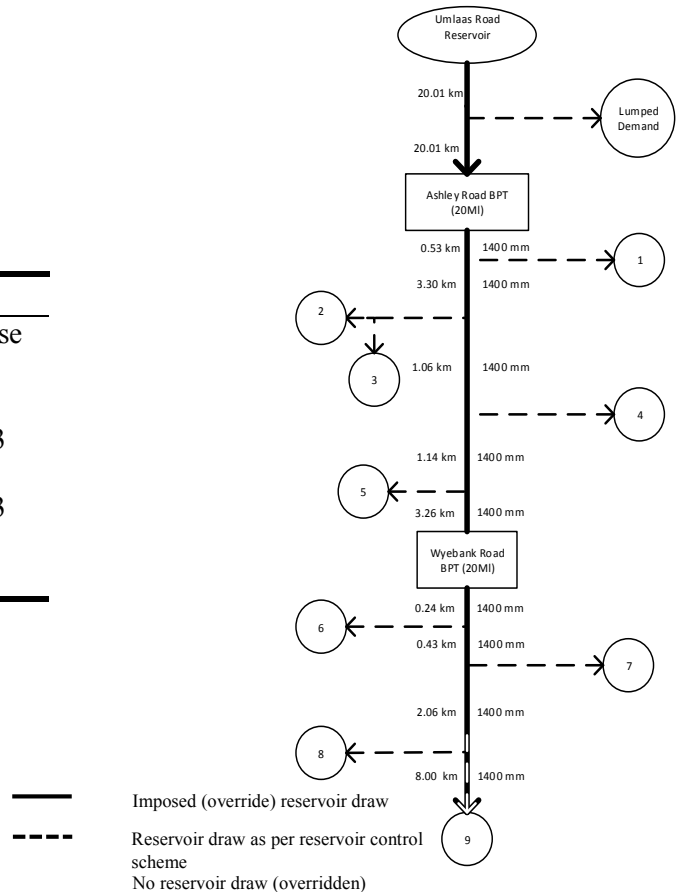

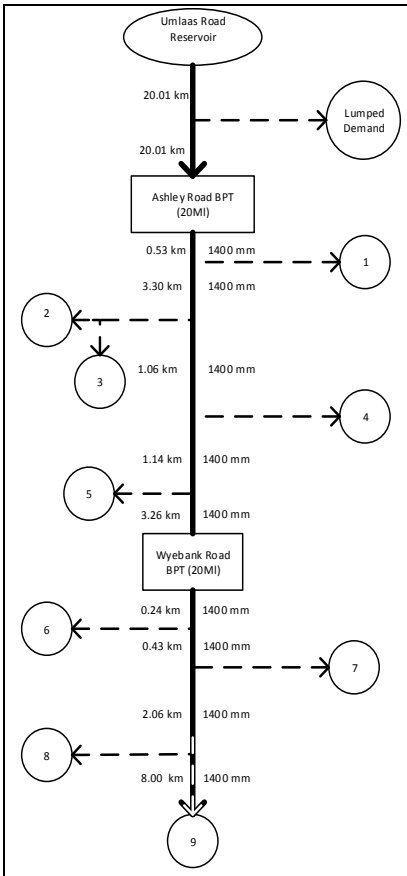

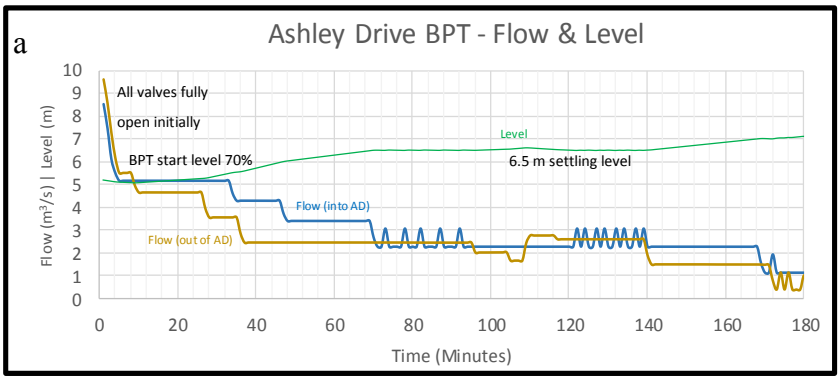

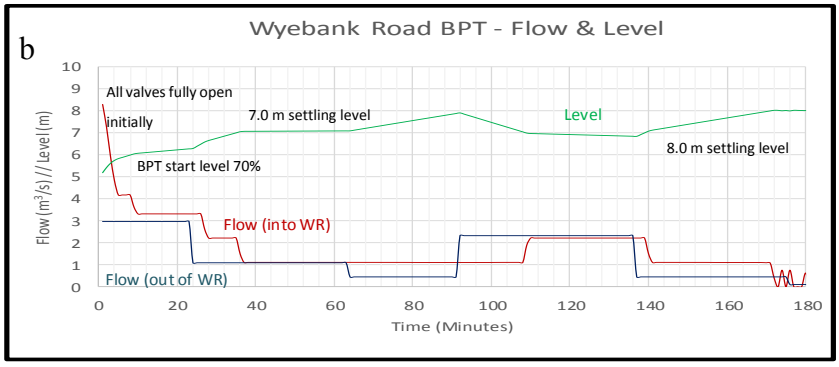

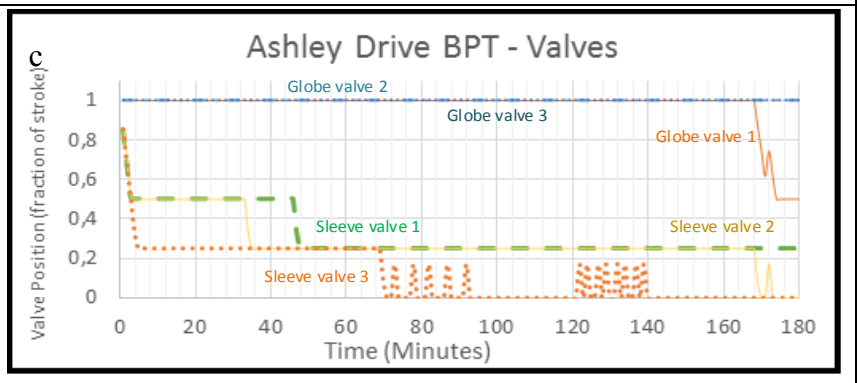

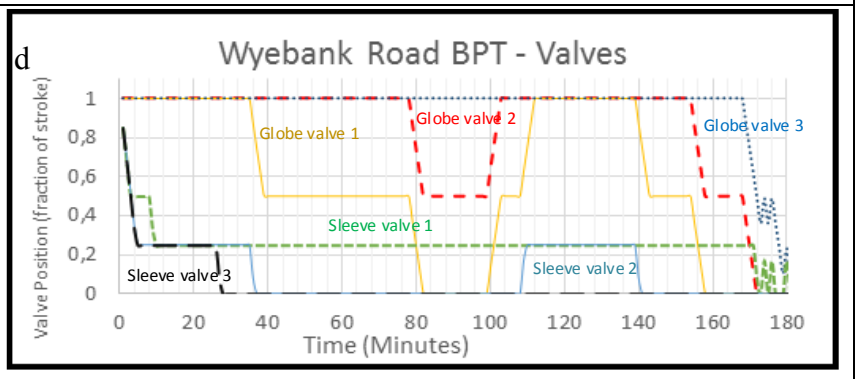

Rates: 2036

1- Represents the most-encountered operational scenario.
2- All consumer draws as per projected schedules. All reservoir draws from mains determined by control systems

Initial Conditions: All valves open, reservoirs 50 %, and BPTs 10% full.

Risk:

1- Valve oscillations - wear risk.
2- Settling level not at NOL (50%) –overflow risk.
3- Globe valve active during normal operation – deviation from design intent due to (2)

AD Initial: WR Initial

S1= 0.85 G1= 1 L^{AD}_{BPT}= 70% of capacity S1=0.85 G1=1

S2= 0.85 G2= 1 L^{WR}_{BPT}=70% of capacity S2=0.85 G2=1

S3= 0.85 G3= 1 L_{res}=50% of capacity S3=0.85 G3=1

Other Observations:

BPT design adequate to establish settling levels when demand variations are encountered. BPT settling levels vary, based upon variations in demand draws. Multiple valves perform duties in response to demand variations.

Figure 32 - Scenario 0 results overview – Normal operation (base case) test – Control 1.0.

- The base case operation was simulated for the design conditions that are anticipated in 2036. The results are important in determining the adequacy of the system to cope with the daily exertions, and to analyse the system behavior under these conditions. The necessity of this scenario is borne from the realisation that this represents the most-encountered (everyday) operational scenario. It is thus important to enact an analysis that can assist in the improvement of operations and possibly prompt optimization-based amendments to the system.
- Figure 32 depicts the simulation results for the AD and WR BPTs at base case conditions. The aforementioned ability of the WR BPT (Section 5.1) to demand a greater inlet draw than the AD BPT, can be most clearly observed by the large difference between inlet and outlet flow to the AD BPT, in Figure 32a. This is attributed to the shorter pipeline length from the AD BPT to the WR BPT (9.34 x10^3 m) compared to that from Umlaas Road to the AD BPT (40.01x10^3 m). The shorter pipeline length results in a lower line, and thus cumulative resistance on the inlet line to the WR BPT, since the valve types, numbers and configurations are identical in both BPTs.
- The maximum visible system throughput is 8.5 $\frac{m^3}{s}$ (734.4 $\frac{M\ell}{day}$) greatly exceeds the maximum design throughput (400 $\frac{M\ell}{day}$). This could be problematic in terms of strength of materials and maintenance. The maximum throughput is governed by the system hydraulics, when the inlet control valves are fully open. The throughput is thus determined by the interplay between the available upstream head, and the line resistance. For this reason, each independent pressure zone (Umlaas Road to AD BPT & AD BPT to WR BPT) would have a different maximum throughput, the smaller of which would be the limiting throughput for the system. This drastic under prediction of the maximum throughput could prove disastrous if a trunk main section were to rupture, especially in the absence of automated, intelligent override control. For example, if the trunk main leading from the AD BPT to the WR BPT were to rupture, the AD BPT control valves would open to 'supply' the rupture point, thus drawing at the maximum throughput rate from the Umlaas Road reservoir.
- The large initial (outlet) draw ($time = 0$) experienced by the AD BPT is due to the combination of the WR control system's required fill rate, in order to reach a *settling* level, and the effect of the simultaneous demands of the reservoirs after the AD BPT.

It should be noted that although the reservoir hydrographs obtained from Stephenson (2012) provide a consumer demand classification in one hour increments, the reservoir draws from the trunk mains are governed by the reservoir control system through its liquid level. The cumulative effect of the reservoir draws, that are most clearly observed as the WR BPT outlet flow (Figure 32b), therefore does not increment according to an hourly schedule, but according to the individual requirements of each reservoirs control system. The behavior of the reservoir levels (between the two BPTs) with time, for this base case scenario are shown in Figure 33.

- The synchrony of the reservoir draws from the trunk mains, which is thus *indirectly* determined by the consumer draws, has a major impact on the results of the model. The magnitude of the impact can be understood from the fact that the 2036 draws are significant with respect to the total capacity of the BPTs. The 2036 average daily demand on all reservoirs after AD is forecasted to be 185.9 $\frac{Ml}{day}$ ($BPT\ daily\ turnover\ rate\ =\ 9.3$) and that for all reservoirs after the WR BPT is forecasted to be 127.9 $\frac{Ml}{day}$ ($daily\ turnover\ rate\ =\ 12.8$). It is thus noted that the accuracy of the reservoir control policy; the projected consumer demand schedules and magnitudes are critical in the construction of an accurate representation of a system.
- The step-like synchronous effect of reservoir draws from the trunk main, is observed in Figure 32b as the WR BPT outlet flow. This step-like behavior can be attributed to the binary toggle that the reservoir control system utilises (valve open/closed or pump on/off) in order to toggle inlet flow (at the characteristic flowrate) to maintain the reservoir levels between the preset deadband limits. Although the consumer demand on each reservoir follows projected schedules and magnitudes (see Section 4.4), the effect on the trunk mains are determined by the level of the reservoir.

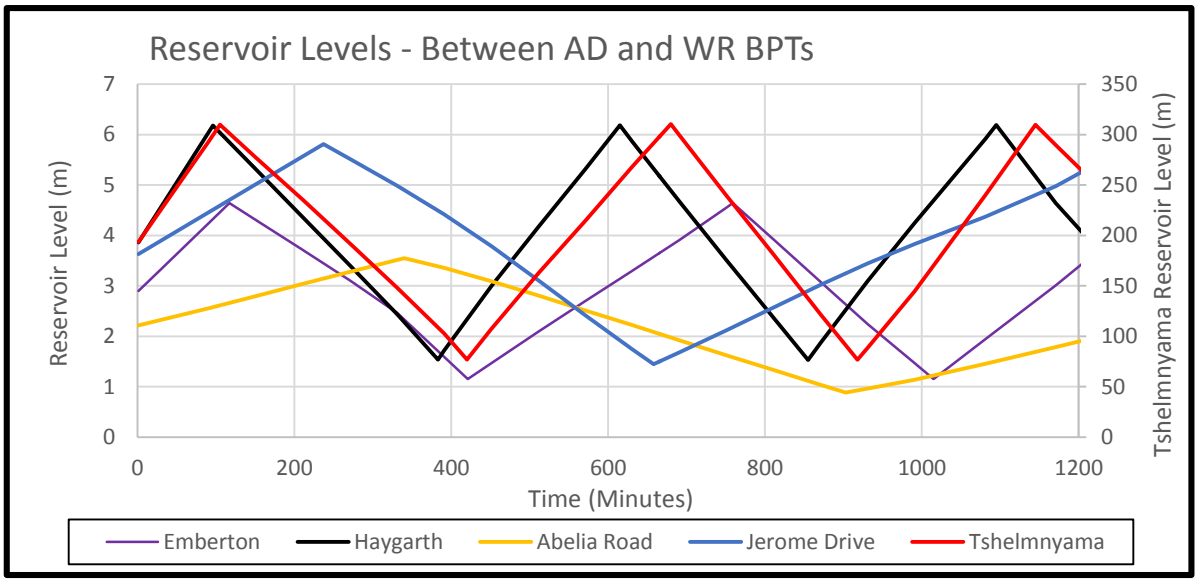

Figure 33 - Simulation results for the reservoirs between the two BPTs for base case conditions. Deadband control can be observed in the individual levels.

- A series of successive BPT (inlet) draw decreases (25 mins<t<35 mins) is observed in Figure 32a and Figure 32b after the initial elevated draw. This corresponds to the sequential closing of the inlet valves to the WR BPT leading up to the attainment of a *settling level* in the WR BPT and two reservoirs breaching their upper deadband limits at t=30 mins and t=70 mins (Haygarth and Tshelmnyama). All reservoirs represented in Figure 33, and the remaining reservoirs after the WR BPT, are still filling during the period t<100 mins, which accounts for the stable outlet flowrate observed for 30 mins<t< 90 mins. The effect of the aforementioned t=70 min reservoir draw toggle (off) is not observed within the AD BPT, as any excess flow is utilized in increasing the WR BPT *settling level.* The WR BPT *settling level* (Figure 30b) can thus be seen to be climbing toward the 8m level, from its current 7 m level. Further patterns are explained through an analogous reasoning process. The ultimate cause of the dynamic (shifting) *settling levels* can thus be said to be the cumulative effect of the diurnal demand profiles of the individual reservoirs. This is in turn due to the proportional-type control of Control 1.0, which must allow the BPT level to decrease to cause the inlet valves to open and thus admit higher flows.
- The dynamic behavior of the control system, as alluded to above, can be more clearly understood from Figure 32. The AD BPT can be seen to establish a settling level of 6.5 m for elevated demand spurts, and sustained demand flows above 1.5 m^3/s. At t=140 mins, upon the decrease of the outlet flow to 1.5 m^3/s, the inlet flow is maintained to adjust the

settling level to 7 m. Numerous instances of this behavior can be observed within both BPTs over the length of the simulation.

- The oscillation patterns (of the inlet flow curve) within the *settling level* maintenance periods in Figure 32a (75 mins<t<95 mins & 120 mins<t<140 mins) vary significantly. This can be attributed to the difference in the outlet (demand) flowrate from the BPT. The valve target positions within these two phases alternate between the same two settings (above and below 6.5 m level). The result is that the incremental, regulated change (valves per interval movement is fixed) in the valve positions (1 sleeve valve only) institutes a different effect on the BPT level. The difference in the effect on the BPT level is caused by the difference between the inlet flowrate change for the permitted valve movement, and the outlet flowrate that is determined by downstream demands (inlet flow does not match outlet demand). Within the first phase, since the outlet (demand) flow is lower, the incremental valve position alteration is sufficient to deliver a level increase that would allow the level to remain above the 6.5 m limit for ~3.5 mins. The greater outlet (demand) flow in the second phase however results in an oscillating pattern whose period is shorter. In this phase, the valve incremental opening can only sustain the level above the 6.5 m boundary for ~2 mins. The period between 40 mins<t<60 mins in Figure 32b does not show oscillatory patterns because a *settling level* has not been established, and the level is thus climbing, albeit at a minimal rate. Both BPTs can be observed to be reaching an individual *settling level* at t=180 mins.

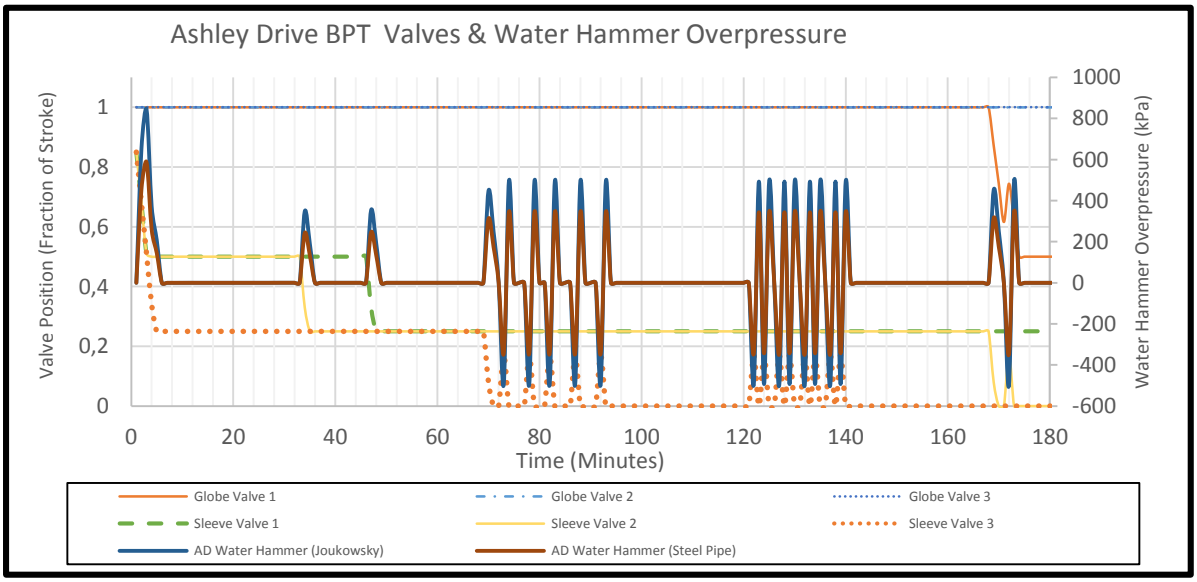

Figure 34 - Simulation results for the waterhammer transient phenomenon at the AD BPT (right axis). Valve positions are represented on the left axis – Control 1.0.

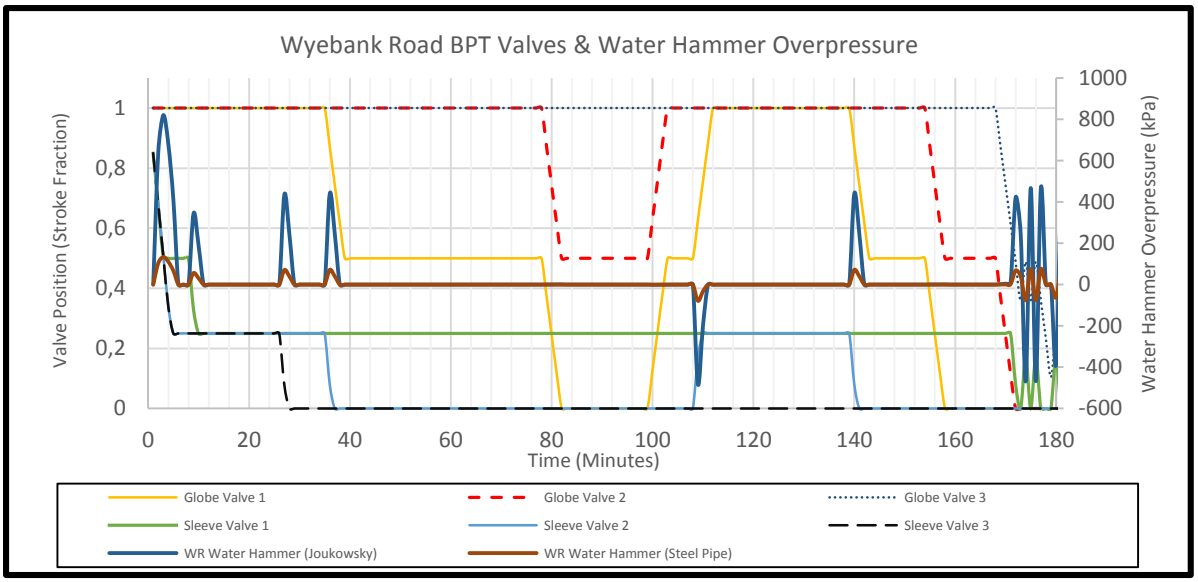

Figure 35- Simulation (Scenario 0) results for the waterhammer transient phenomenon at the WR BPT (right axis). Valve positions are represented on the left axis – Control 1.0.

Figure 34 and Figure 35 display the results of the transient analysis of the AD and WR BPTs respectively. The valve positions are also plotted on the same plot area in order to exhibit the causal relationship between the two variables. The inclusion of both the *steel pipe analogy* and the results of the Joukowsky equation computation is due to the limited applicability of the Joukowsky equation to the system. The limitations of the Joukowsky relationship arise as the valve closure times (600 sec) are greater than the maximum communication time ($\Delta t_{ct} \approx 84$ sec). Furthermore, the Joukowsky equation accounts for a complete valve closure, a situation that is never encountered within these scenarios due to the staggered nature of the PLC control system. This accounts for the drastically larger overpressures calculated for the Joukowsky equation, compared to those for the *steel pipe analogy*. The *steel pipe analogy* itself does not account for the elasticity of the pipe walls, nor for the fluid compressibility, and can thus be expected to *also* overpredict the overpressures.

The overpressure generation can be seen to occur at the same instant as a valve position change, due to the velocity change that accompanies the valve closure. The highest possible overpressure generation can be predicted to occur upon commencement of the simulation if the valve initial starting positions do not correspond to those of the PLC settings (Control 1.0 - Figure 18). This could result in the simultaneous movement of all valves that are out of position (albeit at their regulated movement rate) thus causing the compounding of the overpressure generated. A similar (yet less severe) situation is observed in both Figure 34 and Figure 35 (0

min <t< 4 min), when all three sleeve valves simultaneously move. In any other instance, when compliance to the PLC control system is found, the generated overpressure would tend to be of similar magnitude to one of the two possible magnitudes that could correspond to a single sleeve valve movement or a sleeve valve movement combined with a globe valve movement. The globe valve closures however, can be seen to cause a negligible overpressure. This is due to the fact that according to the control philosophy, upon movement of the globe valves, two of the three sleeve valves are already shut, thus already presenting a large resistance to flow. The result is that the globe valve closure does not correspond to a large change in the flowrate, consistent with its intended (design) purpose. The globe valve movements are however expected to generate appreciable overpressures when they are used to regulate flow in the event of a power outage.

It is observed from Figure 34 that the closure of the valves generates positive (forward) overpressures while opening of the valves generates negative (backward) overpressures, upstream of the valve. This directional analysis corresponds to Newton's Third Law.

The maximum overpressure generated (~8 bar) is appreciable with regard to the maximum static head (194m, 183.5m corresponding to 41.2% and 43.6% of the maximum static head respectively). Although the *steel pipe analogy* computation yielded lower, yet still appreciable results (1.1 bar), a detailed surge analysis is required to allay any doubts about the design integrity of the system, and to identify the need for mitigation measures. The necessity of the surge analysis is compounded by the neglecting of the effect of the Duffs Road (Aloes) reservoir in the original design.

5.3 Scenario 5.1: Triple step override test – Control 1.0

- Stress test to examine the adequacy of the system design to large, sustained demand variations.
- All reservoirs overridden (imposed flows) to draw from the trunk mains, at each reservoirs' respective characteristic flowrate, according to the following user setting:
    - *Step 1: At* $time = 0\ mins$*, all reservoirs overridden to cease drawing from the trunk mains.*
    - *Step 2: At* $time = 180\ mins$*, all reservoirs overridden to begin drawing from the trunk mains, continuously at their respective characteristic flowrates.*
    - *Step 3: At* $time = 360\ mins$*, all reservoirs overridden to cease drawing from the trunk mains.*
- Initial BPT volumes and reservoir levels are set to 50%, valves to their fully open states.
- All flows are based upon projections for 2036.
- Purpose:
    - Represents a string of worst-case scenario situations that could occur due to user demand variations or emergency conditions e.g. (large, widespread wildfires).
    - Determining the adequacy of the system to cope with extraordinary demand variations, and to offer insight to possible procedural improvements for such cases.

Scenario	**5.1**
Classification	Stress – triple step
Start time	00:00
Reservoir draws	Override (all)
Sleeve valves active	AD - 3 WR - 3
Globe valves active	AD – 3 WR - 3
Control system	Control 1.0

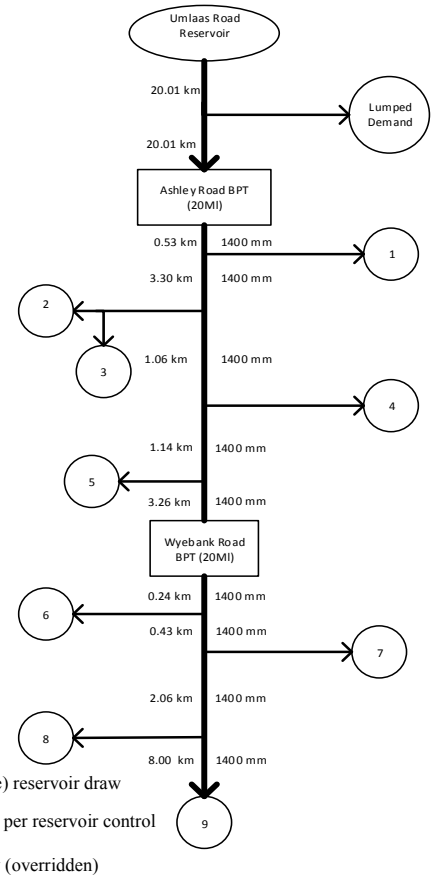

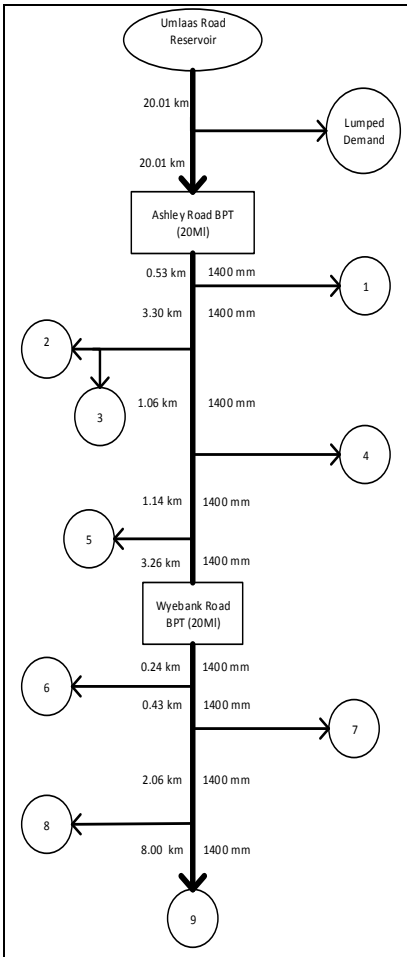

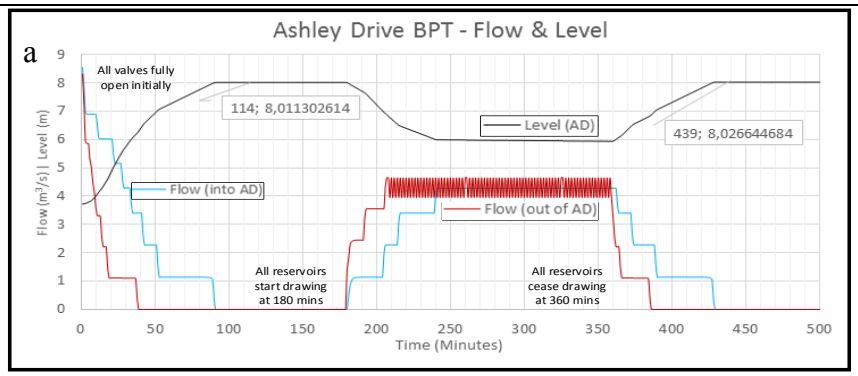

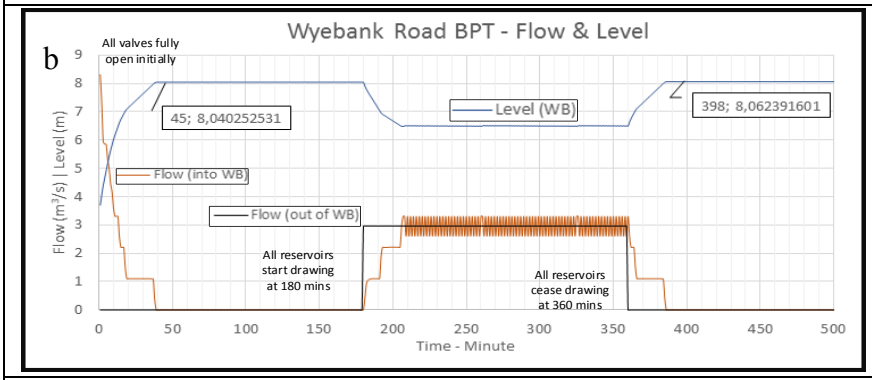

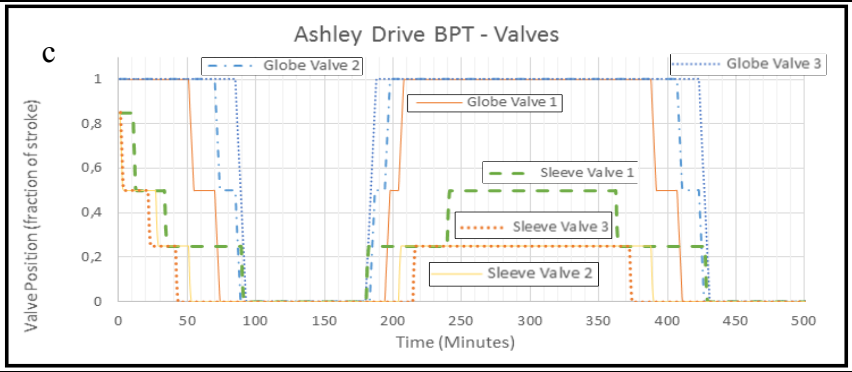

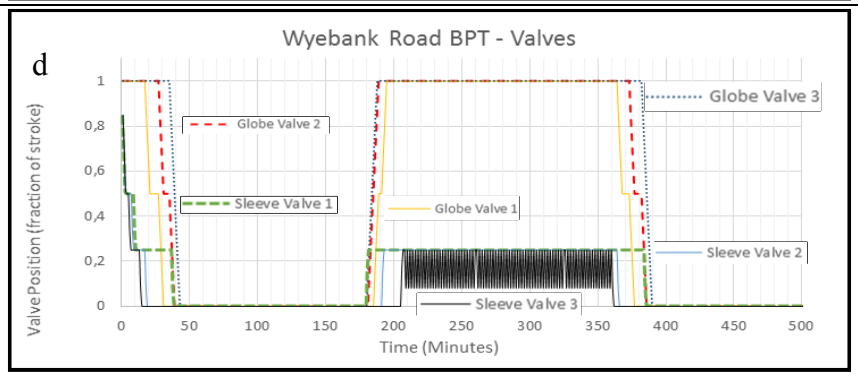

Rates: 2036

1- Represents a string of worst-case scenario situations
2- Used to analyse the WA's capability to cope with large user demand variations

Initial Conditions: All valves open, reservoirs 50 %, and BPTs 10% full.

Risk:

1- Valve oscillations - wear risk.
2- **Overflow risk** on step 1 and step 3
3- Settling level not at 50% level –overflow risk.

AD Initial: WR Initial

S1= 0.85 G1= 1 L^{AD}_{BPT}= 50% of capacity S1=0.85 G1=1

S2= 0.85 G2= 1 L^{WR}_{BPT}=50% of capacity S2=0.85 G2=1

S3= 0.85 G3= 1 L_{res}=50% of capacity S3=0.85 G3=1

Other Observations:

Both BPTs exceed 8.0 m when all downstream demands are ceased. Resumption of downstream demands causes the settling level in AD and WR to be 6.0 m and 6.5m respectively.
System copes well with maximum demand

Figure 36 - Scenario 5.1 results overview – Triple step override test – Control 1.0.

- Scenario 5.1 was designed in order to assess the system's response to rapid changes in demand, and to assess the volume changes within the BPTs under such circumstances. The triple-step stress test represents a string of worst-case scenario tests. This analysis is intended to provide valuable emergency preparedness for situations such as dispersed, runaway wild fires that would require massive, instantaneous water draws from numerous reservoirs around the affected regions. It also enables the evaluation of the valve closure times which aid in preventing transient overpressure, but can render the system sluggish in its reaction to demand cessations, thus causing catastrophic overflows within the BPTs.
- The system response to the lack of demand flows is observed within the starting period in Figure 36a and Figure 36b. The WR BPT (Figure 36d) can be seen to initially rapidly shut its valves in order to decrease the incoming flow, yet the valve closures are slowed between 20 mins and 40 mins. This is due to the restricted valve movement rates and staggered control arrangement and it allows the BPT level to rise to above 100% (8 m), although an overflow will not occur as an allowance as been provided within the BPT height (8.3 m is the overflow level). The filling of the BPTs to above their maximum level is undesirable, and action should be taken to prevent this occurrence.
- The final *settling level* is thus determined by the initial position of the globe valves and the rate to which their movement is restricted. Since no demand flows are stipulated in these test periods, the BPT level cannot not decrease. Thus, if the valves are initially all set to their fully open positions, and the BPT exit flow suddenly stops, a variable settling level, above its target settling level, is likely to occur.
- The similar response observed, from Figure 36a for the AD BPT, is notably slower. While it only takes ~39 mins for the WR BPT to reach its maximum level (stability), the AD BPT takes ~85 mins to reach stability. This can be explained through the volume differences between the two BPTs and their series arrangement. The WR BPT volume is half that of the AD BPT while their depths are equal. This combined with the WR BPTs ability to demand higher rates of inlet flows than the AD BPT, results in the WR BPT achieving an increase in level much faster than the AD BPT. The AD BPT response is thus slowed by its responsibility to supply the WR BPT, at a high rate. The WR BPT draw from the AD BPT is able to exceed the AD BPT inlet draw is because the BPT draws are governed only by the BPT levels and the interplay between the line losses and valve resistances, and not by any outlet flow control. The AD BPT inlet flow will thus always trail its outlet flow (Figure 36a).

- At the 180 min step, the outlet draw from the WR BPT instantly increases from zero to the sum of the characteristic flows (2.96 m^3/s) for the reservoirs downstream of the BPT. The WR BPT can then be observed to establish its new settling level at 6.5 m within ~26 mins (Figure 35b). The AD BPT (Figure 35a) however, due to its aforementioned responsibility to indirectly respond to the WR BPT level, does not exhibit the clarity of the described step increase in outlet flow. The average magnitude of the subsequent increase however, can be seen to be the sum of the characteristic flows of all the reservoirs downstream of it (4.33 m^3/s). The AD BPT reaches stability within ~60 mins of the step, at a level of 6 m. The discrepancy between the stability levels of the BPTs can be explained by the difference between the supply and demand capabilities of the two BPTs. The WR BPT is able to demand more inlet flow than the AD BPT, yet must supply a smaller outflow, allowing its stability level to be higher than that of the AD BPT (according to the PLC scheme in Figure 18, lower levels correspond to lager inflows). The AD BPT's PLC control system must thus satisfy the demand with a lower settling level.

5.4 Sensitivity tests (longevity) – Control 1.0

Various sensitivity tests were conducted in order to examine the limits of the longevity of the WA system, and to assess the change in its performance over an extended time period. Consumer demands increase yearly according to forecasted (y/y) growth factors. This results in the BPT levels decreasing successively, as explained in Section 5.3.

5.4.1 Scenario 5.1

Scenario	**5.1**
Classification	Stress – triple step
Start time	00:00
Reservoir draws	Override (all)
Sleeve valves active	AD - 3 WR - 3
Globe valves active	AD – 3 WR - 3
Control system	Control 1.0

The instantaneous shutting off of all draws from the trunk main results in a slight overshoot of the 8 m (100%) level, necessitating some form of remedial action. In order to assess the impact of sustained elevated demands and rapid demand changes for higher flows, a sensitivity analysis of the time taken for BPT to reach its stability level at the second step (refer to Section 5.3) was conducted. The results of the test, with regards to the BPT stability levels for the second step (all draws *on*) correspond closely to the sensitivity plot for Scenario 4.4 due to the similar conditions, and the discussion will thus be deferred. The settling level for the no-draw steps (step 1 & step 3) remains as 8 m for both BPTs for all years of operation, yet the aforementioned overshoot (below overflow level) always occurs.

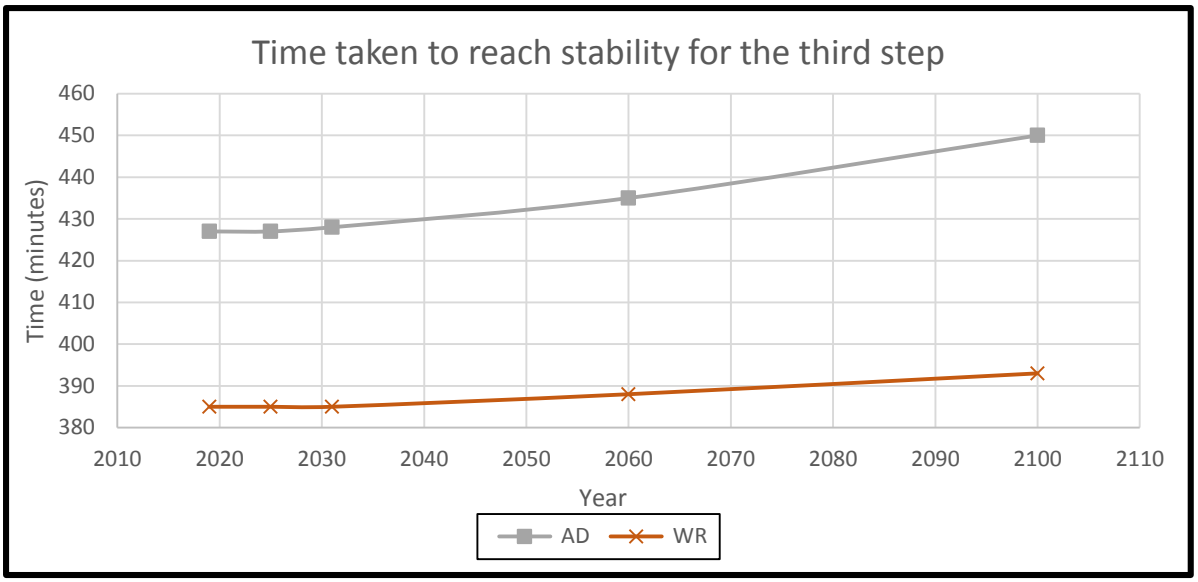

Figure 37 - Sensitivity plot of the time at which stability levels of the BPTs are reached for the third step (toggle draws off) in Scenario 5.1 vs the year of operation – Control 1.0.

It is observed in Figure 37 that the system takes a progressively longer time to establish its settling level. This is due to a consistently decreasing (with year) settling level, that is attained when the reservoir draws are toggled on at t=180 mins. The reason for the decrease in stability level is provided in Section 5.4.3 is thus the increasing downstream demand and the resultant decrease in settling level, that is required cause an increase in the inlet flowrate.

5.4.2 Scenario 4.3

Scenario	**4.3**
Classification	Stress – localized elevated demand
Start time	00:00
Reservoir draws	Override (between BPTs) – no lumped draw
Sleeve valves active	AD - 3 WR - 3
Globe valves active	AD – 3 WR - 3
Control system	Control 1.0

Scenario 4.3 was developed to test the interaction of the BPTs in the absence of draws downstream to the WR BPT. This allowed for the *isolation* of the AD BPT and the reservoirs it supplies directly from the delayed effects of the WR BPT and its downstream draws. All reservoirs between AD BPT and WR BPT were thus set (imposed flows - overridden control system) to draw from the trunk mains at their characteristic flows. All other reservoirs and the

lumped demand term (halfway between Umlaas Road and the AD BPT) were set to cease any draws from the trunk mains. The initial BPT volumes were set to 50%, as were the initial reservoir volumes, while the valves were set to their fully open states.

The overdesign within the BPT subsystems renders the system capable of managing the 2036 flows, in a manner that is similar to, but less stressful to the system than Scenario 5.1.

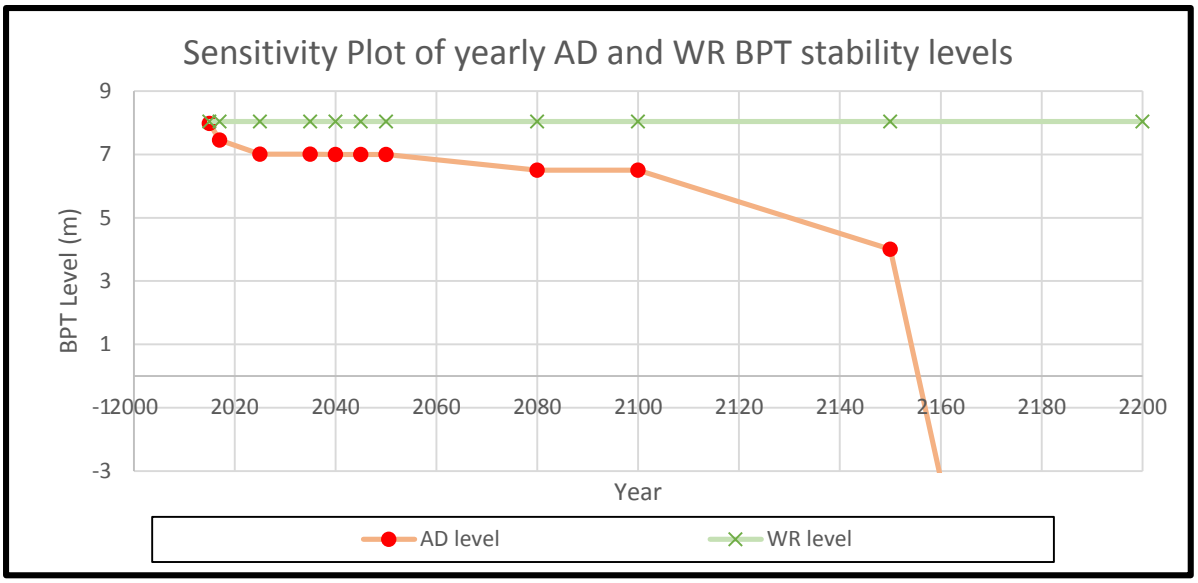

Figure 38 - Sensitivity plot of the stability levels of the BPTs for Scenario 4.3 conditions vs the year of operation – Control 1.0.

Figure 38 presents a sensitivity plot of the BPT stability levels (Scenario 4.3) to the year of operation. The demand flows increase yearly in a compounded manner, thus affecting the operation of the system. Although the sensitivity is plotted against the year of operation, it therefore also applies to a commensurate increase in flow. The WR BPT level remains constant as there are no draws downstream to it, and so the valves simply remain shut, rendering it a *dead end*.

The reasons for the successive decreases in the stability level of the AD BPT have been provided in Section 5.3. The AD BPT can be seen to fail (unable to replenish its level) in the year 2155. The 119 years, between the design year and the year of the projected failure, represents an acceptable (*if not too high*) overdesign margin.

5.4.3 Scenario 4.4

Scenario	4.4
Classification	Stress – localized elevated demand
Start time	00:00
Reservoir draws	Override (After AD) – no lumped draw
Sleeve valves active	AD - 3 WR - 3
Globe valves active	AD – 3 WR - 3
Control system	Control 1.0

Scenario 4.4 was developed to test the response of the system to sustained, elevated draws, which could be realized in the event that fire flows become necessary. The lumped demand upstream of the AD BPT was set to zero in order to negate its effects on the BPTs. All reservoirs after the AD BPT were set (overridden control system) to draw from the trunk mains at their characteristic flows. The initial BPT volumes were set to 50%, as were the initial reservoir volumes, while the valves were set to their fully open states.

The large overdesign within the BPT subsystems also renders the system capable of managing the 2036 characteristic flows, even for a sustained period of time.

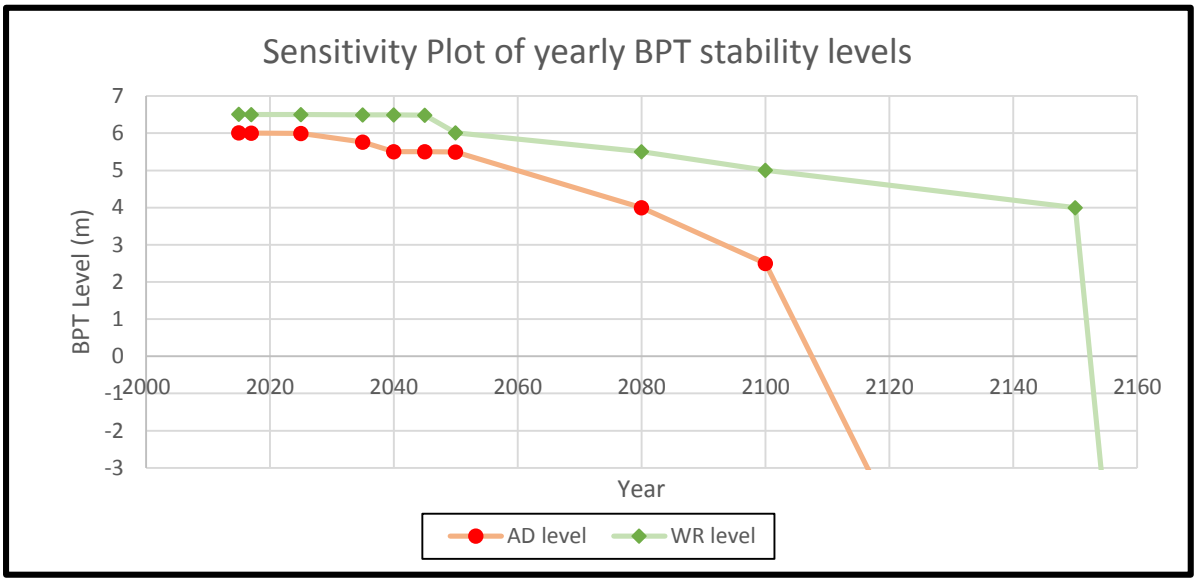

Figure 39 - Sensitivity plot of the stability levels of the BPTs for Scenario 4.3 conditions vs the year of operation.

The sensitivity plot presented in Figure 39 for Scenario 4.4 is analogous to that presented in Figure 38. The activity of the WR BPT, due to the exertions of the sustained downstream draws, however places an additional strain on the AD BPT, which accelerates its decline in adequacy.

The AD BPT can thus be seen to fail during the year 2106 and the WR BPT during 2152. The margin of safety, in terms of the number of years to failure, is sufficient to instill confidence in the design.

5.5 Scenario 6.0: Power loss test - Normal operation – Control 1.0

- The power loss test (under normal operating conditions), is meant to represent the behavior of the Western Aqueduct under normal operating conditions in the event of a loss of electricity.
- The loss of electricity renders the sleeve valves inoperable. The simulation thus involves the sleeve valves adopting a fully-open position upon the loss of electricity.
- AD BPT level shown for multiple scenarios. All other results for Scenario 6.0
- Reservoir consumer demand draws and trunk main draw schedules are as per the test description. (6.0 – normal operation, 6.1 – all reservoirs draw, 6.2 – triple step test) (see Table 10).
- Initial BPT volumes and reservoir levels are set to 50%, valves to their fully open states.
- All flows are based upon projections for 2036.
- Purpose:
    - Represents an oft-encountered scenario, which was given due consideration during the design phase. It is thus important that the system deal adequately with such situations, particularly under normal operating conditions.
    - Determining the adequacy of the system to cope with the daily exertions, and to analyse the system behavior under these conditions

Scenario	6.0
Classification	Stress – power loss
Start time	00:00
Reservoir draws	Diurnal (all)
Sleeve valves active	AD - 3 WR - 3
Globe valves active	AD – 3 WR - 3
Control system	Control 1.0

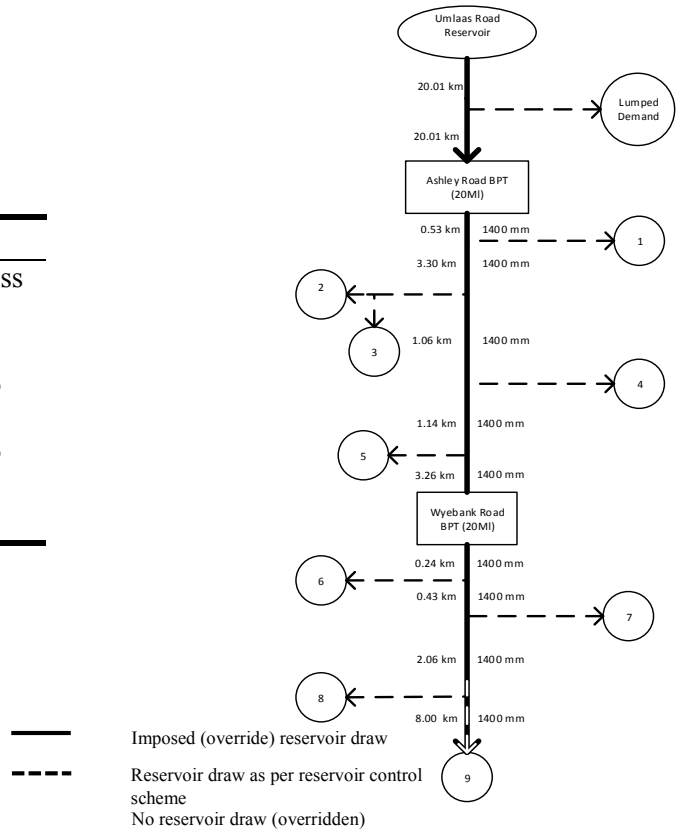

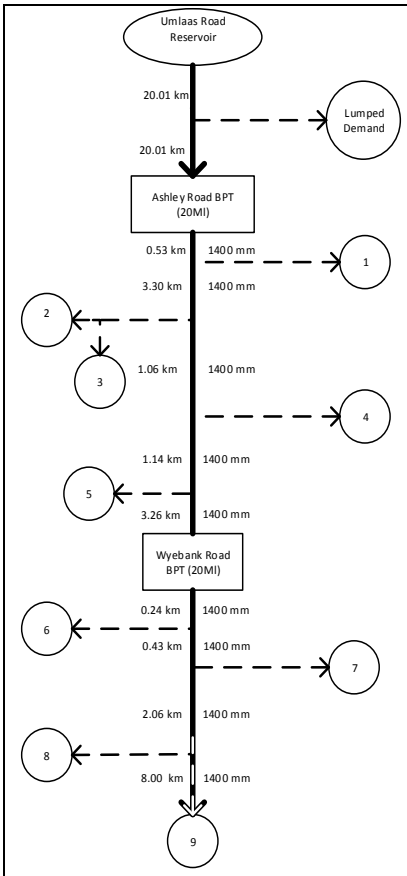

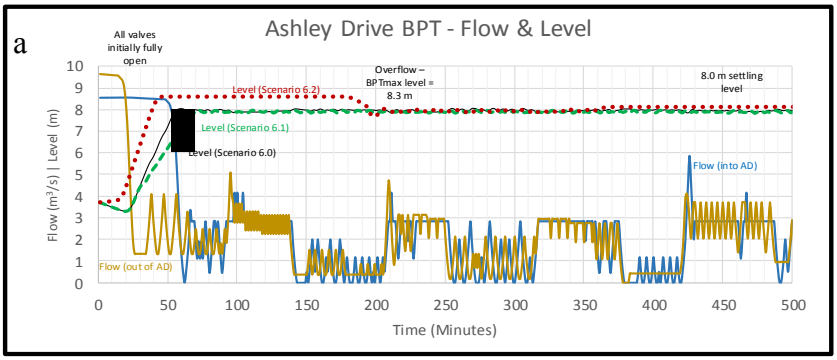

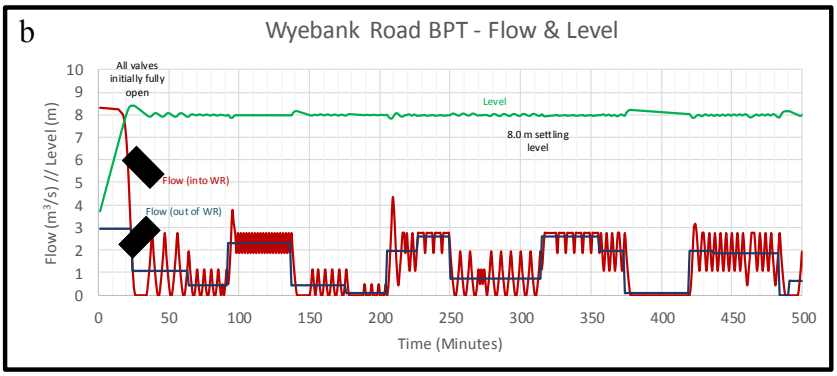

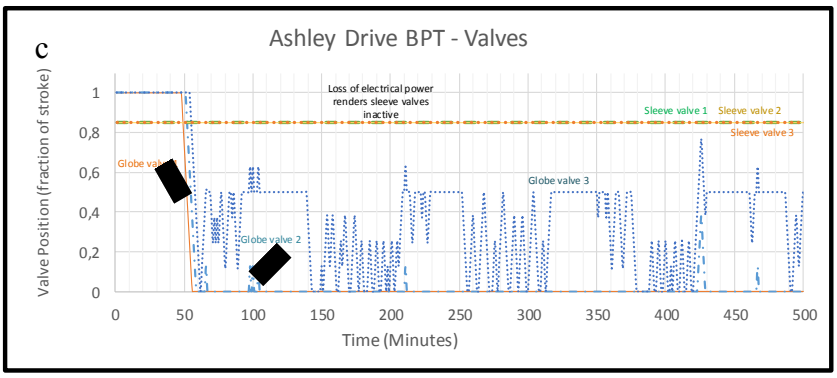

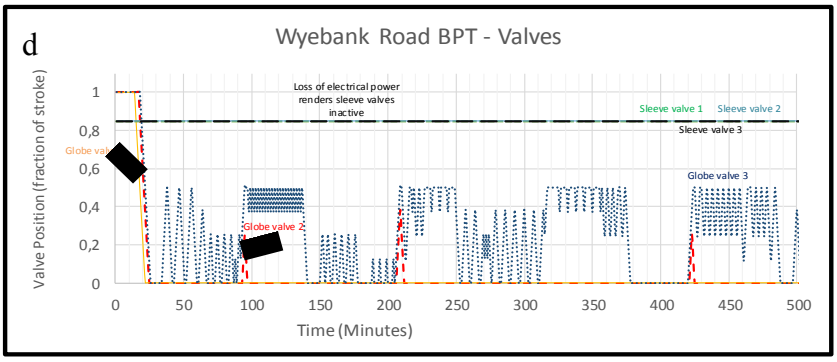

Rates: 2036

1- Simulates the likely situation of a power outage. The sleeve valves are rendered inoperable.
2- Was considered during the design phase

Initial Conditions: All valves open, reservoirs 50 %, and BPTs 10% full.

Risk:

1- Overflow – Both BPTs overshoot their maximum level
2- Valve oscillations - wear risk.
3- Settling level not at 50% level –overflow risk.

AD Initial: WR Initial

S1= 0.85 G1= 1 L^{AD}_{BPT}= 50% of capacity S1=0.85 G1=1

S2= 0.85 G2= 1 L^{WR}_{BPT}=50% of capacity S2=0.85 G2=1

S3= 0.85 G3= 1 L_{res}=50% of capacity S3=0.85 G3=1

Other Observations:
Globe valve reaction too slow, resulting in overflows in both BPTs. Globe valves oscillate with a higher amplitude than when sleeve valves are active – maintenance (wear) risk. Third step produces no significant change (Scenario 6.2).

Figure 40 - Scenario 6.0 results overview – Power loss test (normal operation).

- Scenario 6.0 is a mathematical representation of the very likely situation of a loss of electricity. Scenario 6.1 and 6.2 subject the WA system to stressed operating conditions in the absence of electricity (conditions in Table 10). South Africa has in recent times been plagued with electricity cuts in the form of *load shedding*. Much consideration was given to this situation during the design of the control system and the associated control elements (Section 3.2.1). The results of this scenario therefore will impact on the level of certainty in the design of the BPT control system, and may underpin the necessity for optimization of the PLC control system.
- During the power outage, as shown in Figure 40(a-d), the sleeve valves are rendered ineffective, and so the flow regulating function is assumed by the globe valves. It immediately becomes apparent from the somewhat more rapid and violent oscillations of the BPT-controlled flowrates (Figure 40(a-b)), that the tightness of control is increased. This can be attributed to a greater sensitivity of the inlet flow rate to an incremental change in the globe valve position (higher regulated movement rate), than that for the sleeve valves in combination with the globe valves.
- Observable oscillations within the BPT level curves (Figure 40(a-b)) also reinforce the observation that the sensitivity of the inlet flowrate to the globe valve movements is higher. This will cause the magnitude of the generated waterhammer overpressures to increase significantly. Figure 40(c-d) shows that the globe valve movements are rapid, and of a large magnitude. The high number of oscillations could present a maintenance issue.
- The delayed movement of the globe valves (see Figure 18 for the control algorithm) causes the level to overshoot the 8.0 m settling level. No overshoot is observed in the analogous scenarios when the sleeve valves are active. The delayed movement of the globe valves is particularly perilous in the case of a low initial level. The level curve (Scenario 6.2) in Figure 40(a) shows a large overshoot (8.57 m) from the 8.0 m settling level that extends far over the maximum capacity of the BPTs (8.3 m), thus causing an overflow.
- The BPT response to demand variations is more rapid - this is best observed by the ability of the system to closely maintain the 8.0 m settling level, upon cessation of the demand flows at 180 mins (Figure 40(a) – Scenario 6.2). This can also be seen from the lack of a large overshoot, as observed in the analogous Scenario 5.1, upon the cessation of demands at 360 minutes.

5.5.1 Water hammer analysis – Scenario 6 – Control 1.0

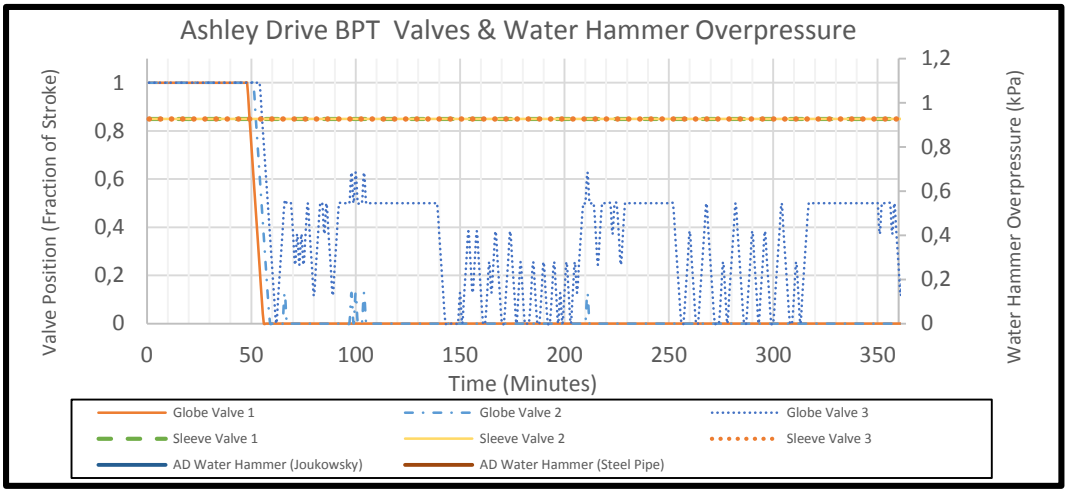

Figure 41 - Results of the water hammer analysis for Scenario 6. Overpressures are plotted on the right axis and valve movements are on the left axis.

Figure 41 presents the results of the water hammer analysis for Scenario 6.2. A significantly higher number of overpressures are generated, with a larger magnitude, than the equivalent scenarios wherein the sleeve valves are active. The large overpressure generated at ~55 minutes is caused by the simultaneous closures of the valves.

5.6 Scenario 7.3: Maintenance (compartment) test – Control 1.0

- Intended to represent the response of the WA to varying conditions during maintenance of a BPT compartment.
- One compartment in each BPT out of service, thus halving the effective volume of the BPTs.
- AD BPT level shown for multiple scenarios. All other results for Scenario 7.3a
- Reservoir consumer demand draws and trunk main draw schedules are as per the test description (7.3a – normal operation, 7.3b – triple step test) (see Table 10). Base case (Scenario 0) shown for comparison.
- Initial BPT volumes and reservoir levels are set to 70% and 50% respectively, valves to their fully open states. All flows are based upon projections for 2036.
- Purpose:
    - The BPT maintenance, and uninterrupted supply during this scenario, was a major consideration during the design phase. Such a scenario is thus important in asessing the resultant design.
    - Useful in drawing up SOPs for maintenance, and in the preparation of maintenance schedules.

Scenario	7.3a
Classification	Stress – BPT compartment maintenance
Start time	00:00
Reservoir draws	Diurnal (all)
Sleeve valves active	AD - 3 WR - 3
Globe valves active	AD – 3 WR - 3
Control system	Control 1.0

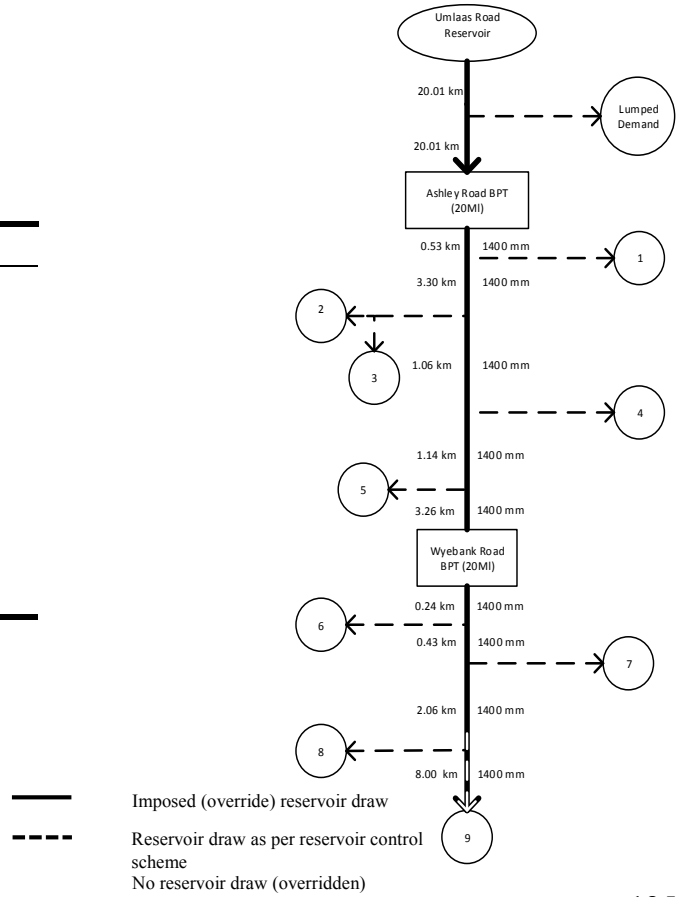

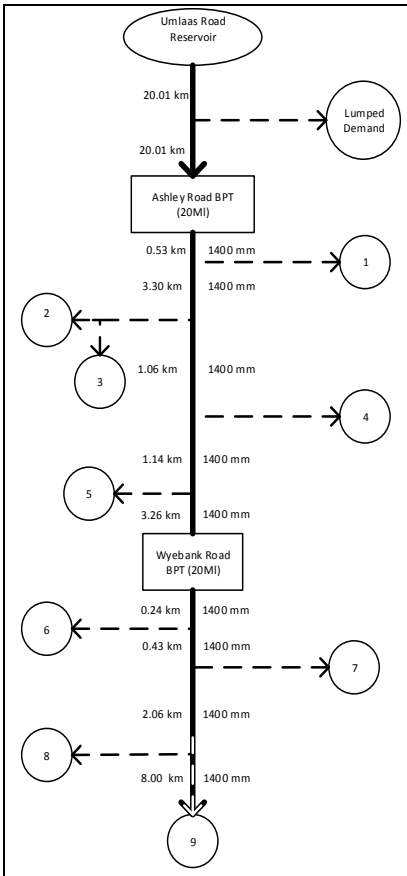

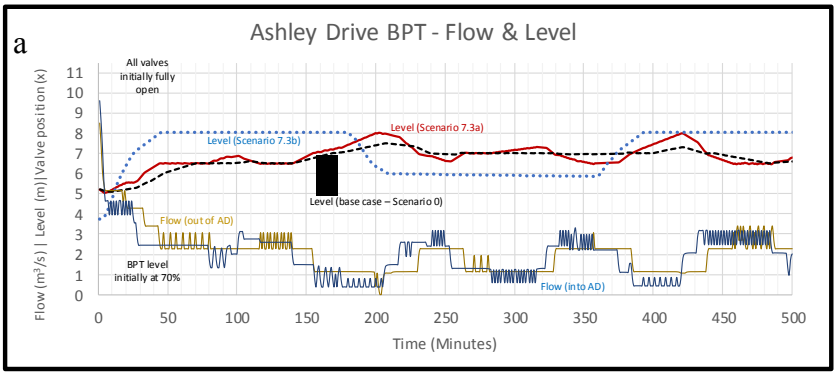

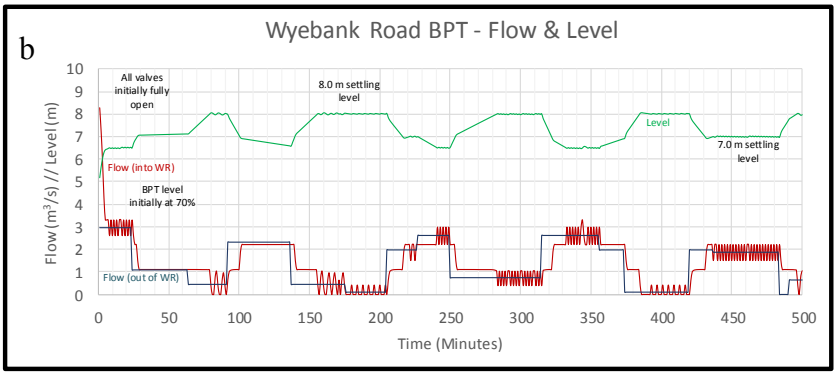

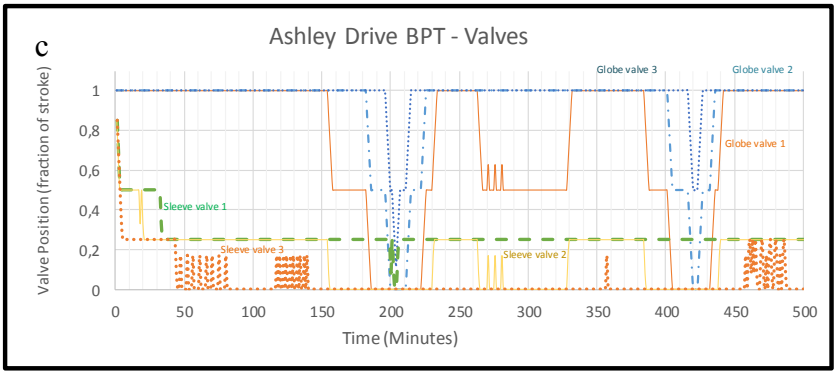

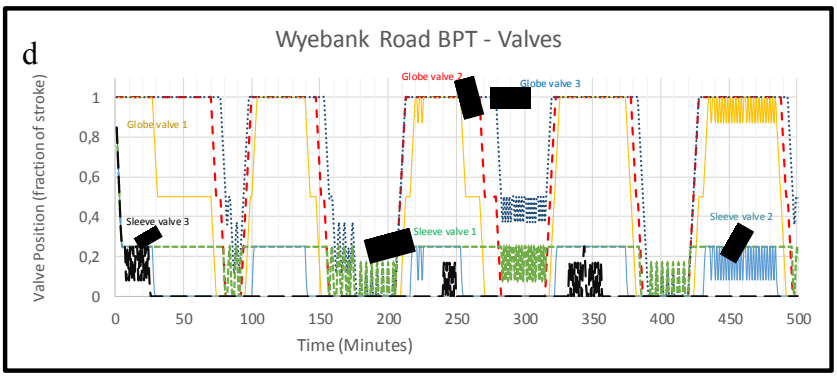

Rates: 2036

1- important in asessing the design.

2- Useful in drawing up SOPs for maintenance, and in the preparation of maintenance schedules.

Initial Conditions: All valves open, reservoirs 50 %, and BPTs 10% full.

Risk:

1- Larger number of valve movements presents a greater maintenance/wear risk
2- No added risks/adverse effects due to maintenance.

AD Initial: WR Initial

S1= 0.85 G1= 1 L^{AD}_{BPT}= 70% of capacity S1=0.85 G1=1

S2= 0.85 G2= 1 L^{WR}_{BPT}=70% of capacity S2=0.85 G2=1

S3= 0.85 G3= 1 L_{res}=50% of capacity S3=0.85 G3=1

Other Observations:

Both BPTs cope satisfactorily under these conditions. The demand draw variations have a larger impact on the level within the BPTs.

Figure 42 - Scenario 7.3a results overview – Maintenance (compartment) test.

- This scenario is intended to represent the WA performance during the simultaneous maintenance of a single compartment within each BPT. The results of the test would thus be used to provide an assurance of the ability of the system to maintain normal supply when maintenance is required. Furthermore, maintenance schedules and standard operating procedures for maintenance can be drawn up, by using the results of this scenario test.
- Figure 42a presents the results of the base case test (Scenario 0) for the AD BPT level together with the results of Scenario 7.3a and Scenario 7.3b. The base case AD BPT level can be seen to be more flat, and thus less sensitive to downstream demand variations than the equivalent results for Scenario 7.3a. This is attributed to the reduced operational surface area within the BPTs. For this reason, the BPT response to the triple step test (~20 mins to reach stability after each step) is markedly more rapid than the response observed in Scenario 5.1 (~45 mins to reach stability after each step).
- Although the reduced operational area causes larger fluctuations in the BPT level due to downstream demand variations, the control system is capable of maintaining supply. This can be observed by the overall adherence of the AD BPT level curve (Figure 42a) to the base case curve. In order to achieve this, the control system can be observed to be demanding a greater number of valve movements (Figure 42(c-d)).
- The ability of the system to cope with Scenario 7.3a conditions is unsurprising, as this scenario was considered during the design phase, and is thus included within the overdesign. Although the level of overdesign is consoling, the necessity of such a large overdesign should be evaluated, considering the associated increase in capital and operations costs.

5.7 Scenario 7.5: Maintenance (sleeve valve) test – Normal operation – Control 1.0

- Intended to represent the response of the WA under normal conditions during maintenance of combinations of varying permutations of the BPT inlet sleeve valves.
- One sleeve valve in each BPT out of service, thus eliminating a parallel leg from the inlet sleeve valve parallel arrangement.
- AD BPT level shown for multiple scenarios. All other results for Scenario 7.5a (7.5a – one valve in each BPT, normal operation; 7.4a – one valve in each BPT, triple step test; 7.5b – two valves in each BPT, normal operation; 7.4d – two valves in AD BPT only, triple step test) (see Table 10).
- Reservoir consumer demand draws and trunk main draw schedules are as per normal operation. Initial BPT volumes and reservoir levels are set to 70% and 50% respectively, valves to their fully open states. All flows are based on 2036 projections.
- Purpose:
    - Important in asessing the efficacy of the design, due to the emphasis placed on this scenario during the design stages.
    - Useful in drawing up SOPs for maintenance, and maintenance schedules.

Scenario	7.5a
Classification	Stress – Sleeve maintenance
Start time	00:00
Reservoir draws	Diurnal (all)
Sleeve valves active	AD - 2 WR - 2
Globe valves active	AD – 3 WR - 3
Control system	Control 1.0

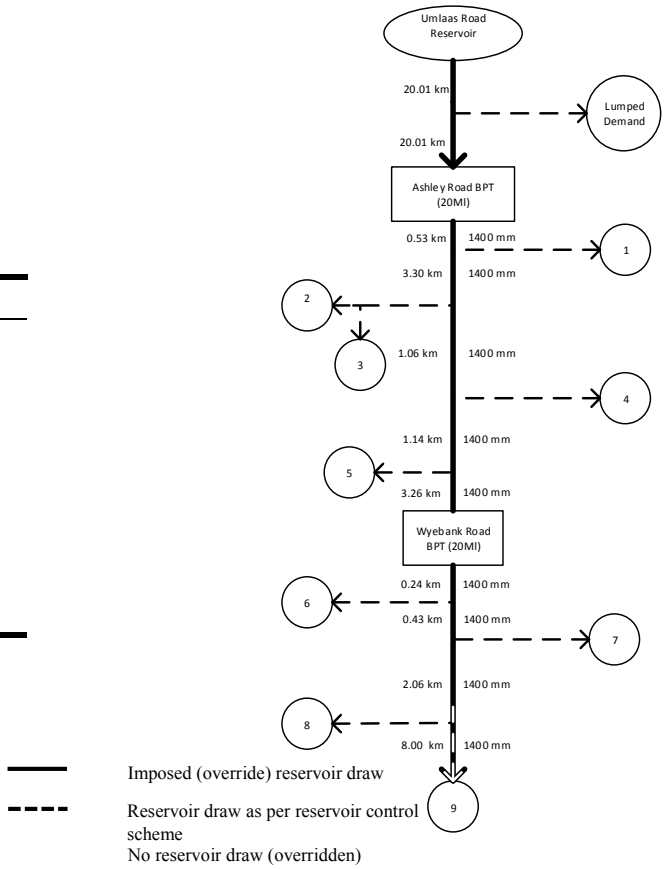

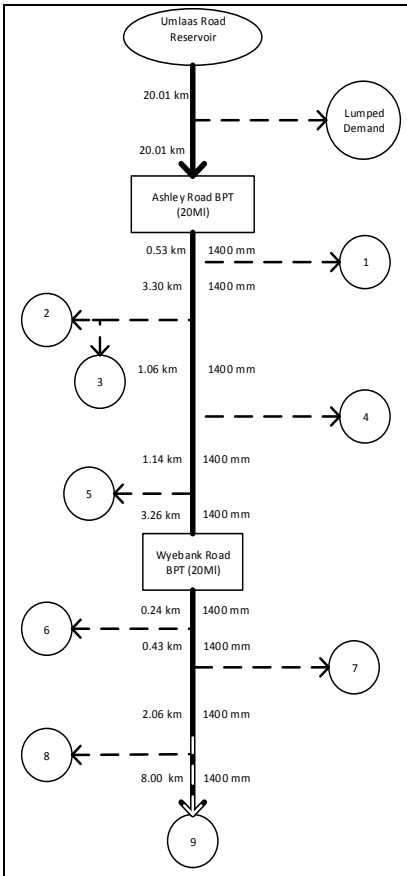

Rates: 2036

1- Important in assessing compliance of the design to design specifications and intent.
2- Preparation of SOPs and maintenance schedules.

Initial Conditions: All valves open, reservoirs 50 %, and BPTs 10% full.

Risk:

1- BPTs stressed when two valves are simultaneously removed from service
2- Valve oscillations - wear risk.
3- Settling level not at 50% level –overflow risk.

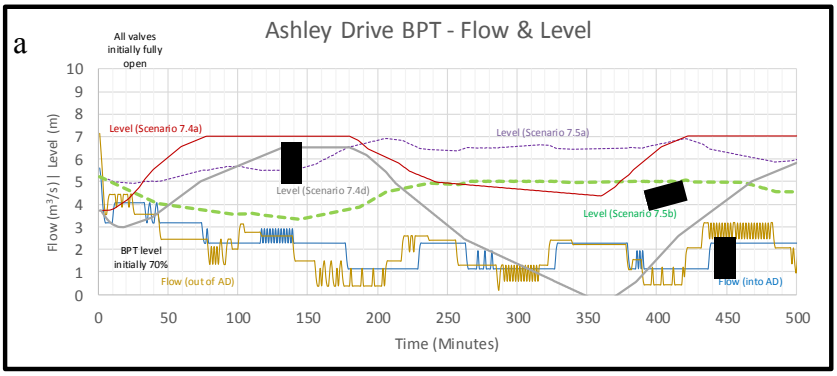

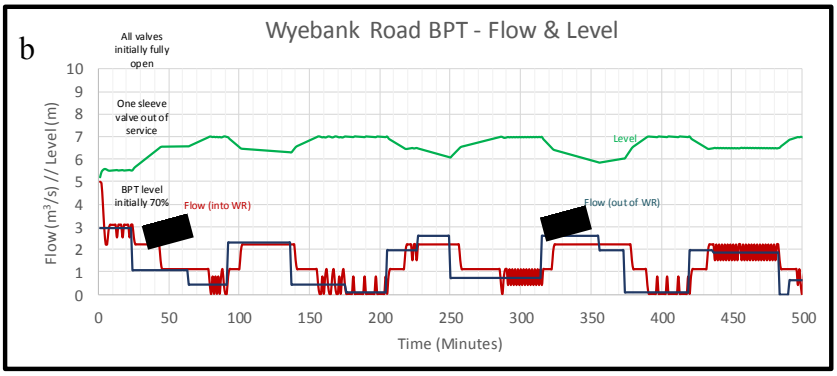

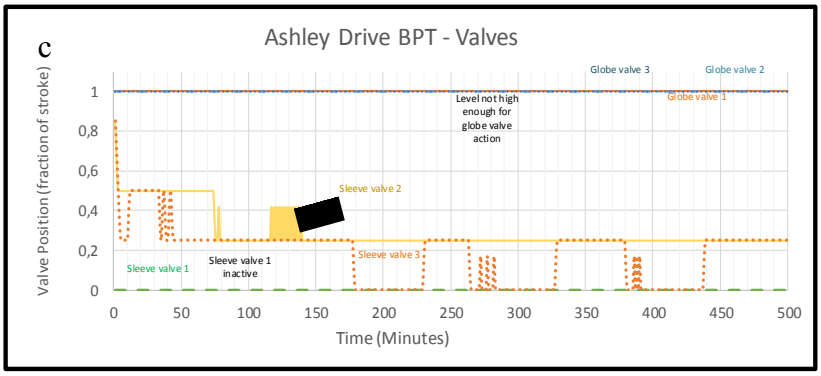

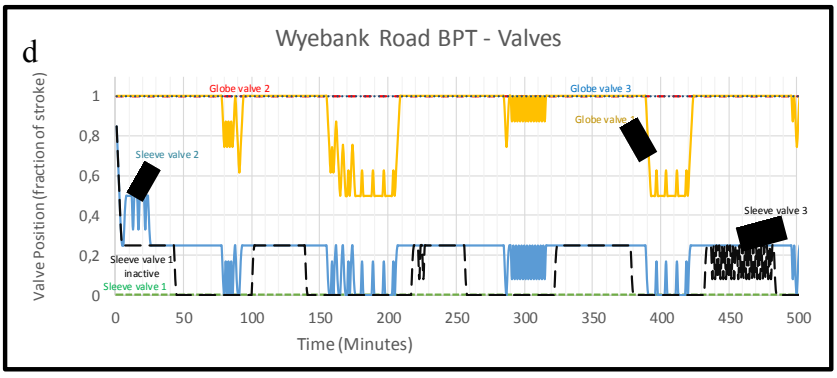

AD Initial: WR Initial

S1= 0.85 G1= 1 L^{AD}_{BPT}= 70% of capacity S1=0.85 G1=1

S2= 0.85 G2= 1 L^{WR}_{BPT}=70% of capacity S2=0.85 G2=1

S3= 0.85 G3= 1 L_{res}=50% of capacity S3=0.85 G3=1

Other Observations:

BPTs cope adequately with only two valves, thus satisfying design specifications. Low throughputs which correspond better to design specifications, are achieved when only two valves are active.

Figure 43 - Scenario 7.5 results overview – Maintenance (sleeve valves) test – Control 1.0.

- Although two sleeve valves could satisfy design specifications, a third valve was added to the parallel configuration in order to allow for unaffected service delivery, even during maintenance. The results of this scenario are therefore critical in the assessment of the efficacy of the proposed design.
- The results presented in Figure 43(a-b) depict a decreased ability of the BPTs to demand high inlet flowrates. This results in a lower maximum throughput, for the fully open (initial) state, than for the scenarios wherein all three sleeve valves are active (see Figure 42 – Scenario 7.3a). This is attributed to the higher resistance presented by the two-leg parallel arrangement. This reduced throughput (~561 $M\ell/day$) corresponds more closely to the design intent (~400 $M\ell/day$). This correspondence desirable in terms of the adequacy of the strength of the materials of construction and the calculated maximum fluid velocity.
- This decreased ability of the BPTs to demand high inlet flows, also allows for the BPT levels to adhere more closely to the design NOL level of 50% (see Section 3.2.1).
- Although a single valve from each BPT is removed from service, the AD BPT is affected more, in terms of its ability to establish a settling level. This is caused by the BPT interactions resulting from the series arrangement (see Section 5.3), and can be seen by the lack of plateaued portions of the AD BPT level curve Figure 43(a), which also indicates a heightened sensitivity of the BPT level to downstream demand variations. These observations are verified by the results of Scenario 7.4d Figure 43(a), which suggests that removing two valves from the AD BPT from service, could result in the AD BPT running empty.
- The results of Scenario 7.5b, which entails the simultaneous removal of two sleeve valves in each BPT, demonstrates that the WA system maintains the capability of adequately supply. This is assuring, particularly from a service delivery perspective, but again (see Section 5.6) raises the question of excessive overdesign.
- In light of the above, operation under the Scenario 7.5a conditions (two valves simultaneously active within each BPT) should thus be considered for normal (everyday) operation of the BPT.

5.8 Scenario 0x: Normal operation (Base case) test – Control 2.0

- **Base case test with revised control system (see Section 3.3.3) – all conditions identical to Scenario 0.**
- Reservoir consumer demand draws determined by the consumer diurnal demand profile for the reservoir.
- Reservoir draw schedules (from the trunk mains) determined by the reservoir control system and the reservoir water level.
- Initial BPT volumes and reservoir levels are set to 70% and 50% respectively, valves to their fully open states.
- All flows are based upon projections for 2036.
- Purpose:
    - **Assess the performance of the new control system in comparison to the original control philosophy.**
    - Represents the most-encountered operational scenario.
    - Determining the adequacy of the system to cope with the daily exertions, and to analyse the system behavior under these conditions
    - Assess the conformity of the system to design expectations

Scenario	0x
Classification	Normal- Base case
Start time	00:00
Reservoir draws	Diurnal (all)
Sleeve valves active	AD - 3 WR - 3
Globe valves active	AD – 3 WR - 3
Control system	Control 2.0

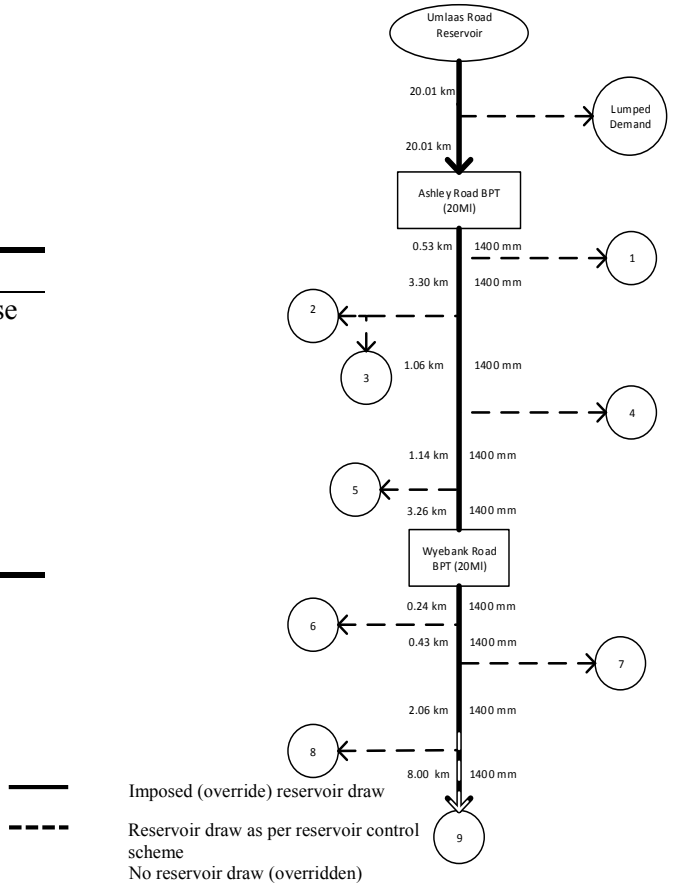

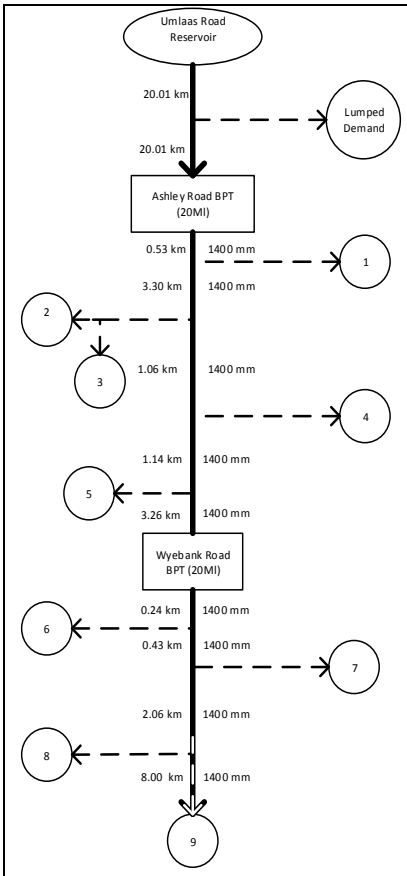

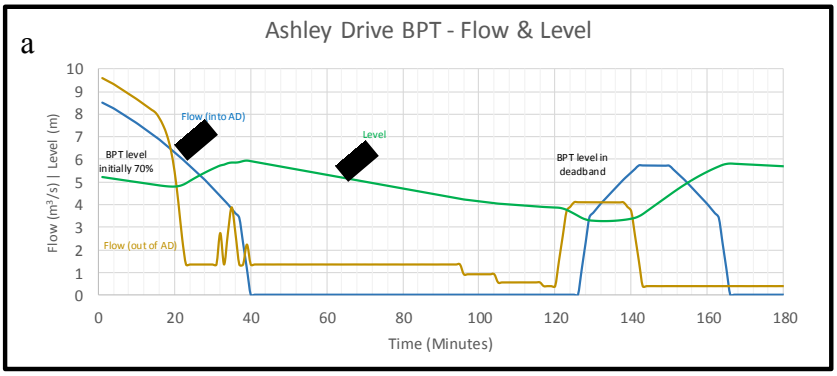

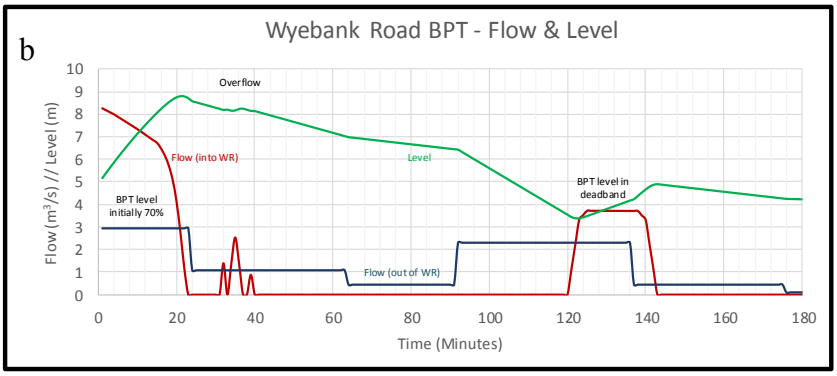

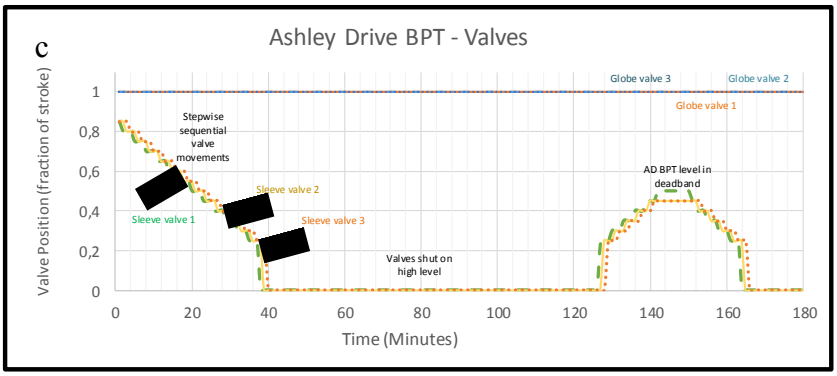

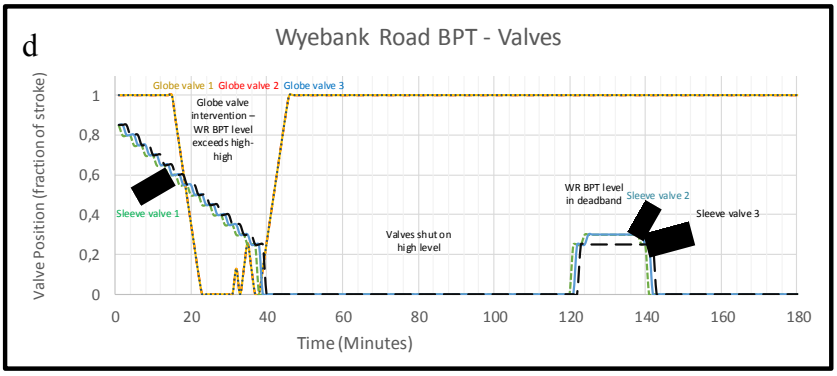

Rates: 2036

1- **Assess the performance of the new control system**
2- Represents the most-encountered operational scenario.

Initial Conditions: All valves open, reservoirs 50 %, and BPTs 10% full.

Risk:

1- **Overflow (WR) -** Sleeve valve response slow, globe valves activate too late.

AD Initial:				WR Initial	
S1=	0.85	G1= 1	L^{AD}_{BPT}= 70% of capacity	S1=0.85	G1=1
S2=	0.85	G2= 1	L^{WR}_{BPT}=70% of capacity	S2=0.85	G2=1
S3=	0.85	G3= 1	L_{res}=50% of capacity	S3=0.85	G3=1

Other Observations:
Sleeve valve reaction.is too slow to prevent an overflow in the WR BPT from the fully open (initial) state. Upon establishing controllability, the system performance is improved.

Figure 44 - Scenario 0x results overview – Normal operation (base case) test – Control 2.0.

- The revised control system was proposed in order to allay the concerns regarding the oscillatory behavior of the valves due to the *localized bang-bang* control philosophy of the original proposal. The revised control system (Control 2.0) is devised around a central deadband region, between 3.5 m and 4.5 m (BPT level), wherein no valve movements are required. This is consistent with the design intent, of maintaining a BPT level of 50% (~4.0 m). Sleeve valve movements, when prompted to occur, occur individually in sequence, with individual movements of 5% (of the valve stroke) per 30 second interval. The movement from fully closed to 25% however, occurs in a single interval. The arrangement of the valve movements can be seen in Figure 44(c-d).
- The presence of the deadband can be observed as plateaued regions of the sleeve valves in both the AD BPT (Figure 44(c) between 142 mins and 148 mins) and the WR BPT (Figure 44(c) between 120 mins and 140 mins)
- The control system, fulfills the intent of preventing the valve oscillations that is a distinguishing defect in the original control philosophy. The result is that amount of valve movements is significantly decreased (Figure 44(c-d)), and the level curves (Figure 44(a-b)) are smoother, and lack the plateau regions.
- The reduction in the amount of requisite valve movements, and the elimination of the *oscillatory stable* state, reduces the generation of water hammer overpressures within the pipelines. The calculated waterhammer overpressures for the revised control system under Scenario 0x conditions are presented in Figure 45 and Figure 46.
- Control 2.0 is also able to satisfactorily cope with routine demand variations.

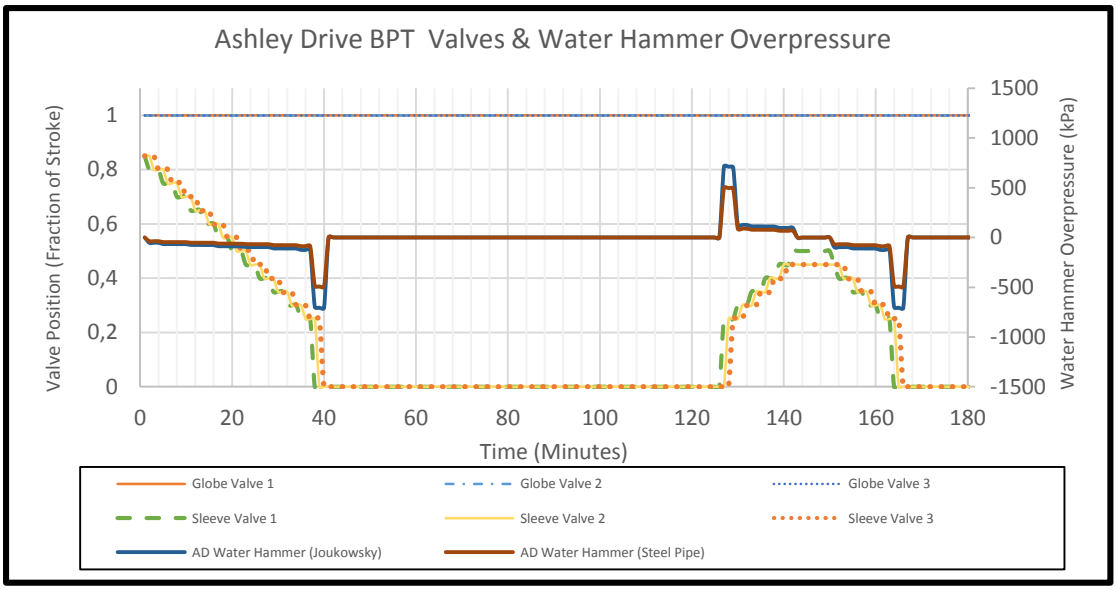

Figure 45- Simulation results (Scenario 0x) for the waterhammer transient phenomenon at the AD BPT (left axis). Valve positions are represented on the right axis – Control 2.0.

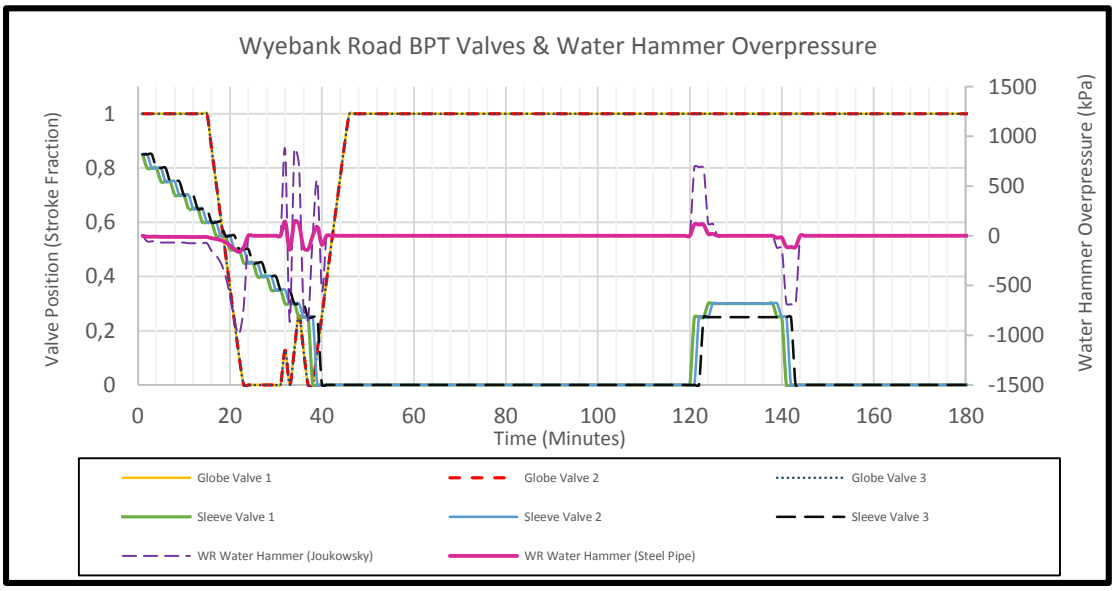

Figure 46- Simulation results (Scenario 0x) for the waterhammer transient phenomenon at the WR BPT (left axis). Valve positions are represented on the right axis – Control 2.0.

- The sequenced arrangement of valve movements, paired with the 5% per interval movement specification, causes the control mechanisms to respond sluggishly. Although this is desirable, in terms of waterhammer concerns, the overflow situation encountered between 15 mins and 40 mins in Figure 44(b) shows that it could result in an overflow, if the initial conditions are unfavourable (all valves initially fully open as per test conditions). A similar peak is observed at 35 mins for the AD BPT (Figure 44(a)), although an overflow is prevented due to the aforementioned interaction between the BPTs and the ability of the

WR BPT to demand a higher inlet flow (from the AD BPT) than the AD BPT is able to acquire from the supply source.

- The configuration of the revised control system, that specifies the simultaneous intervention of the globe valves only at the high-high level (8.3 m), at the original regulated movement rate, is inadequate. The globe valves are unable to prevent the overflow situation due to this configuration. Increasing the rate of closure of the globe valves, to mitigate this, would drastically increase the magnitude of waterhammer overpressures generated. The only feasible adjustment, is thus to decrease the level at which the globe valves begin their intervention. The optimum intervention level should be tested through repetitive runs of this simulation at varying intervention levels.
- The revised control system has the ability to allow the globe valves to assume a bigger proportion of the throttling function during normal operation. This is seen to occur, due to the effect of the sinusoidal-like ripple of the globe valves on the inlet flow to the WR BPT, at ~32 mins in Figure 44(a,b,d). This cannot occur within the original control system's operation, as the sleeve valve and globe valve ranges are separated so that all sleeve valves are shut before the globe valves are shut (to avoid interference of the globe valves on normal control).

5.9 Scenario 7.5cx: Maintenance (sleeve valve) test – Control 2.0

- **Sleeve valve maintenance test with revised control system.**
- Intended to represent the response of the WA under normal conditions during maintenance of varying permutations of the BPT inlet sleeve valves.
- Two sleeve valves in the WR BPT out of service, thus eliminating two parallel legs from the inlet sleeve valve parallel arrangement – all AD valves active.
- WR BPT level shown for two normal operation scenarios. All other results for Scenario 7.5c (two valves only in WR BPT; 7.5a – one valve in each BPT) (see Table 10).
- Reservoir consumer demand draws and trunk main draw schedules are as per normal operation. Initial BPT volumes and reservoir levels are set to 70% and 50% respectively, valves to their fully open states. All flows are based on 2036 projections.
- Purpose:
    - Assess the performance of Control 2.0 under stressed conditions
    - Important in asessing the efficacy of the design, due to the emphasis placed on this scenario during the design stages. Also useful in drawing up SOPs for maintenance, and maintenance schedules.

Scenario	**7.5cx**
Classification	Stress – Sleeve maintenance
Start time	00:00
Reservoir draws	Diurnal (all)
Sleeve valves active	AD - 3 WR - 1
Globe valves active	AD – 3 WR - 3
Control system	Control 2.0

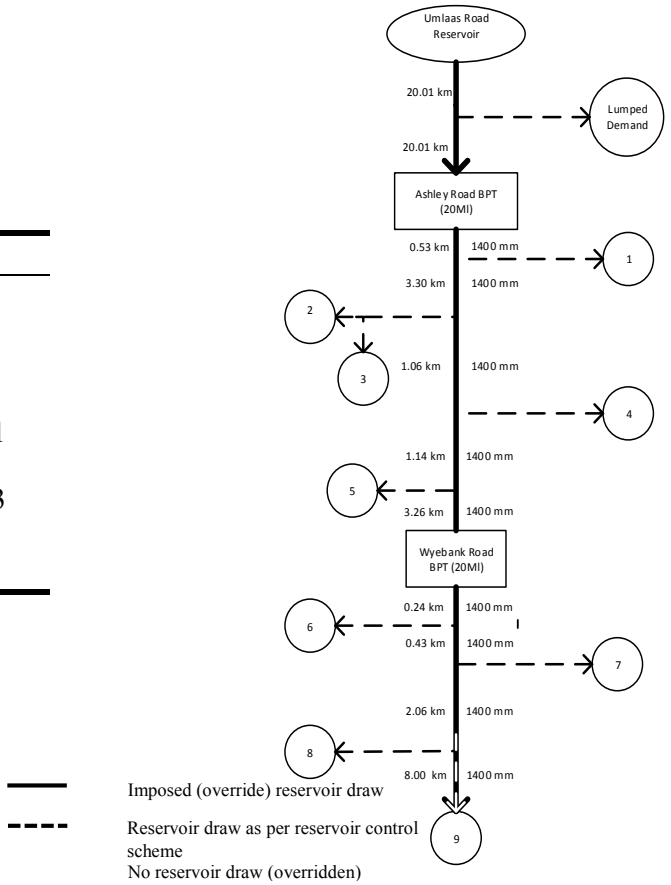

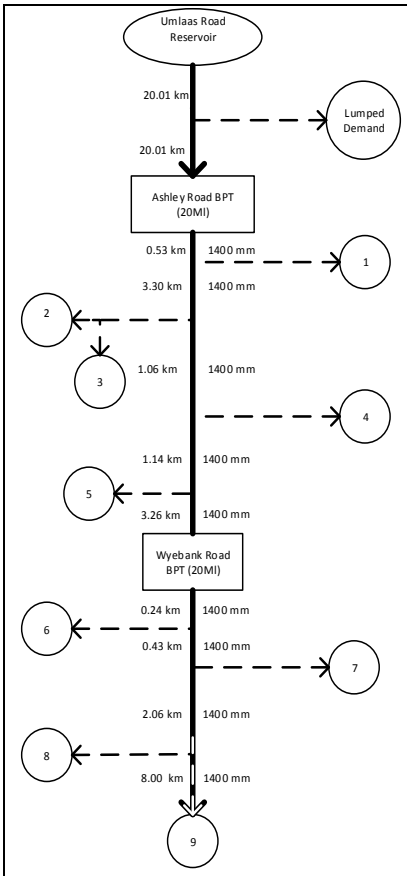

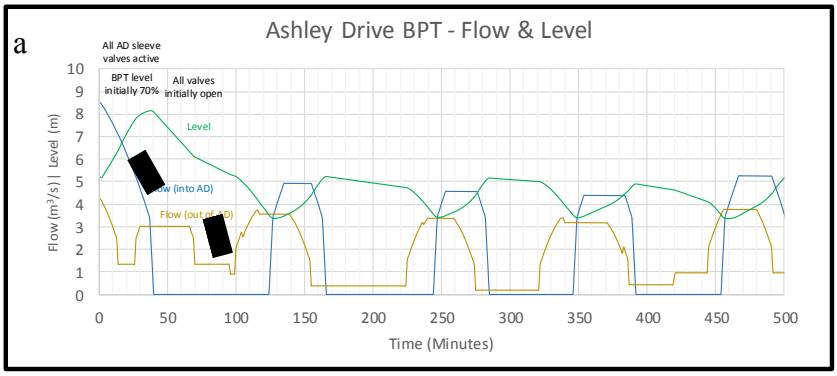

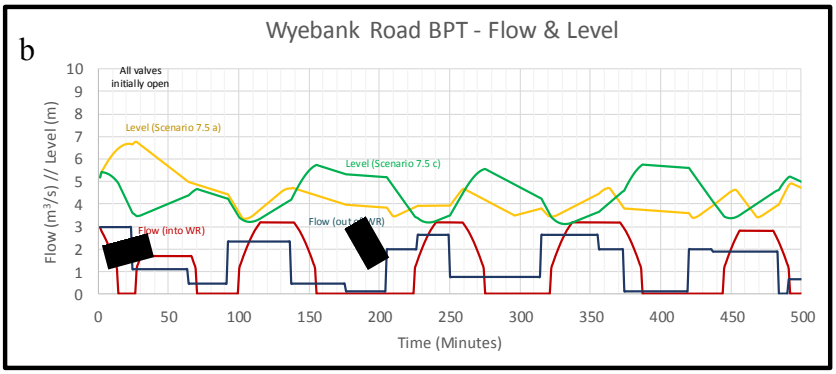

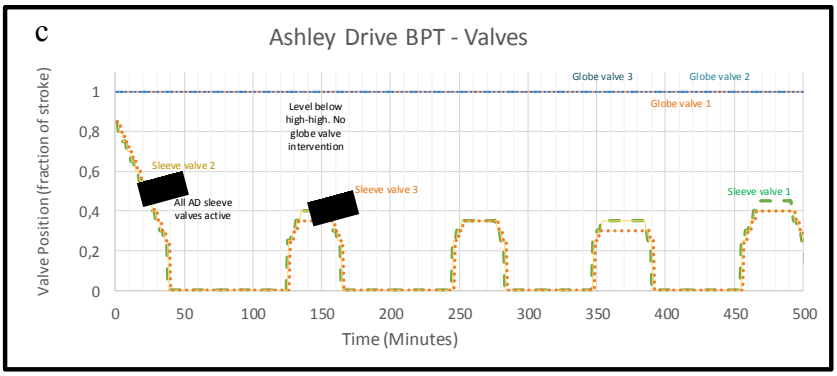

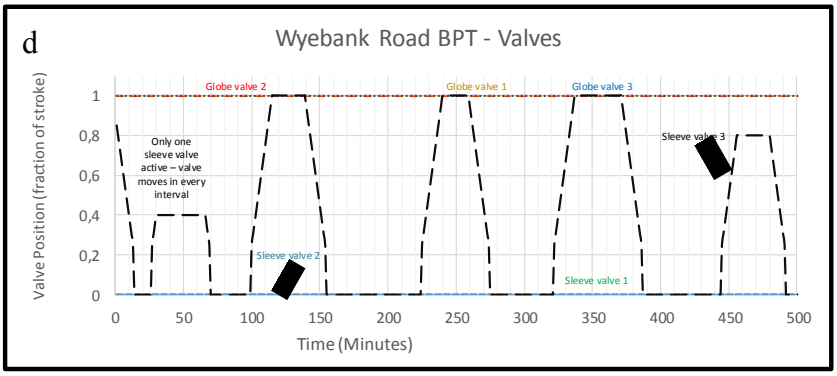

Rates: 2036

1- Assess the performance of Control 2.0 under stressed conditions

Initial Conditions: All valves open, reservoirs 50 %, and BPTs 10% full.

Risk:

1- Overflow risk AD BPT – level breaches 8.0 m

AD Initial: WR Initial

S1= 0.85 G1= 1 L^{AD}_{BPT}= 70% of capacity S1=0.85 G1=1

S2= 0.85 G2= 1 L^{WR}_{BPT}=70% of capacity S2=0.85 G2=1

S3= 0.85 G3= 1 L_{res}=50% of capacity S3=0.85 G3=1

Other Observations:

Control system performance satisfactory. WR BPT robust enough to cope only one sleeve valve active.

Control 2.0 slow to react to decreased demand.

Figure 47 - Scenario 7.5cx results overview– Maintenance (sleeve valves) - Control 2.0.

- This scenario was developed to analyse the system behaviour during sleeve valve maintenance, or if valve breakages are to occur.
- The results of Scenario 7.5c are reassuring, except for the overflow risk, in the AD BPT (Figure 47a), that is noted at 45 mins. This risk, even though it is due to the valves starting fully open, emphasises the aforementioned need (Section 5.9) to improve the sluggish response of Control 2.0 to a reduction in downstream demand. The results of Scenario 5.1 (triple-step stress test - Figure 48) however demonstrate that although the system response is slowed, the system is able to manage a sudden decreased demand under *with all three sleeve and globe valves active* (third step), in a better manner than the original control philosophy. It is thus noted that the overflow situation encountered in Scenario 0x and Scenario 7.5cx is thus a noteworthy exception, but that the revised control system, (Control 2.0) is better suited to the control of the WA than the original control philosophy.

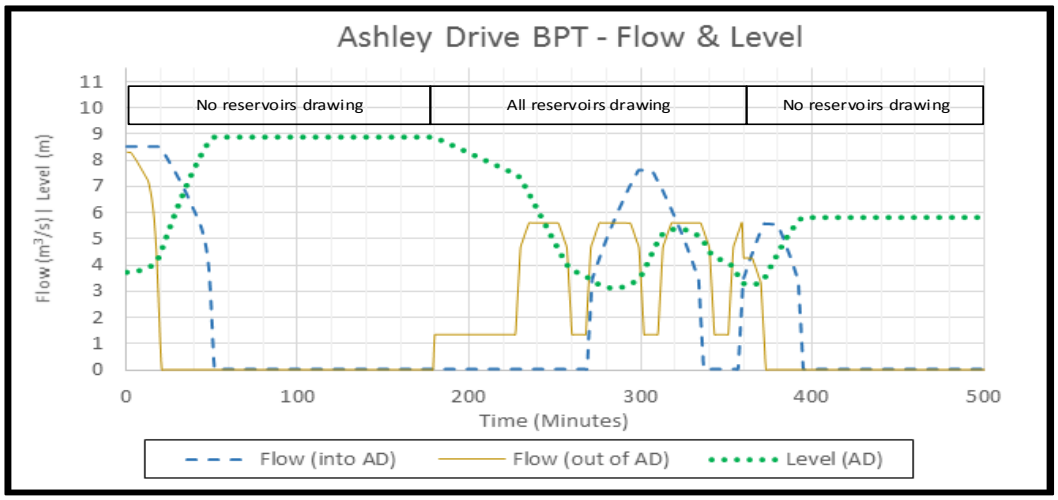

Figure 48 - AD BPT results of Scenario 5.1 with Control 2.0.

- The WR BPT, under Control 2.0, is robust enough to cope adequately with just a single inlet sleeve valve (and three globe valves) active, despite the reduced inlet flowrates. It is expected that due to the series arrangement, which renders the AD BPT as a supply source to the WR BPT and the reservoirs between the two BPTs, that the AD BPT will not perform satisfactorily under similar conditions.

5.10 Darcy-Weisbach calculations (DW) – Control 2.0

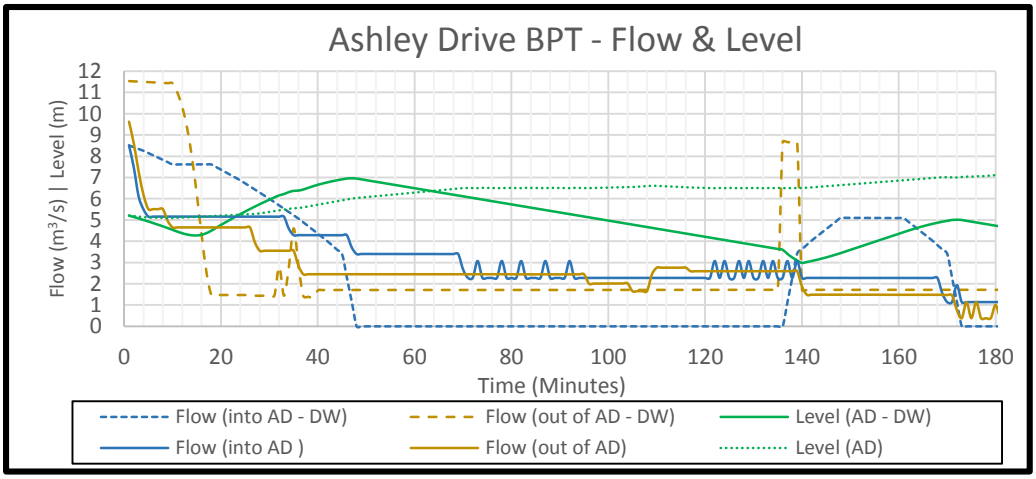

Figure 49 - Results of the Darcy-Weisbach (DW) calculation method (solid) for the AD BPT under base case conditions (Control 2.0). Results of the regression-method calculations are included.

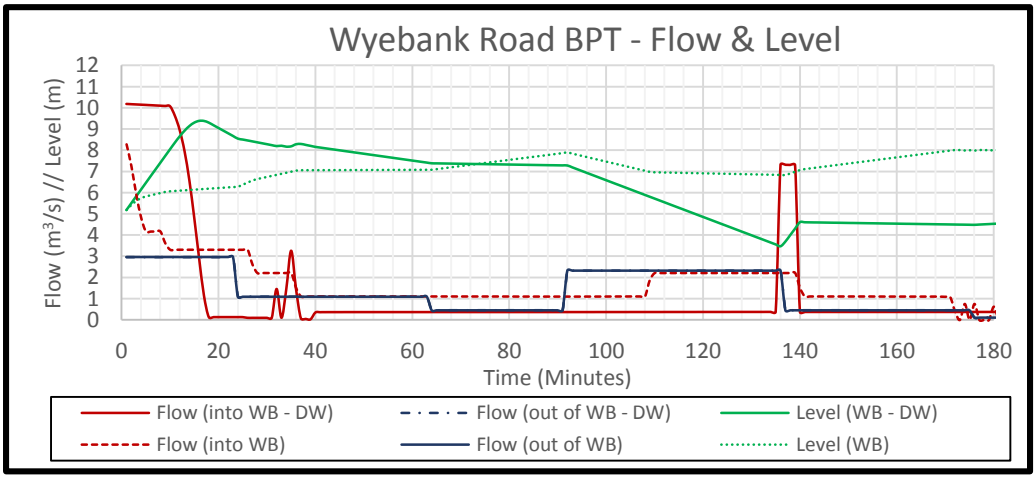

Figure 50 - Results of the Darcy-Weisbach (DW) calculation method (solid) for the WR BPT under base case conditions (Control 2.0). Results of the regression-method calculations are included.

The Darcy-Weisbach calculation method results (Figure 49 and Figure 50) were not used in the analysis of the results due to the lack of conformity between the two calculation methods. As can be observed, from the large discrepancy between the two computations of the initial inlet flowrate to the WR BPT, the Darcy-Weisbach method results in an appreciably lower line resistance. As a result, the predicted performance of the system is altered drastically. Since the WA system is not fully-operational, it was not possible to obtain results for regression to the operation of the physical system. It was thus decided that in order to account for all pipe fittings

and peculiarities that were accounted for within the EPANET design, and thus to ensure the benefit of the analysis to the WA implementation teams, the regression (to the EPANET model – see Section 4.5.2.2) calculations were favoured.

The large discrepancy between the results of the two calculation methods can be noted from the flow characteristics of the pipelines in Figure 51. These results correspond to the aforementioned finding that the Darcy-Weisbach (1845) method predicts a lower line resistance than the k-value regression calculation.

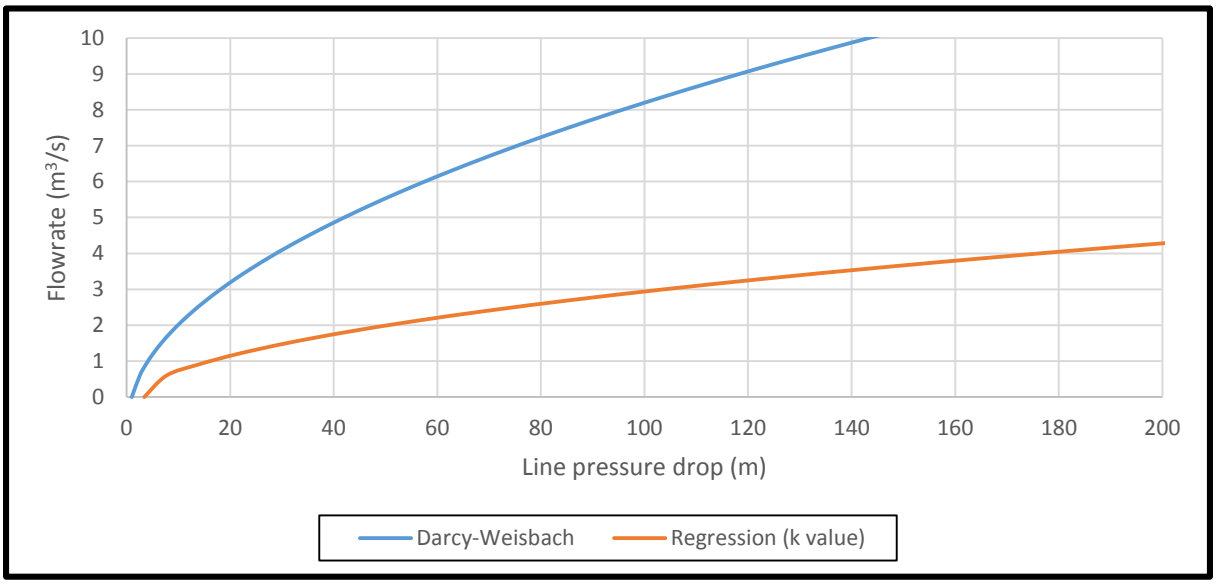

Figure 51 - Comparison of the flow characteristics of the 1 400 mm pipeline when using the Darcy-Weisbach and k-value regression calculation methods.

6 CONCLUSIONS & RECOMMENDATIONS

6.1 Conclusions

- Model assumptions:
    - The reservoirs are controlled by a bang-bang control philosophy with upper and lower limits at 80% and 20% of the total tank volume respectively.
    - Random asynchronous reservoir intakes constitute "Normal Operation"
    - The reservoir draws from the trunk mains can be represented by binary characteristic flows that are unaffected by the pressure within the trunk mains
    - The trunk main's pressure calculation accuracy would not be significantly impacted by simplifying the calculation sequence by decoupling the trunk mains pressure profiles from the offtake pressure profiles (calculated fixed characteristic flows for when reservoir draws switch on)
    - The trunk main pipeline portion between the two BPTs is similar, in terms of its per kilometre line resistance, to the portion from the Umlaas Road reservoir to the AD BPT
    - The EPANET model results (residual pressure) will correspond closely to the fitted characteristics of Western Aqueduct system
    - A regression type calculation, using a fitted flow coefficient (k), would accurately represent both pipeline portions
    - Sleeve valves will fail in their fully open positions during power outages
    - A combination of both the Joukowsky equation and the Newton's II would enable a reasonable, critical estimation of the waterhammer overpressures in the Western Aqueduct system
- The model can be further customised by updating the following:
    - Consumer demand (diurnal) pattern
    - Reservoir characteristic flows
    - Reservoir control strategies

- Data used to obtain the fitted flow coefficient (k), upon commissioning of the WA.

6.1.1 Control 1.0

Control 1.0 (original) consists of several sub-regions at whose (BPT level) boundaries, valve positions are specified. Lower BPT levels allow for higher flow, by successive openings of the valves (see Section 3.3.2).

- The control system acts as a *localized bang-bang* system. An oscillatory settling level is thus formed at a sub-region boundary of the control system.
  - The settling level is dynamic. The sub-region boundary that it will be formed at is determined by the magnitude of the demand (outlet) flow. Large demand flows necessitate lower settling levels (higher inflows due to opening of valves).
- The original design (Control 1.0) is adequate to cope with normal operational conditions in 2036. The following risks are nonetheless existent
  - The maximum system throughput is 8.5 $\frac{m^3}{s}$ (734.4$\frac{M\ell}{day}$) greatly exceeds the normal maximum design throughput (400$\frac{M\ell}{day}$). This could prove disastrous in the event of pipe ruptures, particularly on the trunk main lines.
  - The settling level of the BPTs, until well beyond 2100, is above the design normal operating level (NOL). The settling level resides within the upper 20% of the BPTs, thus presenting an overflow risk.
  - The globe valves are assigned a duty during normal operation (other than power loss scenarios). This is a departure from the intent of the design, and could result in a valve-maintenance issue.
  - Valve oscillations (globe valves and sleeve valves) are prevalent, due to the structure of the control system – this presents a maintenance risk.
  - The globe valve movements are too delayed to be able to individually assume flow control duties upon the loss of electrical power. Due to this delayed movements, the globe valves maintain the BPT level at 8.0 m (100%) for any demand (outlet) flowrate. This represents an overflow risk, particularly when power is restored.

    - Large flow variations (triple step test – cease all demands) cause the BPT levels to breach the 100% (8.0 m) level. This represents an overflow risk.
- High waterhammer overpressures (~8 bar) are predicted by the Joukowsky equation and the *steel pipe analogy.* Although these methods are inaccurate, the magnitude of the predictions (>40% of design pressure) is reason for concern.
- The AD BPT is less robust than the WR BPT due to the series arrangement of the BPTs. The WR BPT thus always leads the AD BPT.
- Based on the forecasted y/y consumer demand growth factors, the AD BPT is expected to be unable to meet demand in the year 2110, and the WR BPT in 2154.
- The WA is able to cope adequately with all connected reservoirs drawing simultaneously (maximum forecasted demand on the WA).
- Simultaneous single BPT compartment maintenance affects the performance of the WA minimally, by increasing the sensitivity of the BPT level to downstream demand variations.
    - Normal operation with one BPT compartment in the AD BPT and WR BPT can be considered
- The WA is able to sustain its performance when simultaneous single and double sleeve valve maintenance is carried out in both BPTs.
    - Due to the series arrangement of the BPTs however, the AD BPT will fail if two sleeve valves are out of service only in the AD BPT (***only*** if all valves in WR are active), and elevated demands are encountered downstream (Scenario 7.4d). The reverse is does not hold for WR.
    - The WA is better suited (in terms of the maximum design throughput and NOL) to be operated with just two sleeve valves active on each BPT.

6.1.2 Control 2.0

Control 2.0 (2016) is a revised control philosophy uses a *true deadband*. No valve movements are specified within the deadband zone (between 3.5 m and 4.0 m). Above the upper deadband limit (4.0 m), the highest position sleeve valve is prompted to close 5% (or 25% if moving to 0% from 25% or vice versa). The opposite holds true when the level falls below 3.5 m. Globe valves only intervene above the *high-high* (8.3 m) level (see Section 3.3.3).

- The revised control system (Control 2.0) is more robust and provides better control of the WA

    - It eliminates the oscillatory settling levels and the accompanying valve oscillations and maintenance concerns
    - The NOL is better adhered to, resulting in a lower overflow risk
    - A decreased number of valve movements are commanded, thus decreasing maintenance requirements on the valves
    - It is however susceptible to overflows due to the slowed valve responses.
- An overflow risk is present if the initial conditions for Scenario 0x (BPTs 70% full, all valves fully open) are encountered. The overall susceptibility of the WA with Control 2.0, is less than that of the WA with Control 1.0. This is due to the improved ability of the WA to maintain the 50% NOL with Control 2.0.

6.2 Recommendations

- Adopt the revised control system for implementation
- Install automated override controls to prevent operation at maximum throughput in the event of trunk main ruptures.
- The possibility of using just two sleeve valves at the entrance of each BPT, during normal operation, should be considered.
- The k-parameter (fitted pipeline flow coefficient) should be revised to use measured data upon the commissioning of the WA, as it greatly affects the predicted performance of the model
- Reservoir draw schedules should be measured accurately, and updated as they greatly affect the simulation results.
- Valve duties should be alternated to avoid excessive wear on active valves
- Detailed surge analyses should be carried out, as the results of the preliminary tests are deemed to be a concern
- The possibility of increasing the movement rate of the globe valves (Control 1.0), decreasing the *high-high* level (globe valves intervention level – Control 2.0) and increasing the sleeve valve movement per 30s (5% - Control 2.0) should be considered in tandem with the results of the detailed surge analysis.
- The possibility of decreasing the inlet resistance to the AD BPT should be considered, in order to decrease the susceptibility of the AD BPT to downstream demands. This could aid in speeding up the response of the AD BPT level to downstream demand fluctuations, by increasing the achievable inlet flowrate.

- Revise the high-high level, at which the globe valves intervene (both control systems). The current settings do not allow the globe valves adequate time to prevent overflows under specific stressed conditions (BPT 50% full with all valves fully open).
- SOPs should be constructed using the results presented above. This includes operator duties for power outages (e.g. adjust the sleeve valve position to x% by turning the hand-wheels etc.), and emergency preparedness training (wildfires etc.). Maintenance schedules can also be tested through simulations.

7 REFERENCES

Albert, R., Jeong, H., & Barabasi, A.-L. (2000). Error and attack tolerance of complex networks. *Nature, 406*(6794), 378-382. Retrieved from http://dx.doi.org/10.1038/35019019

American Water Works Association. (2001). *M2 Instrumentation and Control, Third Edition* (Third Edition ed.).

American Water Works Association. (2005). *Computer Modeling of Water Distribution Systems*: American Water Works Association.

Anderson, G. (2013). HERITAGE SURVEY OF THE ETHEKWINI WATER AND SANITATION WESTERN AQUADUCT: "VOORTREKKER ROAD". Retrieved from http://www.sahra.org.za/sahris/sites/default/files/heritagereports/western%20aquaduct.pdf

Apollo Valves. (2014). Retrieved from http://www.apollovalves.com/_literature/cat_ACVBR9000.pdf

Bailey Valves. (2013). Retrieved from http://www.baileyvalve.com/img/about/02-01s.jpg

BERMAD. (2009). Hydraulic Control Valves

The Biggest of the Best. Retrieved from https://www.bermad.nl/en/docman-documents/waterworks/data-sheet-1/429-ww-large-size-valve-24-36/file.html

Biscos, C., Mulholland, M., Le Lann, M. V., Buckley, C. A., & Brouckert, C. J. (2002). Water Distribution Network Optimization. *WISA Biennial Conference*.

Brebbia, C. A., & Kungolos, A. (2007). *Water Resources Management IV*: WIT Press.

California Polytechnic State University. (2008). Related to Structured Programming. Retrieved from http://users.csc.calpoly.edu/~jdalbey/308/Resources/StructuredProgramming

Cameron. (2015). How does it work: Gate Valves. Retrieved from https://www.c-a-m.com/products-and-services/valves/valve-academy/how-does-it-work-gate-valves

Clark, R. M., Grayman, W. M., & Males, R. M. (1988). Modeling Distribution-System Water Quality; Dynamic Approach. *J. Water Resour. Plann. Manage., 114*(Issue 3), 295-312.

Colebrook, C., & White, C. (1937). Experiments with fluid friction in roughened pipes. *Proceedings of the royal society of london. series a, mathematical and Physical sciences*, 367-381.

Cook, J. (2012). Hydraulic Modeling Improves Water System Reliability, Efficiency. Retrieved from http://www.waterworld.com/articles/wum/articles/print/volume-2/issue-1/features/hydraulic-modeling-improves-water-system-reliability-efficiency.html

Creamer Media. (2015). Western Aqueduct Phase 2 reaches significant milestones. Retrieved from http://www.engineeringnews.co.za/article/western-aqueduct-phase-2-reaches-significant-milestones-2015-06-15

Daily News Reporter. (2015). Bulk water pipeline nears completion. Retrieved from http://www.iol.co.za/dailynews/news/bulk-water-pipeline-nears-completion-1.1820558#.VgD3NvS7prI

Dasic, T., & Djordjevic, B. (2004). Method for water distribution systems reliability evaluation.

Department of Water Affairs and Forestry. (2009). Governing Board Induction Manual: Overview of the South African Water Sector. Retrieved from https://www.dwa.gov.za/io/Docs/CMA/CMA%20GB%20Training%20Manuals/gbtraiingmanualchapter1.pdf

Doorgapershad, A. 2015. Email to Ismaeel Ally. 22 May.

Elker, I., & Kara, T. (2003). Behaviour of a Water Supply System: A Modelling and Simulation Study of Activities with Some Experiments.

Enggcylcopedia. (2012). Self Actuated Pressure Control Valve. Retrieved from http://www.enggcyclopedia.com/2012/02/self-actuated-pressure-contro-valve/

EPANET .DE. (2011). Using EPANET in MATLAB. Retrieved from http://epanet.de/developer/matlab.html.en

eThekwini Municipality. (2011a). Tender Awarded for Western Aqueduct – Phase II. Retrieved from http://www1.durban.gov.za/durban/services/water_and_sanitation/services/western-aqueduct/news-articles/tender_awarded_phaseii

eThekwini Municipality. (2011b). Water Services Development Plan. Retrieved from http://www.durban.gov.za/City_Services/water_sanitation/Policies_Plans_Guidelines/Documents/WSDP2012_Approved.pdf

eThekwini Municipality. (2012). Who we Are? Retrieved from http://www.durban.gov.za/City_Services/water_sanitation/About_Us/Pages/default.aspx

eThekwini Municipality. (2013). About eThekwini Municipality. Retrieved from http://www.durban.gov.za/Discover_Durban/Pages/AboutEM.aspx

Facts About Durban. (2009). The Western Aqueduct. Retrieved from http://www.fad.co.za/Resources/western/aqueduct.htm

Fischer, P. (2014). Design Report on the Inlet Flow Control at the Break Pressure Tanks.

Fischer, P., & van Rooyen, D. (2013). Design Report for the Break Pressure Tanks on the Western Aqueduct.

Fischer, P., & van Rooyen, D. (2015). PARTICULAR SPECIFICATION OP: OPERATING PHILOSOPHY (REVISION 1).

Ghidaoui, M. S., Zhao, M., McInnis, D. A., & Axworthy, D. H. (2005). A Review of Water Hammer Theory and Practice. *Applied Mechanics Reviews, 58*, 49-76. Retrieved from http://hydraulics.unibs.it/hydraulics/wp-content/uploads/2012/04/A_review_of_water_hammer_theory_and_practice.pdf

Groundfos. (2012). Break Tank. Retrieved from http://www.cbs.grundfos.com/india/lexica/Booster/BO_Break_Tank.html?action=Print

Henry Pratt Company. (2008). Sleeve Valves: Energy Dissipators. Retrieved from http://www.spartancontrols.com/~/media/resources/pratt/pf/54_pratt_711_product_document.pdf

Hopkins, M. (2012). Critical Node Analysis for Water Distribution Systems Using Flow Distribution

Ithuba Valves. Sleeve Valves Retrieved from http://www.ithubavalves.co.za/sleeve.php

Karamouz, M., Moridi, A., & Nazif, S. (2010). *Urban Water Engineering and Management*: CRC Press.

KSB Aktlengesellschaft. (2006). Water Hammer. Retrieved from http://www.ksb.com/linkableblob/ksb-za/80892-193671/data/Water_hammer_Know-how_Band_1_en-data.pdf

Kwierniewski, M. (2003). Reliability Modelling of Water Distribution System (WDS) for Operation and Maintenance Needs. *Archives of Hydro-Engineering and Environmental Mechanics, Vol. 51*(No. 1), pp. 88-92.

Macleod, N. (2013). Aqueducts to address Durban's water needs. *Civil Engineering, 21*(5), 30-33.

Mays, L. W. (1999). *Hydraulic Design Handbook*: McGraw-Hill.

Mays, L. W. (2000). *Water distribution systems handbook*: McGraw-Hill.

Mays, L. W. (2010). *Water Transmission and Distribution* (4 ed.): American Water Works Association.

Mays, L. W., & American Water Works Association. (2010). *Water Transmission and Distribution*: American Water Works Association.

Moody, L. F. (1944). Friction factors for pipe flow. *Trans. Asme, 66*(8), 671-684.

Muller, H. (2011). The Right to Water and Sanitation- the South African Experience Retrieved from http://www2.ohchr.org/english/issues/water/Iexpert/docs/StateActors/SouthAfrica.pdf

Neely, A., & Obbayi, S. R. (2010). Structured vs. Object-Oriented Programming: A Comparison. Retrieved from http://www.brighthub.com/internet/web-development/articles/82024.aspx

Netrium. (2014a). Joukowsky Equation. Retrieved from https://neutrium.net/fluid_flow/joukowsky-equation/

Netrium. (2014b). Speed of Sound in Fluids and Fluid in Pipes. Retrieved from https://neutrium.net/fluid_flow/speed-of-sound-in-fluids-and-fluid-in-pipes/#communication-time

Niskanen, M. A. (2003). The Design, Construction, and Maintenance of a Gravity Fed Water System in the Dominican Republic. Retrieved from https://www.mtu.edu/peacecorps/programs/civil/pdfs/matt-niskanen-thesis-final.pdf

Ratnayaka, D. D., Brandt, M. J., & Johnson, M. (2009). *Water Supply*: Elsevier Science.

Rouse, M. (2014). structured programming (modular programming) definition. Retrieved from http://searchsoftwarequality.techtarget.com/definition/structured-programming-modular-programming

SAinfo reporter. (2014). Durban wins prestigious Stockholm water award. Retrieved from http://www.southafrica.info/about/sustainable/water-300514.htm

Shuang, Q., Zhang, M., & Yuan, Y. (2014). Performance and Reliability Analysis of Water Distribution Systems under Cascading Failures and the Identification of Crucial Pipes. *Plos One, 9*(2), 1-11.

Soldi, D., Candelieri, A., & Archetti, F. (2015). Resilience and vulnerability in urban water distribution networks through network theory and hydraulic simulation. *Procedia Engineering, 119*, 1259-1268.

Stephenson, D. (1972). Water Hammer Protection of Pumping Lines. *The Civil Engineer in South Africa*, 382-390.

Stephenson, D. (2012). *Water Supply Management*: Springer Netherlands.

Swartz, M. (2006). xlswrite1. Retrieved from http://www.mathworks.com/matlabcentral/fileexchange/10465-xlswrite1

Tancott, G. (2014). Further contracts in the pipeline for the Western Aqueduct. Retrieved from http://www.infrastructurene.ws/2014/06/24/further-contracts-in-the-pipeline-for-the-western-aqueduct/

The Engineering Toolbox. Adding Kv or Cv for control valves in series or parallel Retrieved from http://www.engineeringtoolbox.com/adding-kv-cv-d_1120.html

The New Zealand Water & Wastes Association Wairos Actearoa. (2009). NATIONAL MODELLING GUIDELINES WATER DISTRIBUTION NETWORK MODELLING. *Draft 01 Rev. 04*.

Trifunovic, N. (2006). *Introduction to Urban Water Distribution: Unesco-IHE Lecture Note Series*: Taylor & Francis.

US Environmental Protection Agency. (2015). EPANET. Retrieved from http://www2.epa.gov/water-research/epanet

Van Rooyen, D. 2015. Email to Ismaeel Ally. 31 August.

Walski, T. M., & Haestad Methods, I. (2003). *Advanced water distribution modeling and management*: Haestead Press.

Watts Canada. (2015). Water Pressure Reducing Valves. Retrieved from http://www.wattscanada.ca/pages/learnAbout/reducingValves.asp?catId=#parallel

Wright, R., Abraham, E., Parpas, P., & Stoianov, I. (2015). Optimized control of pressure reducing valves in water distribution

networks with dynamic topology. *Procedia Engineering, 119*, 1003-1011.

Zessler, U., Shamir, U., & Member, A. (1989). Optimal Operation of Water Distribution Systems. *Journal of Water Resources Planning and Management, 115*(6), 735-752.

APPENDIX A: SUPPORTING MATERIALS

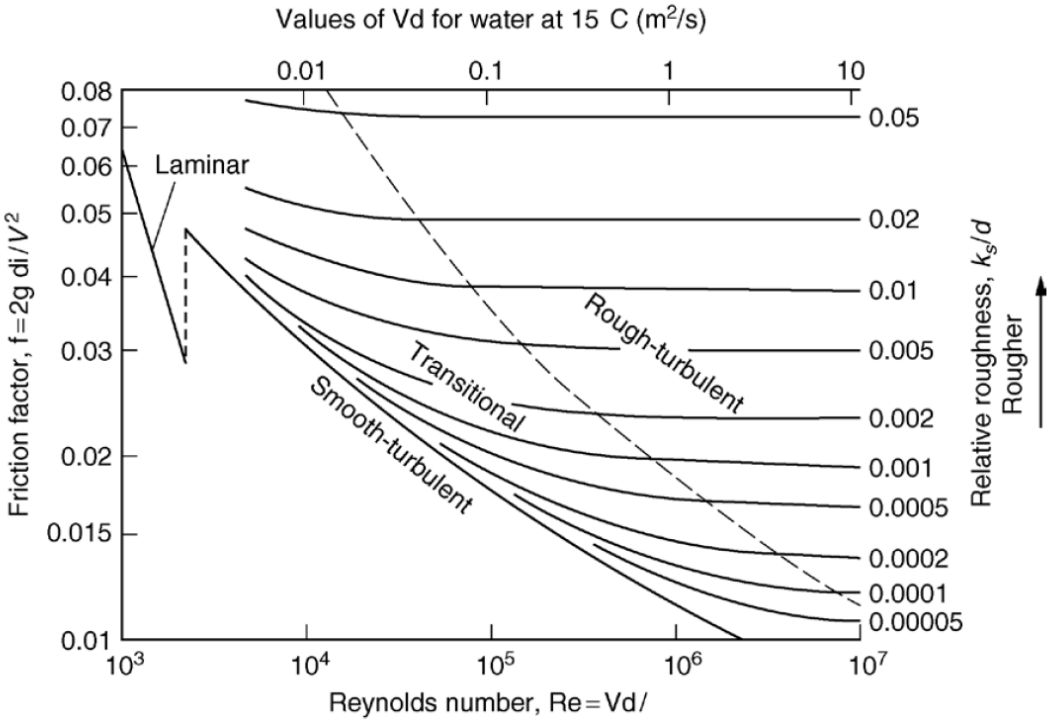

Figure A1- Moody (1944) diagram for the friction factor. The (sloping/horizontal) lines are lines of constant pipeline roughness. The abscissa corresponds to the Reynolds number of the fluid and the ordinate (left) is the dimensionless friction factor.

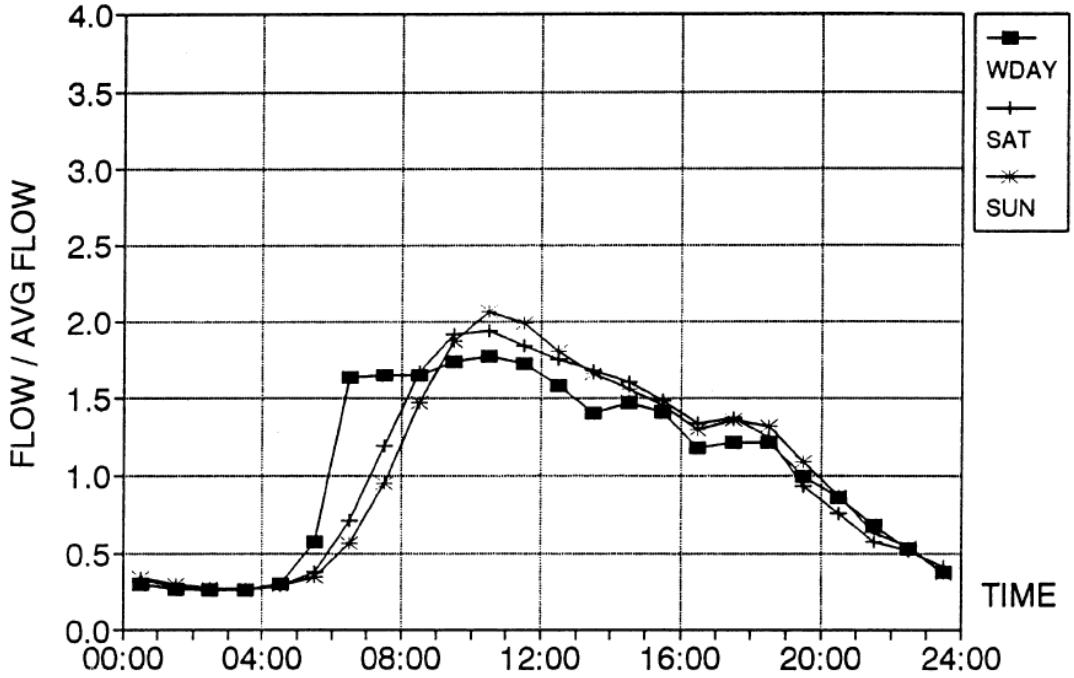

Figure A2 - Hourly demand (normalised) hydrograph for Sunninghill (urban) (Stephenson, 2012).

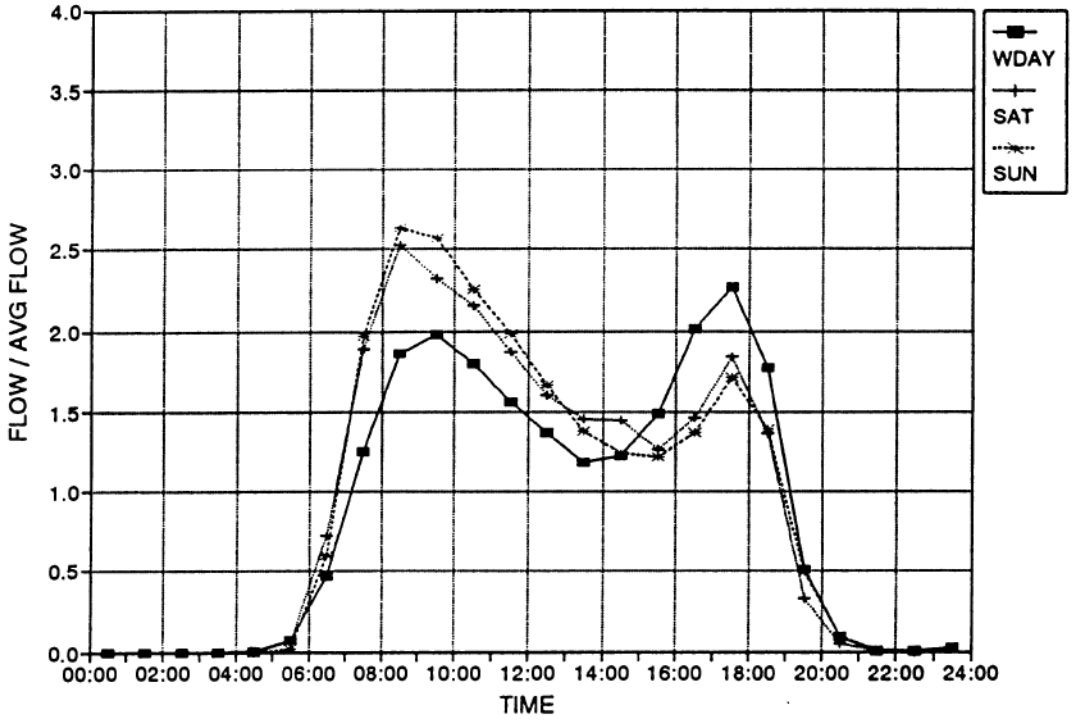

Figure A3 - Hourly demand (normalised) hydrograph for Rabie Ridge (rural) (Stephenson, 2012).

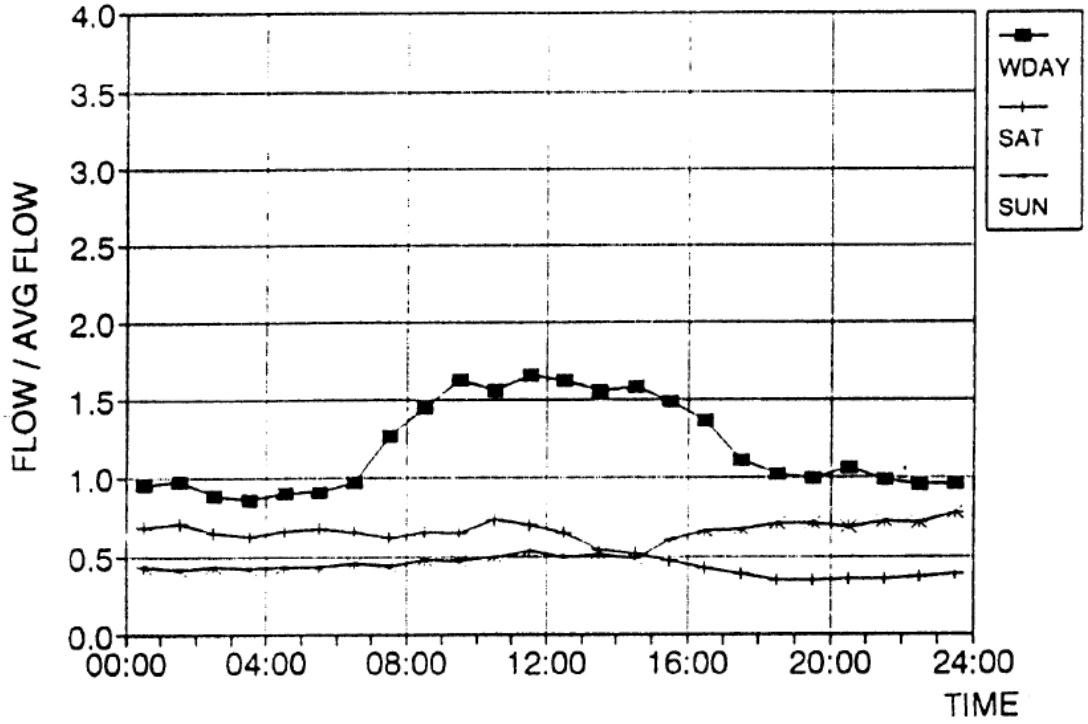

Figure A4 - Hourly demand (normalised) hydrograph for Aeroton (industrial) (Stephenson, 2012).

Technical Data

Dimensions and Weights

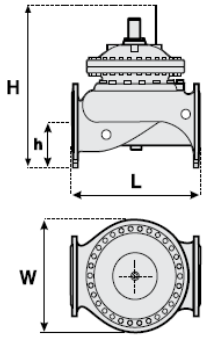

SI Metric

	DN	600	700	750	800	900
ISO PN 10 ; 16	L (mm)	1,450	1,650	1,750	1,850	1,850
	W (mm)	1,250	1,250	1,250	1,250	1,250
	h (mm)	470	490	520	553	600
	H (mm)	1,965	1,985	2,015	2,048	2,095
	Weight (Kg)	3,250	3,700	3,900	4,100	4,250
ISO PN 20 ; 25	L (mm)	1,500	1,650	1,750	1,850	1,850
	W (mm)	1,250	1,250	1,250	1,250	1,250
	h (mm)	470	490	520	553	600
	H (mm)	1,965	1,985	2,015	2,048	2,095
	Weight (Kg)	3,500	3,700	3,900	4,100	4,250

US English

	inch	24"	28"	30"	32"	36"
ANSI 125 ; 150	L	57	65	70	73	73
	W	49	49	49	49	49
	h	18.5	19	20.5	21.8	23.6
	H	77	78	79.3	80.6	82.5
	Weight (lb)	7,150	8,140	8,580	9,020	9,350
ANSI 250 ; 300	L	59	65	70	73	73
	W	49	49	49	49	49
	h	18.5	19	20.5	21.8	23.6
	H	77	78	79.3	80.6	82.5
	Weight (lb)	7,700	8,140	8,580	9,020	9,350

Flow Chart

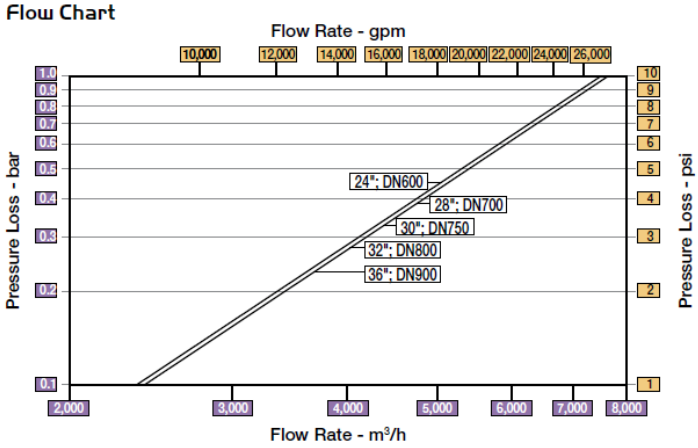

Kv ; Cv to Valve Opening Chart

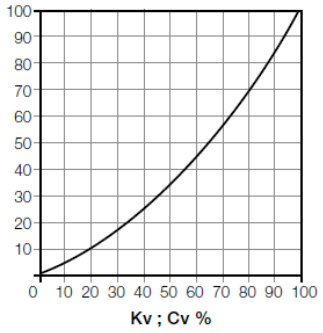

24" - Kv = 7,350 ; Cv = 8,490

28,30,32,36" - Kv = 7,500 ; Cv = 8,670

Figure A5 - Valve characteristics and Kv factor for Bermad Globe valves (BERMAD., 2009).

APPENDIX B – WESTERN AQUEDUCT DATA

Table B1 - Material of construction and wall thickness information for the WA pipes (Van Rooyen, 2015).

Pipe size (DN)	Steel Grade	Wall Thickness (mm)
323	X42	4.5mm
406	X42	4.5mm
508	X42	4.5mm
508	300WA	8mm
610	X42	4.5mm
610	X42	6mm
610	X42	8mm
1016	X42	8mm
1016	X52	8mm
1016	X52	10mm
1016	X52	12mm
1016	X65	12mm
1016	X65	13.5mm
1422	X42	10mm
1422	X52	10mm
1422	X52	12mm
1422	X65	12mm
1422	X65	13.5mm
1626	X42	12mm
1626	X52	12mm
1626	X65	12mm
1626	X65	13.5mm

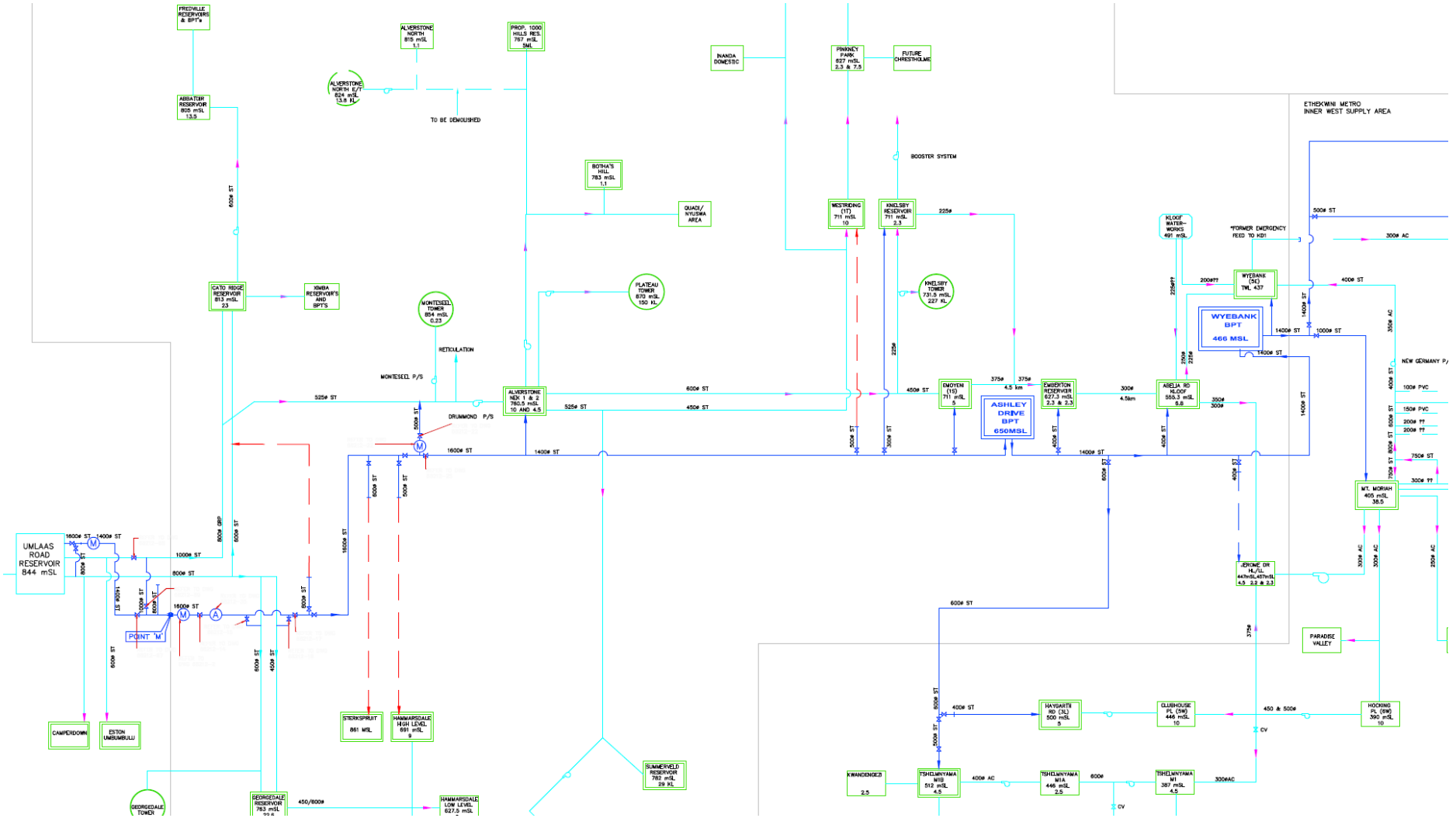

Figure B1 - EWS Western system layout (Supplied by EWS).

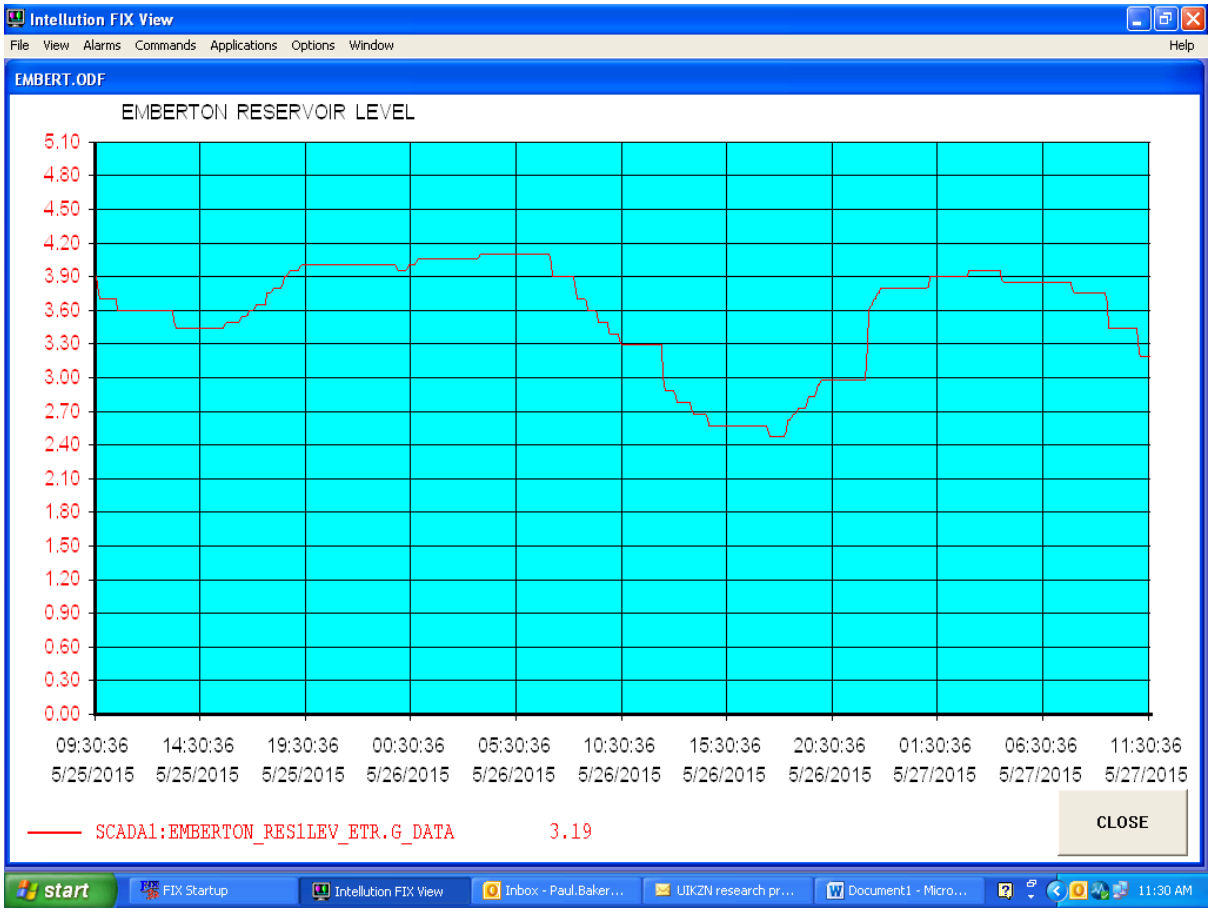

Figure B2 - Example of the time-series representation of one the Emberton reservoirs level from the telemetry system.

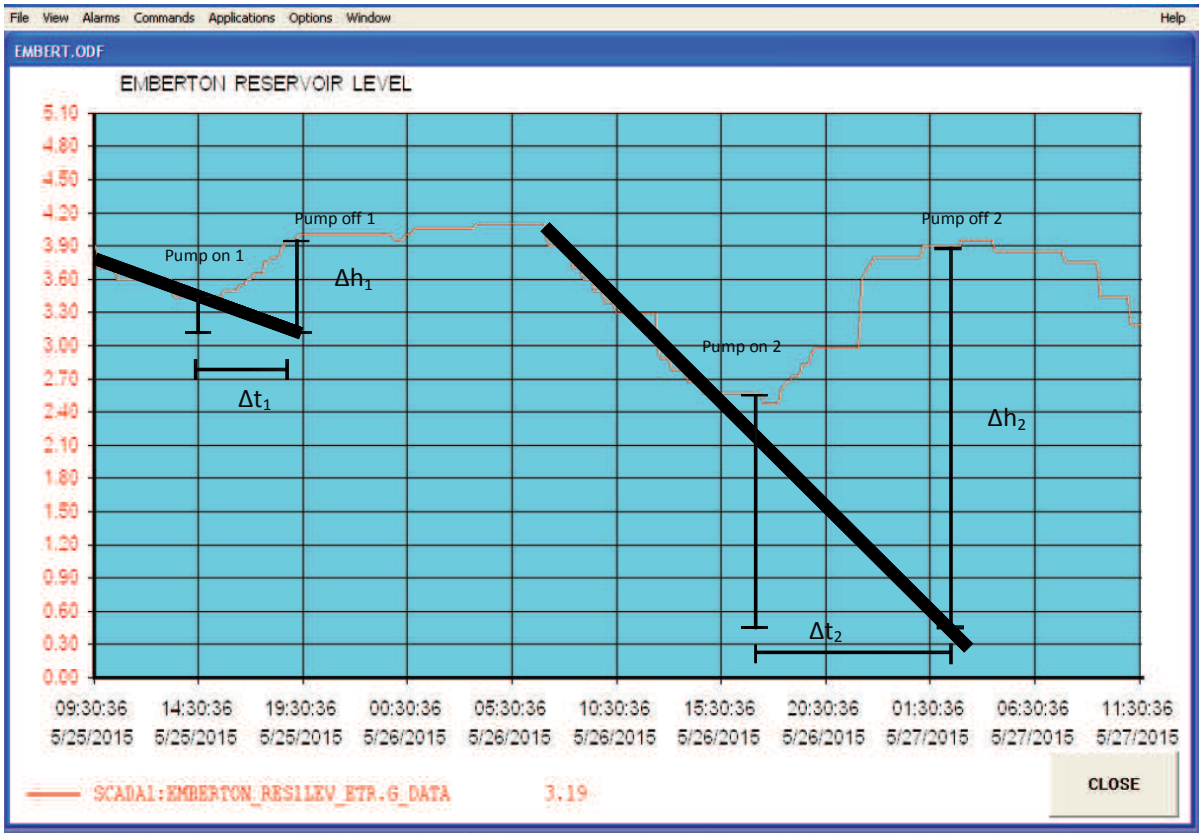

Figure B3 - Example of the procedure followed to obtain an estimate of the characteristic flow of one of the Emberton reservoirs.

APPENDIX C – EXCEL PRESENTATION GRAPHIC

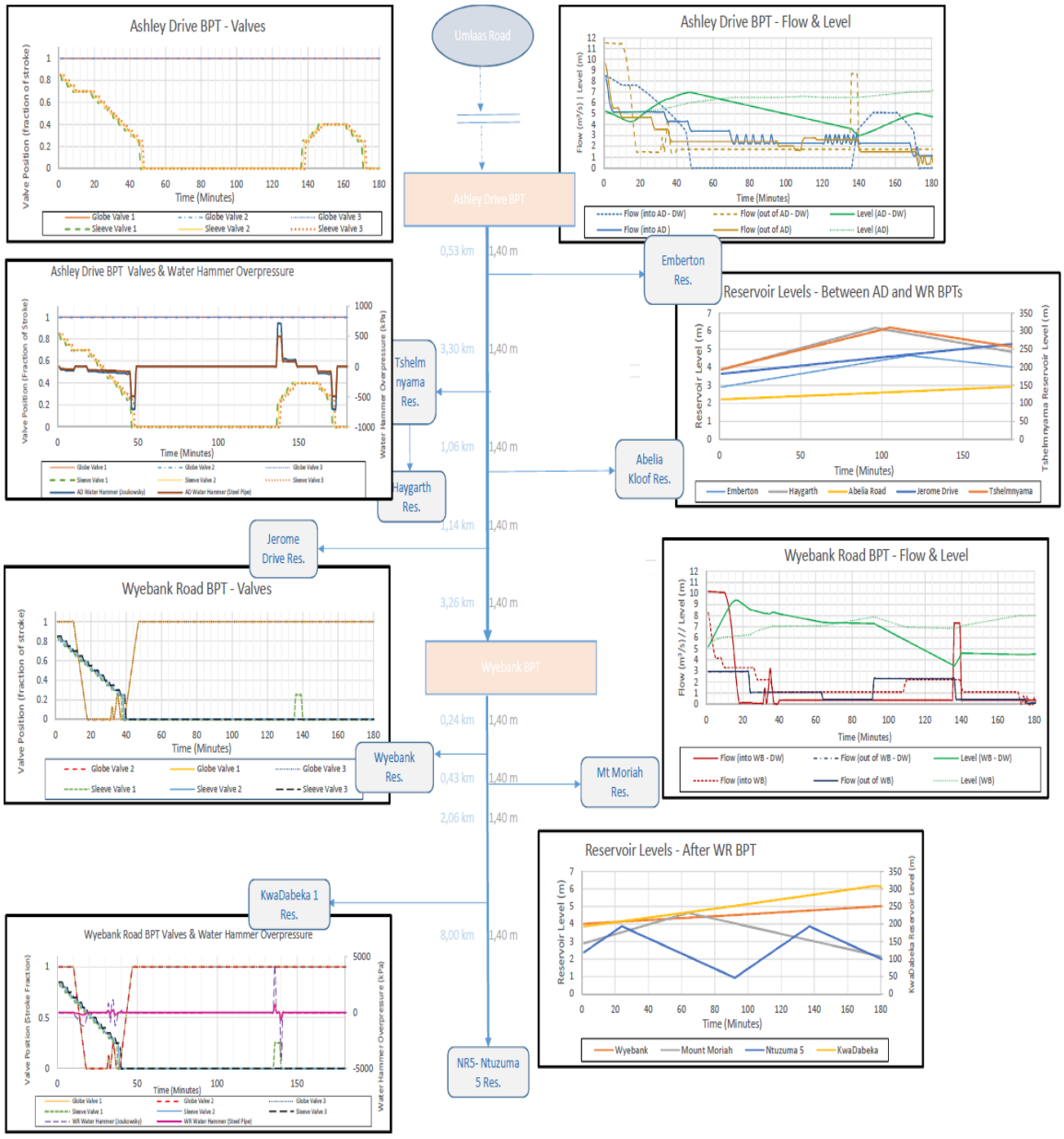

Figure C1 - Microsoft Excel presentation graphic for each simultation run. The above figure corresponds to the results of Scenario 0x.

APPENDIX D – PROGRAM (MATLAB) CODE

```
clc
clear all
close all
global p globeparam


%% time configuration  + increments
totaltime=24; %time in hours
totaltimesec=totaltime*3600; %total time in seconds
increments=totaltimesec/60; % required no of increments
deltat=totaltimesec/increments; %- of time increments in seconds
tcount=0; %initialize a time-based counter
starttime=00; %use 24h clock to set start time
year=2036;

%% Initialize vectors for speed
Fdemand=zeros(floor(increments),5);
ADGVpos=zeros(floor(increments),3);
ADSVpos=zeros(floor(increments),3);
WRGVpos=zeros(floor(increments),3);
WRSVpos=zeros(floor(increments),3);
P1a=zeros(1,floor(increments));
Ff1=zeros(1,floor(increments));
Ff2=zeros(1,floor(increments));
Ff3=zeros(1,floor(increments));
Ff=zeros(1,floor(increments));
dpgvA=zeros(1,floor(increments));
Pash=zeros(1,floor(increments));
Presash=zeros(1,floor(increments));
line1pdrop=zeros(1,floor(increments));
Pintwye=zeros(1,floor(increments));
Pavawye=zeros(1,floor(increments));
Ffw=zeros(floor(increments),5);
FC2=zeros(1,floor(increments));
FC3=zeros(1,floor(increments));
FC4=zeros(1,floor(increments));
FC5=zeros(1,floor(increments));
FC6=zeros(1,floor(increments));
F1w=zeros(floor(increments),1);
```

```
F2w=zeros(floor(increments),1);
F3w=zeros(floor(increments),1);
dpgv2=zeros(1,floor(increments));
PN1=zeros(1,floor(increments));
PN2=zeros(1,floor(increments));
PN3=zeros(1,floor(increments));
PN4=zeros(1,floor(increments));
pdropsWR=zeros(floor(increments),5);
WRresdraws=zeros(floor(increments),5);
Foutashley=zeros(floor(increments),5);
Fdemandla=zeros(floor(increments),4);
AWRresdraws=zeros(floor(increments),4);
ADbptvol=zeros(1,floor(increments));
WRbptvol=zeros(1,floor(increments));
WRoutflow=zeros(1,floor(increments));
ADbptlevel=zeros(1,floor(increments));
WRbptlevel=zeros(1,floor(increments));
timeplot=zeros(1,floor(increments));
ADdPKE=zeros(1,floor(increments));
WRdPKE=zeros(1,floor(increments));
ADdPKE3=zeros(1,floor(increments));
WRdPKE3=zeros(1,floor(increments));
ADdPKE4=zeros(1,floor(increments));
WRdPKE4=zeros(1,floor(increments));
ff=[0 0 0 0 0];
%% initialize vectors (demand)
%%System and BPT information
lengthURAD=40010; %m
totalvolume=[2300 4500 5000 6819 4546]; % volume of reservoirs between ashley drive and wyebank BPTs m^3
areaw=[396.689 11.628 647.501 1538.528 626.171]; % areas of reservoirs between ashley drive and wyebank BPTs m^2
depthw=totalvolume./areaw;
hilimit=depthw.*.8; % dadband high level limit of reservoirs between ashley drive and wyebank BPTs m
lolimit=depthw.*.2; % deadband low level limit of reservoirs between ashley drive and wyebank BPTs m
activew=ones(1,5); % activator vector that toggles to shutoff or turn on characteristic flows to the reservoirs
diamw=ones(1,5)*1.4; % pipe diameters in meters for pipes between ashley drive and wyebank BPTs in the line leading to Wyebank ONLY m
lengthw=[578 3300 1060 1140 3261.27];% pipe lengths in meters for pipes between ashley drive and wyebank BPTs in the line leading to Wyebank ONLY m
volumew(1,:)=totalvolume.*0.5; % volume of water in the reservoirs between ashley drive and wyebank BPTs m^3
activew1=zeros(1,5); % activator vector that toggles to shutoff or turn on characteristic flows to the reservoirs
levelw(1,:)=volumew(1,:)./areaw;  % volume of water in the reservoirs between ashley drive and wyebank BPTs, results from the volume of water and area m
```

```
density=998.2; %density of fluid - kg/m^3
viscosity=8.9e-4; %viscosity of fluid - Pa.s
ADVol=20e3; % Volume of AD BPT- total fixed volume
WRVol=10e3; % Volume of WR BPT- total fixed volume
fillfact=.7; %Initial fill level for both BPTs
ADbptvol(1)=ADVol*fillfact; %Ashley Drive BPT volume filled m^3
WRbptvol(1)=WRVol*fillfact;%Wyebank BPT volume filled m^3
wyearea=26*26*2;%Ashley Drive BPT area m^2
bptarea=2688;%Wyebank BPT area m^2
ADbptlevel(1)=ADbptvol(1)/bptarea; % initial fill height of AD BPT
WRbptlevel(1)=WRbptvol(1)/wyearea; % Initial fill height of WR BPT
Kv=7350;  %m^3/hr/bar^0.5 globe valve coefficient - Bermad
%%AD BPT


%%%%%%%%%%%%%%%%%%%%%%%%%%%%%%%%%%%%%%%%%%%%%%%%%%%%%%%%%%%%%%%%%%%%%%%%%%%%%%%%%%%%%%%%%%%%%%%%%%%%%%%%%%%%%%
%AFTER WYEBANK
totalvolumela=[5000 4540 6800 4929]; % volume of reservoirs after wyebank BPT m^3
activela=[1 1 1 1]; %activator for after wyebank
activela1=[1 1 1 1]; %activator for after wyebank
areala=[623.131 784.517 17.63 1036]; % areas of reservoirs after wyebank BPTs m^2
depthla=totalvolumela./areala;
hilimitla=depthla.*.8; % deadband high level limit of reservoirs after wyebank BPT m
lolimitla=depthla.*.2; % deadband low level limit of reservoirs after wyebank BPT m
volumela(1,:)=totalvolumela.*0.5; % volume of water in the reservoirs after wyebank BPT m^3
levella(1,:)=volumela(1,:)./areala;  % volume of water in the reservoirs after wyebank BPT, results from the volume of water and area m
lengthla=[238.7 429 206.2 8000]; %length of pipe segments after the WR BPT
%AFTER WYEBANK
%%%%%%%%%%%%%%%%%%%%%%%%%%%%%%%%%%%%%%%%%%%%%%%%%%%%%%%%%%%%%%%%%%%%%%%%%%%%%%%%%%%%%%%%%%%%%%%%%%%%%%%%%%%%%%]
%% Physical parameters
poissteel=.295;
bulkmsteel=203.3966e9; % Pa
bulkmwater=2.15e9; %Pa
pipethick=10e-3; %m
%% initiallize valve positions
xg(1,:)=[1 1 1];  %Ashley drive globe valves (1,2,3)
xs(1,:)=[1 1 1]*.85; %Ashley drive sleeve valves (1,2,3)
xgw(1,:)=[1 1 1]; %Wyebank globe valves (1,2,3)
xsw(1,:)=[1 1 1]*.85; %Wyebank sleeve valves (1,2,3)
```

```
%% initialize flow variables + set tolerance +  initialize index
fchar=adwbflow(year); %characteristic flows to resivoirs between the  BPTs
fcharla=wbflow(year); %characteristic flows to resivoirs after WR BPT


%% Regression Block (OPEN)

%%%%%%%%%%%%%%%%%%%% Sleeve valve regression
% READ off points from the supplied graphs (report via email), x and y
% x-vector
xx1=[0 60 120 180 240];

%%measurements of y-vector
yy1=[0 9 13 15 18];
yy2=[0 17 23 28 33];
yy3=[0 24 33 41 47.5];
yy4=[0 30 42 52 61];
yy5=[0 36 51 62 72];
yy6=[0 41 59 71.5 83];
yy7=[0 46 65 80 93];
yy8=[0 51 71 87 102];
yy9=[0 55 76 93 109];
yy10=[0 58 81 99 115];
%values of y-vector corresp. to x-vector
y1=yy1./31;
y2=yy2./31;
y3=yy3./31;
y4=yy4./31;
y5=yy5./31;
y6=yy6./31;
y7=yy7./31;
y8=yy8./31;
y9=yy9./31;
y10=yy10./31;

%Use obtained co-ordinates to regress to a polynomial via matrix regression
%regression function contained in sleeve1linroot function file
p(1,:)=sleeve1linroot(xx1,y1);
p(2,:)=sleeve1linroot(xx1,y2);
p(3,:)=sleeve1linroot(xx1,y3);
p(4,:)=sleeve1linroot(xx1,y4);
```

```
p(5,:)=sleeve1linroot(xx1,y5);
p(6,:)=sleeve1linroot(xx1,y6);
p(7,:)=sleeve1linroot(xx1,y7);
p(8,:)=sleeve1linroot(xx1,y8);
p(9,:)=sleeve1linroot(xx1,y9);
p(10,:)=sleeve1linroot(xx1,y10);
%% K-value (line characteristics) Regressions
%Find the k value for the inlet system to ashley drive
%USE AVERAGE TO DECREASE ERROR
otf=(62.7/185.9)*(1+(1.529641948/100))^(year-2015);
%off take fraction in the supply line, assumed to be halfway to the break pressure tank (ashley drive)
%unit adjustment factor for regression
factor=(8138+((7/8)^5)*(12055+((1-otf)^2)*11345)+((1-otf)^2)*8848);
% Four k-value regressions (incl. 1.5 multiple of peak flow)
kin1=(194-114.91)*24^2*3.6^2/278.8^2/factor;
kin2=(194-154.87)*24^2*3.6^2/factor/185.9^2;
kin3=(194-77.42)*24^2*3.6^2/factor/373.1^2;
kin4=(194-140.82)*24^2*3.6^2/factor/223.1^2;
%Average k-factor
kin=0.25*(kin1+kin2+kin3+kin4);
%%  Globe valve characteristics regression
%regress % open to kv % graph - see BERMAD VALVES literature
kvperc=[0.2 0.8 1];
globex=[0.1 0.7 1];
globeparam=sleeve1(kvperc,globex);
%%Regression Block (CLOSE)


%Calculate the a parameter for the Joukowsky equation
ajou=sqrt(1/((density/bulkmwater)+(density*diamw(1)*(1-poissteel^2)/(bulkmsteel*pipethick))));      %      Wave
propogation velocity for joukowsky equation


%% Timeloop (OPEN)
for time=1:increments
   %% Set the time (OPEN)
   tcount=tcount+1; % Keep a counter to store variables
   cumulativetime=tcount*deltat; % amount of time elapsed in seconds
   time=starttime+cumulativetime/3600; % to give time,
   %e.g. if time is 21:30, display will be 21.5
   if time>24
      time=time-24;
   end %clock reset for 24 hour clock
   %%Set the time (CLOSED)
```

```
%% Set Demands and volumes based on time (OPEN)
Fdemand(tcount,:)=demand(time,year); %set vector of demands
%for reservoirs leading to wyebank from ashley drive
Fdemandla(tcount,:)=demand2(time,year); %set vector of demands
%for reservoirs leading to wyebank from ashley drive

WRresdraws(tcount,:)=activew.*fchar; % Set reservior draws from the
%trunk mains - After WR BPT

if tcount>1
    %Euler integration for the BPT Volumes
    ADbptvol(tcount)=ADbptvol(tcount-1)+((Ff(tcount-1)-FC2(tcount-1))*deltat);
    WRbptvol(tcount)=WRbptvol(tcount-1)+((FC6(tcount-1)-WRoutflow(tcount-1))*deltat);
    %BPT level based upon the Euler method
    ADbptlevel(tcount)=ADbptvol(tcount)/bptarea;
    WRbptlevel(tcount)=WRbptvol(tcount)/wyearea;
    %Reservoir integrations with external function (Euler)
    %Reservoir LEVEL AND AREA between Ashley drive and wyebank BPTs
    volumew(tcount,:)=voladd1(volumew((tcount-1),:),fchar,activew1(tcount-1,:),Fdemand(tcount-
1,:),deltat,totalvolume);
    levelw(tcount,:)=volumew(tcount,:)./areaw;
    volumela(tcount,:)=voladd1(volumela((tcount-1),:),fcharla,activela1(tcount-1,:),Fdemandla(tcount-
1,:),deltat,totalvolumela);
    levella(tcount,:)=volumela(tcount,:)./areala;        %%Reservoir LEVEL AND AREAafter wyebank BPT




    %% Wyebank Road activator - for reservoir draws from trunk mains
    %%according to requirements of individual control systems

    % use binary indices to determine offtake flows, index activated by
    % function call

    %%&&**(())%%]
    if tcount==1
        activew1=activator(levelw(tcount,:),lolimit,hilimit,activew);%% activator toggles the elements of activew
between 0 and 1 to set side-flows
    else
        activew1(tcount,:)=activator(levelw(tcount,:),lolimit,hilimit,activew1(tcount-1,:));
```

```
end
% activew1(tcount,:)=[0 0 0 0 0]; % manual override for imposed flow
%(manual override currenly inactive - base case)
%     %&&**(())%%]

%% Wyebank Road activator

%% After Wyebank Road activator
%%&&**(())%%]
if tcount==1
   activela1=activator(levella(tcount,:),lolimitla,hilimitla,activela);%% activator toggles the elements of activew between 0 and 1 to set side-flows
else
   activela1(tcount,:)=activator(levella(tcount,:),lolimitla,hilimitla,activela1((tcount-1),:));
end
% activela1(tcount,:)=[0 0 0 1];
%%&&**(())%%]
%% After Wyebank Road activator



%% Set Demands and volumes based on time (CLOSED)

%%Valve positioner (OPEN)
% valve positions already initialized - ASHLEY DRIVE
%start 2 layer position stack
% Use external function to set valve position based on level in BPT
%Valve position set in layer 2
if tcount>1;
   xg(1,:)=xg(2,:);
   xs(1,:)=xs(2,:);
end
if tcount==1
   xg(2,:)=xg(1,:);
   xs(2,:)=xs(1,:);
else
   xs(2,:)=positionerrampnew(ADbptlevel(tcount),xs(1,:),deltat);
   xg(2,:)=globepositionerrampnew(ADbptlevel(tcount),xg(1,:),deltat);
end
ADGVpos(tcount,:)=xg(2,:);
ADSVpos(tcount,:)=xs(2,:);
```

```
%stack valve positions for the positioner function -WYEBANK ROAD
if tcount>1
   xgw(1,:)=xgw(2,:);
   xsw(1,:)=xsw(2,:);
end

if tcount==1
   xgw(2,:)= xgw(1,:);
   xsw(2,:)=xsw(1,:);
elseif tcount>1
   xgw(2,:)=globepositionerrampnew(WRbptlevel(tcount),xgw(1,:),deltat);
   xsw(2,:)=positionerrampnew(WRbptlevel(tcount),xsw(1,:),deltat);
end

WRGVpos(tcount,:)=xgw(2,:);
WRSVpos(tcount,:)=xsw(2,:);
%%Valve positioner (CLOSED)



%% Parameter regression (OPEN)
%%%% ASHLEY DRIVE
% Get parameters for Newton Raphson loop for this time step
A(1)=(((3600/Kv/(globeparam(1)*(xg(2,1)^2)+globeparam(2)*xg(2,1)))^2)*10^5/9.81e3);
A(2)=(((3600/Kv/(globeparam(1)*(xg(2,2)^2)+globeparam(2)*xg(2,2)))^2)*10^5/9.81e3);
A(3)=(((3600/Kv/(globeparam(1)*(xg(2,3)^2)+globeparam(2)*xg(2,3)))^2)*10^5/9.81e3);

% f(x) for each globe valve
B(1)=globeparam(1)*(xg(2,1)^2)+globeparam(2)*xg(2,1);
B(2)=globeparam(1)*(xg(2,2)^2)+globeparam(2)*xg(2,2);
B(3)=globeparam(1)*(xg(2,3)^2)+globeparam(2)*xg(2,3);

%conversion factor for Kv into %m^3/s/m(water)^0.5
C=sqrt(9806.38)/(3600*sqrt(1e5));

% Add Cv for valves in parallel
D=Kv*C*(B(1)+B(2)+B(3)); % Identical valves in parallel - m^3/s/m(water)^0.5
```

```
% Cv*f(x)=B*C*Kv
%deltaPglobevalve=(F/Cv/f(x))^2=(F/B/C/Kv)^2
% total deltaP for globe valves=(F/D)^2


% interpolate using valve positions to obtain accurate reults - use
% existing functions
v1a(1)=valveinterpsigsqlin(xs(2,1),xx1(1));
v1a(2)=valveinterpsigsqlin(xs(2,1),xx1(2));
v1a(3)=valveinterpsigsqlin(xs(2,1),xx1(3));
v1a(4)=valveinterpsigsqlin(xs(2,1),xx1(4));
v1a(5)=valveinterpsigsqlin(xs(2,1),xx1(5));
v1=sleeve1linroot(xx1,v1a);

v2a(1)=valveinterpsigsqlin(xs(2,2),xx1(1));
v2a(2)=valveinterpsigsqlin(xs(2,2),xx1(2));
v2a(3)=valveinterpsigsqlin(xs(2,2),xx1(3));
v2a(4)=valveinterpsigsqlin(xs(2,2),xx1(4));
v2a(5)=valveinterpsigsqlin(xs(2,2),xx1(5));
v2=sleeve1linroot(xx1,v2a);

v3a(1)=valveinterpsigsqlin(xs(2,3),xx1(1));
v3a(2)=valveinterpsigsqlin(xs(2,3),xx1(2));
v3a(3)=valveinterpsigsqlin(xs(2,3),xx1(3));
v3a(4)=valveinterpsigsqlin(xs(2,3),xx1(4));
v3a(5)=valveinterpsigsqlin(xs(2,3),xx1(5));
v3=sleeve1linroot(xx1,v3a);
%%%% ASHLEY DRIVE


%%%% WYEBANK ROAD
Aw(1)=(((3600/Kv/(globeparam(1)*(xgw(2,1)^2)+globeparam(2)*xgw(2,1)))^2)*10^5/9.81e3);
Aw(2)=(((3600/Kv/(globeparam(1)*(xgw(2,2)^2)+globeparam(2)*xgw(2,2)))^2)*10^5/9.81e3);
Aw(3)=(((3600/Kv/(globeparam(1)*(xgw(2,3)^2)+globeparam(2)*xgw(2,3)))^2)*10^5/9.81e3);


% f(x) for each valve
Bw(1)=globeparam(1)*(xgw(2,1)^2)+globeparam(2)*xgw(2,1);
Bw(2)=globeparam(1)*(xgw(2,2)^2)+globeparam(2)*xgw(2,2);
Bw(3)=globeparam(1)*(xgw(2,3)^2)+globeparam(2)*xgw(2,3);
```

```
%conversion factor for Kv into %m^3/s/m(water)^0.5
Cw=sqrt(9806.38)/(3600*sqrt(1e5));

% Add Cv for valves in parallel
Dw=Kv*Cw*(Bw(1)+Bw(2)+Bw(3)); % Identical valves in parallel - m^3/s/m(water)^0.5
% Cv*f(x)=B*C*Kv
%deltaPglobevalve=(F/Cv/f(x))^2=(F/B/C/Kv)^2
% total deltaP for globe valves=(F/D)^2

%Re-regression to get analytical equation based on current valve
%positions
v1aw(1)=valveinterpsigsqlin(xsw(2,1),xx1(1));
v1aw(2)=valveinterpsigsqlin(xsw(2,1),xx1(2));
v1aw(3)=valveinterpsigsqlin(xsw(2,1),xx1(3));
v1aw(4)=valveinterpsigsqlin(xsw(2,1),xx1(4));
v1aw(5)=valveinterpsigsqlin(xsw(2,1),xx1(5));
v1w=sleeve1linroot(xx1,v1aw);
%     v1wsl=sleeve1sigstraightline(xx1,v1aw); % option for straight line
%     regression (y=mx+c)

v2aw(1)=valveinterpsigsqlin(xsw(2,2),xx1(1));
v2aw(2)=valveinterpsigsqlin(xsw(2,2),xx1(2));
v2aw(3)=valveinterpsigsqlin(xsw(2,2),xx1(3));
v2aw(4)=valveinterpsigsqlin(xsw(2,2),xx1(4));
v2aw(5)=valveinterpsigsqlin(xsw(2,2),xx1(5));
v2w=sleeve1linroot(xx1,v2aw);
%     v2wsl=sleeve1sigstraightline(xx1,v2aw);


v3aw(1)=valveinterpsigsqlin(xsw(2,3),xx1(1));
v3aw(2)=valveinterpsigsqlin(xsw(2,3),xx1(2));
v3aw(3)=valveinterpsigsqlin(xsw(2,3),xx1(3));
v3aw(4)=valveinterpsigsqlin(xsw(2,3),xx1(4));
v3aw(5)=valveinterpsigsqlin(xsw(2,3),xx1(5));
v3w=sleeve1linroot(xx1,v3aw);
%     v3wsl=sleeve1sigstraightline(xx1,v3aw);
%%%% WYEBANK ROAD
```

```
%%Parameter regression  (CLOSED)

%% Newton Raphson solution loop (OPEN)
%initial guesses for Pint - CHANGES EVERY TIME STEP - USE PREVIOUS
%VALUES AFTER FIRST STEP
if tcount==1
   P1a(tcount)=50;% m of head
else
   P1a(tcount)=Pash(tcount-1); % m of head
   %set initial guess to last convergence value to increase speed
end

%%%%%%%%%%%%%%%%%%%%%%%%%%%%%%%%%%%%%%%%%%%%%%%%%%%%%%%%%%%%%%%%%%%%%%%%%%%%%%%%%%%%%%%%%%%%%%%%%%%%%
    %ASHLEY DRIVE TOLERANCES

    %% set tolerances for loop and sub-loops
    % initialize loop variables and index (Ashley Drive)
    tol1=.001;
    crita=5;
    index=0;
    F1a=0;
    F1b=0;
    F2a1=0;
    F2a2=0;
    F2a3=0;
    F2a=0;
    F2b1=0;
    F2b2=0;
    F2b3=0;
    F2b=0;

    %%Wyebank Road
    tol1w=1e-3;
    critatw=100;
    indextw=0;
    %% ASHLEY DRIVE TOLERANCES
```

```
%%%%%%%%%%%%%%%%%%%%%%%%%%%%%%%%%%%%%%%%%%%%%%%%%%%%%%%%%%%
%%%%%%%%%%%%%%%%%%%%%%%%%%%
    %%&&**(())%%]
    otfi=otf; % set lumped draw to draw according to time-based schedule
    %%&&**(())%%]
    while crita>tol1
      index=index+1; % index to count number of cycle
      movefract=1; %percentage - movement from current point (Newton-Raphson)
      P1b(index)=P1a(index)*(1+movefract/100);% New Pint for % movement
      %Calculate flows in lines upstream to intermediate point between
      %the globe and sleeve valves
      %based upon current pressure, line and globe valve chraracteristics
      F1a(index)=sqrt((194-ADbptlevel(tcount)-P1a(index))/((kin*(1+(1-otfi)^2)+D^-2)));
      %As above, for pressure % away from calculated pressure
      F1b(index)=sqrt((194-ADbptlevel(tcount)-P1b(index))/((kin*(1+(1-otfi)^2)+D^-2)));

      %Calculate flow through sleeve valves based on current pressure
      %(individual)
      F2a1(index)=v1(1)*(P1a(index)/100)+v1(2)*(P1a(index)/100)^0.5;
      F2a2(index)=v2(1)*(P1a(index)/100)+v2(2)*(P1a(index)/100)^0.5;
      F2a3(index)=v3(1)*(P1a(index)/100)+v3(2)*(P1a(index)/100)^0.5;
      %Sum individual flows to get total flow through sleeve valves
      F2a(index)=F2a1(index)+F2a2(index)+F2a3(index);
      %Calculate flow through sleeve valves based on pressure
      % away from calculated pressure (individual)
      F2b1(index)=v1(1)*(P1b(index)/100)+v1(2)*(P1b(index)/100)^0.5;
      F2b2(index)=v2(1)*(P1b(index)/100)+v2(2)*(P1b(index)/100)^0.5;
      F2b3(index)=v3(1)*(P1b(index)/100)+v3(2)*(P1b(index)/100)^0.5;
      %Sum individual flows to get total flow through sleeve valves
      F2b(index)=F2b1(index)+F2b2(index)+F2b3(index);

      %Newton-Raphson convergence criteria - for calc and  %move pressures
      crita= (F1a(index)-F2a(index));
      critb= (F1b(index)-F2b(index));

      %Calculate the gradient for the Newton-Raphson next guess
      gradient=(critb-crita)/(P1b(index)-P1a(index));
      %Over relaxation parameter to avoid overshoots and speed-up
      %convergence
      slowfract=tol1*5;
      %Next guess according to Newton-Raphson algorithm
```

```
    P1a(index+1)=P1a(index)-((crita/gradient)*slowfract);
  end

  % Store the total flow and the flow through each leg
  Ff1(tcount)=F2a1(end);
  Ff2(tcount)=F2a2(end);
  Ff3(tcount)=F2a3(end);
  Ff(tcount)=F2a(end); % Flow through to AD

  dpgvA(tcount)=Ff(tcount)^2/(D^2);%Pressure loss through globe valves

  Pash(tcount)=P1a(index); % Pressure between GV and \SV

  Presash(tcount)=Pash(tcount)+dpgvA(tcount); %Pressure available just
  %before the globe valves - entrance to BPT

  line1pdrop(tcount)=194-Presash(tcount);%Line pressure loss

  %Negative protection reset
  if dpgvA>194
    line1pdrop(tcount)=0;
  end
  %% BEGIN WYEBANK ROAD BPT CALCULATIONS
%%%%%%%%%%%%%%%%%%%%%%%%%%%%%%%%%%%%%%%%%%%%%%%%%%%%%%%%%%
%%%%%%%%%%%%%%%%%%%%%%%%%%%

  %%if statement used to set initial guess to previously calculated
  %%value, to lend speed to the calculation
  if tcount==1
    P1atw(1)=60; %initial guess for intermediate pressure
  else
    P1atw(1)=Pintwye(tcount-1);
  end

  while critatw>tol1w
    indextw=indextw+1;

    %Green portion - inactive - Darcy-Weisbach routine
    %    while critwa>tol1w
    %      indexw=indexw+1;
```

```
%       %start pdrop calc involving intermediate flow and lambda calcs
%
%        movefractw=.1; %percentage
%        ffb(indexw,5)=ff(indexw,5)*(1+movefractw/100); %%%%%%%%%%%%%%
%        CALCULATE FLOWS IN LINES LEADING TO WYEBANK FROM ASHLEY
%        %%%%%%%%%%%%%%% DRIVE
%        ff(indexw,4)=ff(indexw,5)+activew1(5)*fchar(5); % begin
%        calculation of intermediate flows based on gusesses
%        ff(indexw,3)=ff(indexw,4)+activew1(4)*fchar(4);
%        ff(indexw,2)=ff(indexw,3)+activew1(2)*fchar(2)+activew1(3)*fchar(3);
%        ff(indexw,1)=ff(indexw,2)+activew1(1)*fchar(1);
deltapstatic=184-WRbptlevel(tcount); %meters head - design report
epsilon=0.015e-3; %m - Pipe roughness
frictionguess=0.1; %intial guess of the friction factor-for
%successive substitution routine


%find the friction factor (COLEBROOK)
%        frictionfact=lambdafun1(epsilon,diamw,density,ff(indexw,:),viscosity,frictionguess);
%find pressure drops based on friction factor
%        pdrops=deltap1(density, frictionfact, lengthw, ff(indexw,:), diamw);
%        pdrop=sum(pdrops)/9.81e3; % combined pressure drop in m
%        pav=deltapstatic-pdrop; %m of pressure available at entrance to wyebank
%
%        if pav<0
%            pav=0;
%        end
%
%%%%%%%%%%%%%%%%%%%%%%%%%%%%%%%%%%%%%%%%%%%%%%%%%%%%%%%%%%%%%%%%%%%%%%%%%%%%%%%%%%%%%%%%%%%%%%%%%%%%%%%%%%%%%%%%%%%%%%
%        ffb(indexw,4)=ffb(indexw,5)+activew1(5)*fchar(5); % begin calculation of intermediate flows based
on gusesses
%        ffb(indexw,3)=ffb(indexw,4)+activew1(4)*fchar(4);
%        ffb(indexw,2)=ffb(indexw,3)+activew1(2)*fchar(2)+activew1(3)*fchar(3);
%        ffb(indexw,1)=ffb(indexw,2)+activew1(1)*fchar(1);
%        frictionfactb=lambdafun1(epsilon,diamw,density,ffb(indexw,:),viscosity,frictionguess);
%        pdropsb=deltap1(density, frictionfactb, lengthw, ffb(indexw,:), diamw);
%        pdropb=sum(pdropsb)/9.81e3; % combined pressure drop in m
%        pavb=deltapstatic-pdropb;
%
%        if pavb<0
%            pavb=0;
%        end
```

```
%       GVa=(ff(indexw,5)/Dw)^2;
%       GVb=(ffb(indexw,5)/Dw)^2;
%       pintw=pav-GVa;
%       PintwA(indexw)=pintw;
%       pintwb=pavb-GVb;
%       PintwB(indexw)=pintwb;



%       if PintwA(indexw)<1e-6
%          PintwA(indexw)=1e-6;
%       end
%        if PintwB(indexw)<1e-6
%          PintwB(indexw)=1e-6;
%       end


%
%       Pav(indexw)=pav;
%       Pavb(indexw)=pavb;
%       ww=[0 0];
%       tolW(1)=12;
%       sig1=(v1w(1)+v2w(1)+v3w(1));
%       sig2=(v1w(2)+v2w(2)+v3w(2));
% %       sig3=(v1w(3)+v2w(3)+v3w(3));
% %       sig4=v1w(4)+v2w(4)+v3w(4);
%       tolW(2)=5;
% %       if sum(xsw(2,:))>.1
% %       while tolW(1)>innertol
% %          ww(1)=ww(1)+1;
% %          Pdra(1)=Pav(indexw)*.6;
% %          Pdrag(ww(1))=Pdra(ww(1))*(1+movefractw/100);
% %           Pdra(ww(1)+1)=Pdra(ww(1))+10*((((sig1*(Pdra(ww(1))/100)^2+sig2*(Pdra(ww(1))/100)+sig3-
ff(indexw,5))/sig4))^2)-Pdra(ww(1));
% %          tolW(1)=abs(Pdra(ww(1)+1)-Pdra(ww(1)));
% % %       end
% %       while tolW(2)>innertol
% %          ww(2)=ww(2)+1;
% %          Pdrab(1)=Pavb(indexw)*.6;
%                                                                                  %
Pdrab(ww(2)+1)=Pdrab(ww(2))+10*((((sig1*(Pdrab(ww(2))/100)^2+sig2*(Pdrab(ww(2))/100)+sig3-
ffb(indexw,5))/sig4))^2)-Pdrab(ww(2));
% %          tolW(2)=abs(Pdrab(ww(2)+1)-Pdrab(ww(2)));
```

```
% %       end
% %       PwB(indexw)=Pdrab(ww(2)+1);
% %       PwA(indexw)=Pdra(ww(1)+1);

% Lump static terms (coefficients for quadratic equation) into single factor(s)
factor1=sum(lengthw)*kin/lengthURAD+(1/Dw)^2;

factor2=2*kin/lengthURAD*(lengthw(4)*activew1(5)*fchar(5)+lengthw(3)*(activew1(5)*fchar(5)+activew1(4)*fchar(
4))+lengthw(2)*(activew1(5)*fchar(5)+activew1(4)*fchar(4)+activew1(3)*fchar(3)+activew1(2)*fchar(2))+lengthw(1
)*(activew1(5)*fchar(5)+activew1(4)*fchar(4)+activew1(3)*fchar(3)+activew1(2)*fchar(2)+activew1(1)*fchar(1)));

factor3a=kin/lengthURAD*((lengthw(4)*(activew1(5)*fchar(5))^2+lengthw(3)*((activew1(5)*fchar(5)+activew1(4)*f
char(4)))^2+lengthw(2)*(activew1(5)*fchar(5)+activew1(4)*fchar(4)+activew1(3)*fchar(3)+activew1(2)*fchar(2))^2
+lengthw(1)*(activew1(5)*fchar(5)+activew1(4)*fchar(4)+activew1(3)*fchar(3)+activew1(2)*fchar(2)+activew1(1)*f
char(1))^2));

movefract=1; %percentage - move from current value - Newton-Raphson
P1btw(indextw)=P1atw(indextw)*(1+movefract/100); %Pressure at a % from
%the calculated pressure

%Finalize the factors for solving within the quadratic equation
%solver
factor3aa=factor3a-deltapstatic+P1atw(indextw);
factor3bb=factor3a-deltapstatic+P1btw(indextw);

%Use the quadratic equation to solve for the flow through the globe
%valves and upstream line (as per Ashley Drive above)
F1atw(indextw)=(-factor2+sqrt(factor2^2-4*factor1*factor3aa))/(2*factor1);
F1btw(indextw)=(-factor2+sqrt(factor2^2-4*factor1*factor3bb))/(2*factor1);
%       F1atw(indextw)=sqrt((194-WRbptlevel(tcount)-P1atw(indextw))/((kin*(1+(1-otf)^2)+D^-2)));
%       F1btw(indextw)=sqrt((194-WRbptlevel(tcount)-P1btw(indextw))/((kin*(1+(1-otf)^2)+D^-2)));

%Calculate the flow through ech sleeve valve and cumulative flow (as
%per Ashley Drive above)
F2a1tw(indextw)=v1w(1)*(P1atw(indextw)/100)+v1w(2)*(P1atw(indextw)/100)^0.5;
F2a2tw(indextw)=v2w(1)*(P1atw(indextw)/100)+v2w(2)*(P1atw(indextw)/100)^0.5;
F2a3tw(indextw)=v3w(1)*(P1atw(indextw)/100)+v3w(2)*(P1atw(indextw)/100)^0.5;
F2atw(indextw)=F2a1tw(indextw)+F2a2tw(indextw)+F2a3tw(indextw);
%Calculate the flow through ech sleeve valve and cumulative flow (as
%per Ashley Drive above) - for pressure a % away from the calculated
F2b1tw(indextw)=v1w(1)*(P1btw(indextw)/100)+v1w(2)*(P1btw(indextw)/100)^0.5;
F2b2tw(indextw)=v2w(1)*(P1btw(indextw)/100)+v2w(2)*(P1btw(indextw)/100)^0.5;
F2b3tw(indextw)=v3w(1)*(P1btw(indextw)/100)+v3w(2)*(P1btw(indextw)/100)^0.5;
```

```
    F2btw(indextw)=F2b1tw(indextw)+F2b2tw(indextw)+F2b3tw(indextw);

    %Newton-Raphson convergence criteria
    critatw=(F1atw(indextw)-F2atw(indextw))
    critbtw=(F1btw(indextw)-F2btw(indextw));
    %Gradient for next guess calculation for Newton-Raphson algorithm
    gradienttw=(critbtw-critatw)/(P1btw(indextw)-P1atw(indextw));
    %Over relaxation parameter to avoid overshoots and speed-up
    %convergence
    slowfracttw=tol1w*15;
    %next guess calculation according to the Newton-Raphson algorithm
    P1atw(indextw+1)=P1atw(indextw)-((critatw/gradienttw)*slowfracttw);
end
%       AAa=(sig1/sig2)^2;
%       BBa=-((2*ff(indexw,5)*sig1/(sig2)^2)+1);
%       CCa=(ff(indexw,5)/sig2)^2;
%       BBb=-((2*ffb(indexw,5)*sig1/(sig2)^2)+1);
%       CCb=(ffb(indexw,5)/sig2)^2;
%
%       PwA(indexw)=((-BBa-sqrt(BBa^2-4*AAa*CCa))/(2*AAa));
%       PwB(indexw)=((-BBb-sqrt(BBb^2-4*AAa*CCb))/(2*AAa));
%
%       elseif sum(xsw(2,:))<=.03
%           PwA(indexw)=ff(indexw,5)/(0.5/240);
%           PwB(indexw)=ffb(indexw,5)/(0.5/240);
%
%       end
%       critwa= (PintwA(indexw)-PwA(indexw));
%       critwb= (PintwB(indexw)-PwB(indexw));
%       gradientw=(critwb-critwa)/(ffb(indexw,5)-ff(indexw,5));
%
%       slowfractw=5e2*tol1w;
%       ff(indexw+1,5)=ff(indexw,5)-((critwa/gradientw)*slowfractw);



%Store variables for plotting etc.
Pintwye(tcount)=P1atw(indextw); %pressure before sleeve valves - pressure drop accross sleeve valves
Ffw(tcount,:)=F1atw(indextw); %Store flow variables for plotting

%negative protection reset for flow
```

```
FC6(tcount);
if sum(WRSVpos(tcount,:))<6e-5
   FC6(tcount)=0;
else FC6(tcount)=F1atw(indextw);
end

GVa=(FC6(tcount)/Dw)^2;
Pavawye(tcount)=Pintwye(tcount)+GVa; %pressure at entrance to wyebank
FC5(tcount)= FC6(tcount)+activew1(tcount,5)*fchar(5); % begin calculation of intermediate flows based on gusesses
FC4(tcount)=FC5(tcount)+activew1(tcount,4)*fchar(4);
FC3(tcount)=FC4(tcount)+activew1(tcount,2)*fchar(2)+activew1(tcount,3)*fchar(3);
FC2(tcount)=FC3(tcount)+activew1(tcount,1)*fchar(1);
%Pressure drop calculations for pressure profile along the line to the
%Wyebank Road BPT from the Ashley Drive BPT
pdroptw(tcount,1)=kin/lengthURAD*lengthw(1)*FC2(tcount)^2;
pdroptw(tcount,2)=kin/lengthURAD*lengthw(2)*FC3(tcount)^2;
pdroptw(tcount,3)=kin/lengthURAD*lengthw(3)*FC4(tcount)^2;
pdroptw(tcount,4)=kin/lengthURAD*lengthw(4)*FC5(tcount)^2;
pdroptw(tcount,5)=kin/lengthURAD*lengthw(5)*FC6(tcount)^2;
%Pressure profile calculations
pdropstw(tcount,:)=pdroptw(tcount,:)./1; % pressure drops in the lines to wyebank in meters
dpgv2(tcount)=GVa; %Globe valve pressure drops
PN1(tcount)=Pavawye(tcount)+
pdropstw(tcount,5)+pdropstw(tcount,4)+pdropstw(tcount,3)+pdropsWR(tcount,2);
PN2(tcount)=Pavawye(tcount)+ pdropstw(tcount,5)+pdropstw(tcount,4)+pdropstw(tcount,3);
PN3(tcount)=Pavawye(tcount)+ pdropstw(tcount,5)+pdropstw(tcount,4);
PN4(tcount)=Pavawye(tcount)+ pdropstw(tcount,5);

%Calculations for the flow through each sleeve valve
F1w(tcount,:)=v1w(1)*(Pintwye(tcount)/100)+v1w(2)*(Pintwye(tcount)/100)^0.5;
F2w(tcount,:)=v2w(1)*(Pintwye(tcount)/100)+v2w(2)*(Pintwye(tcount)/100)^0.5;
F3w(tcount,:)=v3w(1)*(Pintwye(tcount)/100)+v3w(2)*(Pintwye(tcount)/100)^0.5;

%    Pintwye(tcount)=PintwA(indexw); %pressure before sleeve valves - pressure drop accross sleeve valves
%    Pavawye(tcount)=Pav(indexw); %pressure at entrance to wyebank
%    Ffw(tcount,:)=ff(indexw,5); %Store flow variables for plotting
%    FC2(tcount)=ff(indexw,1);
%    FC3(tcount)=ff(indexw,2);
%    FC4(tcount)=ff(indexw,3);
%    FC5(tcount)=ff(indexw,4);
%    F1w(tcount,:)=v1w(1)*(Pintwye(tcount)/100)+v1w(2)*(Pintwye(tcount)/100)^0.5;
```

```
%     F2w(tcount,:)=v2w(1)*(Pintwye(tcount)/100)+v2w(2)*(Pintwye(tcount)/100)^0.5;
%     F3w(tcount,:)=v3w(1)*(Pintwye(tcount)/100)+v3w(2)*(Pintwye(tcount)/100)^0.5;
%

if F1w(tcount,:)<0
   F1w(tcount,:)=1e-7;
end
if F2w(tcount,:)<0
   F2w(tcount,:)=1e-7;
end
if F3w(tcount,:)<0
   F3w(tcount,:)=1e-7;
end




%     pdrops(tcount,:)=pdrops./9.81e3; % pressure drops in the lines to wyebank in meters
%     dpgv2(tcount)=GVa; %Globe valve pressure drops
%                                                                 PN1(tcount)=Pavawye(tcount)+
pdropsWR(tcount,5)+pdropsWR(tcount,4)+pdropsWR(tcount,3)+pdropsWR(tcount,2);
%     PN2(tcount)=Pavawye(tcount)+ pdropsWR(tcount,5)+pdropsWR(tcount,4)+pdropsWR(tcount,3);
%     PN3(tcount)=Pavawye(tcount)+ pdropsWR(tcount,5)+pdropsWR(tcount,4);
%     PN4(tcount)=Pavawye(tcount)+ pdropsWR(tcount,5);
%



%Create a vector of flows in lines between the two BPTs - referencing
Foutashley(tcount,:)=[FC2(tcount) FC3(tcount) FC4(tcount) FC5(tcount) FC6(tcount)]; %flows in lines leading
to wyebank
%after wyebank calcs




%% Create variables for plotting
AWRresdraws(tcount,:)=activela1(tcount,:).*fcharla;
WRoutflow(tcount)=sum(AWRresdraws(tcount,:),2);
FD1(tcount)=WRoutflow(tcount);
FD2(tcount)=FD1(tcount)-AWRresdraws(tcount,1);
FD3(tcount)=FD2(tcount)-AWRresdraws(tcount,2);
```

```
    FD4(tcount)=FD3(tcount)-AWRresdraws(tcount,3);
    Val(tcount)=AWRresdraws(tcount,4)- FD4(tcount); %check accuracy of calc
    pdropdw(tcount,1)=kin/lengthURAD*lengthla(1)*FD1(tcount)^2;
    pdropdw(tcount,2)=kin/lengthURAD*lengthla(2)*FD2(tcount)^2;
    pdropdw(tcount,3)=kin/lengthURAD*lengthla(3)*FD3(tcount)^2;
    pdropdw(tcount,4)=kin/lengthURAD*lengthla(4)*FD4(tcount)^2;

    if tcount>1
        %     ADdPKE2(tcount)=-(Ff(tcount)^2-Ff(tcount-1)^2)/density/deltat/(pi*diamw(1)^2/4)^2;
        %     WRdPKE2(tcount)=-(FC6(tcount)^2-FC6(tcount-1)^2)/density/deltat/(pi*diamw(1)^2/4)^2;
        ADdPKE(tcount)=-(Ff(tcount)^3-Ff(tcount-1)^3)*density*deltat/2/(pi*diamw(1)^2/4)^2;
        WRdPKE(tcount)=-(FC6(tcount)^3-FC6(tcount-1)^3)*density*deltat/2/(pi*diamw(1)^2/4)^2;
        ADdPKE3(tcount)=-ajou*density*(Ff(tcount)-Ff(tcount-1))/(pi*diamw(1)^2/4)/1000;
        WRdPKE3(tcount)=-ajou*density*(FC6(tcount)-FC6(tcount-1))/(pi*diamw(1)^2/4)/1000;
        ADdPKE4(tcount)=-lengthURAD*density*(Ff(tcount)-Ff(tcount-1))/(pi*diamw(1)^2/4)/deltat/1000;
        WRdPKE4(tcount)=-sum(lengthw)*density*(FC6(tcount)-FC6(tcount-1))/(pi*diamw(1)^2/4)/deltat/1000;
    end
    timeplot(tcount)=tcount;
end
```